eman ta zabal zazu

Universidad del País Vasco
Euskal Herriko Unibertsitatea

Investigating the role of HIF2α and the type I interferon signalling in cancer hypoxia

Tesis presentada por
ESTHER ARNAIZ GONZÁLEZ

2020

(c) 2020 Esther Arnaiz González

Investigating the role of HIF2α and the type I interferon signalling in cancer hypoxia

Tesis presentada por
ESTHER ARNAIZ GONZÁLEZ

Para la obtención del título de doctora en
***Investigación Biomédica* por la**
Universidad del País Vasco/Euskal Herriko Unibertsitatea

Tesis dirigida por
Dr Charles H. Lawrie
Prof Adrian L. Harris

‘Cuando una da un paso valiente, a la vida, el destino o la suerte le da por seguirte la corriente y te facilita las cosas’

Laura Norton

Acknowledgements

First of all, I would like to thank to my thesis directors Dr Charles Lawrie and Prof Adrian Harris. Thank you, **Charles** for giving me the opportunity of joining Molecular Oncology group in Biodonostia Health Research Institute, even if I had one year less to do my PhD, and supporting me during this process. **Adrian**, thank you very much for inviting me to stay longer in Hypoxia and Angiogenesis lab in the Weatherall Institute of Molecular Medicine, it has been decisive for this thesis. Thanks for helping me during this last year, giving new ideas and always being ready to discuss results. Thank you for your support and for your constant encouragement to keep going. I have learnt a lot under your supervision.

Secondly, I would like to thank to Eusko Jaurlaritza for providing me with a PhD grant and a travel grant and helping me in every situation, as well as to EMBO for the travel grant.

Me gustaría agradecer a todas las personas que han formado parte de esta tesis. A pesar de que los resultados mostrados son el trabajo desarrollado en Biodonostia y Oxford en los últimos años, para mí esta tesis comenzó mucho antes. Empezó en el piso de arriba, con las 'Chungas'. Gracias a las dos por introducirme en el mundo científico. A ti **Amaia,** por enseñarme las bases de la ciencia y por demostrarme que las burbujas nunca son buenas, y a ti ***Chunga***, por enseñarme otra forma de trabajar, aunque lo más importante ha sido tu apoyo constante y tus palabras cuando todo era negro. Gracias por ayudarme a tomar cada decisión importante de este camino y por preocuparte por mí durante todos estos años. Gracias también por tus consejos y por ayudarme a poner bonito mi primer CV y decirte que, ¡ya puedo abrir los tubos con una sola mano! No puedo olvidarme de los chicos del piso de abajo. Gracias **Pablo** por animar el ambiente del labo bailando Rafael y por mostrarme que, aunque muchas veces frustrante, el trabajo del laboratorio también es satisfactorio. **Miguel**, darte muchas gracias por tu contagioso entusiasmo y por presentarme a las ranas.

Rubens, no me olvido de ti, no. Gracias por tu apoyo todo este tiempo, por las risas en los momentos más feos y por estar siempre dispuesto a escuchar y ayudar, pero, sobre todo, gracias por no haberte ido antes de tiempo, no sé qué hubiera hecho sin ti.

Agradecer a todos los miembros del grupo, porque cada uno a su manera habéis contribuido en esta tesis. Gracias al grupo de mama, **María Caffarel**, **Angela** y **Andrea**, por dar ideas y estar dispuestas a ayudar, ¡siempre con una sonrisa! Gracias también a **Ibai** por presentarme a HIF y guiarme al principio, y a **María Arestin**, **María Armesto**, **Erika**, **Giovanni** y **Maitena**, por los ánimos durante este tiempo. **Lorea**, zure eguneroko gidagatik, baina askoz gehiago argia erakusteagatik dena ilun zegoenean, mila mila esker. Y **Carla**, jamás hubiera pensado que compartir unas muestras fuera a ser en inicio de una buena amistad. Chispita y Chispón. Gracias por estar siempre dispuesta a ayudar, ya sea científico o no, y por ser mi asesora, secretaria y chófer. Gracias también por preocuparte por mi salud mental y no permitir que me volviera *crazy*. Al grupo de Oncología Celular gracias también por los buenos momentos que hemos compartido. **Mikel** y **Ander**, gracias por sacarme esa risa que nadie imita mejor que vosotros, **Jaione**, mila esker zure animoengatik eta nigatik kezkatzeagatik, **Leire** eta **Juncal**, zueie ere eskerrik asko momentu on guztiengatik. Gracias también a Hepato, por las risas en todo momento, y mencionar a **Álvaro**, porque ver amanecer desde cultivos no tiene precio, a **Ainhoa**, por ser una osa amorosa, y a **Pauli**, mil gracias por todo, por estar siempre dispuesta a escuchar y por los ánimos en los momentos malos, pero también, ¡gracias por los buenos momentos y por todos esos viajes que hemos hecho! A las chicas de Bioingeniería, **Laura** y **Vir** gracias también por el apoyo, eta **Haizea** mila esker zure laguntzagatik, zure aholku zientifiko eta pertsonalengatik eta nire burukominak entzuteagatik. En definitiva, ¡gracias a todos por el apoyo y por soportar mi mal genio!

I cannot forget about everyone in Oxford who has taken part in the development of this thesis. First of all, I would like to thank to Hypoxia and Angiogenesis group members. Thank you, **Karim** for helping with the lipids and for being the only one laughing at my jokes, **Christos** for glucose metabolism, **Helen** for everything related to cell movement, **Esther** for the *in vivo* work and **Koon**, **Ceren** and **Ellen** for introducing me to Oxford's college life and for every laugh we had. I want also to thank **Matteo**, even if you stole my RIPA and left my drug sleeping in your lab coat's pocket, because every time you we were around, I felt closer to home. I would also like to thank **Jana** and **Chris** for no doubting in helping with the microscope. No puedo olvidarme de **Andrés**, **Edu** y **Claudia**, gracias por los ánimos estos últimos meses y por todas las minicharlas entre experimentos que me permitieron desahogarme y me dieron fuerza para seguir. **Prithvi**, **Ria** and **Alberta**, thanks a lot for everything, you cannot imagine how important you guys, have been for me. Thanks for your worries about me and for making me feel good, even if you were laughing at me! You have been a real support, especially during the last months. Alberta's faces, Prithvi's laugh, Ria's dictionary, fado and Portugaaal, every cooking moment, every problem… I will never forget them. Keep in mind girls, that if I don't succeed in science, I will ask for you references to become a Detective!

Ana, me cuesta escribir para darte las gracias, porque no sé por dónde empezar. Ya sabes el papel que has tenido en esta tesis y te lo agradezco infinitamente, perdona no haber podido poner tu nombre más allá de estas líneas. Gracias por ser mi *supervisor* y enseñarme y guiarme en poyata, incluso en la distancia, he aprendido mucho de ti. Nunca olvidaré tus palabras después de la primera reunión con Adrian, y ¿sabes? ¡Lo hemos conseguido! Quiero darte mil gracias también por tu apoyo y tus ánimos, han sido muy importantes todo este tiempo, y por preocuparte por mí. Agradecerte también todos los buenos momentos que hemos pasado dentro y fuera del labo, y por ayudarme a lidiar con los ingleses. Me alegro enormemente de que nuestros caminos se hayan *overlapeado*, porque además de a una científica inigualable, me llevo a una amiga. Millones de gracias por estar dispuesta a ayudar bajo cualquier circunstancia. Gracias por todo, Ana, todo. Nos vemos pronto.

Zuri, mi apoyo incondicional. Tengo que agradecerte muchas cosas, entre ellas, el estar siempre dispuesta quemar el teléfono, ¡no sé cómo hubiera pasado estos años sin hablar contigo! Gracias por escucharme y por darme tu opinión todo este tiempo. Gracias por los ánimos, la alegría y el optimismo que transmites, que por muy lejos que estés, siempre llega. Gracias, y quizás perdón, por preocuparte tanto por mí y por estar pendiente. En definitiva, mil gracias por haber estado a mi lado desde el principio de este camino.

Y por último, a mis **aitas**, sobre todo a mi **ama**, porque sin ti no hubiera llegado hasta aquí. Gracias por no dejarme sola en ningún momento y darme fuerza para seguir adelante.

Abbreviations

12S	Mitochondrially encoded 12S rRNA
2D	2-dimension
2-DG	2-Deoxy-D-glucose
2-DG-P	2-Deoxy-D-glucose-phosphate
3D	3-dimension
3pRNA	5’-triphosphate RNA
A2AR	A2A adenosine receptor
ADAM17	ADAM metallopeptidase domain 17
ADAR1	Adenosine deaminase RNA specific 1
ADAR-p110	Adenosine deaminase RNA specific isoform p110
ADAR-p150	Adenosine deaminase RNA specific isoform p150
ADP	Adenosine diphosphate
AICAR	5-aminoimidazole-4-carboxamide ribose
AMPK	AMP-activated kinase
ANGPTL4	Angiopoietin-like 4
AP2	Adaptin protein 2
ARNT	Aryl hydrocarbon receptor nuclear translocator
ATCC	American Type Culture Collection
ATP	Adenosine triphosphate
ATP6	Mitochondrially encoded ATP synthase membrane subunit 6
AXL	AXL receptor tyrosine kinase
BAF180	BRG1-associated factor 180
BAP1	BRCA1 associated protein 1
BCL2	BCL2 apoptosis regulator
Bev	Bevacizumab
bHLH	Basic helix-loop-helix
BMDAC	Bone-marrow-derived angiogenic cells
BNIP3	BCL2 interacting protein 3
BNIP3L	BCL2 interacting protein 3 like
bp	Base pair
BSA	Bovine serum albumin
C3Orf22	Chromosome 3 open reading frame 22
CA9	Carbonic anhydrase 9
CARD	Caspase recruitment domain
Cas9	Crispr associated protein 9
CCDC78	Coiled coil domain containing 78
CCL28	C-C motif chemokine ligand 28
ccRCC	Clear cell renal cell carcinoma
CD28	Cluster of differentiation 28
CD36	Cluster of differentiation 36
CD39	Cluster of differentiation 39
CD40	Cluster of differentiation 40
CD47	Cluster of differentiation 47
CD73	Cluster of differentiation 73
CD80	Cluster of differentiation 80
CD86	Cluster of differentiation 86

CDCP1	HIF2α-induced CUB domain-containing protein 1
CDK17	Cyclin dependent kinase 17
CDK8	Cyclin-dependent kinase 8
cDNA	Complementary DNA
cGAMP	Cyclic GMP-AMP
cGAS	Cyclic GMP-AMP synthase
CHIP	Carboxyl terminus of Hsp70-interacting protein
CITED2	CBP/p300-interacting transactivator with Glu/Asp (ED)-rich domain 2
c-KIT	Stem cell factor receptor
c-MYC	MYC proto-oncogene
COX1	Mitochondrially encoded cytochrome c oxidase I
CPT	Carnitine palmitoyltransferase
CPT1	Carnitine palmitoyltransferase 1
CPT2	Carnitine palmitoyltransferase 2
Crispr	Clustered regularly interspaced short palindromic repeats
CSC	Cancer stem cells
CSF-1R	Colony-stimulator factor
CT	Computed tomography
CTLA-4	Cytotoxic T lymphocyte-associated antigen 4
CTLs	Cytotoxic T cells
CUL2	Cullin 2
CXCR4	C-X-C motif chemokine receptor 4
CYTB	Mitochondrially encoded cytochrome b
DAI	DNA-dependent activator of IFN-regulatory factors
DAMPs	Damage-associated molecular patterns
DC	Dendritic cells
dCK	Deoxycytidine kinase
ddC	2',3'-dideoxycytidine
ddCTP	Dideoxycytidine triphosphate
DDX41	DExD/Hbox helicase 41
DDX58	DExD/H-box helicase 58
DFS	Disease-free survival
dGK	Deoxyguanosine kinase
D-loop	Displacement loop
DMEM	Dulbecco's modified eagle medium
DMEM/F12	Dulbecco's Modified Eagle Medium: Nutrient Mixture F-12
DMOG	Dimethyloxalyl glycine
DMSO	Dimethyl sulfoxide
DNA	Deoxyribonucleic acid
DNAse	Deoxyribonuclease
dNTP	Deoxynucleoside triphosphate
DOC	Sodium deoxycholate
dsDNA	Double-strand DNA
dsRNA	Double-strand RNA
DSS	Disease-specific survival
ECACC	European Collection of Authenticated Cell Cultures

ECAR	Extracellular acidification rate
ECM	Extracellular matrix
EDTA	Ethylenediaminetetraacetic acid
EGFP	Enhanced green fluorescent protein
EGFR	Epidermal growth factor receptor
EMT	Epithelial-to-mesenchymal transition
EPO	Erythropoietin
EPO-R	Erythropoietin receptor
ER	Estrogen receptor
ERK	Extracellular signal regulated kinase
ETC	Electron transport chain
EZH2	Enhancer of zeste 2 polycomb repressive complex 2 subunit
F	Forward
FACS	Fluorescence-activated cell sorting
$FADH_2$	Flavin adenine dinucleotide
FARP1	FERM, ARH/RhoGEF and pleckstrin domain protein 1
Fas/FasL	Fas cell surface death receptor/Fas ligand
FBS	Fetal bovine serum
FCCP	Carbonyl cyanide-4 (trifluoromethoxy) phenylhydrazine
FDA	Food and Drug Administration
FDG	2-deoxy-2-[^{18}F]-fluoro-D-glucose
FGF	Fibroblast growth factor
FIH	Factor Inhibiting HIF
FLT-3	FMS-like tyrosine kinase
FN1	Fibronectin 1
FSC-A	Forward scatter area
FSC-H	Forward scatter height
GAS	Gamma-activated sequence
GBP4	Guanylate binding protein 4
GFP	Green fluorescent protein
GLUT1	Glucose transporter 1
GLUT3	Glucose transporter 3
gRNA	Guide RNA
G-TPP	Gamitrinib-triphenylphosphonium
HAF	Hypoxia-associated factor
HBSS	Hank’s Buffered Saline Solution
HCA	High-content analysis
HCS	High-content screening
HEPES	4-(2-hydroxyethyl)-1-piperazineethanesulfonic acid
HER2	Human epidermal growth factor receptor 2
HIF1α	Hypoxia-inducible factor 1α
HIF1β	Hypoxia-inducible factor 1β
HIF2α	Hypoxia-inducible factor 2α
HIF3α	Hypoxia-inducible factor 3α
HIG2	Hypoxia-inducible lipid droplet associated
HLA-G	Major histocompatibility complex, class I, G

HMG-CoA	3-hydroxy-3-methyl-glutaryl-coenzyme A
HMGR	3-hydroxy-3-methyl-glutaryl-coenzyme A reductase
HPRT1	Hypoxanthine phosphoribosyltransferase
HRE	Hypoxia response elements
Hsp90	Mitochondrial heat shock protein 90
H-strand	Heavy strand
HSV	*Herpes simplex virus*
HSWB	High salt washing buffer
HTS	High-throughput screening
HUVEC	Human Umbilical Vein Endothelial cells
ICD	Immunogenic cell death
IDH	Isocitrate dehydrogenase
IFI16	Interferon-γ-inducible factor 16
IFIH1	Interferon-induced with helicase C domain 1
IFIT	Interferon-induced protein with tetratricopeptide
IFIT1	Interferon-induced protein with tetratricopeptide repeats 1
IFIT2	Interferon-induced protein with tetratricopeptide repeats 2
IFN	Interferon
IFNAR	IFNα receptor
IFNAR1	IFNα receptor subunit 1
IFNAR2	IFNα receptor subunit 2
IFNGR1	IFNγ receptor
IL-10	Interleukin-10
IL-15	Interleukin-15
IL-2	Interleukin-2
IPS-1	IFNβ promoter stimulator-1
IQCB1	IQ motif containing B1
IRAK-1	Interleukin 1 receptor associated kinase 1
IRAK-4	Interleukin 1 receptor associated kinase 4
IRF3	Interferon-regulatory factor 3
IRF5	Interferon-regulatory factor 5
IRF7	Interferon-regulatory factor 7
IRF9	Interferon-regulatory factor 9
ISG12	Interferon alpha inducible protein 27
ISG15	ISG15 ubiquitin like modifier
ISGF3	IFN-stimulated gene factor 3
ISGs	Interferon-stimulated genes
ISREs	Interferon-stimulated response elements
ISUP	International Society of Urological Pathology
ITH	Transcription initiation sites for the heavy strand
ITL	Transcription initiation sites for the light strand
IVT	*In vitro* transcripts
Iκκ	Inducible IκB kinase
Iκκβ	IκB kinase β
JAK1	Janus kinase 1
JmjC	Jumonji-C

kb	Kilo base
KITL	KIT ligand
KO	Knock out
LB	Luria-Bertani
LC3	Microtubule associated protein 1 light chain 3
LDHA	Lactate dehydrogenase 1
lncRNA462	Long non-coding RNA 462
LOH	Loss of heterozygosity
LPS	Lipopolysaccharides
L-strand	Light strand
Luc	Luciferase
MAVS	Mitochondrial antiviral-signalling protein
MCA	3-methylcholanthrene
MDA5	Melanoma differentiation-associated gene 5
MDSC	Myeloid-derived suppressor cells
MEFs	Mouse embryonic fibroblasts
MES	2-(N-morpholino)ethanesulfonic acid
MET	Mesenchymal-to-epithelial transition
MIC	Major histocompatibility complex class I chain related
min	Minutes
MMP	Matrix metalloproteinase
MMP2	Matrix metalloproteinase 2
MMP7	Matrix metalloproteinase 7
MMP9	Matrix metalloproteinase 9
MOI	Multiplicity of infection
MOPS	3-(N-morpholino)propanesulfonic acid
MRI	Magnetic resonance imaging
mRNA	Messenger RNA
MRP	Mitochondrial ribosomal protein
MRPL1	Mitochondrial ribosomal protein L1
MRPL11	Mitochondrial ribosomal protein L11
MRPL13	Mitochondrial ribosomal protein L13
MRPL21	Mitochondrial ribosomal protein L21
MRPS23	Mitochondrial ribosomal protein S23
MRPS34	Mitochondrial ribosomal protein S34
mtDNA	Mitochondrial DNA
mtdsRNA	Mitochondrial double-strand RNA
mTOR	Mammalian target of rapamycin
mtRNA	Mitochondrial RNA
mtZFN	Mitochondrially targeted zinc-finger nuclease
MX1	MX dynamin like GTPase 1
MX2	MX dynamin like GTPase 2
MyD88	Myeloid differentiation primary response gene 88
NAD/NADH	Nicotinamide adenine dinucleotide
NADPH	Nicotinamide adenine dinucleotide phosphate
NAOAc	Sodium acetate

ND3	Mitochondrially encoded NADH:ubiquinone oxidoreductase core subunit 3
NEB	New England Biolabs
NEO	Neomycin
NF-κB	Nuclear factor-κB
Nix	BCL2 interacting protein 3 like
NK	Natural killer
NKG2D	Natural killer group 2 member D
NO	Nitric oxide
NOD SCID	Non-obese diabetic, severe combined immunodeficiency
NOS	Nitric oxide synthase
NRF2	Nuclear factor, erythroid 2 like 2
OAS	Oligoadenylate synthetase
OCR	Oxygen consumption rate
ODD	Oxygen-dependent degradation domain
OH	Origin of the heavy strand synthesis
OS	Overall survival
OXPHOS	Oxidative phosphorylation system
P/S	Penicillin/Streptomycin
PAC	PAS-associated C-terminal domain
PAI-1	Plasminogen activator inhibitor-1
PAM	Protospacer adjacent motif
PAMPs	Pathogen-associated molecular patterns
PAS	PER-ARNT-SIM
PBAF	Polybromo-BAF
PBMCs	Peripheral blood mononuclear cells
PBRM1	Polybromo 1
PBS	Phosphate buffered saline
PCR	Polymerase chain reaction
PD-1	Programmed death-1
PDGF	Platelet-derived growth factor
PDGFR	Platelet-derived growth factor receptor
PDH	Pyruvate dehydrogenase
PDHA1	Pyruvate dehydrogenase E1 alpha 1 subunit
PDK1	Pyruvate dehydrogenase kinase 1
PD-L1	Programmed death-ligand 1
PD-L2	Programmed death-ligand 2
PET	Positron emission tomography
PFA	Paraformaldehyde
PFS	Progression-free survival
PGC-1α	Proliferator-activated receptor-γ coactivator-1α
PGF	Placental growth factor
PHD	Prolyl hydroxylase
PI3Ks	Phosphatidylinositol-3 kinases
PINK1	PTEN-induced putative kinase 1
pIRF3	Phosphorylated IRF3

PKM2	M2 isoform of pyruvate kinase
PLAUR	Urokinase-type plasminogen activator receptor
PLIN2	Perilipin 2
PNK	Polynucleotide kinase
PNPT1	Polyribonucleotide nucleotidyltransferase 1
POLRMT	Mitochondrial RNA polymerase
poly I:C	Polyinosinic-polycytidylic acid
PR	Progesterone receptor
PRC	Polycomb repressive complex
PRKN	Parkin
PRRs	Pattern-recognition receptors
pSTAT1	Phosphorylated STAT1
PVDF	Polyvinylidene fluoride
qPCR	Quantitative polymerase chain reaction
R	Reverse
RACK1	Receptor of activated protein kinase C
RAG-2	Recombinase activating gene 2
Rb	Retinoblastoma
RBX1	RING box protein 1
RCC	Renal cell carcinoma
ReDo	Repurposing Drugs in Oncology
RET	Neurotropic factor receptor
RIG-I	Retinoid acid-inducible gene I
RNA	Ribonucleic acid
RNAse	Ribonuclease
ROS	Reactive oxygen species
Rot/Ant	Rotenone/Antimycin
rRNA	Ribosomal RNA
RT	Room temperature
RWD	Relative wound density
SCFβ-Trcp	Skp1-Cullin1-F-box protein β transducin repeat-containing protein
SDF1	Stromal-derived factor 1
SDS	Sodium dodecyl sulfate
SDS-PAGE	Sodium dodecyl sulfate polyacrylamide gel electrophoresis
SEM	Standard error of the mean
SETD2	SET domain containing 2, histone lysine methyltransferase
SF	Serum free
sgRNA	Single guide RNA
SHMT2	Serine hydroxymethyltransferase 2
shRNA	Short hairpin RNA
siRNA	Small interfering RNA
SIRT1	Sirtuin 1
SIRT6	Sirtuin 6
SLC35A4	Solute carrier family 35 member A4
SLE	Systemic lupus erythematosus
SOCS	Suppressors of cytokine signalling

SOCS1	Suppressor of cytokine signalling member 1
SOCS3	Suppressor of cytokine signalling member 3
SQSTM1	Sequestosome 1
SSBP	Single-stranded DNA binding protein 1
SSC-A	Side scatter area
ssRNA	Single-strand RNA
STAT	Signal transducer and activator of transcription
STAT1	Signal transducer and activator of transcription 1
STAT2	Signal transducer and activator of transcription 2
STAT3	Signal transducer and activator of transcription 3
STC2	Stanniocalcin 2
STING	Stimulator of interferon genes
SUV3	Suv3 like RNA helicase
SWI/SNF	Switch/sucrose non-fermentable
TAD	Transactivation domain
TAM	Tumour-associated macrophages
TBE	Tris-borate-EDTA
TBK1	TANK binding kinase 1
TBS	Tris-buffered saline
TBS-T	TBS containing 0.1% Tween-20
TCA	Tricarboxylic acid cycle
TCF8/ZEB1	Zinc-finger E-box binding homeobox
TDI	Target Discovery Institute
TFAM	Mitochondrial transcription factor A
TFB1M	Mitochondrial transcription factor B1
TGFα	Transforming growth factor α
TGFβ	Transforming growth factor β
TIR	Toll-IL-1 receptor
TIRAP	TIR domain-containing adaptor protein
TK	Thymidine kinase
TK1	Thymidine kinase 1
TK2	Thymidine kinase 2
TKY2	Tyrosine kinase 2
TLR	Toll-like receptor
TLR3	Toll-like receptor 3
TLR4	Toll-like receptor 4
TLR7	Toll-like receptor 7
TLR8	Toll-like receptor 8
TLR9	Toll-like receptor 9
TMB	Tumour mutational burden
TN	Triple negative
TRAF3	TNF receptor associated factor 3
TRAF6	TNF receptor associated factor 6
TRAILs	TNF superfamily member 10
TRAM	TRIF-related adaptor molecule
Treg	Regulatory T cells

TRIF	TIR domain containing adaptor-inducing IFN
TRIM	Tripartite motif
tRNA	Transfer RNA
UPR	Unfolded protein response
USP18	Ubiquitin specific peptidase 18
UV	Ultraviolet
VCAN	Versican
VEFGR	Vascular endothelial growth factor receptor
VEGFA	Vascular endothelial growth factor A
V-EMCV	*Encephalomyocarditis virus*
VHL	von Hippel-Lindau
Vps34	Vacuolar protein sorting 34
VSV	*Vesicular stomatitis virus*
WHO	World Health Organisation
WT	Wild type
YB-1	Y-box protein 1
ZCCHC17	Zinc-finger CCHC-type containing 17
ZO-1	Zonula occludens-1

Index

1. General introduction 1

1.1. Hallmarks of cancer 3

1.2. Hypoxia 7

1.2.1. HIF transcription factors. Domain organization 7

1.2.2. Post-translational modifications of HIFs 9

1.2.3. The HIF transcriptional program 12

1.2.4. HIFs role in cancer cell survival in hypoxia 13

1.3. Models to study hypoxia 16

1.4. Hypothesis and objectives 17

2. General materials and methods 19

2.1. Cell treatments 21

2.1.1. Hypoxia exposure 21

2.2. Western Blot 21

2.2.1. Protein extraction and quantification 21

2.2.2. SDS-PAGE and Membrane Transference 21

2.2.3. Antibody staining and development 22

2.3. Total RNA extraction 23

2.4. Reverse transcription 23

2.5. Quantitative polymerase chain reaction (qPCR) 25

2.6. Statistical analysis 25

3. The role of HIF2α in renal carcinoma 27

3.1. Introduction 29

3.1.1. Renal cancer 29

3.1.2. RCC classification 29

3.1.3. Clear cell renal cell carcinoma (ccRCC) 32

3.1.3.1. Treatment options for ccRCC 32

3.1.3.2. Genetics of ccRCC 41

3.1.3.3. HIF1α and HIF2α in ccRCC 44

3.2. Objectives ... 50

3.3. Materials and methods ... 51

3.3.1. Cell culture ... 51

3.3.1.1. Lung cancer cell line ... 51

3.3.1.2. Renal cancer cell lines ... 51

3.3.2. Cell treatments ... 51

3.3.2.1. Small-molecule antagonist of HIF2α PT2385 [237] ... 51

3.3.2.2. 2-Deoxy-D-glucose ... 52

3.3.2.3. Cell culture in different glucose media ... 52

3.3.3. Clustered regularly interspaced short palindromic repeats/Cas9 (Crispr/Cas9) ... 52

3.3.3.1. Single guide RNAs ... 52

3.3.3.2. Plasmid digestion and linearization ... 53

3.3.3.3. sgRNA annealing ... 54

3.3.3.4. gRNA precipitation ... 54

3.3.3.5. gRNA and plasmid ligation ... 55

3.3.3.6. Plasmid extraction and amplification ... 55

3.3.3.7. Crispr/Cas9 guide selection ... 56

3.3.3.8. Cell transfection and cell sorting ... 56

3.3.3.9. Validation of cell clones ... 57

3.3.4. Extraction of nucleic acids ... 57

3.3.4.1. Genomic DNA extraction ... 57

3.3.4.2. Plasmid DNA extraction ... 58

3.3.5. Polymerase chain reaction (PCR) ... 58

3.3.6. DNA gel electrophoresis ... 58

3.3.7. Cloning into pGEM®-T Easy Vector ... 58

3.3.8. Sanger Sequencing ... 59

3.3.8.1. PCR product purification ... 59

3.3.8.2. Sanger sequencing reaction ... 59

3.3.9. Production of competent bacteria 59

3.3.10. Transformation of plasmid DNA into competent bacteria 60

3.3.11. Cell transfection 60

3.3.11.1. Cell transfection with Turbofect 60

3.3.11.2. Cell transfection with Fugene 60

3.3.11.3. Cell transfection with Oligofectamine 61

3.3.12. Cell proliferation 62

3.3.13. Colony formation assay 62

3.3.14. Spheroids 62

3.3.14.1. Spheroid formation 62

3.3.14.2. Spheroid disaggregation 63

3.3.15. Migration assay 63

3.3.16. Invasion assay 64

3.3.17. Seahorse metabolic assay 64

3.3.18. Luciferase positive cell line generation 66

3.3.19. *In vivo* metastasis model 66

3.3.20. Immunofluorescence for lipid droplets 67

3.3.21. Flow cytometry for lipid droplets 67

3.4. Results 69

3.4.1. Generation of 786-0 HIF2α KO cell line using Crispr/Cas9 69

3.4.1.1. HIF2α targeting guides are predicted to inactivate the gene 69

3.4.1.2. Successful generation of a 786-0 HIF2α KO cell line 70

3.4.2. Selection of the optimal experimental conditions 74

3.4.3. The role of HIF2α in tumour cell proliferation 76

3.4.3.1. HIF2α deletion inhibits cell proliferation in 2D cultures 76

3.4.3.2. Initial cell density affects the 786-0 KO growth rate 80

3.4.3.3. HIF2α deletion does not affect cell proliferation in 3D cultures 82

3.4.4. HIF2α deletion promotes tumour cell migration but inhibits cells' invasion ability *in vitro*85

3.4.5. HIF2α enhances metastasis *in vivo* 91
3.4.6. HIF2α deletion alters cell metabolism 94
3.4.6.1. HIF2α does not overtake HIF1α's glycolytic role in 786-0 cells 94
3.4.6.2. HIF2α's role in lipid metabolism 95
3.4.6.3. HIF2α KO enhances mitochondrial oxidative phosphorylation 98
3.5. Discussion 102
3.6. Conclusions 116
4. HIF2α conferred resistance to drugs 117
4.1. Introduction 119
4.1.1. Repurposing drugs 119
4.1.2. Repurposed drugs in RCC 119
4.1.3. High-throughput technology 121
4.2. Objectives 123
4.3. Materials and methods 124
4.3.1. Pharmacon MicroSource. HCS 124
4.3.2. HCS data analysis 124
4.3.3. Validation of the Pharmacon screening 125
4.4. Results 127
4.4.1. Drug screening validation 127
4.4.2. HIF2α confers resistance to statins 128
4.5. Discussion 130
4.6. Conclusions 132
5. Type I IFN pathway regulation in hypoxia 133
5.1. Introduction 135
5.1.1. Interferons 135
5.1.2. IFN pathway 135
5.1.2.1. Early phase 135
5.1.2.2. Late phase 137

5.1.3. IFNs and cancer 139

5.1.3.1. Cancer immunoediting 141

5.1.3.2. IFNs and anticancer therapies 143

5.1.3.3. Negative regulation of IFN signalling 145

5.1.4. Hypoxia and the immune system 147

5.1.5. Mitochondria and the type I IFN signalling 150

5.1.5.1. Mitochondria description 150

5.1.5.2. Mitochondria as immunogenic organelles 151

5.1.5.3. Mitophagy 153

5.2. Objectives 156

5.3. Materials and methods 157

5.3.1. Cell culture 157

5.3.1.1. Breast cancer cell lines 157

5.3.1.2. Osteosarcoma cell lines 157

5.3.1.3. Kidney cancer cell line 158

5.3.1.4. Non-tumour cell lines 158

5.3.2. Cell treatments 158

5.3.3. Cell transfection 159

5.3.3.1. Transfection of polyinosinic-polycytidylic acid 159

5.3.3.2. Transfection of siRNA for BNIP3 159

5.3.4. Lactate measurement 160

5.3.5. IFNβ promoter assay 160

5.3.6. Mitochondria extraction 161

5.3.7. Immunofluorescence 161

5.3.7.1. Immunofluorescence for dsRNA 161

5.3.7.2. Immunofluorescence dsRNA image analysis 162

5.3.7.3. Immunofluorescence for mitophagy 164

5.4. Results 165

5.4.1. Hypoxia causes a down-regulation of the type I IFN pathway at basal levels 165

5.4.2. Reoxygenation after hypoxia leads to recovery of the type I IFN pathway 167

5.4.3. Hypoxia down-regulates the type I IFN pathway stimulated with a dsRNA mimic........... 169

5.4.4. HIF1α and HIF2α role in the type I IFN pathway 171

5.4.4.1. Type I IFN pathway is partially dependent on HIF1α 171

5.4.4.2. Hypoxic lactate levels inhibit the type I IFN pathway 173

5.4.4.3. Type I IFN pathway and HIF2α 174

5.4.5. Hypoxic total RNA causes lower IFNβ induction 176

5.4.6. Imaging of dsRNA levels under hypoxia 179

5.4.7. mtDNA and effect of mutation status on dsRNA in hypoxia 185

5.4.8. Hypoxia negatively regulates mtDNA transcription 190

5.4.9. Hypoxia negatively regulates mitochondrial ribosomal protein expression..................... 194

5.4.10. mtRNA is responsible for IFNβ promoter induction... 195

5.4.11. Lower mtRNA in hypoxia is not due to increase mitophagy 197

5.4.12. Effect of mitochondria-targeting drugs in dsRNA levels 199

5.5. Discussion 202

5.6. Conclusions.. 210

6. General summary 211

7. Summary in Spanish...215

7.1. Introducción general 217

7.2. Estudio de HIF2α en carcinoma renal 217

7.2.1. Introducción 217

7.2.2. Resultados 218

7.2.2.1. Papel de HIF2α en la proliferación celular 218

7.2.2.2. La deleción de HIF2α promueve la migración e inhibe la invasión celular *in vitro* 219

7.2.2.3. HIF2α estimula metástasis *in vivo* 219

7.2.2.4. La deleción de HIF2α altera el metabolismo celular 220

7.2.3. Discusión... 220

7.2.4. Conclusiones 221

7.3. Resistencia a drogas mediada por HIF2α 222

7.3.1. Introducción 222

7.3.2. Resultados 222

7.3.3. Discusión........ 222

7.3.4. Conclusiones........ 222

7.4. Regulación de la vía del interferón tipo I 223

7.4.1. Introducción 223

7.4.2. Resultados 224

7.4.2.1. La hipoxia disminuye la activación de la vía del IFN tipo I 224

7.4.2.2. El ARN total procedente de células hipóxicas disminuye la activación del promotor de IFNβ 224

7.4.2.3. Los niveles de dsRNA en hipoxia son más bajos que en normoxia debido a una menor transcripción del mtDNA 225

7.4.2.4. El dsRNA mitocondrial activa al promotor de IFNβ........ 225

7.4.3. Discusión........ 225

7.4.4. Conclusiones........ 226

8. References........227

9. Appendix 255

1. General introduction

1.1. Hallmarks of cancer

Cancer is a heterogenous disease which can arise from almost every cell type. In 2000 Hanahan and Weinberg proposed that despite the diversity between cancer types and between individual tumours of the same origin, all entities had a common pathogenic background [1]. These common characteristics were defined as the 'Hallmarks of cancer', and they included six essential alterations: 1) self-sufficiency in growth signals, 2) insensitivity to growth-inhibitory signals, 3) evasion of apoptosis, 4) limitless replicative potential, 5) sustained angiogenesis and 6) tissue invasion and metastasis.

Later in 2011 [2], they revised this schema and included: genome instability and mutation, tumour-promoting inflammation, reprogramming energy metabolism and evading immune destruction, making a total of ten hallmarks of cancer (Figure 1.1).

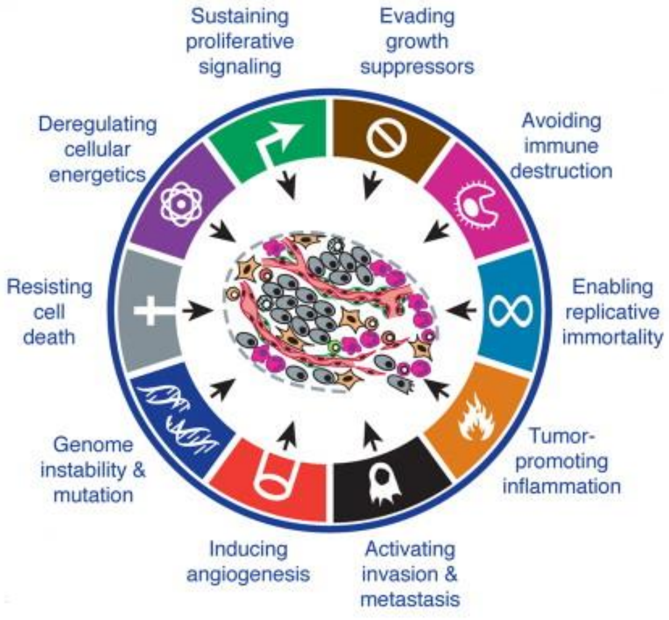
Sustaining proliferative signaling
Evading growth suppressors
Avoiding immune destruction
Enabling replicative immortality
Tumor-promoting inflammation
Activating invasion & metastasis
Inducing angiogenesis
Genome instability & mutation
Resisting cell death
Deregulating cellular energetics

Figure 1.1. The ten hallmarks of cancer. Modified from [2].

1) Self-sufficiency in growth signals

Normal cells require stimulatory signals, also called growth signals, to proliferate. These include growth factors, components of the extracellular matrix (ECM) and cell-to-cell interactions or adhesion molecules. However, tumour cells become independent of the surrounding growth signalling by producing the extracellular growth signals they require themselves, altering the signal transducers or enhancing the intracellular pathway, in this way acquiring the ability to grow self-sufficiently [1]. They can generate their own proliferative signals, such as platelet-derived growth factor (PDGF) and transforming growth factor α (TGFα) [3]. Tumour cells can also overexpress specific receptors for growth factors, making them to be hyper-responsive to basal levels that would not trigger proliferation under normal physiological conditions [3], or switch the type of receptors (e.g. integrins) to those that transmit progrowth signals [4]. In the intracellular pathways, alterations to the cytoplasmic components of the pathway, such as Ras proteins, can occur allowing cell proliferation even without the presence of a stimulatory signal [5].

2) Insensitivity to growth-inhibitory signals

In normal tissue there exist several antiproliferative checkpoint signals to maintain tissue and cellular homeostasis. These can be inhibitory signals which force the cells to entry into a quiescent (G_0), non-proliferative state until the adequate proliferative extracellular signal appears or can be signals inducing cell differentiation [2].

Most antiproliferative signals (e.g. transforming growth factor β (TGFβ)) act through retinoblastoma protein (Rb). In a hypophosphorylated state, Rb blocks proliferation by recruiting E2F transcription factor, which controls the expression of genes involved in cell cycle [6]. In many tumours however, E2F is free to activate the expression of cell cycle genes due to Rb pathway disruption, leading to tumour evasion of antigrowth signals [7].

3) Evasion of apoptosis

Normal cells have a tight control of the signals that determine if they should live or die. Under extracellular death signals (e.g. physiologic stress, pathogen infection or impaired cell-cell/cell-ECM interactions) or intracellular death signals (e.g. DNA damage, oncogene activation or insufficient survival factors) normal cells undergo programmed cell death, also known as apoptosis [8]. However, tumour cells develop mechanisms to overcome these issues, the most common being the loss of the tumour suppressor gene *p53* [1].

4) Limitless replicative potential

In 1997 Hayflick demonstrated that after a certain number of doublings, cells stop growing, a process termed senescence [9]. In contrast, tumour cells appear to be immortalized, having a limitless replicative potential. In human cells, telomere length determines the number of cell's division [10]. With each division telomeres are shortened, however, tumour cells overcome this mechanism by expressing telomerase enzyme that counteracts telomere shortening [2].

5) Sustained angiogenesis

In order to sustain their growth, tumours require a constant supply of nutrients and oxygen. To achieve this, tumour cells secrete soluble angiogenic factors such as vascular endothelial growth factor A (VEGFA) and fibroblast growth factor (FGF) which bind to their respective receptors on the surface of endothelial cells resulting in new blood vessel formation (angiogenesis) [3]. This process is induced at early stages of the malignant transformation [1]. At the same time that tumour cells increase the expression of pro-angiogenic factors, they suppress they expression of the anti-angiogenic ones (e.g. thrombospondin-1) [11]. Moreover, it has been described that proteases can contribute to angiogenesis by releasing the FGF stored in the ECM [12].

6) Tissue invasion and metastasis

Metastasis is the process by which tumour cells escape from their primary site and generate secondary tumours in distant organs. Acquisition of metastatic potential is a process that involves multiple steps: local invasion, intravasation into circulation, survival in circulation (cells lack anchorage during this period), extravasation, colonization and survival in distant organs to form a secondary tumour or metastasis [13].

For a successful invasion and later colonization, cells have developed several mechanisms. First, tumour cells can up-regulate the expression of protease genes, while down-regulating the expression of protease inhibitor genes, for an efficient ECM degradation and cell migration [14]. Then, once in the destination tissue, tumour cells can change their integrin expression, as each integrin subtype has distinct substrate preferences [15].

7) Genome instability and mutation

Cells have diverse DNA monitoring and repairing enzyme complexes for the maintenance of genome integrity, meaning that spontaneous gene mutation is a relatively rare event under physiological conditions. However, tumour cells acquire their neoplastic characteristics primarily through the generation of gene mutations, suggesting that the normal genomic 'caretaker' systems are lost in these cells [16].

Among these systems, the p53 tumour suppressor protein plays perhaps the most prominent role. In response to DNA damage, p53 promotes either cell cycle arrest to allow DNA repair or, if the damage is irreversible, cell apoptosis. However, as this protein is frequently lost in cancers, tumour cells continue proliferating but have much higher levels of genetic instability than normal cells, which in the end create selective advantages for the tumour cells resulting in cancer progression [17]. Similarly, other genes involved in sensing DNA damage or regulating correct chromosomal segregation during mitosis are found to be lost in several cancers [16].

8) Tumour-promoting inflammation

Immune cell infiltration in the tumour mass and the consequent inflammation reflects immune system's attempt to eradicate the tumour. However, it is now known that tumour-associated inflammation can also enhance tumorigenesis and progression [18-20]. Inflammation can contribute to several hallmarks by supplying bioactive molecules (e.g. growth, survival and pro-angiogenic factors or ECM modifying enzymes) to the tumour microenvironment or by releasing signals that activate the epithelial-to-mesenchymal transition (EMT).

9) Reprogramming energy metabolism

Due to the high and often uncontrolled proliferation of tumour cells, they require constant and elevated supply of nutrients. Under aerobic conditions, energy is generated via aerobic respiration, in which glucose is completely oxidized through the tricarboxylic acid cycle (TCA) and energy is produced by the mitochondria through oxidative phosphorylation. However, under anaerobic (hypoxic) conditions, glycolysis is preferred and pyruvate is later transformed to lactate. Cancer cells switch their glucose metabolism to glycolysis regardless the cell origin and independently of the oxygen availability. This phenomenon was first described by Otto Warburg and named 'Warburg effect' or 'aerobic glycolysis' [21].

Even though glycolysis is less efficient than oxidative phosphorylation, with 2 ATP molecules per glucose molecule compared to the 36 ATP molecules generated through oxidative phosphorylation, cells obtain various intermediates for biosynthetic pathways through this process, including those to generate nucleotides and amino acids [2].

Interestingly, it has been shown that two subpopulations of cells symbiotically coexist in some tumours. The first one comprises hypoxic cells residing far from blood vessels which obtain their energy through the Warburg effect and secrete lactate, whereas the second one is formed by better-oxygenated cells which use the lactate generated from their neighbour cells as their main energy source, employing the TCA and mitochondrial respiration [22-24].

10) Evading immune destruction

Both the innate and adaptive immune system prevent tumour establishment and progression by detecting and eliminating cancer cells through immunosurveillance, as explained in more detail in 'Chapter 5'. However, some tumour cells are able to escape this recognition by avoiding the detection of immune cells or by having limited the extent of immunological killing, in both cases evading immune system eradication and promoting tumour development [25].

Tumour cells can escape immune system antitumour activity by overexpressing inhibitory T cell molecules such as programmed death-ligand 1 (PD-L1) or cytotoxic T lymphocyte-associated antigen 4 (CTLA-4), which by binding to their ligands can inhibit effector T cell activation and function [26]. They can also secrete immunosuppressive molecules (e.g. TGFβ) that will inhibit infiltrating cytotoxic $CD8^+$ T cells (CTLs) and natural killer (NK) cells [27, 28] or recruit immunosuppressive inflammatory cells to the tumour, such as myeloid-derived suppressor cells (MDSC) or regulatory T (Treg) cells, that will inhibit the activity of CTLs [29, 30].

1.2. Hypoxia

One of the main characteristics of solid tumours is hypoxia. As tumour cells grow to form a tumour mass, central cells reside further and further away from the blood vessels which supply nutrients and oxygen. Because oxygen can only diffuse 100-180µm from the closest capillary, an oxygen concentration gradient is generated within the tumour mass, whereby internal cells become oxygen deprived otherwise known as hypoxia. In response to the stress generated by oxygen deprivation, cells activate several adaptive responses to match oxygen supply with their energetic demands, most of them driven by the hypoxia-inducible transcription factors (HIFs). Although first identified as a regulator of erythropoietin (EPO) production [31], HIFs are now recognized as the key modulators of the hypoxic response.

1.2.1. HIF transcription factors. Domain organization

HIFs comprise a group of DNA-binding proteins of the PER-ARNT-SIM family, which have a basic helix-loop-helix conformation (bHLH-PAS). These transcription factors function as heterodimers formed by an oxygen sensitive α subunit and a stably expressed β subunit [31-33]. In mammals, there are three α isoforms (HIF1α, HIF2α and HIF3α) and a single β isoform (HIF1β), also named aryl hydrocarbon receptor nuclear translocator (ARNT). While HIF1α is ubiquitously expressed in all cells, HIF2α and HIF3α expression is restrained to some cell types, such as endothelial cells, pneumocytes, renal or liver cells [34]. HIF1α and HIF2α share high sequence homology and they function in a similar way [32, 35], whereas HIF3α displays less similarity and exists as multiple splice variants. Interestingly, oxygen sensitivity and binding affinity with HIF1β varies from one HIF3α splice variant to another, moreover, some of them can even inhibit HIF1α and HIF2α activity [36, 37].

All members of the HIF family possess conserved protein domains: an amino-terminal bHLH domain necessary for DNA binding, PAS-A and PAS-B domains required for heterodimerization and a PAS-associated C-terminal domain (PAC) (Figure 1.2). Both bHLH and PAS domains are highly conserved at sequence level among the HIFs. HIF1α and HIF2α for instance, have 70% and 85% identity between their PAS and bHLH domains, respectively, therefore they are able to bind to the same DNA sequences [32]. In contrast to HIF3α, whose bHLH and PAS domains share 74% and 52-58% identity with HIF1α and HIF2α, respectively [38].

Both HIF1α and HIF2α contain a N- and C-terminal transactivation domain (N-TAD and C-TAD), necessary for target gene expression, while HIF3α has only the N-TAD [39]. TAD domains confer regulatory properties to HIF transcription factors. Interestingly, although N-TAD exhibits higher degree of sequence conservation than C-TAD between HIF1α and HIF2α, it regulates the transactivation of selective genes, whereas C-TAD regulates the expression of common genes [40]. N-TAD is located within the oxygen-dependent degradation domain (ODD) in every α subunit (Figure 1.2). ODD contains key proline residues targeted for hydroxylation in normoxia, with the consequent HIF degradation [41, 42]. Therefore, this domain controls the activity and stability of α subunits.

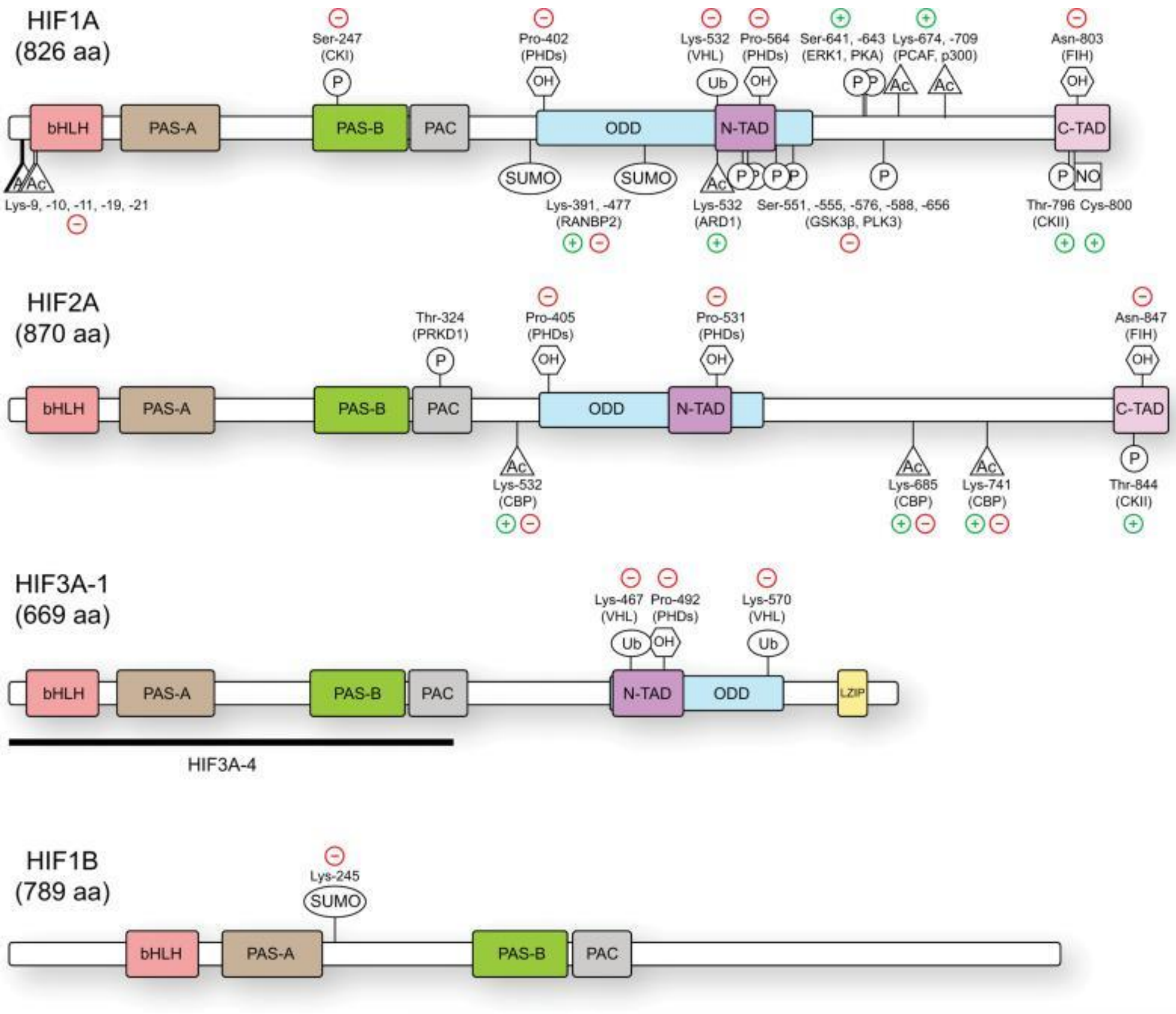
HIF1A
(826 aa)
Ser-247
(CKI)
Pro-402
(PHDs)
Lys-532
(VHL)
Pro-564
(PHDs)
Ser-641, -643
(ERK1, PKA)
Lys-674, -709
(PCAF, p300)
Asn-803
(FIH)
P
OH
Ub
Ac
bHLH
PAS-A
PAS-B
PAC
ODD
N-TAD
C-TAD
SUMO
NO
Lys-9, -10, -11, -19, -21
Lys-391, -477
(RANBP2)
Lys-532
(ARD1)
Ser-551, -555, -576, -588, -656
(GSK3β, PLK3)
Thr-796
(CKII)
Cys-800
HIF2A
(870 aa)
Thr-324
(PRKD1)
Pro-405
(PHDs)
Pro-531
(PHDs)
Asn-847
(FIH)
Lys-532
(CBP)
Lys-685
(CBP)
Lys-741
(CBP)
Thr-844
(CKII)
HIF3A-1
(669 aa)
Lys-467
(VHL)
Pro-492
(PHDs)
Lys-570
(VHL)
LZIP
HIF3A-4
HIF1B
(789 aa)
Lys-245

Figure 1.2. HIF protein domains and post-translational modifications [39].

1.2.2. Post-translational modifications of HIFs

HIF activity is tightly regulated by a number of factors, with oxygen levels being the most important one. Under normal oxygen tension (i.e. normoxia), α subunits are hydroxylated by prolyl hydroxylase enzymes (PHDs) at conserved proline residues within the ODD domain (Figure 1.2) [43, 44]. This allows binding of the von Hippel Lindau (VHL) E3 ubiquitin ligase complex which will polyubiquitinate HIFα targeting it for proteasomal degradation (Figure 1.4) [41, 45].

The *VHL* gene was identified and cloned in 1993 and is located in the short arm of chromosome 3 (3p) [46]. Apart from HIFα subunits, VHL targets other proteins (e.g. protein kinase C and RNA polymerase II subunit A) for ubiquitination and proteasomal degradation [47, 48], and it has been described that VHL interaction with fibronectin, collagen IV α2 and microtubules is important to maintain cell morphology and polarity [49-51].

VHL consists of two domains, α and β. α domain forms a ternary complex (VCB) with elongin C and elongin B proteins [52], while β domain mediates the interactions of VHL with the substrates [45]. VCB complex forms the E3 ubiquitin ligase core together with cullin 2 (CUL2) and RING box protein 1 (RBX1), generating the VCB-CR complex [53, 54] (Figure 1.3). Both elongins link the substrates recognized by VHL β domain to heterodimers of CUL2 and RBX1, which will trigger the ubiquitination of the substrate mediated by E1 ubiquitin-activating and E2 ubiquitin-conjugating enzymes [54]. In the VHL complex, E1 enzyme activates ubiquitin for conjugation using ATP, and further transfers it to E2 enzyme. E2 enzyme interacts with the specific E3-ubiquitin ligase containing the substrate for degradation. E3 subunit then, through RBX1 protein, transfers the ubiquitin to the target protein. Targeted protein can be both mono- or poly-ubiquitinated before degradation [55].

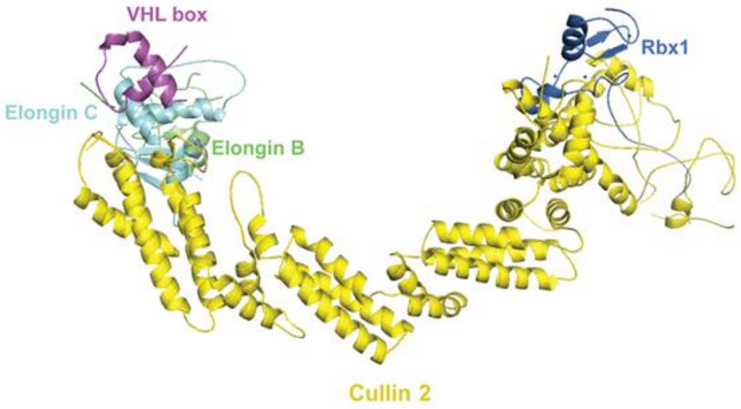

Figure 1.3. Crystal structure of the VHL ubiquitin ligase complex. Modified from [56].

HIF1α and HIF2α are further regulated by hydroxylation. Factor Inhibiting HIF (FIH) hydroxylates an asparagine located in the C-TAD, which will avoid HIF interaction with CBP and p300 coactivators required for the transactivation of the target genes [57, 58].

But under hypoxia, PHDs and FIH are not active due to the absence of oxygen, an essential cofactor, therefore HIFα subunits are not hydroxylated. Stabilized HIFα subunits translocate to the nucleus and dimerize with HIF1β. This heterodimer will bind to specific DNA domains called ‘hypoxia response elements’ (HRE) of target genes and will activate their expression (Figure 1.4).

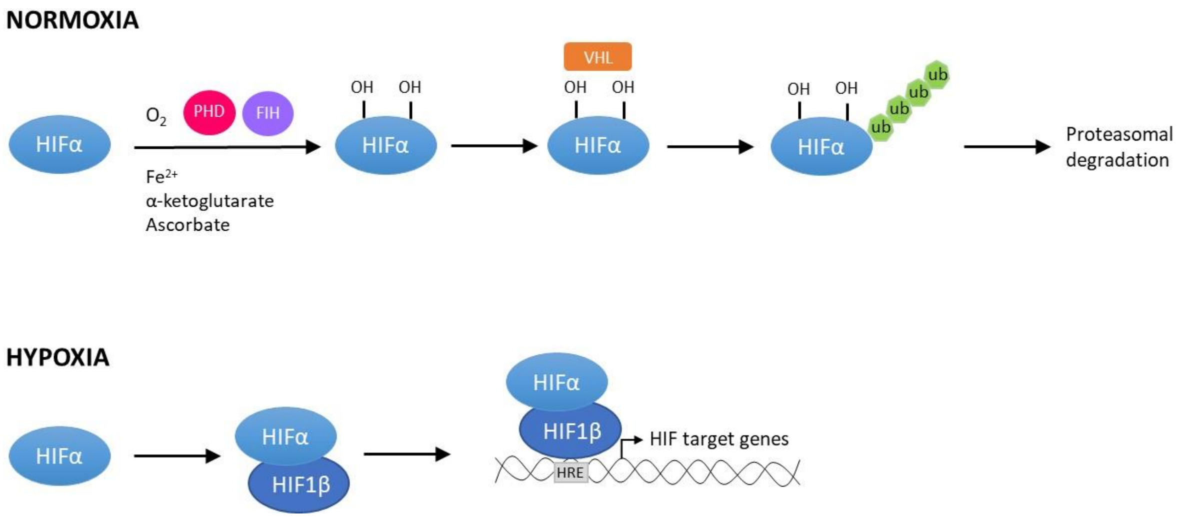

Figure 1.4. Diagram showing the main regulation mechanisms of HIF transcription factors in normoxia and hypoxia.

Some reports have shown that mitochondria also participate in HIF regulation by inhibiting components of the electron transport chain (ETC). For example, it has been demonstrated that in 1.5% hypoxia, mitochondria induce the generation of reactive oxygen species (ROS) (mainly from complex III), which could inhibit PHD's activity and therefore promote HIFα proteins stabilization [59]. It was also observed in another study that hypoxia-induced ROS were located in the intermembrane space of the mitochondria as well as in the cytosol, where they were able to bind to PHD and inhibit their activity [60].

Oxygen-independent mechanisms can also participate in HIF stabilization. PHDs for instance, require iron, α-ketoglutarate and ascorbate in addition to oxygen to hydroxylate HIFα subunits [61]. Therefore, there are some metabolites that can promote HIFα degradation, whereas others, such as fumarate and succinate, can inhibit PHDs by competing with them for iron and ascorbate, and thereby avoid HIFα degradation [62]. It has also been reported that growth factor signalling can stabilize and increase the rate of HIF translation via the activation of mammalian target of rapamycin (mTOR) [63] and that accumulation of lactate and pyruvate results in HIF stabilization [64], further promoting Warburg effect independent of oxygen levels. Other proteins with E3 ubiquitin ligase activity including receptor of activated protein kinase C (RACK1), carboxyl terminus of Hsp70-interacting protein (CHIP) and hypoxia-associated factor (HAF) can ubiquitinate HIFα subunits and target them for proteasomal degradation independently of the oxygen tension [65, 66].

Phosphorylation and acetylation of HIF1α and HIF2α can both have a positive or negative effect. It has been reported that phosphorylation of either subunit enhances the transactivation of target genes by disrupting the interaction with VHL or increasing their affinity for transcriptional coactivators [67], but other studies have shown that phosphorylation can lead to a decrease in HIF stability by inhibiting its binding to HIF1β [68]. Similarly, depending on the location of the acetylated residue, it can have either activating or inhibitory effect on the protein [69].

1.2.3. The HIF transcriptional program

After associating with HIF1β, the HIFα/β heterodimer binds to the core consensus sequence 5’-(A/G)CGTG-3’ within the HRE. Genome-wide analysis of HIF chromatin occupancy have demonstrated that despite the numerous HRE consensus sequences across the genome, under hypoxic conditions less than 1% of sequences are bound by HIFs [70-72], suggesting that other factors determine HIF binding. Moreover, functional HRE can localize both proximal to the promoter of target genes or far from them [39].

Sequence analysis have shown that regions surrounding functional HREs contain motifs characteristic of other transcription factors such as FOS, CREB, CEBPB, NFY, MIF and E2F, suggesting that there could be an interplay between transcription factors which could in turn determine the HIF transcriptional response [70, 73]. It has also been reported that STAT3 helps HIF1α to recruit RNA polymerase II to target genes [74], whereas HIF2α acts with USF, SP1 and ELK DNA-binding proteins in the same enhancer [40, 62]. Therefore, contribution of other factors seems to influence HIF transcriptional response.

Transcription factors can promote the expression of target genes by 1) recruiting general transcription factors and RNA polymerase II to form the pre-initiation complex, 2) remodelling nucleosomes, modifying histones or rearranging the chromatin and 3) modulating RNA polymerase activity at later phases. In all these processes different transcription coactivators and corepressors are involved. The most well studied coactivators in the HIF-mediated response are CBP and p300, which are recruited to the HRE of target genes. They modify the chromatin environment and by interacting with the core transcription machinery facilitate HIF transcriptional activity [75, 76]. The interaction between CBP/p300 and HIF1α/HIF2α happens via HIFα C-TAD domain and it is regulated by hydroxylation [77, 78]. In addition to these coactivators, there are others with the same lysine acetyl-transferase activity which interact with HIF in the transactivation of target genes such as members of the p160 family [77].

Several other factors can promote HIF activity, such as the M2 isoform of pyruvate kinase (PKM2), which catalyses the conversion of phosphoenolpyruvate and ADP to pyruvate and ATP in the last step of glycolysis. It has been shown to act as a coactivator via enhancing HIF binding and p300 recruitment to HREs [79]. Moreover, PKM2 itself is a HIF target gene and it helps HIF in the transactivation of genes involved in the shift from oxidative phosphorylation to glycolysis [79]. On the other hand, cyclin-dependent kinase 8 (CDK8), a component of the Mediator complex, also interacts with HIF1α in the activation of target genes [80], as well as the switch/sucrose non-fermentable (SWI/SNF) nucleosome remodelling complex, which was discovered to target *HIF1α* gene, suggesting that it also enhances HIF1α activity via regulation of HIF1α levels [81]. Interestingly, it has been reported that HIF1β is not just the heterodimerization partner of the α subunit, but it can directly contribute to HIF transactivation by recruiting coactivator proteins through its PAS-B domain [82, 83].

Among the corepressors blocking HIF transactivation of genes, CITED2 (a member of the CBP/p300-interacting transactivator with Glu/Asp (ED)-rich (CITED) family) inhibits HIF1α activity by impeding the interaction with CBP/p300 [84, 85]. Moreover, CITED2 is a HIF target, thus it could be providing a negative feedback in HIF-mediated transcription. Sirtuin 6 (SIRT6) is thought to repress HIF1α via deacetylating histone H3K9 and it seems to prevent HIF-mediated activation of glycolytic genes under normal glucose and oxygen levels, as it has been described to associate with HIF1α in the promoter of glycolytic genes [86]. Similarly, Sirtuin 1 (SIRT1) represses HIF1α transcriptional activity by deacetylation [87], in contrast to HIF2α, whose interaction with SIRT1 enhances its activity [88].

Despite the fact that HIF1α and HIF2α can bind to the same consensus sequence, it is known that some of their target genes differ. The selectivity of HIF1α versus HIF2α depends on the cell type, the oxygen deficiency severity and duration, and the abundance of HIFα proteins [39]. Cell type differences are mostly attributed to chromatin status, RNA polymerase activity and the availability of co-operating transcription factors [73, 80, 89], in addition to HIF2α limited expression to certain tissues. Besides, there seems to be a temporal regulation of HIF1α and HIF2α responses. It was published that under acute hypoxia (<24h) HIF1α was the main driver of the hypoxic response, whereas after longer periods, HIF2α transactivated the expression of target genes [90, 91].

1.2.4. HIFs role in cancer cell survival in hypoxia

HIF activation in hypoxic cells promotes tumour progression, as they activate genes involved in proliferation, angiogenesis, apoptosis, metabolism, DNA damage response, ECM remodelling, cell migration and invasion, which are keys for cancer cell survival.

1) HIFs and proliferation

There are some tumours, e.g. non-small cell lung cancer, head and neck squamous cell carcinoma and neuroblastoma where HIF1α expression is associated with lower cancer stage, whereas HIF2α expression is a negative prognostic factor [34]. This suggests that HIFα subunits contribute differently to tumour progression in certain cancers. In renal carcinoma, it is known that HIF2α is the driver of the disease, rather than HIF1α, possibly due to its interaction with c-MYC oncogene [92]. Moreover, HIF1α stabilizes the tumour suppressor p53, in contrast to HIF2α, which suppresses p53 activity and enhances tumour progression [93].

2) HIFs and angiogenesis

Angiogenesis is an adaptive response to hypoxia that cancer cells exert to support tumour growth. HIFs are master regulators in this vascularization process as they modulate the expression of many genes involved, such as VEGFA, stromal-derived factor 1 (SDF1), angiopoietin 2, placental growth factor (PGF), PDGF or KIT ligand (KITL) [94]. Upon binding to their receptors in the surface of endothelial cells, pericytes and vascular smooth muscle cells, these ligands promote new vessel formation from existing vessels, enhancing oxygen delivery to the tumour [94]. Besides, hypoxic cancer cells can induce bone-marrow-derived angiogenic cells' (BMDAC) movement to circulation and later recruitment within the tumour in a HIF-dependent manner. BMDAC consist of a population of endothelial progenitor cells, mesenchymal stem cells and myeloid cells, which when reaching the tumour will exert pro-angiogenic effects [95, 96]. Nevertheless, although physiological angiogenesis forms functional blood vessels, tumour angiogenesis generates structurally and functionally defective vessels, due to the excessive amount of pro-angiogenic factors and the lack of balance with the anti-angiogenic ones [97].

3) HIFs and metabolism

Tumour cells shift their metabolism from mitochondrial oxidative phosphorylation to glycolysis, a process mediated by both HIFα subunits. HIF1α promotes glucose redirection towards glycolysis by enhancing the expression of glycolytic enzymes and glucose transporters [98]. Under hypoxia, mitochondria releases ROS due to an inefficient ETC. In addition to generate an oxidative stress in the cell, ROS release also induces HIF1α stabilization [99]. Therefore, HIF1α-mediated shift to glycolysis and the consequent decrease in mitochondrial respiration in hypoxia allows reducing the amount of ROS and oxidative stress. This shows a mechanism by which via a stimulus-response loop cells are able to maintain the redox homeostasis.

HIFs further regulate mitochondrial metabolism by inducing mitophagy [99], decreasing fatty acid β-oxidation and promoting fatty acid uptake [100], as well as inducing reductive carboxylation of glutamine [101] and serine or one-carbon metabolism [102]. HIF1α promotes on the other hand, storage of glucose as glycogen [103].

4) HIFs and metastasis

HIFs regulate every step of metastasis: cell acquisition of motile and invasive phenotype (EMT), basement membrane and ECM disruption, inhibition of anoikis (a type of programmed cell death induced after cell detachment from the ECM), extravasation, establishment of premetastatic niches and transition back to an epithelial phenotype (MET) for clonal expansion [104-106].

HIF1α down-regulates the expression of the main component of adherent junctions, E-cadherin, in the first step of the process, while it up-regulates the expression of transcription factors (e.g. SNAIL1, SNAIL2, ZEB1, ZEB2, TWIST and TCF3) that repress the expression of epithelial genes and activate the expression of mesenchymal genes, in order to lose cell-cell adhesion and cell polarity and acquire a motile phenotype [107, 108].

Moreover, HIFs promote the expression of matrix metalloproteinases (MMPs) and the urokinase-type plasminogen activator receptor (PLAUR) involved in matrix remodelling [107]. HIFs can also help in cell migration through the ECM via stimulating collagen crosslinking, which will stiffen the ECM.

Then, cells need to enter into circulation. In this regard, HIF-induced VEGFA facilitates blood vessel permeability [109], while lymphatic endothelial cells can attract cancer cells [110]. PDGF expressed by cancer cells in a HIF-dependent manner can bind to its receptor (PDGFR) expressed by both endothelial and lymphatic endothelial cells [106], therefore facilitating tumour cell intravasation. Once in circulation, tumour cells avoid anoikis death by HIF1α-mediated suppression of integrin αV signalling [111]. And when arrive to the metastatic site, HIFs induce on the one hand, the expression of L1-cell adhesion molecule to promote cancer cell and endothelial cell interaction, and on the other hand the expression of angiopoietin-like 4 (ANGPTL4) to interrupt the interaction between endothelial cells to allow cancer cell extravasation [105].

Finally, cells restore their epithelial phenotype when they arrive to a well oxygenated tissue. There, the hypoxia-induced EMT is lost. It has also been reported that before arriving to the metastatic site, hypoxic tumour cells secrete some factors which will induce the mobilization of bone-marrow-derived cells to the metastatic site, so that they can modify the matrix and prepare it for tumour cell extravasation [112]. HIFs induce the secretion of many of the tumour-secreted factors involved in this establishment of the premetastatic niche [113, 114].

5) HIFs and immune system

It is well established that hypoxia generates an immunosuppressive environment in the tumour, as more detailed in 'Chapter 5'. Hypoxic cells can evade innate immune system by expressing specific molecules in a HIF-dependent manner, such as the 'don't eat me signal' CD47 molecule [115], or the immune checkpoint molecules PD-L1 and CTLA-4 [116, 117], which will bind to macrophages and effector T cells and block their activity. Hypoxic cells can also avoid adaptive immune system destruction via recruitment of MDSC and Treg cells [29, 30]. On the other hand, CD39 and CD73, both HIF target genes, produce extracellular adenosine, which suppresses T cell-mediated antitumour immunity [118]. It has also been reported that the VEGFA generated by hypoxic tumour cells can inhibit dendritic cells' (DC) function and stimulate them to express PD-L1 to further block T cell activity [119]. On the other hand, HIF1α-mediated metabolic shift to glycolysis contributes to immune evasion, as glucose-deprived T cells, due to the high glucose uptake by cancer cells, have lower antitumour effector functions [120, 121].

Additionally, apoptotic cells residing in hypoxic tumour regions produce molecules such as TGFβ, to recruit monocytes and macrophages and enhance their tumour promoting activity [122].

1.3. Models to study hypoxia

In solid tumours, hypoxic regions are often generated as the tumour grows and the disease progresses, but in contrast to most normal cells which cannot survive under these conditions, tumour cells adapt to hypoxia by HIF-driven mechanisms. The main factor regulating HIF activity is the tumour suppressor VHL [41, 45]. Under normoxic conditions VHL targets HIF for proteasomal degradation and avoids an unnecessary hypoxic response, but when oxygen levels are low, VHL cannot act and HIFs can activate their transcriptional program for cell-survival. Similarly, tumours in which *VHL* gene is mutated, such as renal carcinoma, hemangioblastomas, paragangliomas and pheochromocytomas exhibit a hypoxia-like gene signature due to the lack of HIF degradation [123]. Renal cancer is of particular interest in this context because of the constitutive expression of HIF1α and HIF2α due to *VHL* inactivation, which have opposing roles in the progression of the disease [124]. While HIF1α presents a tumour suppressive activity, HIF2α acts as an oncogene and leads tumour development (further reviewed in 'Chapter 3') [125, 126]. It is therefore important to study HIF2α in every step of renal tumour development, from disease initiation to later metastasis.

Hypoxia can further promote cancer development by generating an immunosuppressive environment within the tumour mass, which will allow tumour cells to escape the immune system recognition. This is achieved on the one hand, via recruiting immunosuppressive cells, and on the other hand, via up-regulating molecules which will block immune cell activation (further reviewed in 'Chapter 5') [25]. In this regard, the type I interferon (IFN) pathway regulation and activity under hypoxia has not been studied yet. It is known that an active type I IFN pathway is required for the success of many anticancer therapies, such as radiotherapy, chemotherapy and immunotherapy [127]. Immunotherapeutic drugs, such as recombinant IFNα, have long been used to treat highly immunogenic tumours (e.g. melanoma [128] and lung cancer [129]) as well as renal cancer [130]. Those drugs are now being replaced by immune checkpoint inhibitors, showing promising results [131, 132]. It has been reported that IFNs are potent cytokines to induce PD-L1 expression in tumour cells [133, 134], providing this way increased number of molecules for anti-PD-L1 therapy. Even though the correlation between the expression of PD-L1 in tumour cells and response rate is not clearly stablished, it is clear that IFNs participate in the response. Moreover, successful immunotherapy requires a potent type I IFN pathway, in order to promote the maturation, survival and activity of the immune cells [135].

Hypoxia can also confer resistance to antitumour therapies, as it has been described to induce the expression of membrane proteins that increase drug efflux, as well as inhibit the apoptosis of treated cells by inducing anti-apoptotic gene expression [136]. Therefore, as both cancer cells and immune cells express type I IFNs, and hypoxia is a major characteristic of solid tumours, type I IFN pathway study under hypoxia is required to explore the involvement of this pathway in tumour progression.

Therefore, this thesis proposes to study the role of HIF2α in every step of renal cancer progression as well as its role in the resistance to drugs. In addition, the regulation of the type I IFN pathway in hypoxia will also be investigated in order to describe the implication of this signalling pathway in the immunosuppressive environment generated by hypoxia, using both *VHL* mutated (renal cancer) and non-mutated (breast cancer) cell lines representing common cancer models. The specific objectives to achieve these main aims are detailed in 'Chapter 3', 'Chapter 4' and 'Chapter 5', respectively.

1.4. Hypothesis and objectives

This thesis is based on the fact that hypoxia, or HIF transcription factors, promote tumour progression by affecting different pathways or features of solid tumours, and hypothesise that targeting hypoxia will provide novel therapeutic strategies to repress tumour growth. The general objectives of this thesis are:

1. To investigate the oncogenic role of HIF2α in renal carcinoma.
2. To elucidate if HIF2α is conferring resistance to drugs.
3. To analyse hypoxic regulation of the type I IFN pathway.

2. General materials and methods

2.1. Cell treatments

2.1.1. Hypoxia exposure

Once cells were seeded at the desired density and had attached to the surface of the plate, they were subjected to either 1% or 0.1% hypoxia for the periods specified in each experiment using an InVivO$_2$ hypoxia station (Baker).

2.2. Western Blot

2.2.1. Protein extraction and quantification

Protein extraction was carried out on ice. First, cells were washed with cold PBS, and lysed with 1x RIPA lysis buffer (R0278, Sigma-Aldrich) supplemented with cOmplete™ Protease Inhibitor Cocktail (11697498001, Roche) and Pierce™ Phosphatase Inhibitor Mini Tablets (A32957, Thermo Fisher Scientific™). Cells lysates were vortexed several times while incubated for 30 minutes (min) on ice. Samples were centrifuged at maximum speed (21000g) for 15 min at 4ºC and supernatants were collected and stored at -20ºC. To quantify the total amount of protein of the lysates, DC™ Protein Assay (5000112, Bio-Rad) was used. The reaction taking place is similar to the well-documented Lowry assay. First, a bovine serum albumin (BSA, A3059, Sigma-Aldrich) standard curve was prepared from a 2mg/mL BSA stock solution and a mix of Reagent A and Reagent S was prepared by mixing 1mL Reagent A with 20µL Reagent S. Then, 2.5µL BSA standard or protein lysate was placed in duplicate in a 96-well flat bottom plate. 25µL mix Reagent A+S was added to each well, following the addition of 200µL Reagent B per well. The plate was incubated for 15 min in a shaker at room temperature (RT). After this time, protein concentration was measured at 750nm in a µQuant™ Spectrophotometer (BioTek® Instruments) using the KC4 software.

2.2.2. SDS-PAGE and Membrane Transference

For protein electrophoresis 5-30µg of total protein were loaded into NuPAGE™ 4-12% Bis-Tris gels (NP0336BOX, Invitrogen™) or NuPAGE™ 12% Bis-Tris gels (NP0341BOX, Invitrogen™). NuPAGE™ LDS Sample buffer 4x (NP0007, Invitrogen™) containing 10% β-mercaptoethanol (M6250, Sigma-Aldrich) was added to the samples to a final concentration of 1x, following an incubation step of 5 min at 95ºC to promote the denaturalization of the proteins. Along with samples, Amersham™ ECL™ Rainbow™ Marker - Full range (GERPN800E, GE Healthcare, Sigma-Aldrich) was used to determine the molecular weight. Electrophoresis was carried out under constant voltage (130V) for 2h in 1x NuPAGE™ MOPS SDS Running Buffer (NP000102, Invitrogen™). After SDS-PAGE, proteins were transferred from gels into 0.45µm pore Immobilon-P PVDF Membrane (IPVH00010, Merck) using a semi-dry Invitrogen™ transfer system. In case low molecular proteins were analysed, 1x NuPAGE™ MES SDS Running Buffer (NP000202, Invitrogen™) was used for electrophoresis and proteins were transferred into a 0.2µm pore Immobilon-PSQ PVDF Membrane (ISEQ00010, Merck). Transference was carried out at 0.13A per gel during 90 min in a transfer solution consisting of 10% methanol (322425, Sigma-Aldrich) in 2x NuPAGE™ Transfer Buffer (NP0006, Invitrogen™).

2.2.3. Antibody staining and development

After completion of the transfer, membranes were blocked with 5% non-fat dried milk powder (A0830, PanReac AppliChem) diluted in TBS containing 0.1% Tween-20 (TBS-T, P9416, Sigma-Aldrich) for at least 1h at RT with gentle shaking. Membranes were incubated in the same solution overnight at 4ºC with specific primary antibodies (Table 2.1). Three washes of 10 min with TBS-T were performed before an incubation step of 1h at RT with the correspondent polyclonal horseradish-peroxidase-labelled secondary antibody (Table 2.1) diluted 1:2000 in TBS-T containing 5% non-fat dried milk powder. Membranes were washed three times for 10 min with TBS-T and developed using an ECL™ Prime Western Blotting Detection Reagent (RPN2236, GE Healthcare, Sigma-Aldrich) in an ImageQuant LAS 4000 Mini device (GE Healthcare, Life Sciences). Stripping with Restore™ PLUS Western Blot Stripping Buffer (46430, Thermo Fisher Scientific) was performed for 15 min at RT followed by three TBS-T washes to blot different antibodies in the same membrane.

Table 2.1. Western blot antibodies.

Antibody	Dilution	Reference	Commercial house
HIF1α	1:1000	610958	BD Bioscience
HIF2α	1:500	NB100-122	Novus Biologicals
GLUT1	1:1000	ab652	Abcam
ZO-1	1:1000	9782	Cell Signalling Technology
E-Cadherin	1:1000	9782	Cell Signalling Technology
TCF8/ZEB1	1:1000	9782	Cell Signalling Technology
N-Cadherin	1:1000	9782	Cell Signalling Technology
β-Catenin	1:1000	9782	Cell Signalling Technology
Vimentin	1:1000	9782	Cell Signalling Technology
Snail1	1:1000	9782	Cell Signalling Technology
Slug (Snail2)	1:1000	9782	Cell Signalling Technology
Claudin-1	1:1000	9782	Cell Signalling Technology
PDK1	1:1000	sc-7140	Santa Cruz Biotechnology
LDHA	1:1000	2012	Cell Signalling Technology
STAT1	1:1000	9172	Cell Signalling Technology
pSTAT1-Ser727	1:1000	9177	Cell Signalling Technology
pSTAT1-Tyr701	1:1000	9167	Cell Signalling Technology
IRF3	1:1000	ab76409	Abcam

pIRF3-Ser386	1:1000	ab76493	Abcam
PNPT1	1:1000	ab157109	Abcam
SUV3	1:1000	A303-055A	Bethyl Laboratories
IRF7	1:1000	ab109255	Abcam
IRF9	1:1000	76684	Cell Signalling Technology
ADAR1	1:2000	14175	Cell Signalling Technology
MDA5	1:1000		Built in house (*)
RIG-1	1:1000	LS-C331000	LS BioSciences
MAVS	1:1000	ALX-210-929-C100	Enzo
BNIP3	1:1000	10433	Abcam
c-MYC	1:500	S2931	BD Bioscience
Tubulin β 3 (TUBB3)	1:1000	MMS-435P	BioLegend®
β-Actin-Peroxidase	1:50000	A3854	Sigma-Aldrich
Goat anti-mouse IgG	1:2000	P0447	DAKO
Goat anti-rabbit IgG	1:2000	P0448	DAKO
Rabbit anti-goat IgG	1:2000	P0449	DAKO

*Kindly donated by Dr Jan Rehwinkel

2.3. Total RNA extraction

Cells grown in 6-well plates were lysed directly using Tri Reagent® (T9424, Sigma-Aldrich). Briefly, 500µL of Tri Reagent® was added to the plates and incubated 10 min at RT. Cell lysates were collected into 1.5mL tubes and 100µL of chloroform (C/4960/17, Fisher Chemical) was added. Samples were vortexed for 20 seconds (sec) and left on the bench for 15 min. Samples were centrifuged at maximum speed for 15 min at 4ºC. Aqueous phase was transferred to a new 1.5mL tube and 250µL isopropanol (P/7555/17, Fisher Chemical) was added and mixed by inversion. After 10 min, samples were centrifuged at maximum speed for 10 min at 4ºC. The resulting RNA pellets were washed with 75% ethanol (51976, Sigma-Aldrich) in an additional centrifugation step. After ethanol removal, RNA pellets were left to dry for 10 min at RT. Finally, pellets were resuspended in DEPC-Treated Water (AM9906, Invitrogen™) and placed on ice. RNA quantification was carried out with NanoDrop® ND-1000 spectrophotometer (Thermo Fisher Scientific™). RNA was stored at -80ºC.

2.4. Reverse transcription

Complementary DNA (cDNA) was synthesized from 1µg of total RNA using High-Capacity cDNA Reverse Transcription Kit (4368814, Applied Biosystems™). The reverse transcription master mix was composed of 2µL 10x Reverse Transcription Buffer, 0.8µL 100mM dNTP mix, 2µL 10x Random primers and 1µL (50U) MultiScribe™ Reverse Transcriptase per sample. The reverse transcription reaction was carried out following the manufacturer’s instructions: 10 min at 25ºC, 120 min at 37ºC and 5 min at 85ºC in a Labcycler (SensoQuest). The cDNA was kept at -20ºC until use.

Table 2.2. qPCR primers.

Primer	Sequence (5’-3’)	Primer	Sequence (5’-3’)
HPRT1_F	TGACACTGGCAAAACAATGCA	12S_F	ATATACCGCCATCTTCAGCA
HPRT1_R	GGTCCTTTTCACCAGCAAGCT	12S_R	CTAAATCCACCTTCGACCCT
HIF2α_F	CAACAGAGGCCGTACTGTCA	ND3_F	GGCTTCGACCCTATATCCCC
HIF2α_R	CACATGATGATGAGGCAGGA	ND3_R	TAGGGCTCATGGTAGGGGTA
CA9_F	CCTTTGCCAGAGTTGACGAG	TFB1M_F	TGCTTGCCGCGTATCATG
CA9_R	GCAACTGCTCATAGGCACTG	TFB1M_R	CGGAGGGAGACGGCAAGT
GLUT1_F	GGTTGTGCCATACTCATGACC	MRPL1_F	TTTACAGAGAATGCATCAGAGG
GLUT1_R	CAGATAGGACATCCAGGGTAGC	MRPL1_R	AGGCATTATTTCTGGAACAGC
FN1_F	AGCGGACCTACCTAGGCAAT	MRPL11_F	GAGGCGTTTCCATCAACCAG
FN1_R	GGTTTGCGATGGTACAGCTT	MRPL11_R	CACCTCTTTCCCTGTTTGCC
VEGFA_F	CCTCCGAAACCATGAACTTT	MRPL13_F	TACTAGGAGAAGGACGTACGG
VEGFA_R	ATGATTCTGCCCTCCTCCTT	MRPL13_R	CACAGTCACTCAGTGCATGG
PAI-1_F	TGCTGGTGAATGCCCTCTACT	MRPL21_F	GGAAATGAACTAGACCTTGCGT
PAI-1_R	CGGTCATTCCCAGGTTCTCTA	MRPL21_R	AAGATCCTTTCCGAGGAGTG
EPO_F	TCCCAGACACCAAAGTTAATTTCTA	MRPS23_F	GCTCCCATCCAAGACATCTG
EPO_R	CCCTGCCAGACTTCTACGG	MRPS23_R	TACTTCTCCACAAACCGTTGAC
MYC_F	ACGTCTCCACACATCAGCAC	MRPS34_F	GTGGACTACGAGACCTTGAC
MYC_R	CGCCTCTTGACATTCTCCTC	MRPS34_R	AAAGAGGCGTCTTTGAAGGTC
PLIN2_F	GATGGCAGAGAACGGTGTGAAG	DDX58_F	CAAGCCTTCCAGGATTATATCCG
PLIN2_R	CAGGCATAGGTATTGGCAACTGC	DDX58_R	AGTCCAGAATAACCTGCATGGT
HIG2_F	TGATGGAGTCCCTAGAGGGCTT	IFIH1_F	TTAACAGGCTCTGATTGCTC
HIG2_R	GCCAGTATGGAAGGAGGTCTTAT	IFIH1_R	TCTCTTCATCTGAATCACTTCCC
CD36_F	GTGCCTATTCTTTGGCTTAATGA	MAVS_F	GTACCCGAGTCTCGTTTCCT
CD36_R	TTACTTGACTTCTGAACATGTTTGC	MAVS_R	ATGAAGTACTCCACCCAGCC
CPT1A_F	GTGAACAGGTATCTACAGTCGG	IRF3_F	CTCGTGATGGTCAAGGTTGTG
CPT1A_R	GGTAGATGTACTCCTCCCAC	IRF3_R	AGTTTATTGGTTGAGGTGGTGG
PDK1_F	TTGGTACAAAGCTGGTATATCC	IRF7_F	AAGGGCTTCCCCTGACTG
PDK1_R	CTTGTATTCAATCACACCCTGG	IRF7_R	TCTACTGCCCACCCGTACA
PDHA1_F	TGGAGTCAGTTACCGTACAC	STAT1_F	TACACCTACGAACATGACCCT
PDHA1_R	CATCCTCAATCTCCTTCCTCAC	STAT1_R	TCACCAACAGTCTCAACTTCAC
LDHA_F	GAATGAATGTTGCTGGTGTCTC	STAT2_F	CCCGCTGACTGAAATCATCC
LDHA_R	CCGTAAAGACCCTTAATCATGG	STAT2_R	AGTTCATCCACCTGTCTATTAGAG
BNIP3_F	AAACAGCTCACAGTCTGAGGA	ISG15_F	GCGAACTCATCTTTGCCAGTA
BNIP3_R	GACGCCTTCCAATATAGATCCC	ISG15_R	CCAGCATCTTCACCGTCAG
Slug_F	TGGTTGCTTCAAGGACACAT	ADARp150_F	CTTCCAGTGCGGAGTAGCG
Slug_R	GCAAATGCTCTGTTGCAGTG	ADARp150_R	GTGACGGTGTCTGCTTTCCA
SHMT2_F	CAAGACTGGCCGGGAGATC	MX1_F	GTTACCAGGACTACGAGATTGAG
SHMT2_R	GGGAACACGGCAAAGTTGAT	MX1_R	GATGAGTGTCTTGATCTTATACCC
ATP6_F	GGACTCCTGCCTCACTCATT	IFIT1_F	TACCTGGACAAGGTGGAGAA
ATP6_R	AAGTGGGCTAGGGCATTTTT	IFIT1_R	GTGAGGACATGTTGGCTAGA
TFAM_F	GCTAAGGGTGATTCACCGCA	IFIT2_F	TGTGCAACCTACTGGCCTAT
TFAM_R	ATCCTTTCGTCCAACTTCAATC	IFIT2_R	TTGCCAGTCCAGAGGTGAAT
POLRMT_F	AGGTCAAGCAAATAGGAGGTG	IFNAR1_F	ATTTCGCAAAGCTCAGATTGGT
POLRMT_R	CAGCGAGTGGATGAAGTTGG	IFNAR1_R	CATCCAAAGCCCACATAACAC
CYTB_F	CGCATGATGAAACTTCGGCT	IFNAR2_F	GCCAGGCCTCAGAATCAGCA
CYTB_R	ATTTGGAGGATCAGGCAGGC	IFNAR2_R	TGTAAATGACCTCCACCATATCCA

2.5. Quantitative polymerase chain reaction (qPCR)

qPCR reaction was carried out in a QuantStudio™ 5 Real-Time PCR System (Applied Biosystems™) with standard cycling conditions: 10 min at 95ºC and 40 cycles of 15 sec at 95ºC followed by 1 min at 60ºC. Briefly, 10ng cDNA was mixed with 5µL SensiMix™ Sybr Green® No-ROX (QT650-05, Bioline), 0.8µL primer mix (Forward+Reverse mix, 5µM each) and DEPC-Treated Water in a final volume of 10µL per reaction. Primers were designed using PerlPrimer v1.1.21 software to span exon-exon junctions, to have a GC content close to 50%, with a melting temperature around 60ºC, and to produce a product of 80-300 base pairs (bp) size. Maximum difference of melting temperatures between primer pairs was 3ºC. Gene expression was analysed with the Ct method using hypoxanthine phosphoribosyltransferase (*HPRT1*) expression for normalization. Primers used are listed in Table 2.2.

2.6. Statistical analysis

For statistical analysis, GraphPad Prism 5.0 statistical analysis software (GraphPad Software) was used. If not otherwise specified, all the experiments were performed in biological triplicates. When analysing the influence of two different independent variables (e.g. oxygen levels and genotype or genotype and time) on one dependent variable (e.g. gene expression), 2-way ANOVA was applied. The 2-way ANOVA test assesses the main effect of each variable but also if there is any interaction between them on the dependent variable. When two means were compared, t-test was performed if samples followed a normal distribution or Mann-Whitney if there was not a normal distribution. In the graphs, the error bars depict the standard error of the mean (SEM).

3. The role of HIF2α in renal carcinoma

3.1. Introduction

3.1.1. Renal cancer

Renal cell carcinoma (RCC) is the sixth most frequently diagnosed cancer in men and the tenth in women, representing 5% and 3% of all the oncological diagnoses, respectively [137]. In 2018 there were 403,262 new cases diagnosed and 175,098 deaths from kidney cancer worldwide [138]. After Asia, Europe was the continent with the second highest incidence and mortality from RCC, whereas in Spain, kidney tumours accounted for only 3% of the new cases [138]. Worldwide, the incidence rate of RCC has increased about 20% in the last ten years due to better incidental detection by abdominal imaging (e.g. ultrasonography, computed tomography (CT) and magnetic resonance imaging (MRI)) carried out for non-related musculoskeletal or gastrointestinal complaints [139]. Indeed, nearly half of all RCC diagnoses are made in this manner.

If the tumour is detected early enough, while still localized in the kidney, surgical resection or nephrectomy can be performed, and the 5-year survival rate is nearly 92% [140]. However, if diagnosis is made after the tumour has spread locally but non-systemically, the 5-year survival rate decreases to 70%, whereas if distant metastasis are present (17% of patients harbour distant metastasis at the time of diagnosis [141]), the 5-year survival rate drops to just 12% [140].

3.1.2. RCC classification

RCC is a heterogenous collection of neoplasms that affect the kidney, with at least 20 different subtypes recognised by the World Health Organisation (WHO) [142]. The International Society of Urological Pathology (ISUP) proposed an updated classification for RCC tumours in a conference in Vancouver in 2012 based on chromosomal alterations, histological subtypes and molecular pathway abnormalities (Table 3.1) [143].

Table 3.1. Vancouver RCC classification.

Vancouver RCC classification
Papillary adenoma
Characterized by papillary/tubular structures
Oncocytoma
Made up of oncocytes, epithelial cells with excessive number of mitochondria
Clear cell renal cell carcinoma
Formed by malignant epithelial cells with clear cytoplasm. Highly vascular
Multilocular clear cell renal cell neoplasm of low malignant potential
Papillary renal cell carcinoma
Originates in the renal tubular epithelium
Chromophobe renal cell carcinoma
Hybrid oncocytic chromophobe tumour
Carcinoma of the collecting ducts of Bellini
Originates in the papillary duct of the kidney
Renal medullary carcinoma
MiT family translocation renal cell carcinoma
Xp11 translocation renal cell carcinoma
t(6;11) renal cell carcinoma
Carcinoma associated with neuroblastoma
Mucinous tubular and spindle cell carcinoma
Characterized by a mixture of cuboidal and spindle cells and mucinous stroma
Tubulocystic renal cell carcinoma
Composed predominately of tubules and cysts lined by a single layer of cells
Acquired cystic disease-associated renal cell carcinoma
Clear cell (tubulo) papillary renal cell carcinoma
Hereditary leiomyomatosis-associated renal cell carcinoma
Renal cell carcinoma, unclassified

The most common subtypes of renal tumours are clear cell RCC (ccRCC, 70-85% of cases), papillary RCC (7-15%), chromophobe RCC (5-10%) and tumours of the medullary and collecting system (5%) [139]. Histological and genetic classification can help in treatment decisions. For example, papillary carcinomas, that lack the VHL-HIF-VEGF pathway, do not respond to anti-angiogenic therapy [144]. As well as subtype, the staging system is a major factor in deciding on the treatment to give a RCC patient.

The most prevalent system used for RCC staging is the TNM staging system, as defined by the American Joint Committee on Cancer (Table 3.2) [145]. This system takes into account the size of the primary tumour (T), regional lymph node involvement (N) and the presence or not of distant metastasis (M).

Table 3.2. TNM staging of the American Joint Committee on Cancer.

TNM	Description
TX	Primary tumour cannot be assessed
T0	No evidence of primary tumour
T1	Tumour ≤7 cm in greatest dimension, limited to the kidney
T1a	Tumour ≤4 cm in greatest dimension, limited to the kidney
T1b	Tumour >4 cm but ≤7 cm in greatest dimension, limited to the kidney
T2	Tumour >7 cm in greatest dimension, limited to the kidney
T2a	Tumour >7 cm but ≤10 cm in greatest dimension, limited to the kidney
T2b	Tumour >10 cm, limited to the kidney
T3	Tumour extends into major veins or perinephric tissues but not into the ipsilateral adrenal gland and not beyond the Gerota fascia
T3a	Tumour grossly extends into the renal vein or its segmental (muscle-containing) branches or tumour invades perirenal and/or renal sinus fat but not beyond the Gerota fascia
T3b	Tumour grossly extends into the vena cava below the diaphragm
T3c	Tumour grossly extends into the vena cava above the diaphragm or invades the wall of the vena cava
T4	Tumour invades beyond the Gerota fascia (including contiguous extension into the ipsilateral adrenal gland)
NX	Regional lymph nodes cannot be assessed
N0	No regional lymph node metastasis
N1	Metastasis in regional lymph node(s)
M0	No distant metastasis
M1	Distant metastasis

Briefly, the TNM scheme defines Stage I disease as when the tumour is confined to the kidney, within the renal capsule, and further subclassifies tumours on the basis of size, with T1a tumours being ≤4 cm in diameter and T1b tumours >4 cm but ≤7 cm in diameter. Stage II tumours are larger (>7 cm), but still confined to the kidney, whilst Stage III tumours include those that have extended beyond the renal capsule but are within Gerota's facia or have invaded the veins (Figure 3.1). When tumours have spread beyond Gerota's facia they are classified as Stage IV. Metastasis are divided into Stage N for regional lymph nodes and Stage M for distant metastasis. RCC usually metastasizes through both the venous or lymphatic systems, and the most common sites of distant metastasis are lungs (45%), bone (39%), lymph nodes (22%), liver (20%), adrenal glands (9%) and brain (8%) [146].

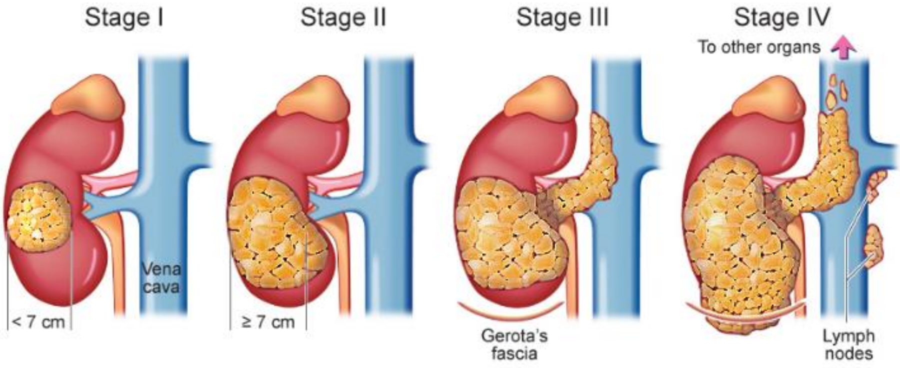

Figure 3.1. Picture showing the different stages of renal carcinoma [147].

As mentioned above, RCC are usually detected by imaging (ultrasonography) and later confirmed by CT scan or MRI, which allows determination of the degree of invasiveness of the tumour. In addition, tumour biopsies are carried out to provide histological confirmation of the disease and pathological classification of the subtype, which in turn dictates treatment options [148].

3.1.3. Clear cell renal cell carcinoma (ccRCC)

ccRCC accounts for 70-85% of diagnosed kidney cancers and it is considered the most aggressive subtype of the disease [139]. Patients with ccRCC tend to have a worse prognosis compared to patients with other histologic subtypes, as the 5-year disease-specific survival (DSS) for ccRCC patients is lower (50-69%) than papillary RCC (67-87%) and chromophobe RCC (78-87%) cases [149]. Originating from the epithelial cells of the proximal tubule of the nephron [150], ccRCC is characterized by being highly vascular and having tumour cells with robust lipid and glycogen accumulation in the cytoplasm [151].

3.1.3.1. Treatment options for ccRCC

1) **Surgery**

Localized RCC measuring up to 7 cm (Stage I) are normally managed surgically with partial or radical nephrectomy [139]. Ablative approaches (e.g. cryoablation or ablation by radiofrequency) are chosen for patients with small tumours (≤3 cm) with high surgical risk, such as compromised renal failure or multiple bilateral tumours, among others [139]. For patients harbouring tumours smaller than 4 cm, with significant comorbidities, or patients whose life expectancy is short, active surveillance is usually recommended [139]. Stage II tumours are generally managed with laparoscopic radical nephrectomy, whereas Stage III tumours are treated with radical nephrectomy. Treatment of Stage IV cancers depends on the cancer extension and the patient's health. Surgery is the first option for those patients whose primary tumour is removable and the cancer has only spread to one area, but these cases are rare. Sometimes, although extensive metastasis, if the primary tumour is removable, surgery might still be helpful. However, in the majority of cases, metastatic RCC are initially treated with systemic therapies such as chemotherapy, targeted drugs or immunotherapy [139].

Until the last decade, treatment options for metastatic RCC were limited to interleukin 2 (IL-2) and IFNα. But due to the low response rates and high toxicity [152-155], several alternative therapies have developed since then, such as anti-angiogenic therapies, immune checkpoint targeting therapies or a combination of both.

2) Anti-angiogenic therapy

Altered hypoxia signalling leads to increased angiogenesis in ccRCC, and consequently, many molecules involved in this pathway have been the subject of therapeutic advances in recent years [156, 157]. Anti-angiogenic therapies target either tyrosine kinase receptors or circulating VEGFA, and they have been the first-line treatments for ccRCC patients for many years (Table 3.3).

Tyrosine kinase inhibitors

Sunitinib is an oral multikinase inhibitor targeting tyrosine kinase receptors, including platelet-derived growth factor receptor (PDGFR), vascular endothelial growth factor receptor (VEGFR), stem cell factor receptor (c-KIT), FMS-like tyrosine kinase (FLT-3), colony-stimulator factor (CSF-1R) and neurotropic factor receptor (RET) [158]. It is the first-line therapy for ccRCC Stage IV or unresectable cases [159-161].

Pazopanib is another oral anti-angiogenic targeting VEGFR, PDGFR and c-KIT. Results from a phase III trial comparing sunitinib or pazopanib administration in locally advanced or metastatic RCC patients showed similar effects and toxicity with both drugs [162].

Cabozantinib is a small molecule inhibitor of the tyrosine kinase receptors VEGFR, MET and AXL [158]. It was approved by the Food and Drug Administration (FDA) for use as first-line agent, based on the results from a phase II clinical trial which showed that it was more effective than sunitinib [163].

Axitinib is a second-line tyrosine kinase inhibitor that targets VEGFR [158]. It was shown to provide patients who had been previously treated with sunitinib or cytokine therapy with longer progression-free survival (PFS), compared to sorafenib [164]. Sorafenib, another tyrosine kinase inhibitor, was one of the earliest to be approved, based on the better response generated over IFNα [152], but it is less specific to VEGFR compared to sunitinib, pazopanib or axitinib [165].

VEGFA targeting antibodies

Bevacizumab is a recombinant humanized monoclonal antibody which binds to circulating VEGFA, thus avoiding VEGFA binding to its receptor and the consequent pathway activation. It was shown to improve patients' PFS, without any changes in the overall survival (OS) [166, 167].

Despite of the suitability of anti-angiogenic drugs for ccRCC treatment, clinical trials indicate that as single therapy, they are only modestly effective (Table 3.3). Furthermore, several patients develop resistance to tyrosine kinase inhibitors [168].

Table 3.3. Summary of the clinical trials with anti-angiogenic drugs in ccRCC. Results correspond to the drug's group. '+' means longer/higher, '=' means no differences. PFS (progression-free survival), OS (overall survival), DFS (disease-free survival).

Drug	Clinical trial	Result	Reference
Sunitinib	Phase III (Sunitinib vs IFNα) Phase III (Sunitinib vs placebo)	+ PFS and OS + DFS, + toxicity	[159, 160] [161]
Pazopanib	Phase III (Pazopanib vs placebo) Phase III (Sunitinib vs pazopanib)	+ PFS, = OS = effects, = toxicity	[169] [162]
Cabozantinib	Phase II (Cabozantinib vs sunitinib)	+ PFS and OS	[163]
Axitinib	Phase III (Axitinib vs sorafenib) Phase III (Axitinib vs sorafenib)	+ PFS = PFS, = OS	[164] [170]
Bevacizumab (Bev)	Phase III (Bev+IFNα vs placebo+IFNα) Phase II (dose increment)	+ PFS and OS + PFS, = OS	[166] [167]

3) mTOR inhibitors

In parallel with VEGFR tyrosine kinase inhibitors, mTOR inhibitors are also approved for ccRCC treatment. mTOR is a protein kinase member of the phosphatidylinositol-3 kinase-related kinase family, a family of serine/threonine-protein kinases similar to phosphatidylinositol-3 kinases (PI3Ks) [171]. mTOR regulates cell proliferation, motility, metabolism, apoptosis and angiogenesis, among other processes [172]. Temsirolimus and everolimus, both mTOR inhibitors, are typically used as second-line treatment in the management of ccRCC (Table 3.4).

Temsirolimus was the first mTOR inhibitor approved by the FDA based on a phase III study [173], and it is nowadays the only mTOR inhibitor used as first-line monotherapy for advanced ccRCC patients with poor prognosis.

Everolimus is a treatment option for metastatic patients refractory to tyrosine kinase inhibitor therapy [174]. As it is orally administrated, in contrast to the intravenous infusion of temsirolimus, it is preferred in the second-line mTOR inhibitors therapy.

Table 3.4. Summary of mTOR inhibitors' clinical trials in ccRCC. Results correspond to the drug's group. '+' means longer/higher. PFS (progression-free survival), OS (overall survival).

Drug	Clinical trial	Result	Reference
Temsirolimus	Phase III (Temsirolimus vs IFNα and temsirolimus vs temsirolimus+IFNα)	+ PFS and OS	[173]
Everolimus	Phase III (Everolimus vs placebo)	+ PFS	[174]

4) Immunotherapy

Some tumours, such as melanoma or lung cancer, respond to immunotherapy due to the high tumour mutation burden (i.e. the number of mutations per coding area of the tumour genome) (TMB), which facilitates recognition by the immune system [130]. The observation that some patients with metastatic disease experienced spontaneous regression following surgical removal of the primary tumour suggested that the immune system was playing an important role in tumour eradication [175, 176]. However, as somatic mutation rates are typically low, the exact mechanism by which ccRCC responds to immunotherapy is still unknown [130]. Moreover, ccRCC has been shown to be a highly immune-infiltrated tumour [177, 178]. Treatments based on immune system stimulation (IL-2 and IFNα) have long been used to treat the disease, and in the last few years immune checkpoint inhibitors have shown very promising results as well [131, 132]. It is believed that immune checkpoint inhibitors success is due to the high pre-existing T cell infiltration within the tumour [179]. Since preclinical data showed that blockade of immune checkpoints could result in tumour eradication [180], several antibody-based therapies blocking different steps of the antitumour immune response have been developed.

Among the antibody therapies that act to interrupt the molecular mechanisms by which tumours escape immune recognition (i.e. checkpoint inhibitors), antibodies directed against CTLA-4, programmed cell death protein 1 (PD-1) and PD-L1 are the most well-studied (Table 3.5).

Ipilimumab is a monoclonal antibody against CTLA-4, which got FDA approval for the treatment of melanoma in 2011 [181]. A trial for advance ccRCC treatment revealed positive results but, in contrast to melanoma, no complete responses were achieved [182].

Nivolumab is an anti-PD-1 monoclonal antibody that impairs the PD-1/PD-L1 signalling pathway, avoiding immune response blockade against tumour cells [183]. Nivolumab is currently the only FDA-approved PD-1 inhibitor for the treatment of patients with metastatic ccRCC and has also been approved as second-line therapy for those advanced ccRCC cases in which anti-angiogenic therapy has failed. It was approved in 2015 based on a phase III study called CheckMate 025 [184].

Anti-PD-L1 antibodies such as BMS-936559 (also known as MDX 1105), durvalumab and atezolizumab have also been tested as immune checkpoint inhibitors in ccRCC. These antibodies block PD-L1/PD-1 signalling, but allow PD-L2/PD-1 interaction to persist, although PD-L2/PD-1 induced signalling seems not to be as strong as PD-L1/PD-1 signalling [185]. Atezolizumab effectiveness was studied in a phase I trial in metastatic ccRCC patients who had received previous treatment [186]. Durvalumab, on the other hand, has been studied as a monotherapy in patients with brain metastasis from epithelial-derived tumours (NCT02669914).

Table 3.5. Summary of the clinical trials with immune therapies in ccRCC. Results correspond to the drug's group. '+' means longer/higher, '=' means no differences and '-' means less. PFS (progression-free survival), OS (overall survival).

Drug	Clinical trial	Result	Reference
Ipilimumab	Phase II (dose increment)	+ response, + toxicity	[182]
Nivolumab	Phase III (Nivolumab vs everolimus)	+ OS, = PFS, - toxicity	[184]
BMS-936559	Phase I	+ PFS	[187]
Atezolizumab	Phase I	+ PFS	[186]

One of the main concerns regarding immunotherapy in ccRCC is the development of predictive biomarkers to determine which patients will benefit from the therapy. According to the National Cancer Institute, a biomarker is defined as 'a biological molecule found in blood, other body fluids, or tissues that is a sign of a normal or abnormal process or of a condition or disease'. An ideal biomarker should be highly specific, sensitive and have a robust predictive power.

The expression levels of PD-L1 and PD-1 in tumour cells and in tumour-infiltrating lymphocytes are widely used predictive biomarkers for anti-PD-L1 and anti-PD-1 therapies in RCC (and other cancers) [188]. However, the use of PD-L1 immunohistochemistry as a biomarker is far from perfect. PD-L1 has highly heterogeneous intratumour expression and expression changes over the course of the disease progression [189]. Furthermore, there is a lack of consistency between studies, some of which use differing antibodies and variable cut-off thresholds and vary in whether staining is measured in tumour cells or immune cells [190].

Despite some studies observing a correlation between high PD-L1 tumour expression and response rate, lack of PD-L1 expression did not exclude patients from having an objective response [184, 191, 192]. Indeed, some studies have seen that high PD-L1 expression in tumour cells was associated with shorter OS, compared to low PD-L1 expression patients [193, 194]. Whereas in the CheckMate 214 study, high PD-L1 expression was correlated with better response and PFS after either nivolumab or ipilimumab treatment [195].

Therefore, it is clear that although PD-L1 is still used to predict response to immunotherapy in the clinic, better predictive biomarkers are needed. Among the alternative biomarkers proposed, gene expression signatures and TMB have garnered much interest. For example, high TMB has been associated with a better response to checkpoint inhibitor immunotherapies in various types of cancer [196]. Similarly, whole exome sequencing performed in 35 tumours of metastatic ccRCC patients previous to be treated with nivolumab, showed that biallelic loss of polybromo 1 (*PBRM1*) was associated with increased clinical benefit from immune checkpoint therapy [197]. These studies suggest that omic studies analysing tumour cell mutations or gene expression signatures would be suitable to predict patients' response to immune checkpoint inhibitors.

5) Combination therapy

In order to improve single-agent therapies, combinations with other immunotherapy, radiotherapy, chemotherapy or targeted therapies are also under study for ccRCC [198].

Regarding immune checkpoint combinations, one of the best studied is ipilimumab plus nivolumab. These antibodies target different stages of T cell activation, with ipilimumab blocking early T cell activation, whereas nivolumab inhibits T cell activation in primary lymph organs [199, 200]. A phase III melanoma trial comparing either combination therapy or single-agent therapy showed an increase response rate in the former group [201]. Results from a phase I trial in metastatic RCC (both ccRCC and non-clear cell RCC) which analysed the combination of nivolumab with sunitinib, pazopanib or ipilimumab showed that combination with ipilimumab generated the least adverse effects on patients [202], therefore, the study was continued with the combination of the two immune checkpoint inhibitors (CheckMate 016) [203]. In this trial they studied different doses in non-treated and previously treated patients. The promising results of this study motivated the design of a phase III clinical trial (CheckMate 214) to compare nivolumab plus ipilimumab versus sunitinib as first-line treatment for metastatic ccRCC patients [204]. This study found that in patients with intermediate- and poor-risk characteristics, PFS was higher in the combination group, as well as the discontinuation due to adverse effects, whereas in the favourable-risk cohort, sunitinib achieved better outcomes. On the basis of CheckMate 016 and CheckMate 214, the FDA approved nivolumab and ipilimumab combination therapy for patients with previous VEGFR tyrosine kinase therapy and as first-line therapy for intermediate- or poor-risk patients who had not been under previous treatment, respectively.

Combination therapies of immune checkpoint inhibitors with anti-angiogenic treatments also show promise, as anti-angiogenic therapies have been found to reduce tumour-induced immunosuppression [205]. For example, VEGFA has potent immunomodulatory effects and can induce the development of MDSC and Treg cells that impair the function of effector T cells and alter DC maturation, suggesting that anti-VEGFA agents could be useful to reactivate tumour-inhibited immune responses [206, 207]. In the first trial combining tremelimumab (anti-CTLA-4) with sunitinib (anti-VEGFR), the combination was poorly tolerated, and the study was stopped [208]. Similarly, the phase I CheckMate 016 trial studying the combination of nivolumab (anti-PD-1) with sunitinib, pazopanib or ipilimumab showed poor tolerability in the combination with anti-angiogenic inhibitors, and was consequently stopped [202]. A combination of cabozantinib and nivolumab, with the addition of ipilimumab or not, in patients with genitourinary tumours, showed promising results for ccRCC, and therefore this combination is being further explored [209].

These studies highlight that selection of anti-angiogenic therapies with no overlapping toxicities with immune checkpoint inhibitors is of crucial importance to ensure a safe therapy and achieve good outcomes. In addition, blocking the molecules that promote VEGFA expression, such as HIF2α, could further provide an alternative way of stimulating the immune system and therefore, synergy anti-HIF2α and immune checkpoint inhibitors therapy.

6) Targeting the HIF pathway

Another promising therapeutic option for ccRCC is targeting HIF transcription factors. This will block the activation of all downstream genes, and therefore, inhibit several pathways by which the tumour could progress [210].

Even though targeting transcription factors is believed to be the most direct way to target a tumour [211], due to the helix-loop-helix conformation and lack of active sites usually used for small-molecule binding, HIF molecules have proved difficult to target [212].

Several HIF inhibitors have been developed over the last years, targeting HIF in different ways (Table 3.6). Some of them inhibit HIF1α mRNA expression, e.g. the antisense oligonucleotide EZN-2698 or aminoflavone [213, 214], while others block HIF protein translation, such as cardiac glycosides, PX-478 or topoisomerase I inhibitors (topotecan, EZN-2208, a pegylated form of the active metabolite of camptothecin SN38, or the nanoparticle-drug conjugate CRLX101) [106, 215-220]. Regarding the DNA binding motif of HIF, echinomycin, a cyclic peptide antibiotic, and anthracyclines have been found to inhibit HIF activity by blocking its binding to the HRE sequence in the DNA [96, 221]. Chetomin and bortezomib have shown to inhibit HIF transcriptional activity by inhibiting the recruitment of the p300 coactivator [222-224].

Some of the above mentioned drugs are currently being evaluated in clinical or preclinical trials, whereas results are already available for others [225]. For example, the nanoparticle-drug conjugate CRLX101 showed good results for metastatic RCC patients (ccRCC, papillary RCC and chromophobe RCC patients) when used in combination with bevacizumab [226]. On the other hand, EZN-2968, EZN-2088 or PX-478 have shown modest activity in phase I trials, and their investigation in metastatic ccRCC has consequently stopped [227-229].

Table 3.6. HIF inhibitors.

Drug	Mechanism of action	Selectivity	Reference
EZN-2698	Inhibition of HIF1α mRNA expression	HIF1α	[213]
Aminoflavone	Inhibition of HIF1α mRNA expression	HIF1α	[214]
Glycosides	Inhibition of HIF1α protein translation	HIF1α and HIF2α	[220]
PX-478	Inhibition of HIF1α protein translation	HIF1α	[218]
Topotecan	Inhibition of HIF protein translation	HIF1α and HIF2α	[215, 216]
EZN-2208	Inhibition of HIF1α protein translation	HIF1α	[217]
CRLX101	Inhibition of HIF protein translation	HIF1α and HIF2α	[219]
Echinomycin	Inhibition of HIF1α binding to the DNA	HIF1α	[221]
Anthracyclines	Inhibition of HIF binding to the DNA	HIF1α and HIF2α	[96]
Chetomin	Inhibition of HIF transcriptional activity	HIF1α and HIF2α	[222]
Bortezomib	Inhibition of HIF transcriptional activity	HIF1α and HIF2α	[223]

Most of the above mentioned inhibitors target both HIF1α and HIF2α, without clear selectivity for one isoform [230]. In ccRCC, HIF2α is expressed in all tumour types, in contrast to HIF1α [231]. Moreover, as HIF2α is the oncogenic driver of the disease [125], molecules targeting this isoform are likely to be the most promising.

The PAS-B domain of HIF2α contains a relatively large cavity where possible cofactors can bind and generate an allosteric conformation change, avoiding this way the union to HIF1β subunit [212]. Scheuermann *et al.* showed that small-molecule ligands can actually bind to this hydrophobic cavity, induce a conformational change, avoid the heterodimerization with HIF1β and finally impair the activation of downstream target gene expression [232-234]. Moreover, these compounds are specific for HIF2α as they cannot antagonize HIF1α isoform [235], due to three different residues between the PAS-B pocket of HIF1α and HIF2α [236]. The work performed by Key *et al.* in 2009 is the first example of inhibitors targeting the protein-protein interaction of HIF2α/HIF1β complex [232]. In this work, they generated more than 130 inhibitory structures and based on selectivity, binding strength and orally available molecules, prioritised PT2385 and PT2399 as clinical candidates.

Both PT2385 and PT2399 can bind to HIF2α and allosterically block its dimerization with HIF1β. These two antagonists are structural and functional analogues, and in spite of differing slightly in the structure, their physical, chemical and biochemical properties are similar. PT2385 showed to inhibit the expression of HIF2α target genes in ccRCC cell lines and tumour xenografts [237]. Under a good safety profile, PT2385 administration promoted tumour regression faster than sunitinib in a subcutaneous xenograft model. Moreover, PT2385 demonstrated its antitumour efficacy by inhibiting tumour growth in a patient-derived xenograft model. This tumour was derived from a patient who had progressed after sunitinib and everolimus treatment [237]. A phase I clinical trial was performed in previously treated patients with advanced ccRCC to determine the best dose for a phase II study. In this study there were no dose limiting toxicities, and PT2385 was well tolerated, with anemia, peripheral edema and fatigue the most common adverse effects of the drug [238]. This study suggested that PT2385 has a favourable safety profile and is active in patients with pretreated ccRCC.

Similarly, PT2399 was found to decrease HIF2α-induced transcription and tumour growth in a ccRCC model [239]. Using a patient-derived xenograft model, the authors showed that PT2399 suppressed tumorigenesis in 56% of the cases. PT2399 was better tolerated and presented greater activity than sunitinib, and was effective in sunitinib-resistant tumours [239]. However, long-term PT2399 treatment ultimately led to resistance in initially sensitive tumours, although resistance took the double amount of time to develop when compared to the tumours treated with sunitinib [239]. Furthermore, one of the patients whose tumour had originated a sensitive xenograft achieved disease control for more than 11 months after treatment with the analogue PT2385. This data validates PT2399 suitability as ccRCC therapeutic target, but shows that tumours have different sensitivity. Another study further highlighted the variable sensitivity to PT2399 in preclinical mouse models of primary and metastatic ccRCC cases [240].

In addition to PT2399 and PT2385, PT2977 is also under investigation and there are currently three ongoing clinical trials: a phase I study to identify the maximum tolerated dose of PT2977 tablets and the recommended dose for phase II (NCT02974738), a phase II trial to investigate PT2977 as a treatment for VHL disease associated ccRCC (NCT03401788) and a phase II to study the effect of PT2977 in combination with cabozantinib (NCT03634540).

Although there are only minor effects from combination therapies of HIF inhibitors plus anti-angiogenic therapy [226] or proteasome inhibitors (NCT01100242), a combination with immunotherapy is currently still under investigation. HIF is known to generate an immunosuppressive environment within the tumour [119], therefore, therapies combining HIF inhibitors and immune checkpoint inhibitors seem promising to enhance the antitumour immune response both by down-regulating the immunosuppressive environment and promoting immune cell activation. In addition, it has been reported that in ccRCC HIF2α regulates PD-L1 expression, rather than HIF1α [241, 242], further showing that the combination treatment might be beneficial for the patient. This strategy is already being evaluated in clinical trials to analyse the efficacy of nivolumab plus PT2385 (NCT02293980).

Similar to immunotherapeutic options, the lack of appropriate biomarkers to assess the response of HIF inhibitors therapy has slowed down the development of these therapies. Several different end-points have been used in clinical trial designs including the measurement of HIF protein expression by western blot or immunohistochemistry, mRNA expression of HIF target genes or indirect measurement of microvessel density inside the tumour [230]. However, HIF inhibitor application in the clinic awaits further research into which specific tumours rely on this pathway, suitable biomarkers to both identify those tumours and detect the therapy response, as well as further clinical trials studying them in combination [243]. Moreover, studies analysing HIF2α inhibition in ccRCC would also be beneficial to stablish the consequences of blocking the main oncogenic driver of the disease.

3.1.3.2. Genetics of ccRCC

The central genetic events in ccRCC include biallelic inactivation of the *VHL* tumour suppressor gene, occurring in 80% of ccRCC cases, followed by mutations in genes encoding for chromatin modifying enzymes such as *PBRM1*, SET domain containing 2, histone lysine methyltransferase (*SETD2*) and BRCA1 associated protein 1 (*BAP1*). *PBRM1* mutations are found in 40% of ccRCC cases, whereas *SETD2* and *BAP1* mutations appears in 10-15% of diagnosed ccRCC [244]. In addition, copy number alteration in chromosomes, such as loss of chromosome 3p, gain of chromosome 5q and loss of chromosome 14q have also been found in 91%, 67% and 49% of ccRCC tumours, respectively [245]. Moreover, chromosome 3p and 14q harbour multiple tumour suppressor genes, whereas chromosome 5q contains several oncogenes [245].

1) ***VHL* gene**

VHL gene was named after Arvid Lindau and Eugen v. Hippel first described angiomas in the eye [246] and in the cerebellum and spine cord [247], respectively. This syndrome was later defined as VHL disease. VHL disease is a hereditary condition caused by genetic mutations in *VHL* gene, in which highly vascularized tumours, as well as cysts, arise in different organs, e.g. eyes, cerebellum, spinal cord, kidneys and adrenal glands [248]. In this syndrome, patients inherit only one functional copy of *VHL* gene, and subsequent loss of heterozygosity (LOH) results in the disease [248]. As a consequence, affected individuals are more likely to develop retinal and central nervous system hemangioblastomas, ccRCC, pheochromocytomas and pancreatic neuroendocrine tumours [249]. Although such tumours are typically non-malignant, they can cause serious or life-threatening problems and 73% of deaths in

VHL patients are directly due to the disease [250]. The frequency of ccRCC development among VHL patients increases with age, as by 60 years old, 70% of VHL patients will have developed ccRCC [249].

Even though most ccRCC cases are sporadic, 1-4% are associated with inherited syndromes, such as VHL disease [244]. Normally, hereditary cancers develop at earlier ages (mean of 37 years) than spontaneous ccRCC (mean of 61 years), and they can be bilaterial (occur in both kidneys) and multifocal [251]. However, copy number deletion, inactivating mutation or epigenetic silencing by promoter hypermethylation of *VHL* gene is the main genetic event in both cases [245].

VHL gene mutations are only detected in 50% of the patients, whereas promoter methylation is associated with 10-20% of the cases. This suggests that in addition to the direct mutation or hypermethylation in *VHL* gene, some tumours have VHL protein function compromised due to genetic or epigenetic alterations in other genes that are affecting *VHL* expression [252, 253]. In contrast to ccRCC, other RCC subtypes such as papillary RCC, chromophobe RCC or tumours from the collecting system do not ussually present *VHL* gene mutation [254].

2) ***PBRM1* gene**

Loss of *VHL* leads to senescence of renal tubular cells, indicating that loss of *VHL* alone is not sufficient to generate ccRCC tumours, other molecular changes are necessary for malignant transformation [255]. The *PBRM1* gene is located in chromosome 3p21 and it is the second most common mutated gene after *VHL* [256]. *PBRM1* encodes for BRG1-associated factor 180 (BAF180) protein, a subunit of the chromatin remodelling complex polybromo-BAF (PBAF) of the SWI/SNF family [257]. By altering the position of nucleosomes along the DNA, this complex regulates cellular processes such as cell proliferation, replication, repair and transcription of DNA. It was reported that silencing *PBRM1* enhanced proliferation, clonogenic potential and migration of various ccRCC cell lines, suggesting a tumour suppressor role in ccRCC [257, 258].

3) ***SETD2* gene**

The *SETD2* gene is also localized in chromosome 3p and it encodes for histone H3 lysine 36 trimethyltransferase, which promotes transcriptional activation of target genes by methylation [259]. It has been shown that depletion of *SETD2* reduced nucleosome stabilization and chromatin compaction and increased replication stress [260], suggesting a role of SETD2 in maintaining genome integrity *in vitro*. On the other hand, HIF binds to methylated CpG regions in gene promoters and an open conformation of the chromatin facilitates the interaction [72, 261], suggesting that mutations in chromatin modifying enzymes change the chromatin accessibility to HIF transcription factors within a *VHL* defective background. Consistent with this idea, a study demonstrated that mutations in *SETD2* increased chromatin accessibility to HIFs in kidney tumour samples and also generated alterations in RNA processing levels of 25% of all expressed genes [262]. The authors concluded that mutations in chromatin regulatory proteins could lead to tumour development through RNA processing defects and enhanced HIF-mediated gene transcription.

4) *BAP1* gene

The *BAP1* gene is located between *VHL* and *PBRM1* on chromosome 3p [256]. The BAP1 protein is a deubiquitination enzyme also involved in transcriptional regulation as it forms part of the multiprotein polycomb repressive complex (PRC) [263]. PRC consists of the highly conserved transcriptional repressors polycomb-group of proteins and the catalytic subunit BAP1, which silence target gene expression via histone modification [264]. Mutations in *BAP1* have been associated with higher tumour stage and grade, as well as worse prognosis in ccRCC [265]. Moreover, mutations in *BAP1* are mutally exclussive with *PBRM1* [263].

5) Copy number alterations of chromosome 3p, 5q and 14q genes

In addition to the mutations of *VHL*, *PBRM1*, *SETD2* and *BAP1* tumour suppressor genes located in chromosome 3p, this chromosome can further undergo genetic translocations associated with higher risk of ccRCC development [266]. These translocations are mainly associated to hereditary RCC cases and have been described to increase the risk of tumour development up to 80% [267].

The first report linking chromosome 3p translocations to ccRCC came in 1979 from a study of ccRCC cases that occurred in 10 members of the same family [268]. The authors realized that tumours developed earlier than sporadic ccRCC and were also present in both kidneys and in several renal sites. They linked these tumours with the presence of translocations between chromosomes 3 and 8, suggesting a genetic mechanism for tumour development. Since then, other translocations involving chromosome 3 have been reported, mainly associated to hereditary ccRCC [269].

Similarly, loss of chromosome 14q genes, such as *HIF1α*, can further promote ccRCC tumorigenesis, as it has been reported that HIF1α acts as a tumour suppressor in ccRCC [270, 271], in contrast to the oncogenic driver HIF2α [125]. Moreover, many ccRCC cases with exclusive expression of HIF2α isoform have been described [270].

Regarding chromosome 5q genes, sequestosome 1 (*SQSTM1*) has been found to be frequently amplified in ccRCC patient samples and cell lines [272]. It encodes p62 protein, which activates the nuclear factor, erythroid 2 like 2 (NRF2) transcription factor that regulates the expression of antioxidant proteins involved in the resistance to oxidative stress. Moreover, it has been published that suppression of *SQSTM1* decreases ccRCC progression by reducing mTOR signalling [273]. Other genes located in chromosome 5q, e.g. enhancer of zeste 2 polycomb repressive complex 2 subunit (*EZH2*), stanniocalcin 2 (*STC2*) and versican (*VCAN*) were found to be amplified and transcriptionally overexpressed in ccRCC samples, suggesting them as potential 5q oncogenes [274, 275].

3.1.3.3. HIF1α and HIF2α in ccRCC

The best characterized VHL targets are HIF1α and HIF2α. Loss of function of *VHL* in ccRCC leads to stabilization of both subunits even in the presence of oxygen, generating a 'pseudohypoxic' transcriptional response [124]. Although there exists an overlap between HIF1α and HIF2α targets, there are some genes activated only by one subunit [39, 276]. Moreover, several genes bind both HIF1α and HIF2α, but only one isoform is able to induce the transactivation. HIF activated genes are involved in cell proliferation, migration, angiogenesis, oxygen transport and metabolism, which in ccRCC context, will help in the development of the tumour.

1) HIFs and proliferation in ccRCC

Even though both HIF1α and HIF2α appear to be involved in ccRCC initiation [277], they have contrasting roles as the disease develops [125]. Several reports suggest that HIF1α functions as a tumour suppressor in ccRCC by attenuating tumour cell growth, whereas HIF2α promotes tumour development [125, 126]. Immunohistochemical analysis of kidney samples of patients with VHL disease showed that both isoforms could be detected in precancerous lesions, as well as the known HIF targets carbonic anhydrase 9 (CA9), glucose transporter 1 (GLUT1) or cyclin D1. But in normal tubular cells only HIF1α was expressed, suggesting that HIF2α is a tumour driver in these cells [278].

Studies in mouse xenograft models revealed that HIF2α overexpression in ccRCC cells led to increase tumour burden [125, 126], whereas shRNA mediated silencing of HIF2α reduced tumour mass [279]. HIF1α on the other hand, had the opposed effect. Overexpression of HIF1α reduced tumour size, in contrast to the increase cell proliferation seen when HIF1α was silenced [125, 270]. These observations support the hypothesis that in ccRCC HIF2α acts as an oncogene by promoting tumour cell proliferation, in contrast to a tumour suppressor role of HIF1α. Further supporting HIF1α's tumour suppressor role, it was described that HIF1α transcriptional activity was increased after silencing FIH, with the consequent impairment of ccRCC cell growth [280], as HIF1α is more sensitive than HIF2α to FIH-mediated degradation [281].

Another study carried out by Gordan *et al.* found that VHL-defective ccRCC cases expressed HIF2α, with some of them even having the HIF1α isoform inactivated [231]. They distinguished three ccRCC subtypes: those with wild type *VHL*, those with *VHL* inactivated and expressing both HIF1α and HIF2α, and those with *VHL* inactivated and only expressing HIF2α. They found that tumours expressing only HIF2α had the highest rates of proliferation. Moreover, cyclin D1 oncogene was found to be exclusively regulated by HIF2α but not HIF1α in ccRCC [282], and was also induced in early kidney lesions of patients with VHL disease [278]. Taken together, these results suggest that HIF2α plays a key role in early ccRCC development. Several studies showed that ccRCC cases that only express HIF2α have increased cell proliferation and adverse prognosis [93, 283].

HIF2α promotes ccRCC cell growth through the interaction with several oncogenes, e.g. MYC proto-oncogene (c-*MYC*) and the epidermal growth factor receptor (*EGFR*). c-MYC promotes cell cycle and regulates cell metabolism by controlling the expression of the genes involved [245]. HIF isoforms have contrasting effects on c-MYC. While HIF1α impairs c-MYC transcriptional activity, with the consequent reduction in the expression of genes involved in cell cycle, HIF2α enhances c-MYC's activity [284]. By interacting with c-MYC, HIF2α increases the expression of cell cycle regulators such as cyclin D2 [231], in contrast to HIF1α that increases the expression of the cell cycle inhibitors p21 and p27 [231, 284]. This further supports HIF1α suppressor and HIF2α oncogenic role in ccRCC development. Apart from cyclin D2, cyclin D1 is another tumour-promoting HIF2α target specifically found in ccRCC [125]. Cyclin D1 did not enhance cancer cell proliferation *in vitro*, but it appeared to be relevant to sustain *in vivo* tumour growth [285].

HIF2α promotes *TGFα* expression, which induces EGFR downstream signalling and the consequent cell growth [286]. Interestingly, HIF2α can directly enhance EGFR pathway by promoting its transcription via binding to an HRE [287] and by reducing EGFR endocytosis [288].

In addition, HIF2α also prevents the activity of the tumour suppressor p53 protein [93]. Moreover, HIF2α induces the expression of antioxidant enzymes which would restrict p53 activation by oxidative stress [93]. Altogether, HIF2α avoids the accumulation of ROS and DNA damage, bypassing cell death and promoting ccRCC cell survival.

All these studies show that through several mechanisms, HIF2α can enhance ccRCC tumour cell growth both *in vitro* and *in vivo*, demonstrating the importance of HIF2α in this disease. However, RCC tumours in which *VHL* is not mutated (e.g. papillary RCC, chromophobe RCC or tumours from the collecting system) do not present high HIF2α expression [289], showing that up-regulation of HIF2α due to *VHL* mutation is of particular relevance in ccRCC oncogenesis.

2) HIFs and angiogenesis in ccRCC

Deregulated vascular growth promote the onset and progression of many tumour types [1]. Under normal conditions, blood vessel development sustains tissue oxygenation and metabolic activity [290], but the enhanced metabolism and disrupted oxygen sensing mechanism found in kidney cancer induce structural changes of the vasculature, leading to aberrant neovascularization and angiogenesis. This process is mainly due to HIF pathway deregulation [94, 291] and *VHL* mutations [292, 293].

Among the HIF-induced genes, there are several that are pro-angiogenic factors contributing to ccRCC's high vasculature [94], such as VEGFA, PDGF and galectin-1. Tumour hypoxia induces *VEGFA* expression to promote the generation of blood vessels as the lesion expands [291]. But in ccRCC, hypoxia is not necessary to promote angiogenesis as high HIF levels due to *VHL* mutation promote *VEGFA* expression [293]. In addition, HIF can enhance tumour vascularization by affecting PDGF signalling pathway [294], which is important in the recruitment of pericytes and maturation of the new blood vessels [295]. The HIF1α target galectin-1 is overexpressed in ccRCC, and by binding to integrin and ECM proteins promotes tumour cell migration and invasion [296]. It has been demonstrated that galectin-1 enhanced cell movement via the HIF1α-mTOR pathway [296]. mTOR, another HIF2α target, promotes tumour development by inducing cell growth [297], migration and invasion [296] and adaptation to metabolism in ccRCC [298].

These studies show that in ccRCC, aberrant HIF signalling leads to the induction of genes involved in angiogenesis and thus promotion of tumour growth.

3) HIFs and metabolism in ccRCC

High lipid and glycogen accumulation in the cytoplasm of tumour cells is a morphological hallmark of ccRCC, which gave rise to the name 'clear cell' RCC. Alterations in metabolic pathways, such as glucose, lipids and amino acids contribute to the clear cell phenotype [151]. Moreover, ccRCC has long been classified as a metabolic disease due to all these alterations [210, 299].

The Warburg effect is mainly driven by HIF1α [98, 271], and this phenomenon is amplified in VHL defective ccRCC due to HIF overexpression. HIF1α controls the glucose flux through several mechanisms to avoid pyruvate entry to the TCA. First, HIF1α inhibits the conversion of pyruvate to acetyl-CoA by pyruvate dehydrogenase (PDH) by enhancing the expression of pyruvate dehydrogenase kinase 1 (PDK1), which will inactivate PDH and consequently avoid pyruvate entry to the TCA cycle [300, 301]. Second, HIF1α induces the expression of lactate dehydrogenase (LDHA), which converts pyruvate to lactate [302, 303]. In this manner, HIF1α redirects the glucose flux from mitochondrial respiration to glycolysis (Figure 3.2). But, as a consequence, the energy generated is lower, 36 ATP via mitochondrial respiration compared to 2 ATP generated by glycolysis. Therefore, to overcome this issue, HIF1α up-regulates the expression of glucose transporters GLUT1 and GLUT3 in the cell membrane to increase the glucose uptake for glycolysis [302, 304].

Through glycolysis, tumour cells can also obtain the glycolytic intermediates necessary to generate the building blocks for nucleotides, proteins and lipids [305], and they have been shown to be highly elevated in ccRCC [245, 306]. For instance, phosphate pentose pathway starts with the first intermediate of glycolysis, glucose-6-phosphate, and this pathway is important for lipid and nucleotide production [307]. Moreover, in spite of the transition from aerobic respiration to aerobic glycolysis, oxidative phosphorylation is not completely abolished [308], and reduction in the activity of the ETC leads to increase ROS [309]. To avoid oxidative stress, tumour cells can use the NADPH generated during phosphate pentose pathway to reduce oxidized glutathione. In this way, phosphate pentose pathway helps cells to maintain their antioxidant capacity [310].

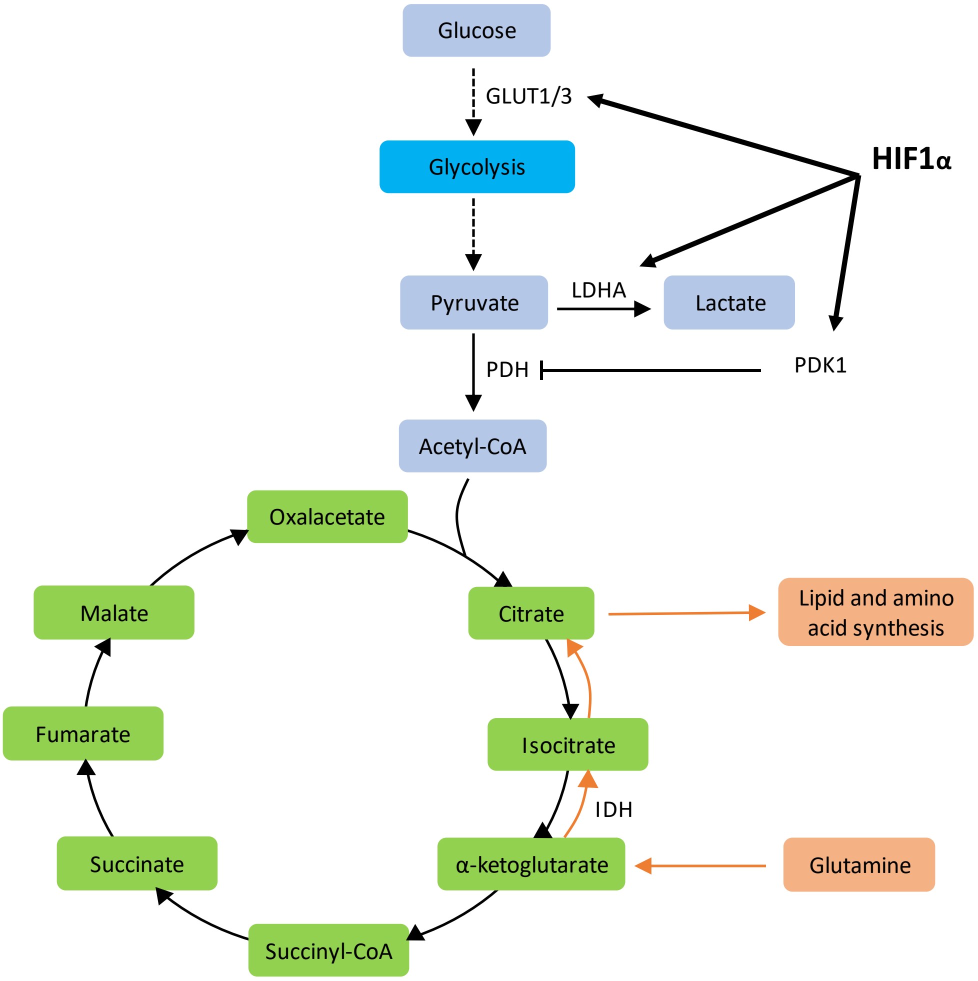
Glucose
GLUT1/3
Glycolysis
HIF1α
Pyruvate
LDHA
Lactate
PDH
PDK1
Acetyl-CoA
Oxalacetate
Citrate
Lipid and amino acid synthesis
Malate
Isocitrate
Fumarate
IDH
Succinate
α-ketoglutarate
Glutamine
Succinyl-CoA

Figure 3.2. HIF transcription factors generated metabolic adaptations.

Although glycolysis shift is mainly executed by HIF1α, HIF2α is a potent inducer of GLUT1 [125, 126] and enolase 2 [285] in ccRCC, allowing the shift to glycolysis also in ccRCC cases only expressing HIF2α.

HIF2α not only increases the glycolytic rate by promoting GLUT1 expression, but also reduces glucose oxidation by increasing glutamine reductive carboxylation [311]. These metabolic actions were thought to be regulated by HIF1α, but it was demonstrated that they can be driven by HIF2α too [311]. Reductive glutamine metabolism provides metabolic intermediates for the synthesis of macromolecules. In hypoxic, highly proliferating cells, or in the context of ccRCC, HIF-expressing cells, glutamine is used to generate citrate through the reductive carboxylation of α-ketoglutarate, catalysed by isocitrate dehydrogenase (IDH), providing this way intermediates for lipid [101, 312] and amino acid [313] synthesis (Figure 3.2). Moreover, renal cancer cell lines showed to prefer the citrate derived from reductive carboxylation, rather than glucose-derived citrate generated by oxidation, for lipid biosynthesis, even at normal oxygen levels [101].

In addition to the reprogramming of glucose and glutamine metabolism, ccRCC has several alterations in lipid metabolism, at levels of fatty acid degradation (β-oxidation), synthesis and storage. Through β-oxidation cells break lipids into acetyl-CoA, generating in the process NADH and $FADH_2$ which will be used to generate ATP in the oxidative phosphorylation. In contrast to normal renal proximal tubule epithelial cells, which have high rates of β-oxidation [314], ccRCC cells display reduced mitochondrial content and activity [315]. Moreover, it has been described that HIF1α activates mitophagy through the up-regulation of BCL2 interacting protein 3 (BNIP3) and BCL2 interacting protein 3 like (BNIP3L, also known as Nix), impairing glucose and fatty acid oxidation in the mitochondria [316, 317].

Contributing to the clear cell phenotype, ccRCC is characterized by the accumulation of lipid droplets in the cytoplasm [318]. Lipid droplets, also known as lipid bodies or adiposomes, are specialized organelles in which the cell stores neutral lipids, such as triglycerides, steryl esters or cholesterol. Lipid droplets are surrounded by a monolayer membrane which arises from the endoplasmic reticulum, and contains several coating proteins, e.g. proteins of the perilipin family [319]. It has been demonstrated that lipid droplets are not just lipid storage places within the cell, as these droplets are physically and functionally connected to the endoplasmic reticulum, they are fundamental to avoid endoplasmic reticulum stress and facilitate ccRCC progression [318]. Furthermore, in glioblastoma and breast cancer, lipid droplet accumulation protected cells from ROS and promoted cell survival after hypoxia-reoxygenation [100]. Suppression of either HIF1α or HIF2α reduced lipid droplet content in ccRCC [318, 320, 321].

In ccRCC lipid accumulation is driven by HIF2α, although HIF1α also participates. On the one hand, HIF2α promotes lipid storage by inhibiting fatty acid oxidation, mainly via inhibition of carnitine palmitoyltransferase 1 (CPT1), the rate-limiting enzyme for fatty acid β-oxidation [320]. In contrast to short and medium chain fatty acids, long fatty acids are unable to cross the mitochondrial membranes by simple diffusion, they need to be imported by the carnitine palmitoyltransferase (CPT) system [322, 323]. The first component of the system is CPT1, a mitochondrial outer membrane protein, which transfers the long-chain acyl group of the acyl-CoA ester to carnitine, generating acyl-carnitine which diffuses through the outer mitochondrial membrane to the intermembrane space, and gets into the mitochondrial matrix via a translocase. In there, acyl-carnitine is back converted to acyl-CoA by CPT2 for further oxidation (Figure 3.3). CPT1 is tightly regulated by the first intermediate in the fatty acid biosynthesis, malonyl-CoA. Therefore, allowing the regulation of β-oxidation based on the availability of fatty acids [322, 324]. On the other hand, HIF2α can reduce mitochondrial content and inhibit mitochondrial biogenesis, explaining both reduction of fatty acid β-oxidation and glucose oxidation in ccRCC [271, 325, 326]. Moreover, it has been reported that HIF2α, and not HIF1α, promotes the expression of the lipid droplet coat protein perilipin 2 (PLIN2) [318]. This HIF2α-dependent lipid droplet formation enhances fatty acid accumulation in the cell, likely as a consequence of low β-oxidation, and protects cancer cells from cytotoxic endoplasmic reticulum stress [318], altogether promoting ccRCC progression.

All these studies suggest that in ccRCC HIF2α decreases fatty acid β-oxidation with a concomitant increase in lipid synthesis and storage to promote tumour progression.

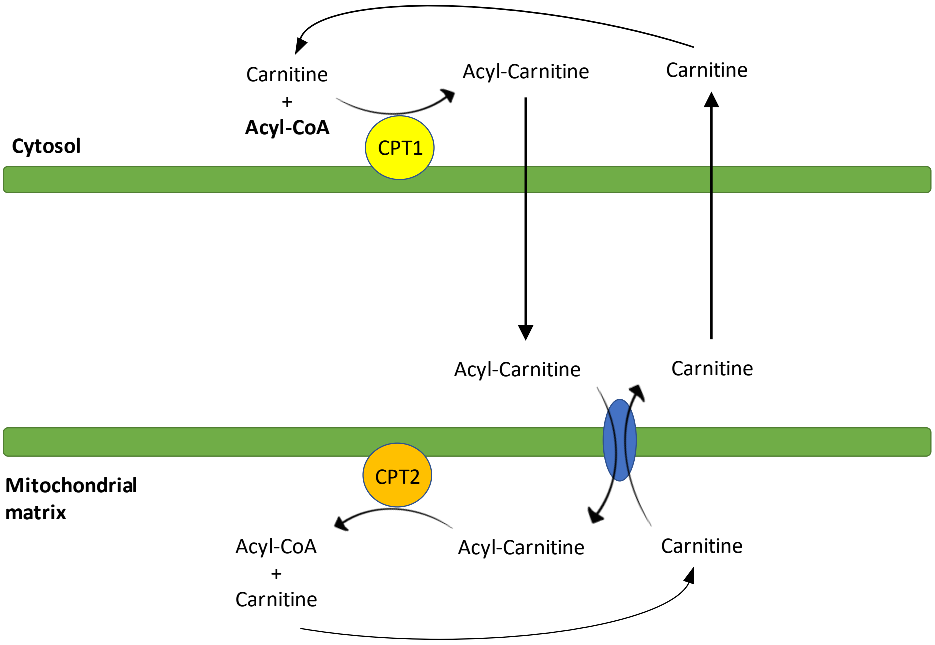

Figure 3.3. CPT system.

3.2. Objectives

HIF1α and HIF2α are the main transcription factors generated in hypoxia, which is one of the main characteristics of solid tumours. Moreover, in ccRCC HIF2α appears to be the relevant isoform for the disease, as it initiates tumour growth and promotes tumour development by affecting several pathways. Therefore, the main objective of this chapter is to study HIF2α involvement in ccRCC by generating a stable HIF2α knock out (KO) ccRCC cell line. The aims are:

1. To determine how HIF2α is involved in cell proliferation to promote tumour cell growth in both normoxic and hypoxic conditions.
2. To investigate the role of HIF2α in tumour cell dissemination and metastasis by studying the migratory and invasive ability of renal tumour cells.
3. To analyse the different nutritional requirements mediated by HIF2α.
4. To study the differences between the complete absence of HIF2α and a partial silencing, by using the HIF2α antagonist PT2385, in terms of cell proliferation, migration, invasion and metabolism.

3.3. Materials and methods

3.3.1. Cell culture

3.3.1.1. Lung cancer cell line

The A549 non-small cell lung cancer cell line was obtained from the American Type Culture Collection (ATCC®). This hypotriploid cell line was grown in Dulbecco's Modified Eagle Medium: Nutrient Mixture F-12 (DMEM/F12, 31331093, Gibco™) supplemented with 10% Fetal Bovine Serum (FBS, 10500064, GIBCO™) (complete DMEM/F12). Cells were tested for mycoplasma every three months using MycoAlert™ Mycoplasma Detection Kit (LT07-118, Lonza) and subcultured when they reached 80% confluence. As A549 cell line proliferates fast and is easy to grow and transfect, this cell line was used to validate the Crispr/Cas9 guides.

3.3.1.2. Renal cancer cell lines

The 786-0 ccRCC cell line was obtained from ATCC®. The 786-0 cell line is the parental cell line (wild type, 786-0 WT) of the HIF2α Crispr/Cas9 knock out (786-0 KO) cell line generated in this thesis. The 786-0 cell line contains a single *VHL* allele with a frameshift nonsense mutation resulting in the absence of VHL protein [327]. In addition, it lacks HIF1α expression while it expresses HIF2α constitutively [328]. Both cell lines were grown in low glucose (1g/L) Dulbecco's Modified Eagle Medium (DMEM, 31885023, Gibco™) and supplemented with 10% FBS (complete DMEM). They were routinely tested for mycoplasma contamination and subcultured when confluent enough. In addition, 786-0 cell line expressing *VHL* gene (786-0 VHL$^+$) was used for specific experiments in 'Chapter 4'. This cell line was also grown in complete DMEM.

RCC4 *VHL* mutant cell line [329] was obtained from European Collection of Authenticated Cell Cultures (ECACC). It was commercially available stably expressing an empty vector (RCC4 WT) or a vector for *VHL* overexpression (RCC4 VHL). These cell lines were also grown in complete DMEM. They were tested for mycoplasma contamination every three months and subcultured when reached confluence.

3.3.2. Cell treatments

3.3.2.1. Small-molecule antagonist of HIF2α PT2385 [237]

PT2385 compound (B1920, BioVision) dissolved in dimethyl sulfoxide (DMSO, D1435**,** Sigma-Aldrich) was added to cell cultures at different final concentrations (0.1µM, 1µM or 10µM) as previously described [237]. For hypoxia-treated cells, cell cultures were placed into the hypoxic incubator for at least 4h before compound addition and maintained under hypoxic condition for the duration of the treatment.

3.3.2.2. 2-Deoxy-D-glucose

$5x10^4$ 786-0 cells were seeded per well in 6-well plates. The following day, 2-Deoxy-D-glucose (2-DG, D8375, Sigma-Aldrich) was added to the cells at final concentrations of 2mM and 6mM for 5 days. Prior to addition to the cells, the compound solution was filtered.

3.3.2.3. Cell culture in different glucose media

For metabolism studies and when specified, $5x10^4$ 786-0 cells were seeded per well in 6-well plates and grown in DMEM no glucose, no glutamine, no phenol red (A1443001, Gibco™) supplemented with different amounts of glucose (G8769, Sigma-Aldrich), 4mM glutamine (17-605C, Lonza), 1mM sodium pyruvate (11360070, Gibco™) and 10% FBS for 5 days.

3.3.3. Clustered regularly interspaced short palindromic repeats/Cas9 (Crispr/Cas9)

3.3.3.1. Single guide RNAs

Specific single guide RNAs (sgRNAs) for *HIF2α* were designed using the CRISPR Design Tool from Genome-Engineering webpage (http://crispr.mit.edu/). Guides were designed in exons to ensure changes in protein expression. The program suggests several guides, specifying the genomic sequence, locus, score and off-targets. Those guides with the highest score and least off-target genes were selected. Once the guides were selected, both ‘forward’ (sgRNA_F) and ‘reverse’ (sgRNA_R) sequences were designed as sgRNA following the format showed in Table 3.7. This format allows a perfect annealing with the overhangs generated by BbsI enzyme used for plasmid digestion and the two guanines immediately before the forward sequence facilitate DNA polymerase III transcriptional activity. Specifically, 2 guides designed in the 5th and 6th exons were selected for *HIF2α* (Table 3.8). The designed guides must immediately precede a Protospacer Adjacent Motif (PAM) sequence (5’-NGG-3’), required for the Crispr/Cas9 system to cleave the DNA.

Table 3.7. Format of the guides for Crispr/Cas9 editing.

Oligo	Format
sgRNA_F	5’-CACCGG_$N_{20\ (sense)}$- 3’ (towards PAM)
sgRNA_R	5’-AAAC_$N_{20\ (antisense)}$_CC-3’

Table 3.8. HIF2α guide sequences.

Guide name	Sequence (5’-3’)
HIF2α guide 1-F	CACCGGCATGAAGAAGTCCCGCTCTG
HIF2α guide 1-R	AAACCAGAGCGGGACTTCTTCATGCC
HIF2α guide 2-F	CACCGGTAGCCACACAGACTATTGTG
HIF2α guide 2-R	AAACCACAATAGTCTGTGTGGCTACC

3.3.3.2. Plasmid digestion and linearization

Guides were cloned into pX330 EGFP/2A NEO-NEO construct (pX330 EGFP, modified from pX330 and kindly provided by Dr Joey Riepsaame). The parental pX330 plasmid was designed by Zhang’s laboratory [330] (Plasmid #42230, Addgene) for the expression of a chimeric guide RNA (gRNA), the human codon optimized Cas9 enzyme and the ampicillin resistance gene (Figure 3.4). It was further modified for the additional expression of the enhanced green fluorescent protein (EGFP) and neomycin (NEO) resistance gene.

The digestion was performed by mixing 10µg pX330 EGFP plasmid, 10µL NEBuffer™ 2.1 (B7202S, New England Biolabs, NEB), 10µL BbsI digestion enzyme (R0539S, NEB) and DEPC-Treated Water in a final volume of 100µL for digestion during 15 min at 37ºC, followed by an inactivation step of 20 min at 65ºC. Next, the digested plasmid was gel-purified running the digestion product in a 1% agarose gel (A8963, Ecogen), harvesting the bands under ultraviolet (UV) light and extracting the DNA using QIAquick Gel Extraction Kit using a Microcentrifuge (28704, QIAGEN). The purified plasmid was eluted in DEPC-Treated Water and quantified in a NanoDrop® ND-1000 spectrophotometer.

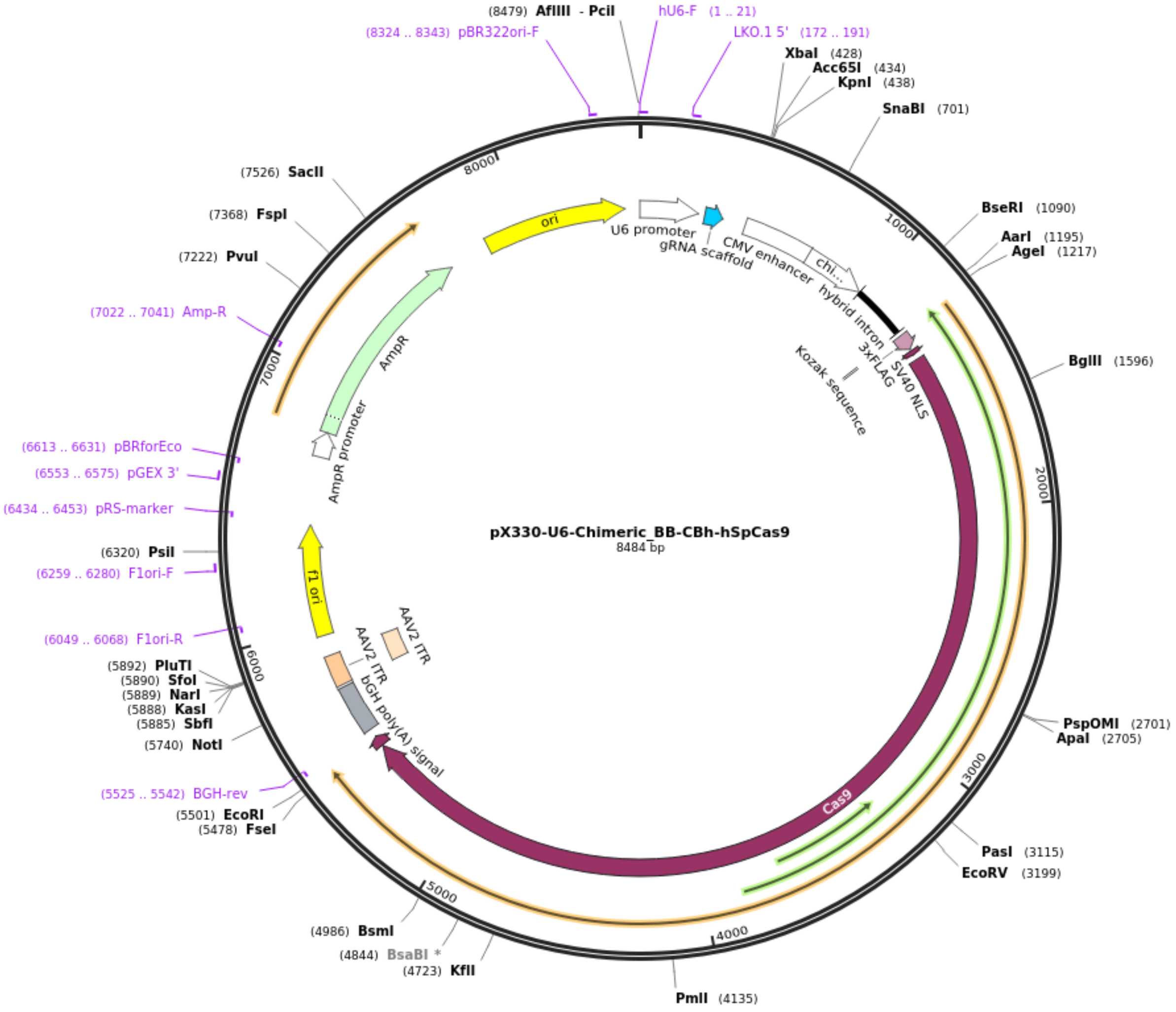
(8479) AflIII - PciI
(8324 .. 8343) pBR322ori-F
hU6-F (1 .. 21)
LKO.1 5' (172 .. 191)
XbaI (428)
Acc65I (434)
KpnI (438)
SnaBI (701)
BseRI (1090)
AarI (1195)
AgeI (1217)
BglII (1596)
PspOMI (2701)
ApaI (2705)
PasI (3115)
EcoRV (3199)
PmlI (4135)
(4986) BsmI
(4844) BsaBI *
(4723) KflI
(5525 .. 5542) BGH-rev
(5501) EcoRI
(5478) FseI
(5892) PluTI
(5890) SfoI
(5889) NarI
(5888) KasI
(5885) SbfI
(5740) NotI
(6049 .. 6068) F1ori-R
(6320) PsiI
(6259 .. 6280) F1ori-F
(6434 .. 6453) pRS-marker
(6553 .. 6575) pGEX 3'
(6613 .. 6631) pBRforEco
(7022 .. 7041) Amp-R
(7222) PvuI
(7368) FspI
(7526) SacII
8000
1000
2000
3000
4000
5000
6000
7000
ori
U6 promoter
gRNA scaffold
CMV enhancer
chi...
hybrid intron
3xFLAG
SV40 NLS
Kozak sequence
AmpR
AmpR promoter
f1 ori
AAV2 ITR
AAV2 ITR
bGH poly(A) signal
Cas9
pX330-U6-Chimeric_BB-CBh-hSpCas9
8484 bp

Figure 3.4. pX330 parental plasmid map (Plasmid #42230, Addgene).

3.3.3.3. sgRNA annealing

Before cloning the guides into the plasmid, double-stranded oligos (gRNA) were generated by annealing the Forward and Reverse sgRNAs. Annealing was based on serial brief incubation steps at high temperature. First, 10µM forward guide and 10µM reverse guide were mixed in DEPC-Treated Water in a final volume of 100µL and incubated in a ThermoBlock (Eppendorf) for 5 min at 99ºC. Then, the ThermoBlock was switched off and the 1.5mL tubes containing the guides were held half out of the machine for 5 min. Later, the 1.5mL tubes were left lying down on the ThermoBlock for another 5 min. Finally, guides were incubated for 7 min at RT.

3.3.3.4. gRNA precipitation

For gRNA precipitation, 30µL 3M sodium acetate (NaOAc) pH 5.6 and 300µL 100% ethanol were added to the annealed guides prior to centrifugation at 15000rpm for 30 min at 4ºC. Supernatant was discarded and precipitated guides were washed with 500µL 70% ethanol by centrifugation at 15000rpm for 10 min at RT. After ethanol removal, gRNA pellets were left to dry for 30 min at RT. Finally, pellets were resuspended in DEPC-Treated Water and placed on ice. Quantification was carried out with a NanoDrop® ND-1000 spectrophotometer.

3.3.3.5. gRNA and plasmid ligation

In order to ligate the gRNA and the digested plasmid, gRNAs must be previously phosphorylated. To achieve this, 1µg gRNA was mixed with 2µL T4 DNA Ligase Reaction Buffer (B0202S, NEB) and 1µL T4 Polynucleotide kinase (PNK, M0201S, NEB) in a final volume of 20µL, and incubated for 1h at 37ºC. In this process, PNK transfers γ-phosphates from ATP to the 5' end of the DNA, being ready for the ligation. To ligate the gRNAs into the linearized plasmid, 1µL T4 DNA Ligase Reaction Buffer, 0.5µL gRNAs, 20ng digested pX330 EGFP and 1000U T4 DNA Ligase (M0202T, NEB) were mixed in a final volume of 10µL and incubated for 1h at RT.

3.3.3.6. Plasmid extraction and amplification

5µL of the ligation product were transformed into XL1-Blue competent bacteria and bacteria were later grown on LB Agar (1083, Condalab) plates containing 1µg/mL ampicillin (624619, Laboratorios Normon) as described in the 'Transformation of plasmid DNA into competent bacteria' section. Individual ampicillin resistant colonies were picked and grown in 3mL LB Broth media (1231, Condalab) with 1µg/mL ampicillin overnight at 37ºC in a shaker Incubator OPAQ (10000-01068, OVAN). The following day, glycerol stocks of the samples were harvested and the plasmids were isolated using the QIAprep Spin Miniprep kit (27104, QIAGEN) following manufacturer's instructions. Plasmids were eluted in 50µL DEPC-Treated Water and quantified in a NanoDrop® ND-1000 spectrophotometer. Prior to sequencing, 50ng plasmid were amplified by PCR using specific primers for the plasmid (Table 3.9), and after cleaning the PCR product with ExoSAP-IT™ PCR Product Cleanup Reagent (78201, Applied Biosystems™), samples were Sanger sequenced, using both the forward and reverse primer (Table 3.9) in order to verify the correct cloning of the guides into the plasmid.

Table 3.9. Primers to amplify the genomic region of pX330 EGFP plasmid where the guides are cloned.

pX330 EGFP sequencing primers	Sequence (5'-3')
pX330 EGFP-F	GCCTGGTATCTTTATAGTCC
pX330 EGFP-R	CTTGATGTACTGCCAAGTGG

Once the cloning was verified and one colony was selected, bacteria from the glycerol stock were picked for further amplification in 300mL LB Broth media containing 1µg/mL ampicillin by incubation overnight in a shaker Incubator OPAQ. Plasmids were isolated using the QIAGEN Plasmid Maxi Kit (12162, QIAGEN).

3.3.3.7. Crispr/Cas9 guide selection

In order to predict the modification created by the guides in the genome and the impact at protein level, several transfections were performed prior to cell sorting. As described in 'Cell transfection with Turbofect' section, A549 cells were individually transfected with the guides targeting *HIF2α* (Table 3.8). 72h post-transfection, DNA was extracted and amplified by PCR using the primers listed in Table 3.10. To obtain enough amplified DNA (100ng), 4 amplifications were performed per sample. PCR product size was checked in a 1.5% agarose gel and further purified and concentrated prior to cloning into pGEM®-T Easy Vector, as described in 'Cloning into pGEM®-T Easy Vector'. Positive colonies were Sanger sequenced and analysed using BioEdit Sequence Alignment Editor [331] to see the modification at sequence level, and ExPaSy Translate tool to predict the impact of this genetic modification in protein translation.

Table 3.10. Specific primers to amplify the genomic region of interest of the guides.

HIF2α guides	Sequencing primers	Sequence (5'-3')
Guide 1 and 2	HIF2α_seq-F	GGGCCCCTCTCATGAATATC
	HIF2α_seq-R	ACTTCATGTCCATGCTGTGG

HIF2α genomic sequence was downloaded from Ensembl (https://www.ensembl.org/index.html) and manually modified according to Sanger sequencing results. This new sequence was translated using ExPaSy Translate tool (https://web.expasy.org/translate/). ExPaSy gave the amino acid sequence and the theoretical molecular weight of the proteins generated from the six open reading frames (three from the forward strand (5'-3') and another three from the reverse strand (3'-5')). This information was used to see the impact of each genomic modification at protein level. The guide which was predicted to generate the most promising modification was selected for cell transfection and cell sorting.

3.3.3.8. Cell transfection and cell sorting

Cells were transfected with the desired guide as described in 'Cell transfection' section. 72h post-transfection, cells were trypsinized and resuspended in Sorting buffer (Hank's Buffered Saline Solution (HBSS, BE10-547F, Lonza) containing 25mM HEPES (15630-056, Gibco™), 5mM EDTA and 1% BSA) to a final concentration of 1x10^6 cells/mL. Cells were sorted in a BD FACSJazz™ (BD Bioscience) in the Flow

Cytometry Facility of Achucarro Basque Centre for Neuroscience (Leioa, Spain) upon positive GFP expression, and each cell was seeded in a well of 96-well V-bottom Cellstar® cell culture plates (651180, Greiner) and allowed to grow.

3.3.3.9. Validation of cell clones

Individual cell clones were expanded and cells were seeded under normoxia or hypoxia for DNA, RNA and protein isolation, in order to validate the clones at DNA level by Sanger sequencing, at transcriptional level by qPCR and at protein level by western blot, as described in the corresponding sections. Genomic DNA was extracted with QIAamp DNA Mini Kit (51304, QIAGEN), amplified on the genomic regions of interest using specific primers (Table 3.10), run on an 1.5% agarose gel to verify the amplification and Sanger sequenced to detect mutations in *HIF2α* gene. Furthermore, predicted guide off-targets were also analysed at sequence level using the primers in Table 3.11.

Table 3.11. Primers to sequence the predicted off-targets of *HIF2α*-targeting guide 2.

Guide	Predicted off-target	Sequence (5'-3')
Guide 2 for HIF2α	FARP1_F	GCTGAGATTGGGGATTTTGA
	FARP1_R	TAGGTGACCACGTCCCTTTC
	ZCCHC17_F	AGCAGCTGCCTGAATGAGTT
	ZCCHC17_R	ATGGGAAAAGTGAGCACCAC
	CDK17_F	TACAGGTGTGAGCCATGCAC
	CDK17_R	GCTTCCATTTCTGGGCATT
	lncRNA462_F	GTGGACCTCAGGAAACCAAA
	lncRNA462_R	TTCCCCAGGAGGAAAGAGTT
	CCDC78_F	AGCCCAAGAACACCATGAAC
	CCDC78_R	GGGTCTCCCTGAAGCTATCC
	SLC35A4_F	ACCACCAGCCCCTTACTCTT
	SLC35A4_R	CTTGGTCAGCTCAGTCAGCA
	C3Orf22_F	GGGGCCTCTCCTAGAGACTG
	C3Orf22_R	GGAGGCAAAGTGATCATTCC
	IQCB1_F	CTGGTGGAAGAAGCTTGGAG
	IQCB1_R	GAAAACAGGGAAATGTCCTTCA

3.3.4. Extraction of nucleic acids

3.3.4.1. Genomic DNA extraction

Genomic DNA was extracted from 2x10^5 cells pellets with Nucleospin® Tissue Kit (740952, Macherey-Nagel) according to manufacturer's instructions. To extract the DNA of sorted clones prior to sequencing, QIAamp DNA Mini Kit was used instead. Both kits use proteinase K for cell lysis and DNA binding is based on silica membrane technology. DNA was eluted in DEPC-Treated Water and quantified with NanoDrop® ND-1000 spectrophotometer.

3.3.4.2. Plasmid DNA extraction

For plasmid DNA isolation, Miniprep and Maxiprep methods were performed. These methods had two steps, first bacterial lysis and then DNA isolation. For lower yields, QIAprep Spin Miniprep kit was used, starting from an overnight bacterial culture of 3mL and following manufacturer's instructions. For higher yields, QIAGEN Plasmid Maxi Kit was used, starting from an overnight bacterial culture of 300mL and following manufacturer's instructions. Isolated DNA was eluted DEPC-Treated Water and stored at -20ºC.

3.3.5. Polymerase chain reaction (PCR)

50ng DNA was amplified by mixing 2.5µL buffer 10x, 1µL $MgCl_2$, 0.5µL dNTPs, 0.5µL forward primer (10µM), 0.5µL reverse primer (10µM), 0.2µL BIOTAQ™ DNA Polymerase (Bio-21040, Bioline) and DEPC-Treated Water in a final volume of 25µL. The PCR reaction was carried out with a single first denaturalization step of 1 min at 95ºC, followed by another denaturalization step of 30 sec at 95ºC, an annealing step of 30 sec at the optimized temperature for each primer pair, and an elongation step of 45 sec at 72ºC. These three steps were repeated for 35 times prior to a final elongation step of 3 min at 72ºC. PCR reaction was performed in a Veriti Thermal Cycler (Applied Biosystems™).

3.3.6. DNA gel electrophoresis

Agarose gels at varying concentrations of 0.8-2% were prepared to effectively separate DNA fragments according to their size. GelRed® Nucleic Acid Stain (41003, Biotium) fluorescent nucleic acid dye was used at 1:10000 concentration to enable visualization of DNA bands under UV light. Along with loaded samples, ϕX174 DNA-Hae III ladder was used (N3026S, NEB) to detect bands in the range of 100-1000bp while 1kb DNA Ladder (N3232L, NEB) was used for bigger bands (up to 10kb). Samples were run at 110V for 45 min.

3.3.7. Cloning into pGEM®-T Easy Vector

PCR amplicons were purified using NucleoSpin® Gel and PCR Clean-Up (740609, Macherey-Nagel), eluted in 20µL DEPC-Treated Water but further concentrated to 10µL using a Savant™ DNA SpeedVac™ (13442549, Thermo Fisher Scientific™). PCR product was cloned into pGEM®-T Easy Vector (A1360, Promega) by mixing 5µL 2x Rapid Ligation Buffer, 1µL (50ng) pGEM®-T Easy Vector, 3µL concentrated PCR product and 1µL T4 DNA Ligase (3U/µL). The reaction was incubated 1h at RT. Ligation product was transformed into competent bacteria (see section ‘Transformation of plasmid DNA into competent bacteria') and 150µL of these bacteria were plated in LB Agar plates containing 1µg/mL ampicillin and left growing overnight at 37ºC. Resistant colonies were picked, put into 50µL distilled H_2O and boiled for 5 min at 95ºC. To ensure the presence of the insert, 2µL were used as template for the PCR using vector-specific primers (Table 3.12). These primers surround the cloning region, so that the presence of the insert can be easily distinguished by the PCR product size in an agarose gel.

Table 3.12. Primers to amplify the clonig region of pGEM®-T Easy Vector.

pGEM®-T Easy Vector primers	Sequence (5'-3')
M13-F	GTAAAACGACGGCCAGT
M13-R	CAGGAAACAGCTATGAC

3.3.8. Sanger Sequencing

3.3.8.1. PCR product purification

After amplifying the desired fragments by PCR and verifying the band size on an agarose gel, PCR products were cleaned with ExoSAP-IT™ PCR Product Cleanup Reagent. Briefly, 2.5µL PCR product were mixed with 1µL ExoSAP and incubated 15 min at 37ºC followed by 15 min at 80ºC. Cleaned-up products were diluted 1:10 in RNAse and DNAse free water before proceeding with Sanger Sequencing reaction. Alternatively, in some cases PCR clean-up was performed by extracting the DNA fragment directly from the gel, upon UV visualization, and performing a silica membrane-based purification using QIAquick Gel Extraction Kit.

3.3.8.2. Sanger sequencing reaction

For Sanger sequencing reaction BigDye® Terminator v3.1 Cycle Sequencing Kit's (4337454, Applied Biosystems™) was used. First, 7.05µL of the purified PCR product were mixed with 0.5µL Ready reaction premix 2.5x, 1.25µL BigDye sequencing buffer 5x and 1.5µL sequencing primer (5µM). The PCR conditions used were: 3 min at 94ºC for initial denaturalization, 25 cycles of 10 sec at 96ºC, 5 sec at 50ºC and 4 min at 60ºC and a final cool down to 4ºC. Samples were sequenced in an ABI PRISM 3130 genetic analyzer (313001R, Applied Biosystems™) in Biodonostia Health Research Institute's Genomic Platform Service. Finally, sequences were analysed using Mutation Surveyor® software (SoftGenetics®) and BioEdit Sequence Alignment Editor [331].

3.3.9. Production of competent bacteria

Competent bacteria were produced in-house from XL1-Blue *Escherichia coli* strain using a $CaCl_2$ and glycerol-based treatment. To achieve this, XL1-Blue bacteria were grown overnight in 3mL LB Broth media in a shaker Incubator OPAQ. The following day, grown bacteria (3mL) were added to 300mL LB Broth media for further growth until the optical density at 600nm was between 0.5 and 0.8, so they were still in the exponential growing phase. Absorbance measurement was performed every hour by removing 1mL of the culture and measuring in a GeneQuant pro spectrophotometer (Amersham). Then, bacteria were poured into 50mL centrifuge tubes and kept on ice for 10 min, prior to centrifugation at 2600rpm for 10 min at 4ºC. Supernatant was discarded and each bacteria pellet was resuspended in 10mL cold sterile solution of 100mM $CaCl_2$ and 15% glycerol (131339, PanReac). Cells were pooled into two tubes (30mL/tube) and incubated on ice for 30 min. After centrifuging at 2600rpm for 10 min at 4ºC, each bacteria pellet was resuspended in 6mL sterile solution of 100mM $CaCl_2$ and 15% glycerol. 350µL bacteria were aliquoted into 1.5mL tubes on ice and placed immediately in a -80ºC freezer.

3.3.10. Transformation of plasmid DNA into competent bacteria

XL1-Blue competent bacteria were defrosted on ice prior to plasmid transformation. Plasmid transformation was carried out by mixing 10µL pGEM®-T vector or 5µL pX330 EGFP plasmid and bacteria, following an incubation of 30 min on ice, a heat shock of 2 min at 42ºC and incubation for additional 3 min on ice. For pGEM®-T transformation, 250µL warm LB Broth media were added to bacteria, whereas for pX330 EGFP transformation 1mL warm LB Broth media was added, without antibiotics in both cases, and incubated for 1h at 37ºC in a shaker Incubator OPAQ for recovery. Afterwards, different volumes of bacteria were seeded in LB Agar plates containing 1µg/mL ampicillin and left to grow overnight at 37ºC.

3.3.11. Cell transfection

3.3.11.1. Cell transfection with Turbofect

For guide selection, transfections were performed in 6-well plates. $1.5x10^5$ A549 cells were seeded in each well and allow attaching for 8h. Then, 1.1µg plasmid was diluted in 400µL serum free (SF) DMEM/F12 containing 4.5µL vortexed TurboFect™ Transfection Reagent (R0533, Thermo Fisher Scientific™) and kept 20 min at RT. Cell culture media of cells was replaced with 450µL complete DMEM/F12 and plasmid was added dropwise. The next day, culture media was replaced with 2mL complete DMEM/F12.

3.3.11.2. Cell transfection with Fugene

Due to the toxicity TurboFect™ Transfection Reagent exerted on 786-0 cells, these cells were transfected using FuGENE® HD Transfection Reagent (E2311, Promega) (6:1 ratio) prior to cell sorting.

Briefly, 8.4x10^5 786-0 cells were seeded in duplicate in 10cm^2 plates. 8h later, transfection mix was prepared by mixing 500µL Opti-MEM™ I Reduced Serum Medium (31985070, Gibco™), 4.2µg plasmid and 25.2µL FuGENE® HD Transfection Reagent (E2311, Promega) and kept 10 min at RT. Then, cell culture media was replaced with 4.5mL complete DMEM and DNA-lipid complexes were added dropwise. The following day, media was replaced with 10mL complete DMEM.

3.3.11.3. Cell transfection with Oligofectamine

Transfection of siRNA for HIF2α (siHIF2α, a pool of three siRNAs, Dharmacon™) or siRNA control (siCON, Dharmacon™) (Table 3.13) was performed in Opti-MEM™ I Reduced Serum Medium at a final concentration of 20nM. To check the duration of siHIF2α inhibition, transfection was performed in 6-well plates in a final volume of 2mL Opti-MEM™ I Reduced Serum Medium. Briefly, on the one side, 500µL Opti-MEM™ I Reduced Serum Medium were mixed with siRNA (siCON or siHIF2α) (Mix A), and on the other side, 485µL Opti-MEM™ I Reduced Serum Medium were mixed with 15µL Oligofectamine™ Transfection Reagent (12252011, Invitrogen™) (Mix B). Both mixes were kept 5 min at RT. Then, 500µL Mix B were added to Mix A, and incubated for 20 min at RT. Meanwhile, cells were trypsinized and counted. 1mL of Mix A+B was put in each 6-well plate well and cells were further seeded in another 1mL Opti-MEM™ I Reduced Serum Medium. 5h later 20% FBS was added, and the following day media was replaced with complete DMEM.

For migration and invasion experiments, transfection was performed in Opti-MEM™ I Reduced Serum Medium at a final concentration of 20nM in a final volume of 200µL. As explained above, Mix A and Mix B were prepared. After 5 min at RT, Mix B was added to Mix A and incubated for 20 min at RT. During this time cells were trypsinized and counted. 100µL Mix A+B was added in each well of the 96-well plate, and 1.2x10^4 786-0 WT cells were seeded in additional 100µL Opti-MEM™ I Reduced Serum Medium per well. Similarly, 5h later 20% FBS was added and the following day the scratch was performed as explained in 'Migration assay' and 'Invasion assay' sections.

Table 3.13. siCON and siHIF2α sequences. TT* overhang.

siRNA	Sequence (5'-3')
siCON	ACGACACGCAGGUCGUCAUTT*
siHIF2α	TAACGACCTGAAGATTGAATT*
	CAAGCCACTGAGCGCAAATTT*
	TGAATTCTACCATGCGCTATT*

3.3.12. Cell proliferation

CyQUANT™ Cell Proliferation Assay (C7026, Invitrogen™) kit was used to determine cell proliferation. The main component of the assay is CyQUANT® GR, a dye that exhibits strong fluorescence when bound to nucleic acids. This way, it is possible to measure DNA content, and indirectly, cell presence. The assay was conducted on cells grown in 96-well black microplates (165305, Thermo Fisher Scientific™). 250, 500, 1000 or 3000 cells per well were seeded in triplicate and left on culture. At the desired time point, medium from each well was removed and plates were frozen at -80ºC for at least 24h. The day of the assay, 1x lysis and cell dye solution was prepared by diluting the 20x cell-lysis buffer stock solution and the 400x CyQUANT® GR dye to 1x each in MilliQ water. Plates were thawed and cells were incubated with 200µL of the prepared 1x CyQUANT® GR dye/cell-lysis buffer for 5 min in the darkness. Fluorescence of samples was measured using a fluorescence microplate reader (SpectraMax M2^e, Molecular Devices) at excitation/emission wavelengths 485/538 nm.

3.3.13. Colony formation assay

1000 cells were plated in 10cm^2 plates and cultured under normoxia or 0.1% hypoxia for 10 days. Media was removed and Coomassie blue solution (H_2O containing 50% methanol, 7% acetic acid glacial (A/0360/PB17, Thermo Fisher Scientific™) and 0.1% Brillant Blue R (B7920, Sigma-Aldrich)) was added to fix and stain the colonies for 2h. Then, Coomassie blue solution was recovered and plates were washed with tap water. Plates were allowed to dry overnight and scanned using UMAX MagicScan software. Colony count was manually performed using Fiji Image J Software.

3.3.14. Spheroids

3.3.14.1. Spheroid formation

2500 cells per well were seeded in 96-well Clear Round Bottom Ultra-Low Attachment Microplates (7007, Corning®) in a final volume of 200µL. Cells were centrifuged at 2000rpm for 10 min to encourage the formation of a single spheroid per well. 18 replicates of each condition were plated in each biological replicate. When PT2385's effect was tested, the inhibitor was added 24h after spheroids generation at a final concentration of 1µM. Every three days, 100µL cell culture old media was replaced with fresh and every two days spheroids were photographed in an EVOS™ XL Core Imaging System (Thermo Fisher Scientific™) at 10x magnification. Spheroids were cultured for 15 days before the final analysis. To measure the volume and circularity of spheroids Fiji Image J Software was used. Spheroid area was calculated using a previously published macro [332]. Spheroid area was used to determine spheroid radius ($R = \sqrt{(area/\pi)}$), from which the volume ($V = (4/3)\ \pi R^3$) was calculated.

3.3.14.2. Spheroid disaggregation

At day 15, spheroids were disaggregated and counted. 10 spheroids per condition were combined into 1.5mL tubes and let them sink. Media was removed and 200µL PBS was added to wash. After letting spheroids to sink again, PBS was removed very carefully to not disturb spheroids and 100µL Accumax™ solution (A7089, Sigma-Aldrich) was added per tube and incubated for 10 min at 37ºC. Spheroids were resuspended and returned to 37ºC for another 5 min to ensure complete disaggregation. After dissociation, cells were washed with 200µL PBS by centrifuging at 300g for 5 min at 4ºC. PBS was removed, cells were resuspended in Trypan Blue Solution (T8154, Sigma-Aldrich) and counted.

3.3.15. Migration assay

1.2×10^4 786-0 cells or 2×10^4 RCC4 cells were seeded per well in 96-well ImageLock™ plates (4379, Essen BioScience) and incubated for 24h. A minimum of 18 wells per condition were seeded in each biological replicate. If the effect of PT2385 was tested, the compound was added to the wells once the cells were attached. The WoundMaker™ (4563, Essen BioScience) is a 96-pin mechanical device designed to create 700-800µm wide homogeneous wounds in cell monolayers on 96-well ImageLock™ plates. Prior to use after storage, the WoundMaker™ lid was washed with sterile distilled water for 5 min and with 70% ethanol for another 5 min. After washing, the scratch was performed to create precise wounds in all wells of the ImageLock™ plate. After wounding, cells were washed with fresh media to prevent dislodged cells from settling and reattaching. When PT2385 was tested, the new media contained 1µM or 10µM PT2385. Once the wound was made, plates were placed into the IncuCyte ZOOM® for 48h in the case of 786-0 cells or 72h in the case of RCC4 cells. Scanning was performed using a 10x objective and scheduled every 2h. After using the WoundMaker™ the lid was washed with 1% Rely+ON™ Virkon™ (330003, LANXESS) for 5 min, sterile distilled water for 5 min and finally with 70% ethanol for another 5 min. Migration ability of different cells and conditions was analysed through two integrated metrics that the IncuCyte™ Software calculates based on the processed images: wound width and wound confluence. Wound width represents the average distance (µm) between the leading edge of the population of migrating cells (scratch wound mask) within an image. Wound confluence determines the percentage of wound area that is occupied by cells, and it relies on the initial scratch wound mask to differentiate the wounded from the non-wounded region. Debris or other matter within the wound is quantified as confluence and is not background subtracted. Therefore, the wound confluence values at the initial time point may not be 0%.

3.3.16. Invasion assay

96-well ImageLock™ plate wells were coated with a thin layer of Matrigel® Growth Factor Reduced Basement Membrane Matrix (354230, Corning®). To this end, Matrigel® stock solution was dissolved in cold cell culture media to a final concentration of 100µg/mL. Wells were coated with 50µL of the solution and the plate was placed in a 37ºC incubator, 5% CO_2 overnight. Matrigel® was removed and, either $1.2x10^4$ cells in the case of the 786-0 cell line or $2x10^4$ cells in the case of the RCC4 cell line were seeded per well and incubated for 24h. In this case, a minimum of 10 wells per condition were used per biological replicate. When necessary, PT2385 was added to the wells once the cells were attached. After this time, the scratch was performed to create precise wounds in all wells of the ImageLock™ plate. Wells were washed once with cell culture media and 50µL Matrigel® (8mg/mL) was added to each well carefully, avoiding the formation of bubbles. The plate was placed in the incubator for 30 min prior to the addition of 100µL cell culture media containing PT2385 or not. The plate was then placed into the IncuCyte ZOOM® for 5 days. Scanning was performed using a 10x objective and scheduled every 4h. The WoundMaker™ was washed before and after using as described in 'Migration assay'. The invasion ability was analysed using the relative wound density (RWD). Like wound confluence, RWD also relies on the initial scratch wound mask to differentiate between cell-occupied and cell-free regions of the image, because it calculates the density of the wound region relative to the density of the cell region. This parameter is the only recommended metric for cell invasion because 1) the mild texture of the ECM can hinder the ability of the analysis algorithm to apply an appropriate initial scratch wound mask and confluence mask and consequently result in a misleading wound confluence metric, and 2) cells invading through a 3D matrix usually exhibit an elongated phenotype with filopodia that extend into the ECM. Furthermore, one leader cell is generally followed by numerous other cells, forming tracts, as opposed to a leading edge of cells seen in a migration assay. For this reason, the scratch wound masks may not best represent the invading population and wound width measure can thus be inaccurate and misleading.

3.3.17. Seahorse metabolic assay

$2x10^4$ cells per well were seeded in Seahorse XF96 V3 PS Cell Culture Microplates (101085-004, Agilent Technologies) 24h prior to the experiment. If PT2385 was tested, 1µM or 10µM PT2385 was added to cell cultures once the cells were attached. A minimum of 8 wells per condition were seeded in each experiment. One Seahorse XFe 96 Extracellular Flux Assay calibration plate was filled with 200µL MilliQ water and 25mL Sehorse XF Calibrant pH 7.4 (100840-000, Agilent Technologies) were aliquoted into a tube per run. Both the plate and tube were incubated overnight in a 37ºC, non-CO_2 Seahorse chamber. The day of the assay, MilliQ water from the calibration plate was replaced with 200µL

Sehorse XF Calibrant pH 7.4 and left in the 37ºC, non-CO_2 Seahorse chamber for 45-60 min. 100mL Seahorse XF DMEM media pH 7.4 (103575-100, Agilent Technologies) was supplemented with 10mM glucose (G8769, Sigma-Aldrich), 2mM glutamine (17-605C, Lonza) and 1mM sodium pyruvate (11360070, Gibco™) final concentrations to generate the working Seahorse media. Cells were washed twice with warmed Seahorse media and additional 155µL Seahorse media per well was added before placing the cells in the 37ºC, non-CO_2 Seahorse chamber for 1h. Meanwhile, oligomycin, carbonyl cyanide-4 (trifluoromethoxy) phenylhydrazine (FCCP) and rotenone/antimycin (Rot/Ant) mix drugs (103015-100, Agilent Technologies) were resuspended as per manufacturer's instructions and prepared in Seahorse media 8x, 9x and 10x concentrated, respectively, so that the final concentration in the cells' plate was 2µM for 786-0 and 1µM for RCC4 oligomycin, 0.5µM FCCP and 0.5µM Rot/Ant. After removing possible bubbles from the calibration plate, 25µL drug per well was loaded. Seahorse XFe 96 Extracellular flux Analyzer (Agilent Technologies) was used to run the XF Cell Mito Stress Test assay.

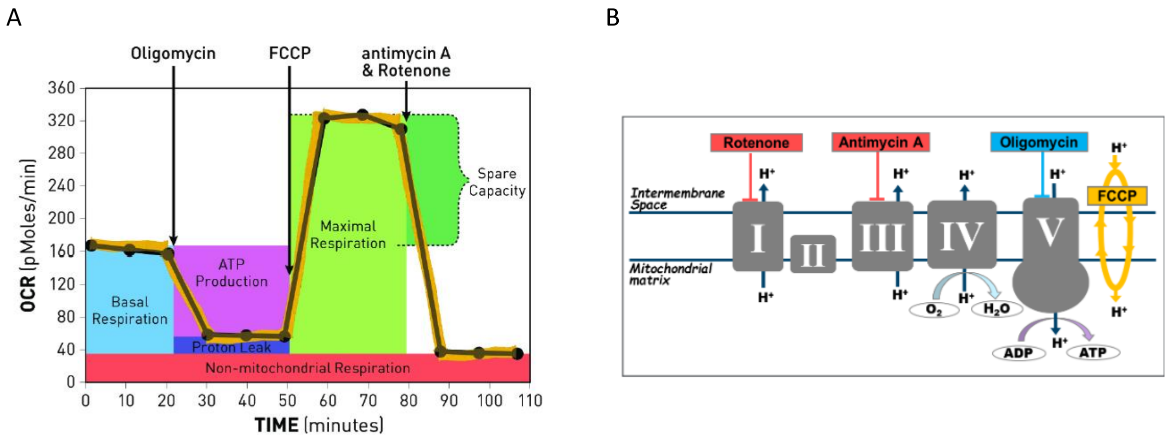

Figure 3.5. A) Representative diagram of Seahorse OCR results after the injection of the drugs. B) Mitochondrial ETC. Diagram from Agilent Seahorse XF Cell Mito Stress Test Kit User Guide.

Oxygen consumption profiles were determined via measurements prior to and following sequential injection of oligomycin, FCCP and Rot/Ant. Oligomycin blocks the ATP synthase (complex V), forcing the basal oxygen consumption level drop to its minimum. It is therefore used to obtain the level of oxygen consumption that is used for ATP synthesis. Following the administration of oligomycin, cells have to rely on glycolysis for energy production. FCCP is a proton ionophore, so its injection disrupts the proton gradient and the mitochondrial membrane potential. It increases proton conductance, forcing the oxygen consumption by complex IV to reach its peak. But the collapse of the mitochondrial membrane potential leads to a rapid consumption of energy and oxygen without the generation of

ATP. Both oxygen consumption rate (OCR) and extracellular acidification rate (ECAR) will increase in this case, OCR due to uncoupling, and ECAR due to the cells' effort to sustain their energy levels by using glycolysis to generate ATP. Rotenone and antimycin A inhibit complexes I and III, respectively. These two drugs are added to determine non-mitochondrial respiration.

After the assay, media was removed and plates were stored at -80ºC for CyQUANT™ Cell Proliferation Assay. OCR and ECAR values were normalized to cell viability values, determined by Cyquant fluorescence intensity.

3.3.18. Luciferase positive cell line generation

$2x10^5$ 786-0 WT and 786-0 KO cells were seeded in 24-well plates. After 24h, media was replaced with fresh and cells were transduced with CMV-Luciferase (firefly) lentiviral particles (LVP325-PBS, Amsbio) at a multiplicity of infection (MOI) of 125, as per manufacturer's instructions. 72h after the infection, cells were transferred into a 6-well plate and media was replaced with media containing 2µg/mL puromycin (A1113803, GIBCO™) for selection. Due to the high cell death generated by puromycin, the concentration was lowered to 0.5µg/mL, and selection was carried out during two weeks. Cells were assayed for luciferase activity by addition of 100µg/µL Beetle Luciferin, Potassium Salt (E1603, Promega) and measuring light in an ImageQuant LAS 4000 Mini device. Successfully infected cells were further amplified to inject into the mice (here after, 786-0 WT Luc^+ or 786-0 KO Luc^+ cells).

3.3.19. *In vivo* metastasis model

Procedures were carried out according to the boundaries and guidelines of PPL licence 30-3197 under the Home Office license for Animal testing and research. 4-5 weeks old female non-obese diabetic, severe combined immunodeficient (NOD SCID) mice were used for the tail vein injection. These mice are characterized by an absence of functional T cells and B cells, whereas their macrophage and NK cell population are intact. 10 mice per group were injected with $5x10^5$ 786-0 WT Luc^+ or 786-0 KO Luc^+ cells in 100µL PBS. Briefly, mice were warmed in a hot box for 1h to dilate the vessels and later anesthetized with isoflurane prior to the tail vein injection of tumour cells using insulin needle to avoid clumping of cells and damage to veins. After the injection, mice were weighted and monitored until full recovery. Mouse welfare changes were confirmed daily assessing behaviour, grooming and mobility changes, as well as weighting them twice per week at least. Imaging of metastasis was carried out every 7 days for the first 4 weeks from the day of the injection, then, according to licence boundaries, in the last two weeks of endpoint tumour growth (licence permitted six imaging events), in an IVIS® Lumina LT Series III In Vivo Imaging System (CLS136331, PerkinElmer) using a Living Image® 4.5.5 Software. Prior to bioluminescence image acquisition, mice were anesthetized with isoflurane and intraperitoneally injected with 5mg Beetle Luciferin, Potassium Salt per 20g weight diluted in 100µL PBS. Five minutes after the injection, once the luciferin gets into the system, mice were imaged.

At the end of the experiment (16th week) mice were killed and lungs were injected with 100µg/µL Beetle Luciferin, Potassium Salt to identify the metastasis.

3.3.20. Immunofluorescence for lipid droplets

786-0 WT and 786-0 KO cells were seeded on borosilicate glass coverslips (631-0150, VWR Collection) and placed into normoxia or 0.1% hypoxia for 48h. Positive controls were incubated in normoxia with 200µM Oleate-BSA (O3008, Sigma-Aldrich) diluted in cell culture media for 24h prior to fixation. Oleic acid is a potent inducer of triglyceride synthesis and storage, but as it is a free fatty acid with detergent-like properties and poorly soluble in aqueous media, binding to BSA is necessary for its uptake. After this time, cells were washed with PBS and fixed in 4% paraformaldehyde (PFA, 28908, Thermo Fisher Scientific™) for 10 min at RT. Cells were later washed three times with PBS containing Hoechst 33342 (H3570, Invitrogen™) at 1:1000 concentration and incubated with 0.1µg/mL Nile Red (19123, Sigma-Aldrich) for 10 min at RT in the darkness. Nile Red is used to localize and quantify neutral lipids within the cells. Coverslips were washed twice with PBS containing Hoechst 33342 and one last time with PBS. Coverslips were mounted with Vectashield® Mounting Medium for Fluorescence without DAPI (H-1000, Vector Labs) and sealed with nail polish. Slides were imaged in a Zeiss 880 Inverted confocal microscope (Zeiss) using a ZEN fluorescence microscopy system (Zeiss) and a 63x Plan-Apochromat objective. Laser properties, acquisition mode and detectors were manually adjusted for each experiment.

3.3.21. Flow cytometry for lipid droplets

$6x10^4$ 786-0 WT and 786-0 KO cells were incubated in normoxia or 0.1% hypoxia for 48h. Positive controls were incubated in normoxia with 200µM Oleate-BSA (O3008, Sigma-Aldrich) diluted in cell culture media for 24h prior to fixation. After this time, cells were trypsinized and centrifuged at 300g for 5 min at RT. Cell pellet was washed with PBS and fixed in 4% PFA for 10 min at RT. Cells were later washed three times with PBS by serial centrifugations of 300g for 5 min. Cell pellets were resuspended in 500µL of Nile Red dye at 0.1µg/mL concentration and kept 10 min at RT in the darkness. After the incubation with Nile Red, cells were washed with PBS three times before being resuspended in 500µL of PBS for flow cytometry analysis. Cells were analysed in an Attune NxT Analyser (Thermo Fisher Scientific™). Briefly, first Forward Scatter Area (FSC-A) and Side Scatter Area (SSC-A) distribution was used to select living cells and discard cell debris. FSC intensity is proportional to the diameter of the cell, thus it gives information about cell size, whereas SSC provides information about the internal complexity (granularity) of the cells. Selected cells were plotted in FSC-A and FSC-H (FSC-Height) graph. This combination of axis was used to discard doublets, because doublets have increased area whilst similar height to single cells. Single cells were then plotted in a histogram, and the mean intensity value of the positive staining was recorded for each cell population.

3.4. Results

3.4.1. Generation of 786-0 HIF2α KO cell line using Crispr/Cas9

3.4.1.1. HIF2α targeting guides are predicted to inactivate the gene

With the aim of studying the role of HIF2α in renal cancer Crispr/Cas9 gene edition technology was used to generate a stable KO in 786-0 cells. This technique allows the specific editing of the genome with a complete deletion of the gene of interest, instead of the partial knock down obtained when using siRNA or shRNA [333]. To achieve a suitable model with a clean background, first, the modifications generated by *HIF2α* targeting guide 1 and guide 2 were studied as explained in 'Crispr/Cas9 guide selection'.

As depicted in Figure 3.6, not all the ampicillin resistant colonies had been transformed with pGEM®-T Easy Vector containing the insert. Lower bands correspond to the amplification product of those colonies that did not incorporate pGEM®-T Easy Vector with the insert of interest. This means that the vector circularized without the insert and that bacteria were transformed with an empty vector.

pGEM-T Easy + HIF2α guide 1

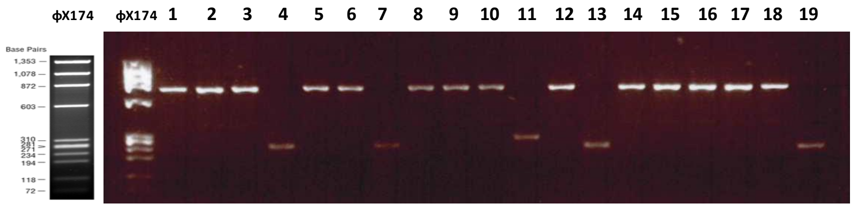
ϕX174
ϕX174
1
2
3
4
5
6
7
8
9
10
11
12
13
14
15
16
17
18
19
Base Pairs
1,353
1,078
872
603
310
281
271
234
194
118
72

pGEM-T Easy + HIF2α guide 2

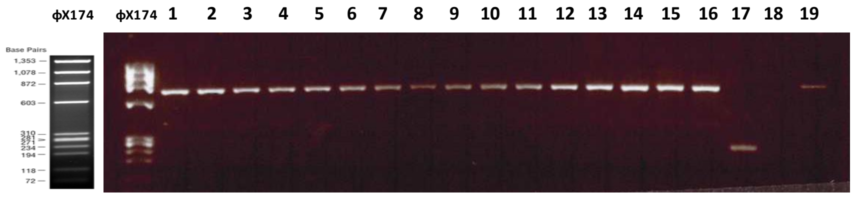
ϕX174
ϕX174
1
2
3
4
5
6
7
8
9
10
11
12
13
14
15
16
17
18
19
Base Pairs
1,353
1,078
872
603
310
281
271
234
194
118
72

Figure 3.6. PCR amplification of bacterial DNA previously transformed with pGEM®-T Easy Vector containing the amplified product of the HIF2α guide 1 or guide 2 targeted genome region.

Positive colonies were further processed for Sanger sequencing. As the DNA cloned into pGEM®-T Easy Vector came from a population of non-sorted cells, some cells might had been successfully transfected with *HIF2α* targeting guides, while others might not. Therefore, not all the cells would have *HIF2α* gene modified. In fact, most of the sequenced PCR products had *HIF2α* gene intact. Among the clones harbouring *HIF2α* alterations, guide 1 generated three different deletions in *HIF2α* gene: one of 174bp just after the guide targeting sequence, another one of the entire guide-targeting sequence, and the last one of the first 10bp of the target sequence. While guide 2 created a deletion of the first 11bp of the target sequence.

According to ExPaSy Translate tool, all the modifications that guide 1 and guide 2 could make would generate a protein without the first amino acids of the bHLH domain, in some cases part of the PAS sequence could also be lost. In any case, without bHLH domain, HIF2α cannot bind to the DNA, and therefore it cannot transactivate gene expression.

As both guides were able to modify *HIF2α* gene to the extent that the modification would generate a non-functional protein if translated, 786-0 cells were transfected with both guide 1 or guide 2 targeting *HIF2α*.

3.4.1.2. Successful generation of a 786-0 HIF2α KO cell line

After cell sorting, cells transfected with guide 1 were not able to grow from a single cell. Single cell growth is essential to have a population of cells harbouring the same mutation. Nevertheless, although only 4% of the total cell population transfected with guide 2 were GFP$^+$, it was enough to get seven possible HIF2α KO clones. DNA from these seven clones was extracted, amplified using primers covering the guide region (Table 3.10) and run on an agarose gel (Figure 3.7).

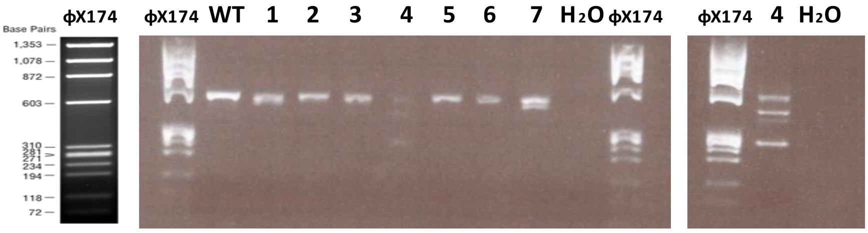

Figure 3.7. Agarose gel of the 786-0 parental cell (WT) and the seven possible HIF2α KO clones.

Clone 4 and clone 7 were discarded because of the presence of several amplification products. Clones 1, 2, 3, 5 and 6 were Sanger sequenced. According to Mutation Surveyor, clone 3 appeared to have a homozygous deletion of an adenine (A) in 336 position, as shown in Figure 3.8A, whereas clone 5 and clone 6 harboured a heterozygous deletion of the same A (Figure 3.8B and 3.8C). The rest of the sequenced clones did have some sequence alteration, but they were discarded from further analysis due to unclear modification at sequence level.

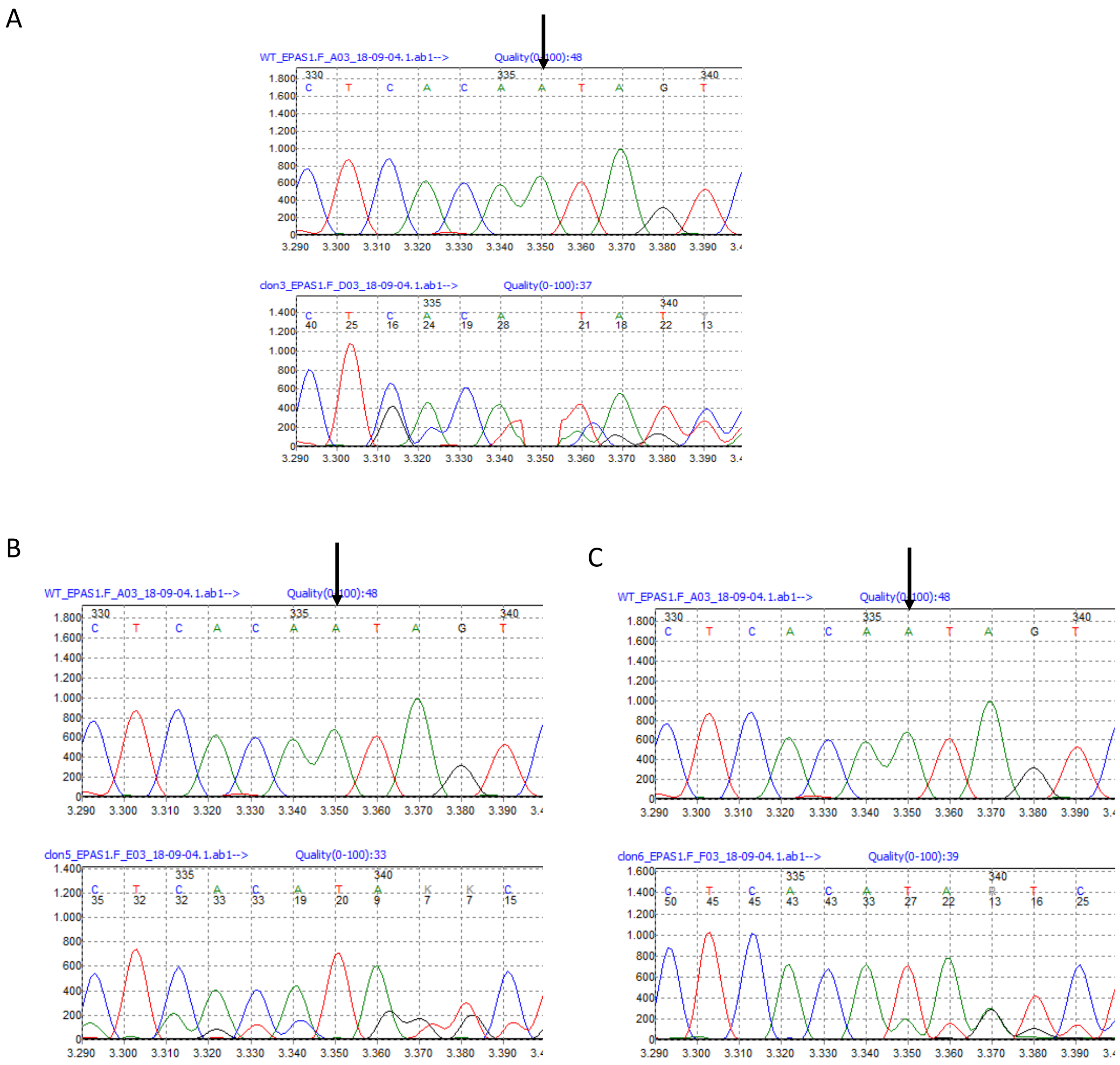

Figure 3.8. Sanger sequencing results of clone 3 (A), clone 5 (B) and clone 6 (C) analysed with Mutation Surveyor.

Next, clone 3, clone 5 and clone 6 were exposed to normoxia or 1% hypoxia for 10h, 24h or 48h to analyse HIF2α at mRNA and protein level. As illustrated in Figure 3.9A, clone 3 had the lowest *HIF2α* mRNA levels at every tested time point, whereas clone 5 and clone 6 showed between 3- and 5-fold higher levels than clone 3 with a tend to increase at 24h and 48h, respectively, under hypoxia. However, western blot revealed that only clone 3 was KO for HIF2α (named from now on 786-0 KO) (Figure 3.9B).

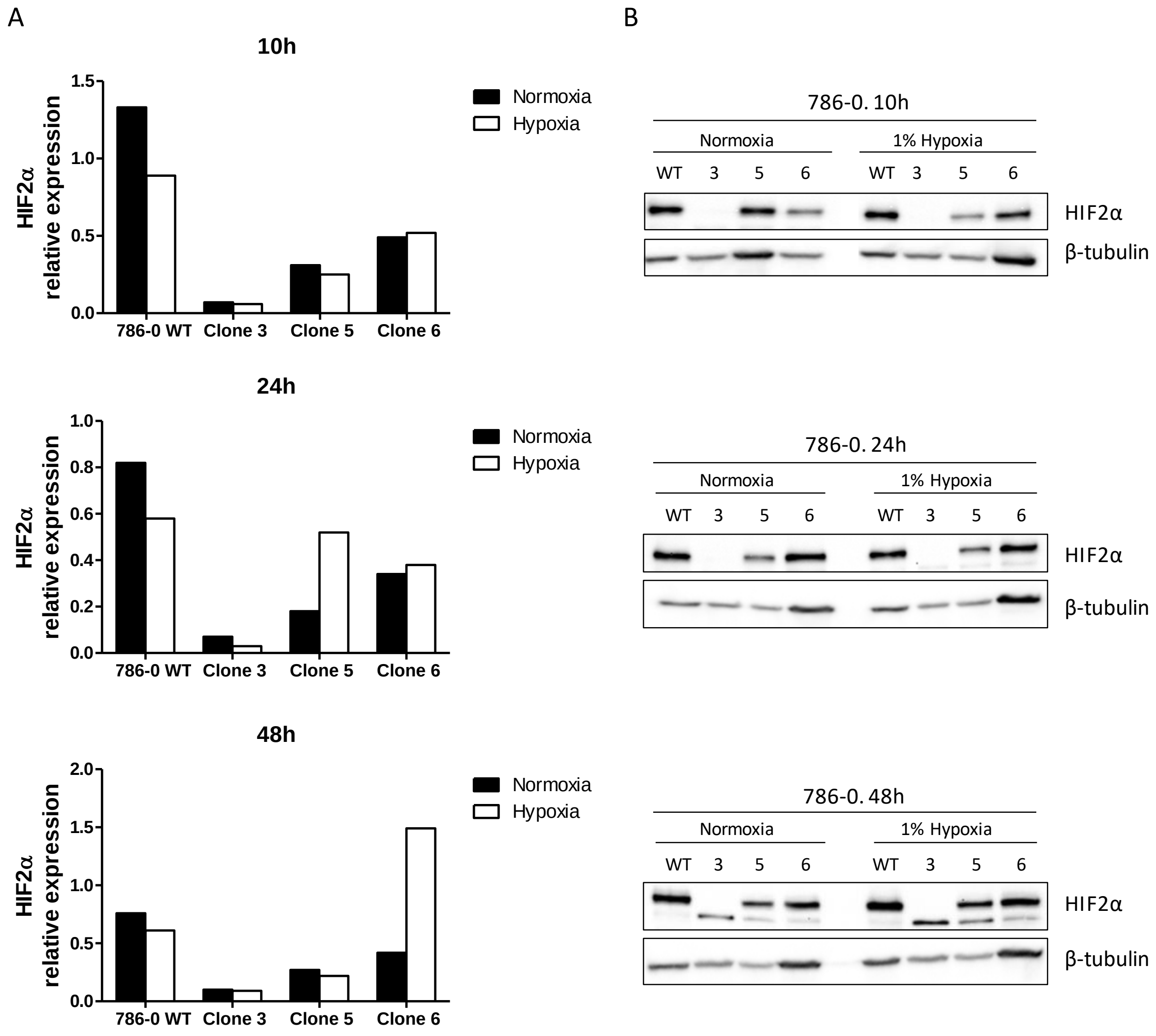

Figure 3.9. HIF2α mRNA (A) and protein (B) levels at 10h, 24h and 48h in 786-0 wild type (786-0 WT, WT), clone 3 (3), clone 5 (5) and clone 6 (6) cultured under normoxia or 1% hypoxia. n=1.

To further validate clone 3, HIF2α guide 2 predicted off-targets were analysed. Together with the guide sequence and the score, CRISPR Design Tool gives the possible genome off-targets sites of the guide. These off-targets sites are genomic regions with high similarity to the target sequence, and therefore, the guide could bind and make an inappropriate modification in those regions. HIF2α guide 2 had eight predicted exonic off-target sites which were amplified and analysed by Sanger sequencing. All of them appeared to be intact, so HIF2α guide 2 did not make any additional modification, as far as analysed, in these cells.

Despite not knowing the genomic modification caused by the HIF2α guide 2 in clones 1 and 2, they were also tested for HIF2α expression by western blot (Figure 3.10A). Both clones expressed HIF2α in normoxia and 0.1% hypoxia, but GLUT1, a known HIF2α target gene, was not as highly expressed as in the parental cell line (786-0 WT), suggesting that these two clones could be knock down. To explore this idea further, gene expression of several HIF2α targets was tested in these cells by qPCR (Figure 3.10B). *HIF2α* levels were 3- and 5-fold higher in both clones compared to 786-0 KO, whereas *GLUT1* levels were similar to 786-0 WT cells (p>0.05). On the other hand, *VEGFA* and fibronectin 1 (*FN1*) levels were close to those observed in 786-0 KO cells (p>0.05). These results suggested that clone 1 and clone 2 had an intermediate phenotype between 786-0 WT and 786-0 KO cells.

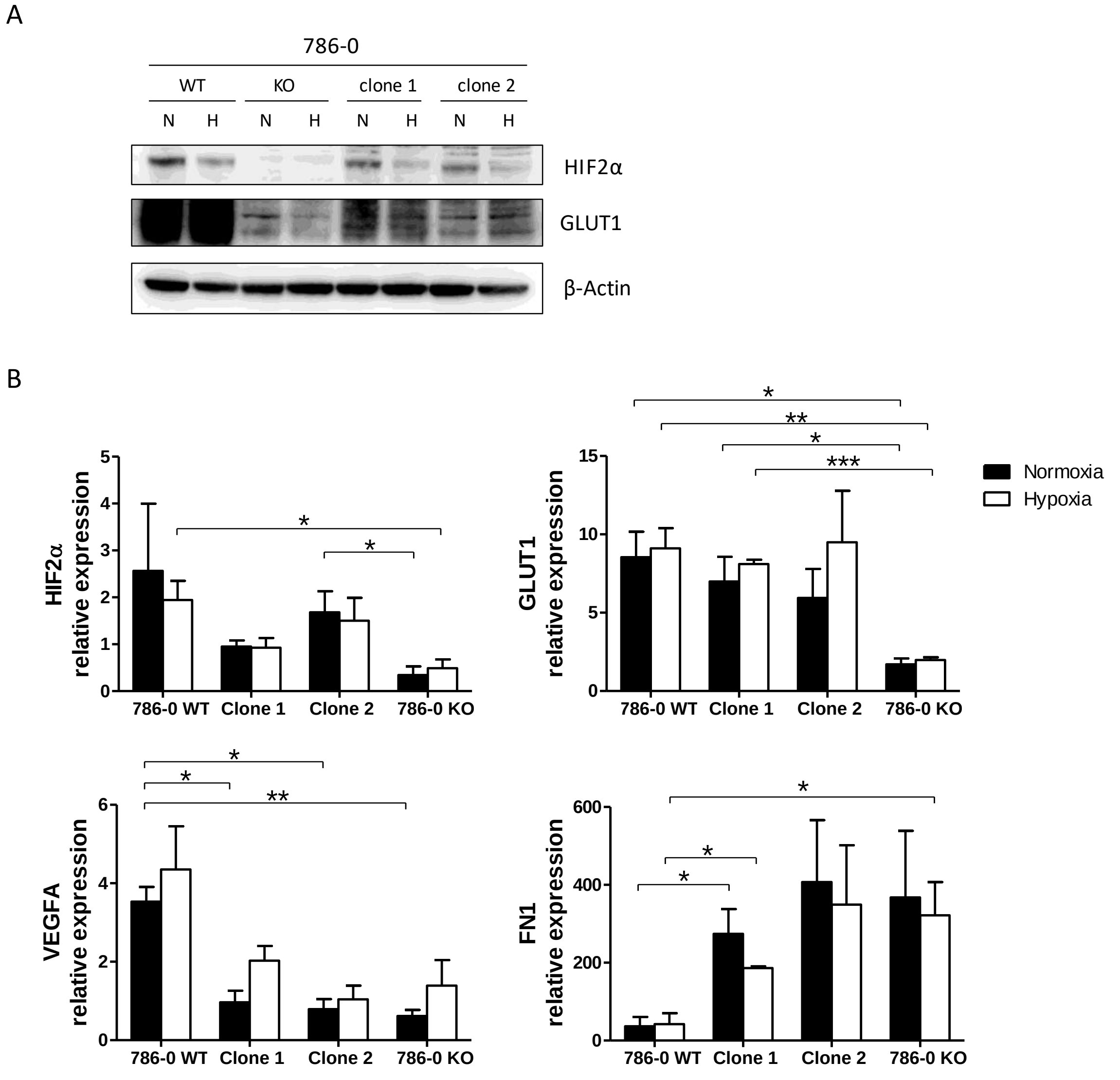

Figure 3.10. A) HIF2α and GLUT1 proteins levels in 786-0 WT (WT), 786-0 KO (KO), clone 1 and clone 2 cultured in normoxia (N) or 0.1% hypoxia (H) for 48h. n=3. B) HIF2α target gene expression in 786-0 WT, clone 1, clone 2 and 786-0 KO cells cultured in normoxia or 0.1% hypoxia for 48h. n=3. * p<0.05, ** p<0.01, *** p<0.001.

3.4.2. Selection of the optimal experimental conditions

In order to select the best time point and hypoxic conditions for future experiments, 786-0 WT and 786-0 KO cells were cultured under normoxia and hypoxia (1% and 0.1%) for 8h, 16h, 24h and 48h. As shown in Figure 3.11A, *HIF2α* and *GLUT1* expression was more than 50% suppressed in 786-0 KO compared to 786-0 WT cells at every time point analysed, whereas the levels increased in the parental cell line at 48h. HIF2α and GLUT1 protein expression followed the same pattern (Figure 3.11B). *CA9* on the other hand, a well-known HIF1α target gene, was used as a negative control due to the presence of a *HIF1α* inactivating mutation in 786-0 cell line [328].

As the hypoxic induction of *HIF2α* and *GLUT1* mRNA expression occurred mainly at 48h and there were no differences among the different oxygen levels, future experiments were carried out for 48h in 0.1% hypoxia, unless it is specified.

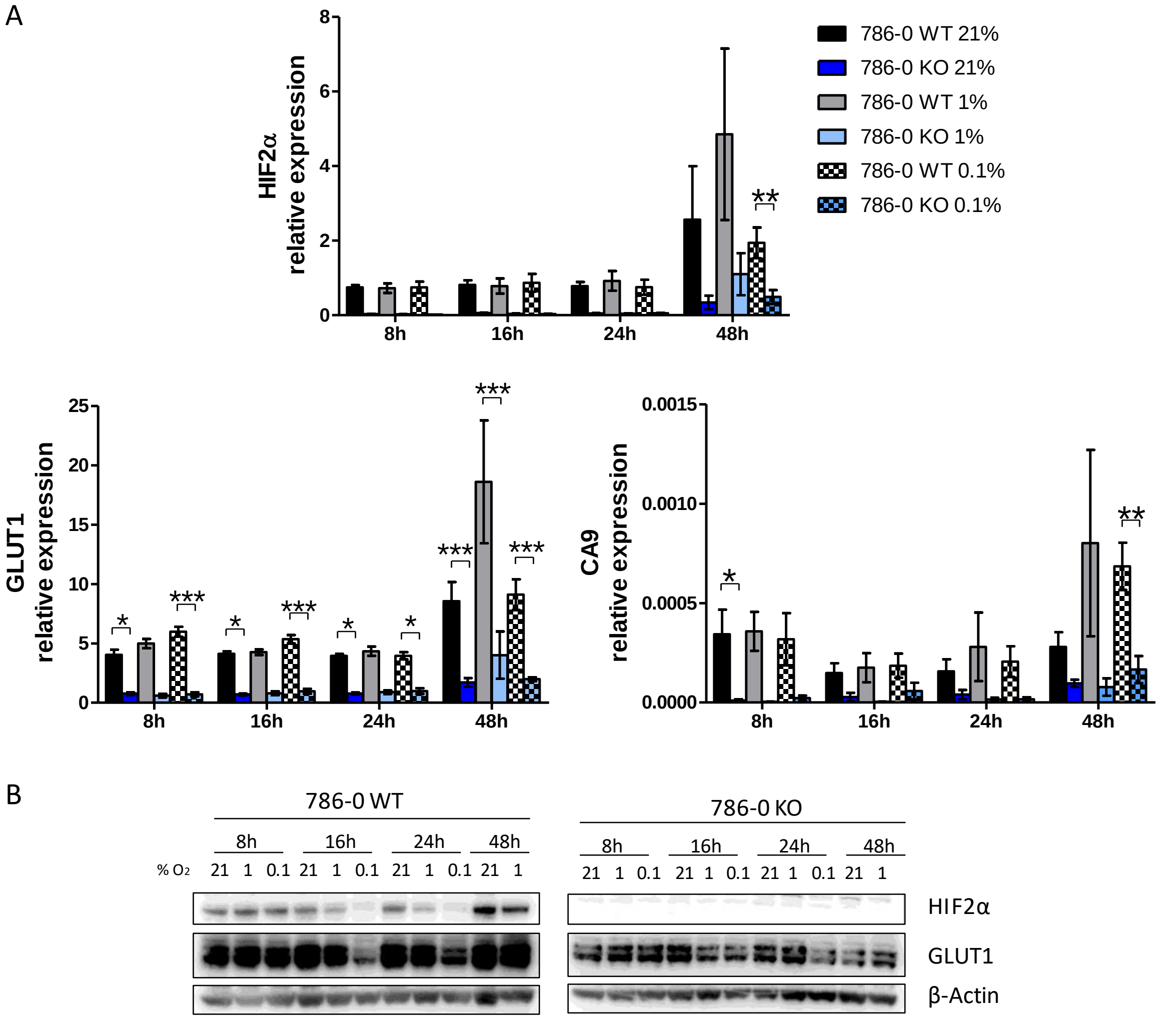

Figure 3.11. Time course experiment of 786-0 WT and 786-0 KO cells cultured at different oxygen concentration for 8h, 16h, 24h or 48h. A) Relative mRNA expression of *HIF2α*, *GLUT1* and *CA9*. n=3. * $p<0.05$, ** $p<0.01$, *** $p<0.001$. B) HIF2α and GLUT1 protein expression. n=3.

As only one clone (clone 3, 786-0 KO) showed complete HIF2α deletion, the RCC4 cell line was also used to confirm the results obtained in this thesis. RCC4 is a renal carcinoma cell line with a mutation in the *VHL* gene, thus resulting in stable expression of HIF1α and HIF2α even in normoxia. RCC4 cells stably transfected with an empty vector (RCC4 WT) and RCC4 cell line stably transfected with an overexpressing vector for *VHL* (RCC4 VHL, which promotes HIF1α and HIF2α proteasomal degradation under normoxic conditions) were used. RCC4 WT cell line could resemble 786-0 WT, while RCC4 VHL could be compared to 786-0 KO (Figure 3.12).

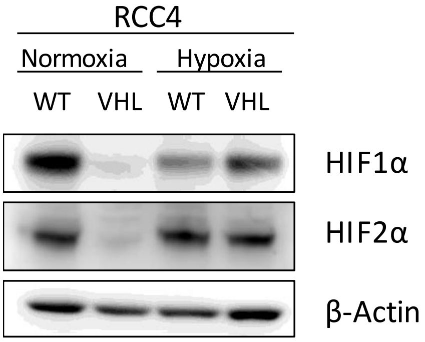

Figure 3.12. HIF1α and HIF2α protein expression in RCC4 cell lines stably transfected with an empty vector (RCC4 WT) and transfected with a vector for *VHL* (RCC4 VHL) cultured under normoxia or 0.1% hypoxia for 48h. n=1.

Time course experiments in RCC4 cell lines (Figure 3.13) showed that RCC4 VHL had more than 2-fold lower levels of *HIF2α* and *GLUT1* than RCC4 WT both in normoxia and hypoxia at every tested time. As a positive control, *CA9* was only detected in HIF1α-expressing RCC4 WT cells, and the levels were increased in hypoxia in a time-dependent manner.

As for 786-0 cell line, 48h and 0.1% hypoxia were selected as the best experimental settings for RCC4 cells and they were used in future experiments.

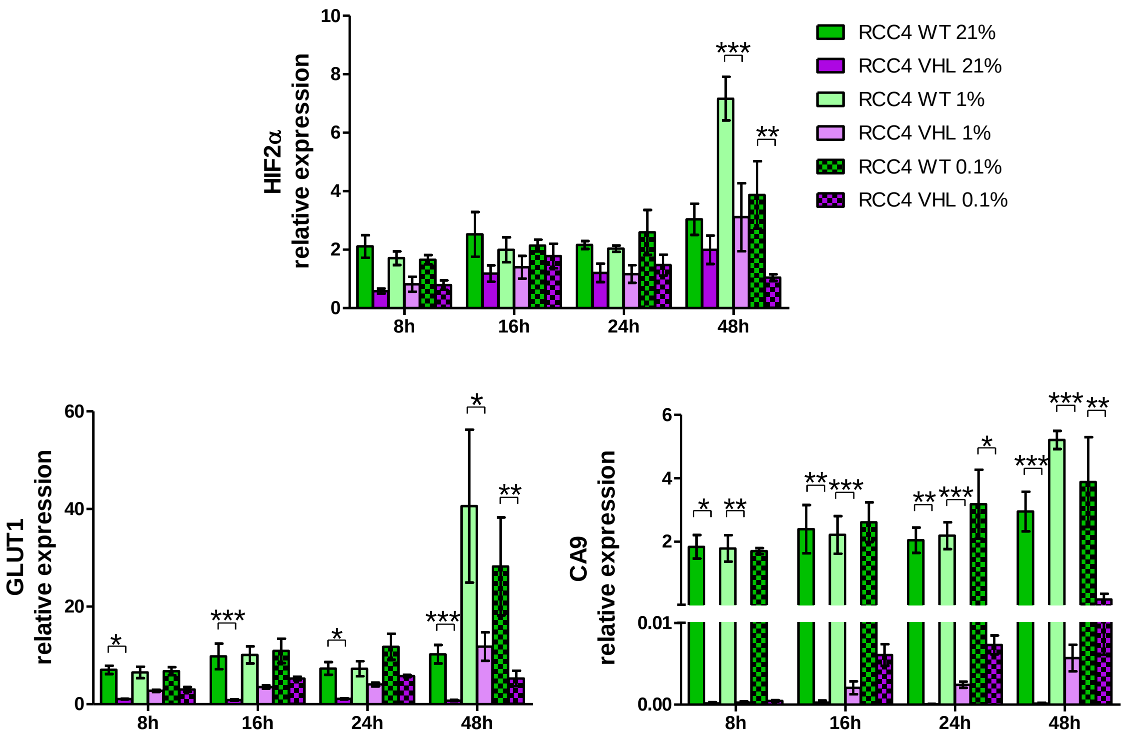

Figure 3.13. Time course experiment of RCC4 WT and RCC4 VHL cell lines cultured at different oxygen concentration for 8h, 16h, 24h and 48h. Relative expression of *HIF2α*, *GLUT1* and *CA9* is shown. n=3. * $p<0.05$, ** $p<0.01$, *** $p<0.001$.

3.4.3. The role of HIF2α in tumour cell proliferation

3.4.3.1. HIF2α deletion inhibits cell proliferation in 2D cultures

In order to characterise the effect of HIF2α deficiency on ccRCC cell growth, the proliferation rate of 786-0 KO cells was compared to 786-0 WT cells in 2-dimensional (2D) culture systems. 3000 786-0 WT and 786-0 KO cells were seeded and cultured under normoxia or 0.1% hypoxia for four days. Both 786-0 WT and 786-0 KO cells proliferated at a similar rate ($p>0.05$). Low oxygen conditions decreased the proliferation of 786-0 KO cells at day 4, but not significantly ($p>0.05$) (Figure 3.14A). The effect of the HIF2α antagonist PT2385 on tumour cell growth was also tested. PT2385 is a small molecule inhibitor that binds to a region in HIF2α PAS-domain and allosterically blocks its dimerization with the HIF1β/ARNT transcriptional partner, consequently inhibiting HIF2α downstream pathways [237]. As it was previously reported, the HIF2α antagonist did not suppress cell growth at any tested concentrations (Figure 3.14B and 3.14C).

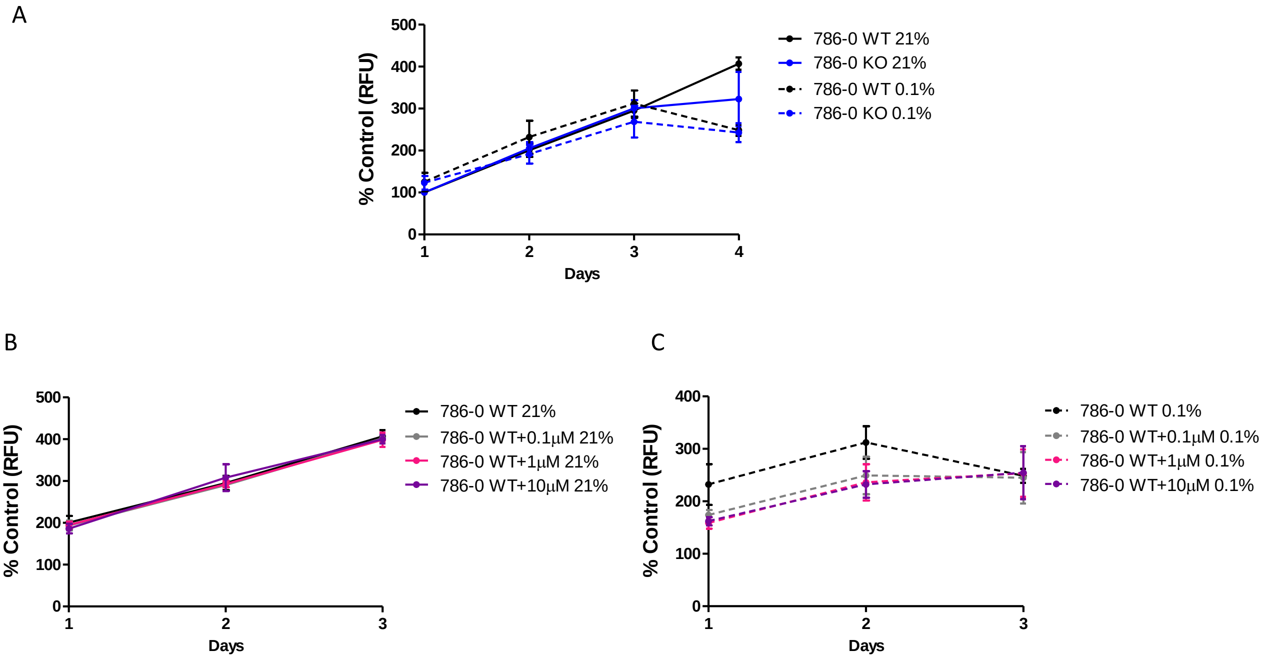

Figure 3.14. Proliferation results of A) 786-0 WT and 786-0 KO cells cultured up to four days in normoxia and 0.1% hypoxia, and PT2385's effect on 786-0 WT cell proliferation in B) normoxia and C) 0.1% hypoxia. n=3. * p<0.05, ** p<0.01, *** p<0.001.

The expression of HIF2α downstream genes was also analysed when 786-0 WT cells were treated with PT2385 to confirm its efficacy. As previously described [237], PT2385 inhibited HIF2α target gene expression in a concentration-dependent manner (Figure 3.15), achieving 75% inhibition at 10µM. 786-0 KO cells were used as positive control. The expression levels for each gene in 786-0 KO cells was similar to that obtained with 10µM PT2385.

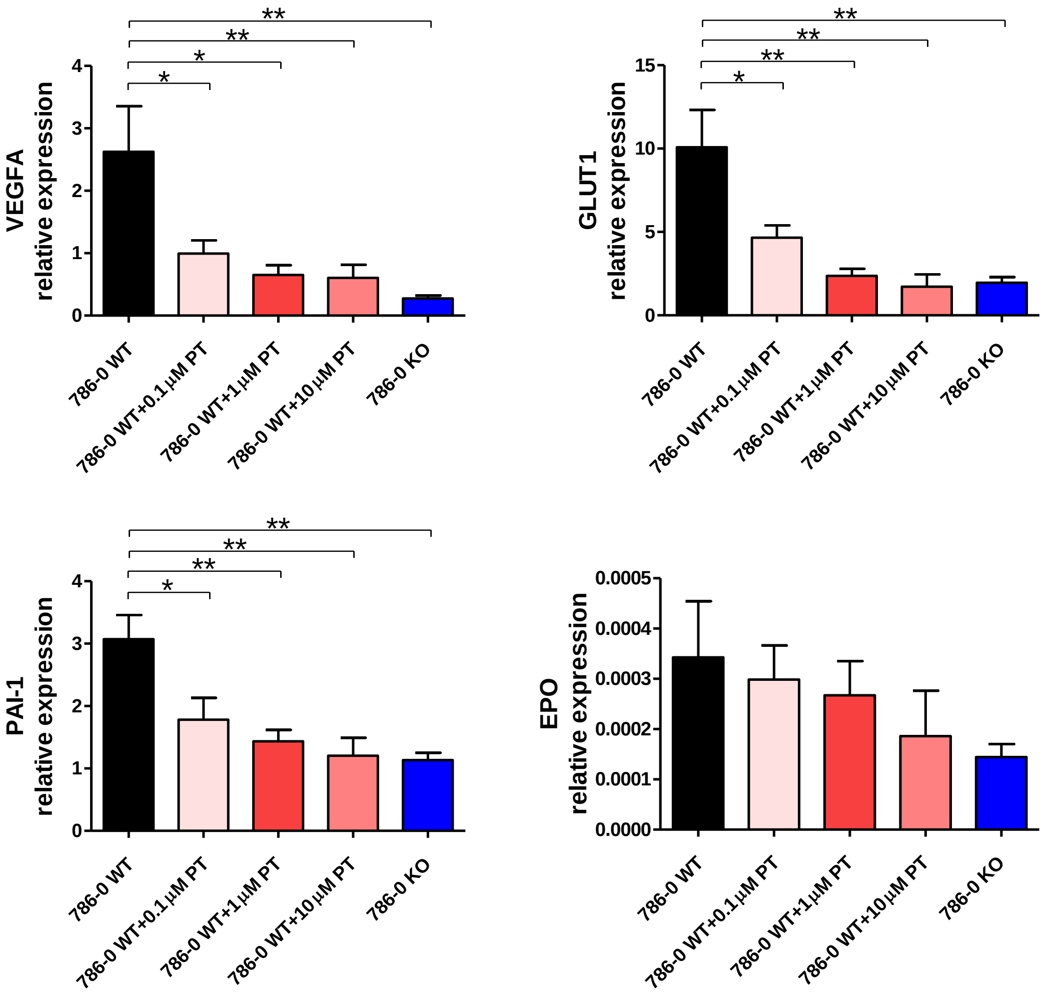

Figure 3.15. Relative expression of the HIF2α target genes *VEGFA, GLUT1,* plasminogen activator inhibitor-1 (*PAI-1*) and *EPO* in 786-0 WT, 786-0 WT+PT2385 and 786-0 KO cells cultured in normoxia for 48h. n=3. * $p<0.05$, ** $p<0.01$, *** $p<0.001$.

To further check the effect of HIF2α deletion in cell proliferation, clonogenic assays were performed in both 786-0 and RCC4 cell lines. From this assay, the cells ability to grow as a colony starting from a single cell can be assessed. Despite both being renal tumour cell lines, 786-0 cells formed quite spread colonies, in contrast to the colonies formed by RCC4 cell line (Figures 3.16 and 3.17).

Moreover, 786-0 KO cells formed 40% less colonies than 786-0 WT, and they were smaller. Low oxygen concentrations significantly inhibited the clonogenic potential of both cell lines in a similar way ($p<0.01$) (Figure 3.16). HIF2α activity blockage was also tested with the inhibitor PT2385, and as previously reported [237] and demonstrated in this thesis (Figure 3.14), it did not affect proliferation from a single cell either, as 786-0 WT cells were able to form colonies at a concentration up to 10µM (Figure 3.16), further showing that this HIF2α antagonist is not toxic for the cells.

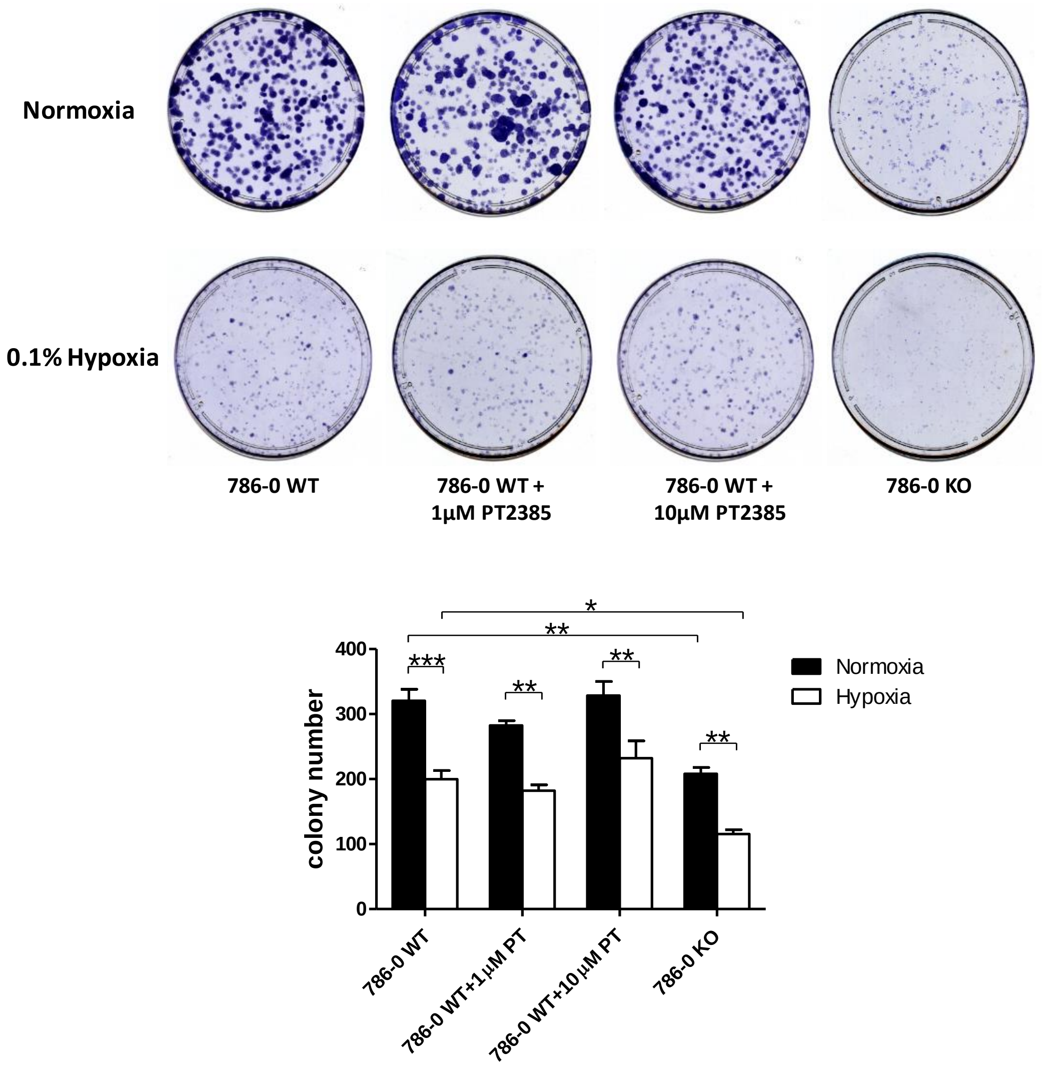

Figure 3.16. Representative images of 786-0 WT, 786-0 WT+PT2385 and 786-0 KO clonogenic assays and colony count. n=3. * $p<0.05$, ** $p<0.01$, *** $p<0.001$.

The same experiments were performed in RCC4 cell lines. In contrast to 786-0 KO cell line, HIFα inducible RCC4 VHL cells formed 30% more colonies than RCC4 WT under normoxic conditions ($p<0.001$), as shown in Figure 3.17. Hypoxia also suppressed the colony formation ability of both RCC4 cell lines ($p<0.001$), generating a more pronounced effect on RCC4 VHL cells, as it inhibited by 60% the clonogenic potential of these cells (Figure 3.17), showing that stress conditions such as oxygen deficiency have a greater effect on the high proliferative RCC4 VHL cell line. The addition of PT2385 to the cultures did not impair RCC4 cells' ability to form colonies (Figure 3.17).

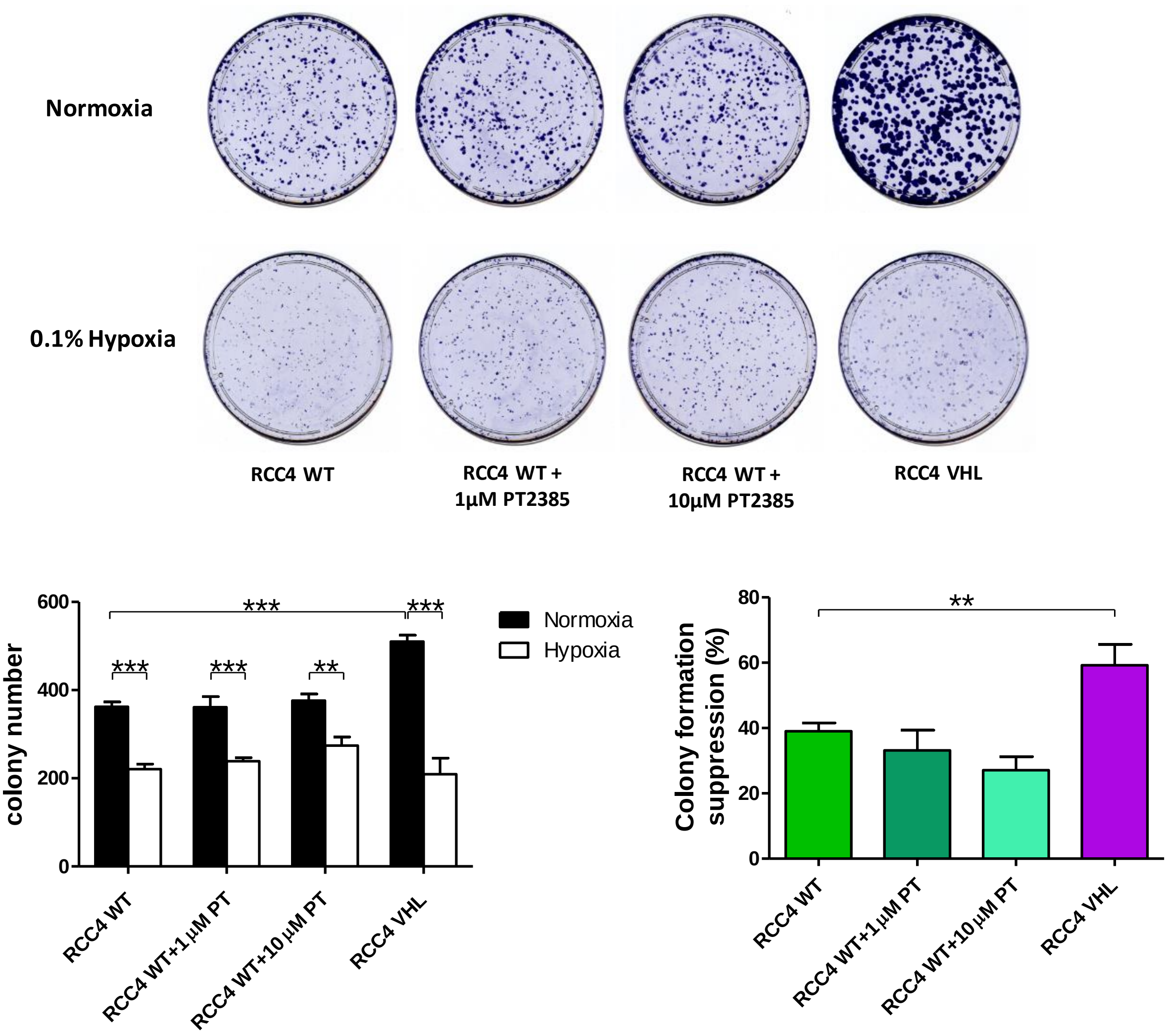

Figure 3.17. Representative images of RCC4 WT and RCC4 VHL clonogenic assays, colony count and colony suppression graph. n=3. * p<0.05, ** p<0.01, *** p<0.001.

3.4.3.2. Initial cell density affects the 786-0 KO growth rate

As shown before, 786-0 WT and 786-0 KO cells proliferated similarly when they were confluent enough in the wells (Figure 3.14A), but when few cells were in culture, such as occurs in the clonogenic assay, 786-0 KO formed less colonies (Figure 3.16). These results suggested that HIF2α might exert a different effect on cell proliferation depending on the initial cell density. To further explore this idea, various cell densities were seeded and left in culture for 5 days (Figure 3.18).

When seeding few cells (250, 500 or 1000 cells), 786-0 KO cell line proliferated significantly less than 786-0 WT ($p<0.001$), but when the initial cell density was high (3000 cells), they proliferated in a similar way (Figure 3.18A). Hypoxia negatively affected the proliferation of both cell lines, but it was only significant for 786-0 KO cells (p<0.01). This further suggests that cell-cell contact or even the concentration of secreted molecules to the media might have an impact on the proliferation rate.

Initial seeding cell density did not have any effect on RCC4 cell lines. In all conditions, RCC4 VHL cells proliferated nearly 2-fold more than RCC4 WT under normoxia, whereas hypoxia inhibited the proliferation of both cell lines, achieving 40-60% inhibition in RCC4 VHL cells (p<0.001) (Figure 3.18B).

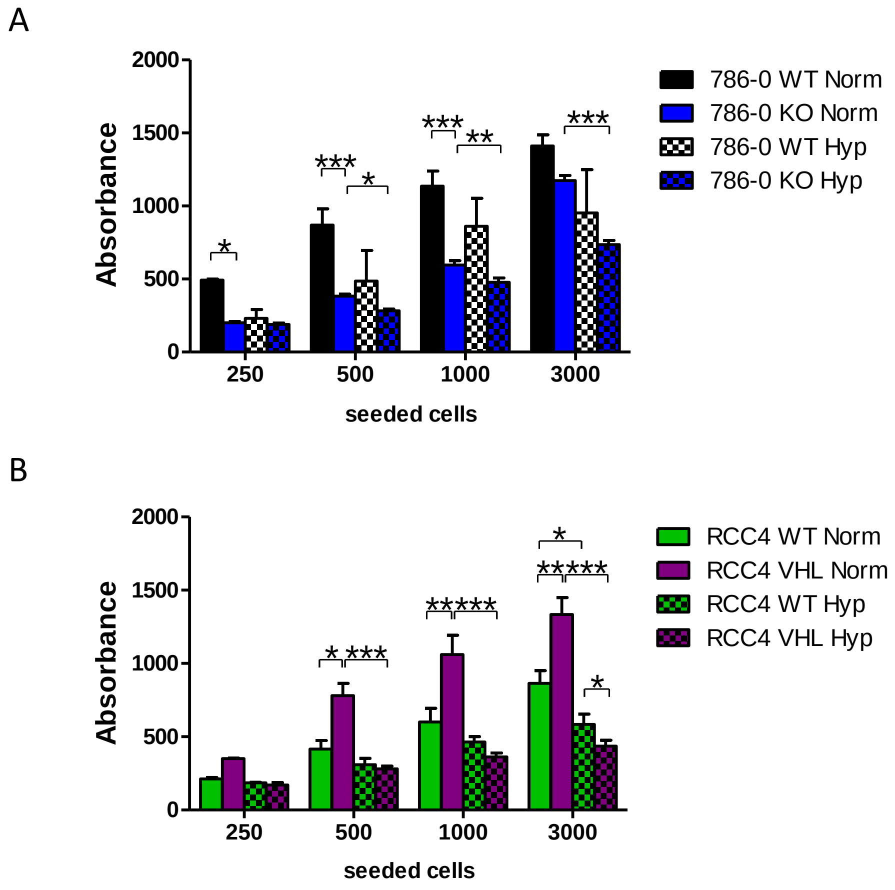

Figure 3.18. Different cell densities (250, 500, 1000 and 3000 cells) of 786-0 (A) and RCC4 (B) cell lines were cultured under normoxia and 0.1% hypoxia for 5 days. Cell proliferation was measured after this time. n=3. * p<0.05, ** p<0.01, *** p<0.001.

These results support clonogenic assay, where 786-0 KO forms less colonies than 786-0 WT and RCC4 VHL forms more than RCC4 WT. Independently of the initial seeding cell density, hypoxia negatively affected the proliferation ability of all cells, but the effect was bigger in 786-0 WT and RCC4 VHL cell lines, which proliferate faster.

3.4.3.3. HIF2α deletion does not affect cell proliferation in 3D cultures

In order to model tumour cell proliferation more realistically, 3-dimensional (3D) spheroid formation assays were performed. Spheroid assay offers the possibility of modelling *in vitro* tumour growth, mimicking hypoxic conditions usually found within the tumour mass as well as tumour 3D growth. As shown in Figure 3.19A and 3.19C, 786-0 spheroids did not get bigger with time ($p>0.05$). Because the spheroids were establishing during the first 5 days, a reduction in volume was observed. However, from day 5 until day 15, it kept constant, suggesting that cells form more compact spheroids with time or that apoptotic and proliferation rates compensate each other. While 786-0 WT and 786-0 KO spheroids had a similar volume, addition of 1µM PT2385 to 786-0 WT spheroids made them significantly bigger that 786-0 WT spheroids ($p<0.05$) (Figure 3.19A and 3.19C).

Moreover, spheroid circularity was also analysed. Circularity is represented as a value between 0 and 1, being 1 a perfect circle and 0 an elongated shape. Figure 3.19B depicts that 786-0 KO spheroids had the most defined edges. Moreover, PT2385 addition to 786-0 WT spheroids reduced cell compaction to form a perfect spheroid ($p<0.05$) (Figure 3.19B and 3.19C). This HIF2α inhibitor made spheroids less compact, which can be explained by the bigger volume (Figure 3.19A) and the blebbing seen in the edge of the structures (Figure 3.19C), measured as a low circularity value (Figure 3.19B).

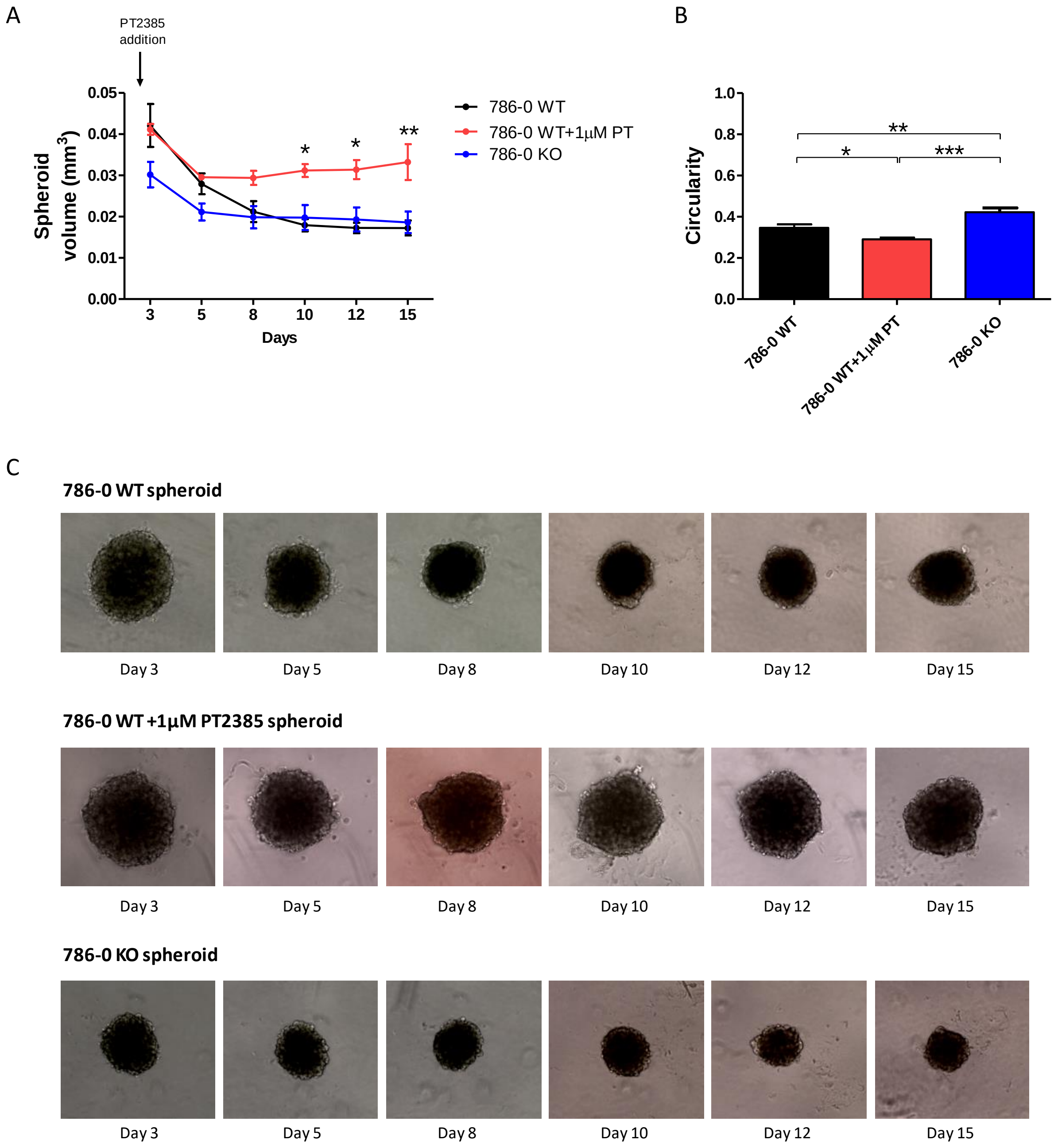

Figure 3.19. 786-0 WT, 786-0 WT+1μM PT2385 and 786-0 KO spheroid volume (A) and spheroid circularity (B) during 15 days. n=3. * $p<0.05$, ** $p<0.01$, *** $p<0.001$. Representative images of spheroids are shown in C.

At the end of the experiment, spheroids were disaggregated and manually counted. The total number of cells was similar in all groups (Figure 3.20A). However, 786-0 WT spheroids had more viable cells than 786-0 KO and 786-0 WT cells treated with 1μM PT2385 ($p<0.05$) (Figure 3.20B), suggesting that HIF2α would be involved in the survival to low oxygen concentrations generated by seeding the cells in 3D. Although not highly significant ($p>0.05$), PT2385 effect on the viability of cells forming spheroids can be supported by studies analysing this antagonist *in vivo* [237]. Spheroids are *in vitro* models of real tumours, so in line with previously published studies, PT2385 induced tumour regression might be represented here as less viable cells within the spheroids.

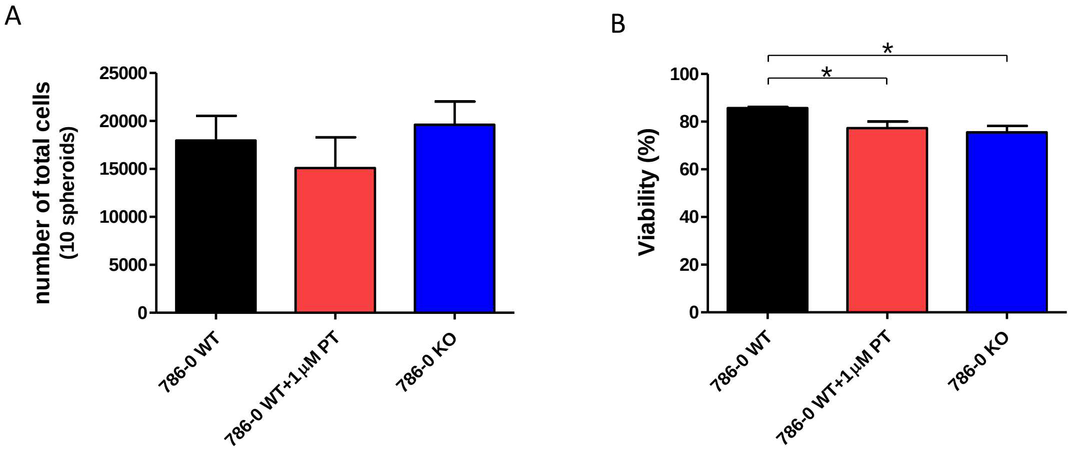

Figure 3.20. A) Number of total cells per 10 spheroids of 786-0 WT, 786-0 WT+1μM PT2385 and 786-0 KO cells. B) Viability of the cells forming 786-0 WT, 786-0 WT+1μM PT2385 and 786-0 KO spheroids. n=3. * $p<0.05$, ** $p<0.01$, *** $p<0.001$.

Overall, HIF2α deletion made a difference in the proliferation of 786-0 cells in 2D cultures, and this effect was greater under normoxic conditions. 786-0 KO cells were more sensitive to the lack of cell contact, as shown in clonogenic assays and in the different cell density proliferation assays, although they grew quite similarly to 786-0 WT cells under low oxygen concentrations. This suggests that HIF1α mutated 786-0 cells rely not only on HIF2α, but also on other molecules to resist to hypoxia. This idea was further confirmed with the spheroids, where the presence of HIF2α did not increase the proliferation rate of cells forming spheroids, but increased the viability.

Even though both RCC4 and 786-0 are renal cancer cell lines, their proliferation follows different patterns. RCC4 VHL cells grew faster than RCC4 WT in all tested conditions. In this case however, hypoxia inhibition on cell proliferation had a more profound effect in the fast proliferating RCC4 VHL cell line as it lowered its proliferation rate to RCC4 WT cell line's levels, suggesting that HIF transcription factors might inhibit proliferation of RCC4 cell lines.

3.4.4. HIF2α deletion promotes tumour cell migration but inhibits cells' invasion ability *in vitro*

It is well described that HIF transcription factors promote EMT during the development of the tumour, making the tumour to acquire an invasive, malignant phenotype [334, 335]. Therefore, migration and invasion ability of 786-0 and RCC4 cells was studied.

To study the migratory potential, wound healing assay using the IncuCyte ZOOM® technology was carried out. Figure 3.21A shows a representative image of 786-0 cells migrating. Dark blue region corresponds to the initial scratch wound, whereas light blue represents the wound lacking of cells at the compared moment. As seen in those pictures and represented as the wound confluence and wound width (Figure 3.21B), 786-0 KO cells migrated significantly faster than 786-0 WT ($p<0.001$) as they had completely closed the wound 12h after making the scratch, whereas 786-0 WT cells did not. In addition to this, HIF2α inhibition using the PT2385 inhibitor had no effect on 786-0 WT cell's migration.

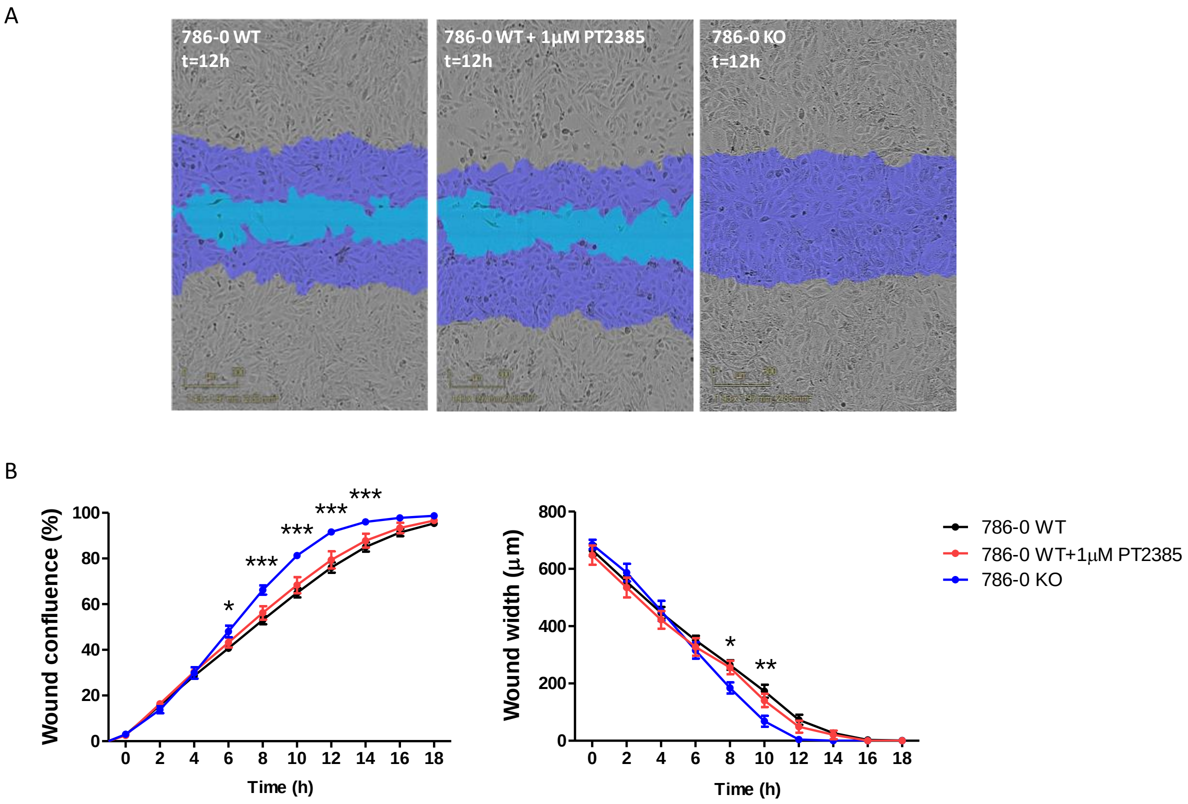

Figure 3.21. A) Representative images of 786-0 WT, 786-0 WT+1µM PT2385 and 786-0 KO cells migrating 12h after the scratch. B) Wound confluence and wound width measurement until the complete closure of the wound. n=3. * $p<0.05$, ** $p<0.01$, *** $p<0.001$.

In this experiment, RCC4 cell line resembles 786-0 cell's phenotype, although RCC4 cells migrate much slower than 786-0 possibly as they represent an earlier tumour stage. 12h after making the scratch 786-0 cells had almost, if not completed, closed the wound (Figure 3.21), whereas it took 48h to completely close the wound to RCC4 cells. HIF1α and HIF2α inducible RCC4 VHL cell line migrated faster than RCC4 WT as soon as 4h after making the wound (p<0.001) (Figure 3.22). Interestingly, PT2385 addition to RCC4 WT cells promoted their migration (p<0.001) (Figure 3.22) generating an intermediate phenotype between RCC4 WT and RCC4 VHL cells. This suggests that in RCC4 cell line, not only HIF2α but also HIF1α is repressing cell migration.

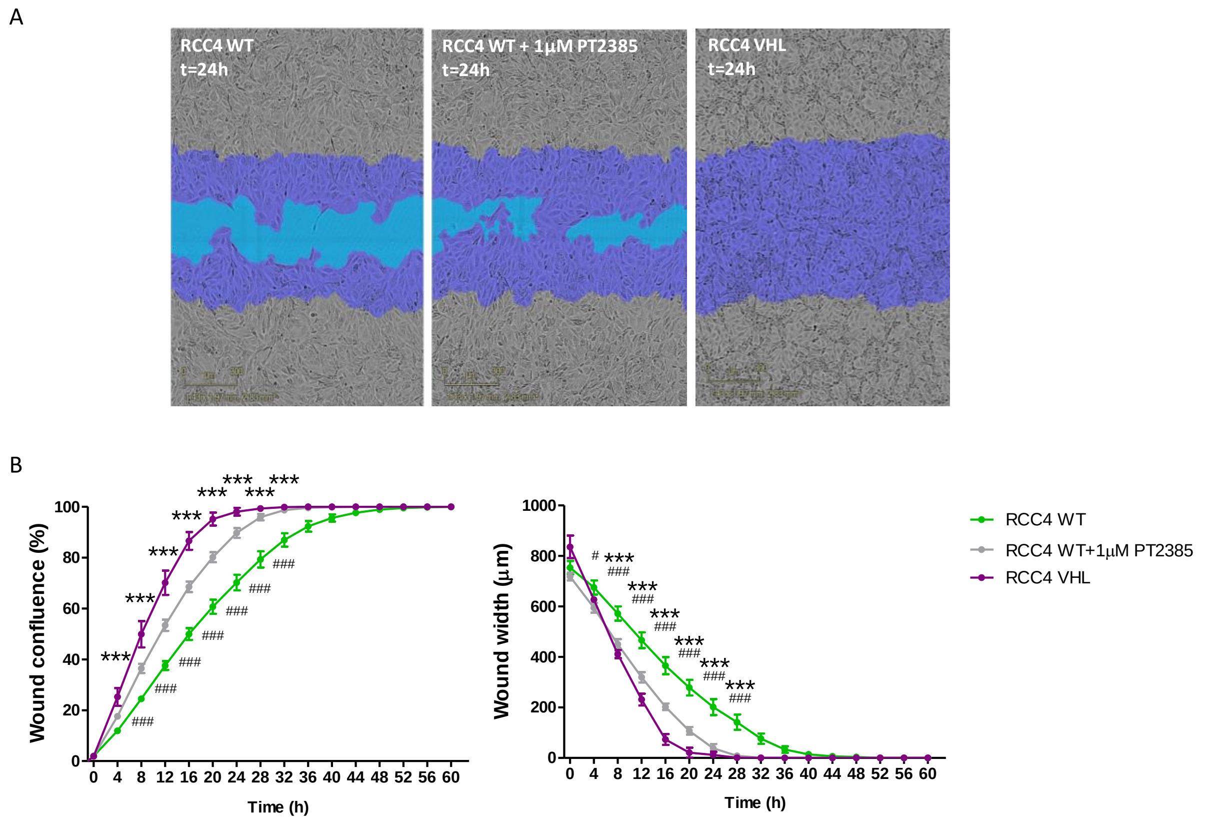

	Wound confluence				Wound width			
	RCC4 WT vs RCC4 VHL		RCC4 WT vs RCC4 WT+1μM PT		RCC4 WT vs RCC4 VHL		RCC4 WT vs RCC4 WT+1μM PT	
Time	**P value**	**Summary**	**P value**	**Summary**	**P value**	**Summary**	**P value**	**Summary**
0	P>0.05	ns	P>0.05	ns	P>0.05	ns	P>0.05	ns
4	P<0.001	***	P>0.05	ns	P>0.05	ns	P<0.05	#
8	P<0.001	***	P<0.001	###	P<0.001	***	P<0.001	###
12	P<0.001	***	P<0.001	###	P<0.001	***	P<0.001	###
16	P<0.001	***	P<0.001	###	P<0.001	***	P<0.001	###
20	P<0.001	***	P<0.001	###	P<0.001	***	P<0.001	###
24	P<0.001	***	P<0.001	###	P<0.001	***	P<0.001	###
28	P<0.001	***	P<0.001	###	P<0.001	***	P<0.001	###
32	P<0.001	***	P<0.001	###	P>0.05	ns	P>0.05	ns
36	P>0.05	ns	P>0.05	ns	P>0.05	ns	P>0.05	ns
40	P>0.05	ns	P>0.05	ns	P>0.05	ns	P>0.05	ns

Figure 3.22. A) Representative images of RCC4 WT, RCC4 WT+1μM PT2385 and RCC4 VHL cells migrating 24h after the scratch. B) Wound confluence and wound width measurerement until the complete closure of the wound. n=3. * p<0.05, ** p<0.01, *** p<0.001.

Regarding the invasive potential, the wound healing assay using the IncuCyte ZOOM® in the presence of Matrigel® was performed. As depicted in Figure 3.23, 786-0 WT cells invaded significantly more than 786-0 KO cells ($p<0.001$), showing that HIF2α enhances 786-0 cells' invasion. This was further supported by addition of PT2385, as the HIF2α antagonist impeded invasion of cells in a concentration-dependent manner ($p<0.001$) (Figure 3.23). In contrast to the migration potential where HIF2α suppresses cell movement, HIF2α promotes tumour cell invasion, suggesting that HIF2α could play a major role in later stages of the metastatic process.

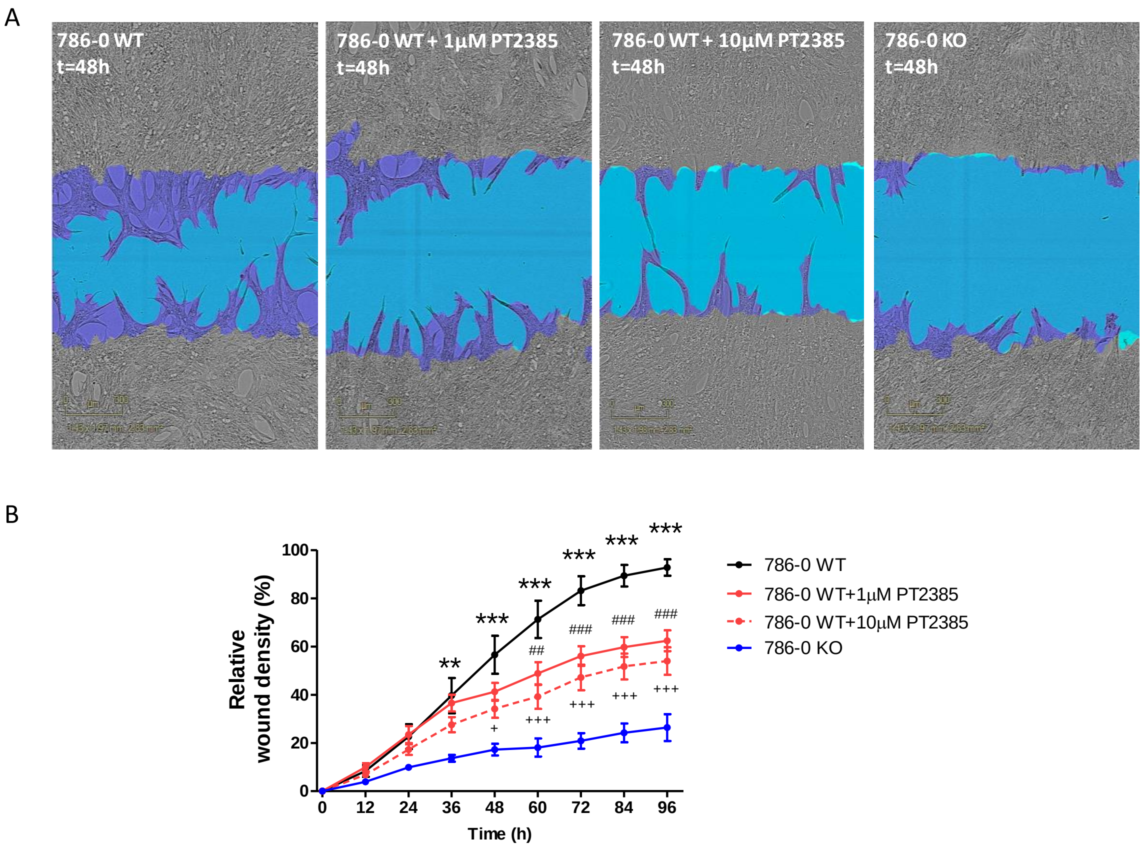

	Relative wound density					
	786-0 WT vs 786-0 KO		786-0 WT vs 786-0 WT+1µM PT2385		786-0 WT vs 786-0 WT+10µM PT2385	
Time	**P value**	**Summary**	**P value**	**Summary**	**P value**	**Summary**
0	P>0.05	ns	P>0.05	ns	P>0.05	ns
12	P>0.05	ns	P>0.05	ns	P>0.05	ns
24	P>0.05	ns	P>0.05	ns	P>0.05	ns
36	P<0.01	**	P>0.05	ns	P>0.05	ns
48	P<0.001	***	P>0.05	ns	P<0.05	+
60	P<0.001	***	P<0.01	##	P<0.001	+++
72	P<0.001	***	P<0.001	###	P<0.001	+++
84	P<0.001	***	P<0.001	###	P<0.001	+++
96	P<0.001	***	P<0.001	###	P<0.001	+++

Figure 3.23. A) Representative images of 786-0 WT, 786-0 WT+1µM/10µM PT2385 and 786-0 KO cells invading 48h after the scratch. B) RWD measurement until 96h after wound performing. n=3. * $p<0.05$, ** $p<0.01$, *** $p<0.001$.

Conversely, neither RCC4 WT nor RCC4 VHL cells were able to invade through the Matrigel® (Figure 3.24). This could be explained as this cell line arises from an earlier tumour stage compared to 786-0 cell line, thus they might not be malignant enough to invade other tissues. Curiously, the low invasion ability of 786-0 KO (RWD=20% at 96h) is similar to RCC4 WT and RCC4 VHL cell lines (RWD=40% at 96h) (Figure 3.23 and 3.24), suggesting that HIF2α deletion could trigger the loss of the invasive potential in RCC.

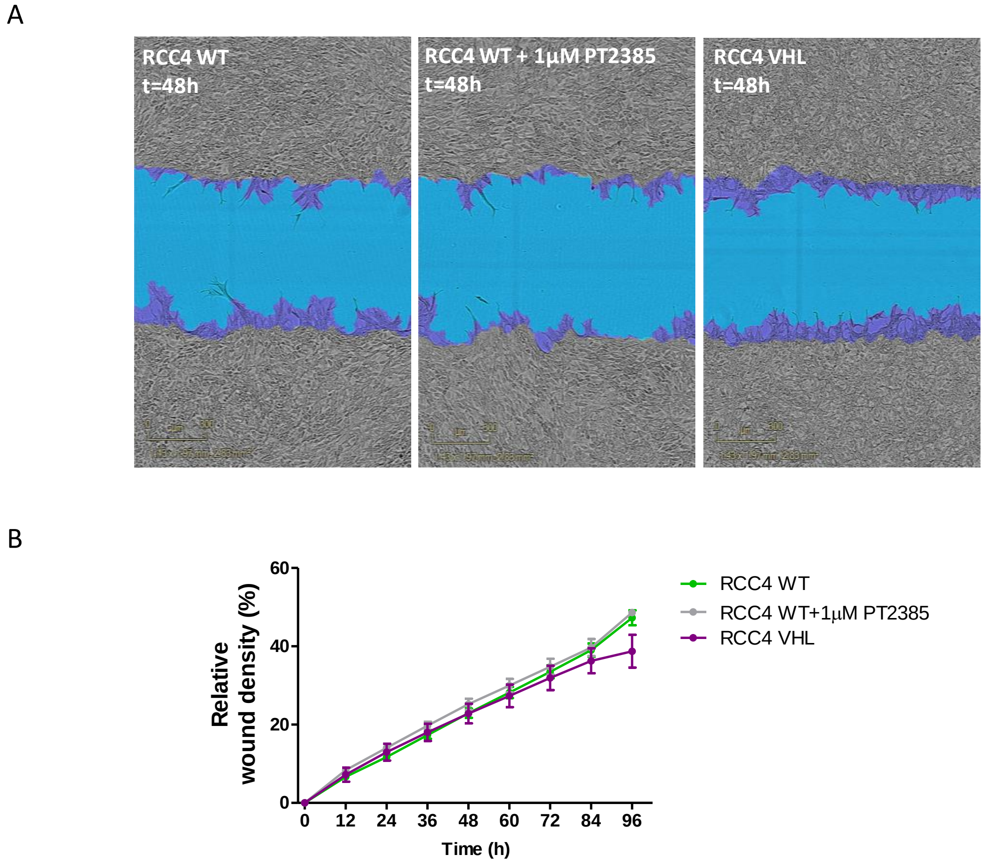

Figure 3.24. A) Representative images of RCC4 WT, RCC4 WT+1µM PT2385 and RCC4 VHL cells invading the wound 48h after the scratch. B) RWD measurement until 96h after wound performing. n=3. * $p<0.05$, ** $p<0.01$, *** $p<0.001$.

To confirm these results with a different approach, 786-0 WT cells were transfected with either siRNA control (siCON) or siRNA for HIF2α (siHIF2α) and their migratory and invasion potential was analysed. In this case, partial deletion of HIF2α did not enhance the migratory ability of 786-0 WT cells nor blocked their invasion potential (Figure 3.25), as observed in 786-0 KO cells. This suggests that completely lack of HIF2α is responsible for the 786-0 KO phenotype as the low HIF2α remaining levels after the knock down could be enough to affect migration and invasion.

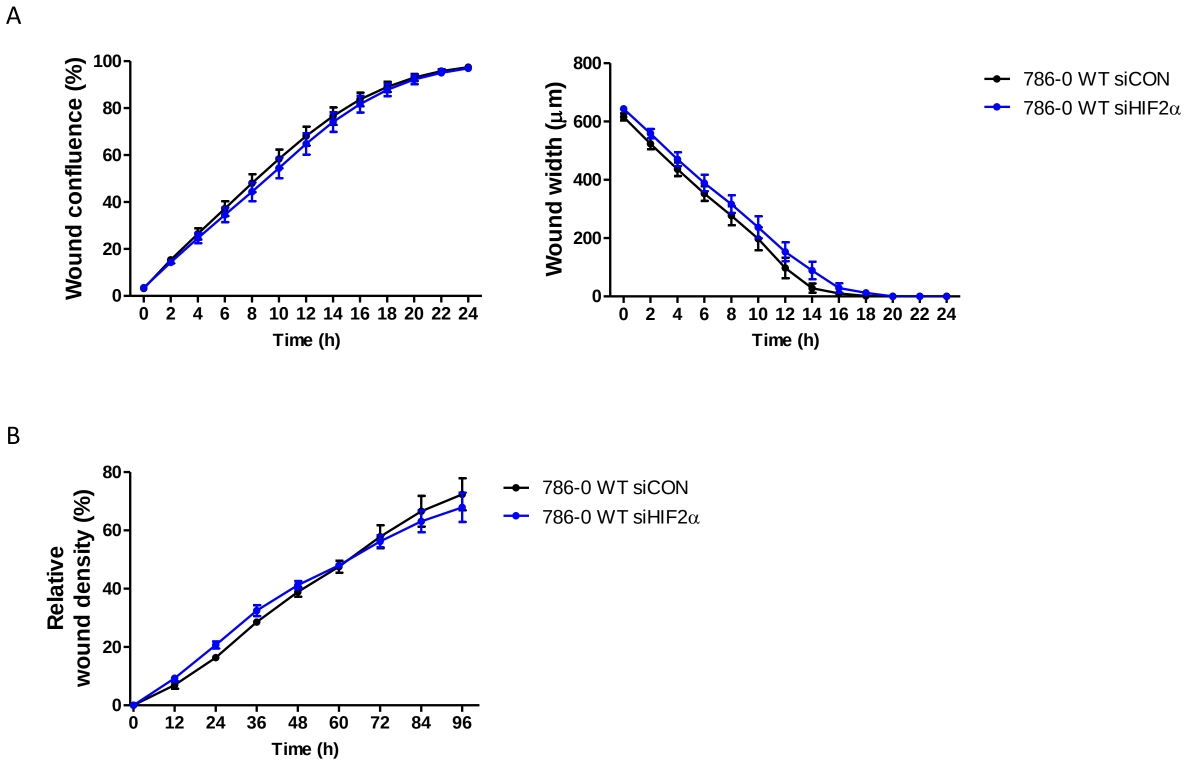

Figure 3.25. Representation of 786-0 WT siCON and 786-0 WT siHIF2α cells' migration (A) and invasion (B), presented as wound confluence and wound width measure and RWD, respectively. n=3. * $p<0.05$, ** $p<0.01$, *** $p<0.001$.

As siRNA silencing is temporary, in order to discard a possible residual HIF2α effect in the observed phenotype of 786-0 WT siHIF2α cells, the expression of HIF2α and known HIF2α target genes was analysed every 24h until the end of the experiment. The initial time (0h) in both migration and invasion experiments corresponds to the moment in which the scratch is done, which is 24h post-transfection. As Figure 3.26 shows, HIF2α was not induced over time, or its targets *GLUT1* and *VEGFA*. This shows that silencing of HIF2α was maintained during the whole migration and invasion experiment, and further shows that the lack of differences was not due to the re-expression of HIF2α.

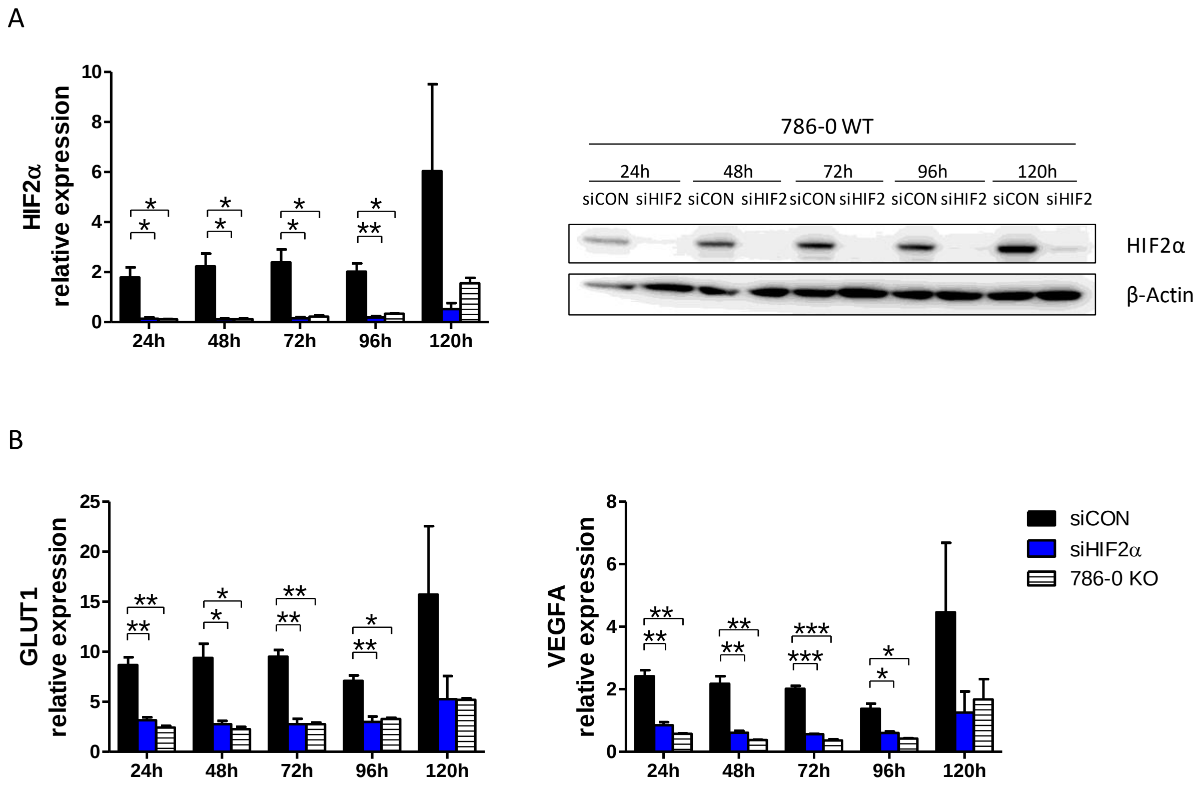

Figure 3.26. A) mRNA and protein expression of HIF2α in 786-0 WT cells transfected with siCON or siHIF2α and cultured in normoxia for 24h, 48h, 72h, 96h or 120h. B) mRNA expression of *GLUT1* and *VEGFA* in 786-0 WT cells transfected with siCON or siHIF2α and 786-0 KO cells cultured in normoxia for 24h, 48h, 72h, 96h or 120h. n=3. * p<0.05, ** p<0.01, *** p<0.001.

EMT is a process in which cells lose their epithelial characteristics and acquire mesenchymal features. This process has been associated with tumour malignancy in several ways, including tumour initiation, progression, tumour cell stemness, migration, intravasation to the blood, metastasis and resistance to therapy [336]. Thus, the expression of different genes involved in EMT was determined both at protein (Figure 3.27A) and mRNA level (Figure 3.27B) in order to see if they could explain the differences observed in migration and invasion. Both epithelial (zonula occludens-1 (ZO-1), E-cadherin, claudin-1) and mesenchymal (zinc-finger E-box binding homeobox 1 (ZEB1), N-cadherin, vimentin, snail, slug, β-catenin) markers were analysed in 786-0 WT and 786-0 KO cells (Figure 3.27A). Only the tight junction protein claudin-1 showed noticeable differences between 786-0 WT and 786-0 KO cells both in normoxia and in 1% hypoxic conditions. Lower expression of claudin-1 in 786-0 KO cells might explain the enhanced migration ability of these cells. Slug was slightly more expressed in 786-0 KO cells, being this up-regulation enhanced in 1% hypoxia, although not significant in either case. *Slug* expression was also checked at mRNA level (Figure 3.27B). It was higher expressed in 786-0 KO than 786-0 WT under normoxia (p>0.05), whereas no differences were detected in 0.1% hypoxia, as reflected at protein level. Slug is a transcription factor which suppresses the expression of the adhesion molecule E-cadherin, thus it could contribute to increase the tumour migration. However, E-cadherin levels were not altered (Figure 3.27B). Moreover, these differences in claudin-1 and slug expression between 786-0 WT and 786-0 KO were lost when culturing the cells in 0.1% hypoxia.

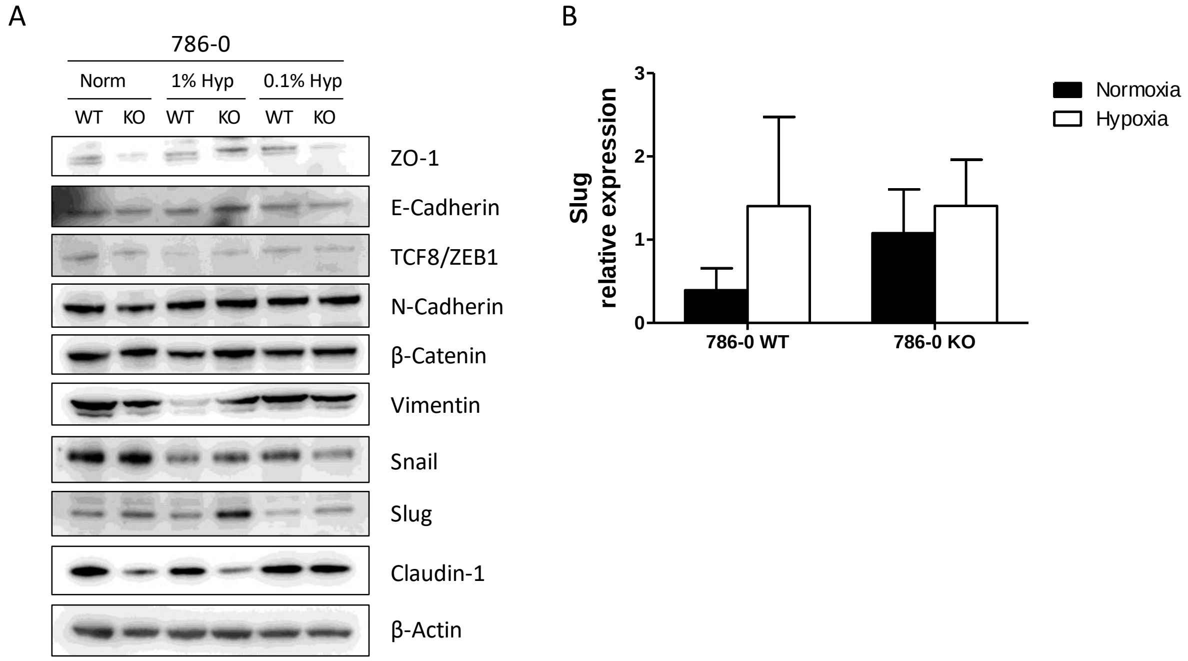

Figure 3.27. A) Western blot of EMT proteins in 786-0 WT and 786-0 KO cells cultured under normoxia and hypoxia (1% and 0.1%) for 48h. B) Relative expression of *Slug* in 786-0 WT and 786-0 KO cells cultured under normoxia and 0.1% hypoxia for 48h. n=3. * p<0.05, ** p<0.01, *** p<0.001.

3.4.5. HIF2α enhances metastasis *in vivo*

To study HIF2α invasion *in vivo*, 786-0 WT Luc$^+$ or 786-0 KO Luc$^+$ cells were injected via the tail vein injection in NOD SCID mice and colonization of tissues was analysed. As shown in Figure 3.28, none of the mice injected with 786-0 KO Luc$^+$ cells (786-0 KO mice) developed any metastasis, confirming HIF2α's role in metastasis and further supporting the *in vitro* invasion results. Mice injected with 786-0 WT Luc$^+$ cells (786-0 WT mice) developed metastasis two weeks after tumour cell injection, but at week 4 metastasis of every mice disappeared, as previously seen in patients who underwent nephrectomy [337]. This suggests that even using NOD SCID mice without functional T and B cells, the low macrophage and NK cell activity present in the host might be enough to induce metastasis regression. However, reappearance of metastasis 10 weeks after suggests that some cells, e.g. cancer stem cells (CSC), could be avoiding NK cells and macrophages mediated antitumour activity and give rise to a new tumour cell population.

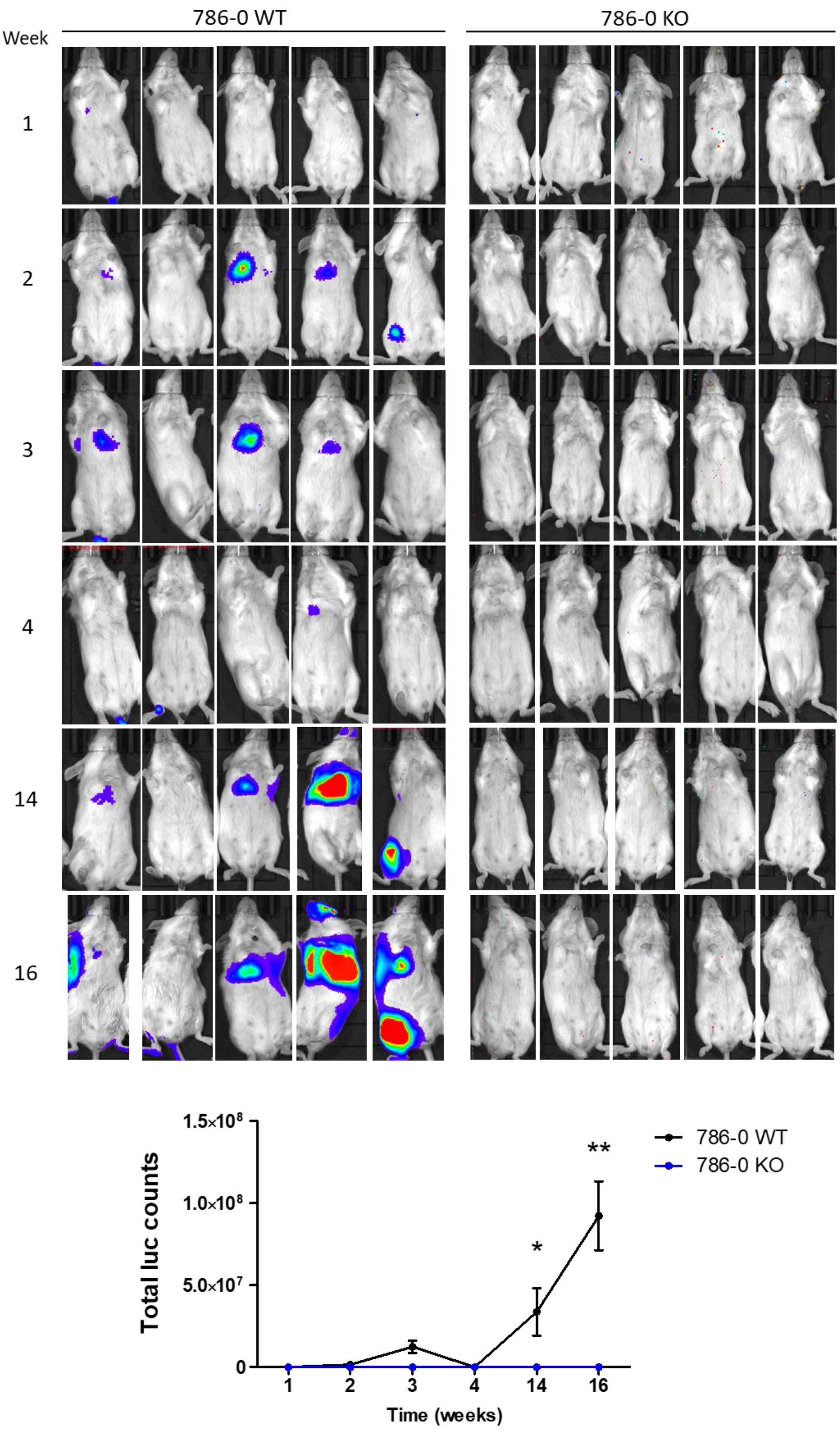
786-0 WT
786-0 KO
Week
1
2
3
4
14
16
Total luc counts
1.5×10⁸
1.0×10⁸
5.0×10⁷
0
**
*
1
2
3
4
14
16
Time (weeks)
786-0 WT
786-0 KO

Figure 3.28. Representative bioluminescence images and total luminescence count of the five mice which ended the experiment at week 16. n=10 (until week 4), n=5 (from week 4 until week 16). * $p<0.05$, ** $p<0.01$, *** $p<0.001$.

At week 16, mice were imaged again and metastasis in the lungs, brain and mammary fat pad were recorded. As sometimes the amount of emitted light is not enough to escape from the mouse and be detected, mice were injected with Beetle Luciferin, Potassium Salt prior to sacrificing and lungs were imaged for bioluminescence emission. All lungs from 786-0 WT mice emitted bioluminescence (Figure 3.29), in contrast to the whole mice images where one mouse did not show any metastasis (Figure 3.28).

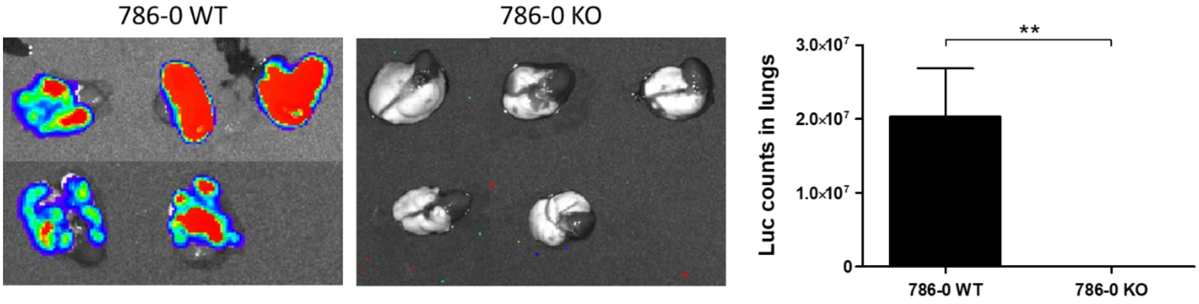

Figure 3.29. Lung bioluminescence images and measurement at week 16. n=5. * $p<0.05$, ** $p<0.01$, *** $p<0.001$.

In addition, the weight of the lungs was significantly higher in mice harbouring metastasis than in mice which did not develop metastasis ($p<0.001$) (Figure 3.30), showing that the metastasis burden in this organ is increased in 786-0 WT mice. Similarly, 786-0 WT mice presented enlarged spleens, comparing to 786-0 KO mice ($p<0.001$). The spleen and lymph nodes are important lymphoid organs for the host's immune response, as antitumour effector cells are developed in those organs [338]. Moreover, the spleen produces various cytokines [339] which migrate to the liver and enhance NK cell cytotoxicity in the liver [340]. NK cells can further act to eradicate the tumour and its metastasis [341]. Therefore, bigger spleens show an enhance immune response against the metastatic tumour cells.

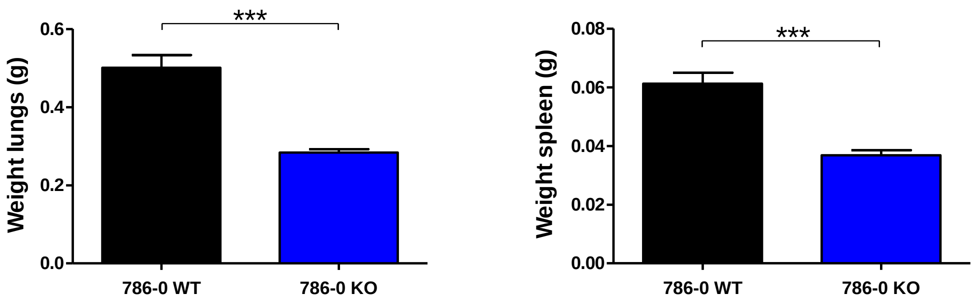

Figure 3.30. Weight of the lungs and spleen of the mice at the endpoint (week 16). n=5. * $p<0.05$, ** $p<0.01$, *** $p<0.001$.

3.4.6. HIF2α deletion alters cell metabolism

3.4.6.1. HIF2α does not overtake HIF1α's glycolytic role in 786-0 cells

In order to analyse if glucose was the main energy source of 786-0 cell lines, 786-0 WT and 786-0 KO cells were seeded in media containing different concentration of D-glucose for 5 days. As depicted in Figure 3.31A, 786-0 KO cells had significantly more difficulties than 786-0 WT (p<0.01) to grow when glucose concentration was low (1.25mM or 2.5mM). No glucose in the media impaired the growth of both cell lines at the same rate. To further explore the use of glucose in these cell lines, the effect of the D-glucose analogue 2-DG was tested (Figure 3.31B). 2-DG is a D-glucose molecule in which the 2-hydroxyl group has been replaced by a hydrogen. In spite of being uptaken by glucose transporters of the cells and phosphorylated by hexokinase to form 2-deoxy-D-glucose-phosphate (2-DG-P), 2-DG-P cannot be further metabolized by phosphoglucose isomerase leading to its accumulation and inhibition of glycolysis. The growth of both 786-0 WT and 786-0 KO cells was indistinctly impaired by 2-DG treatment.

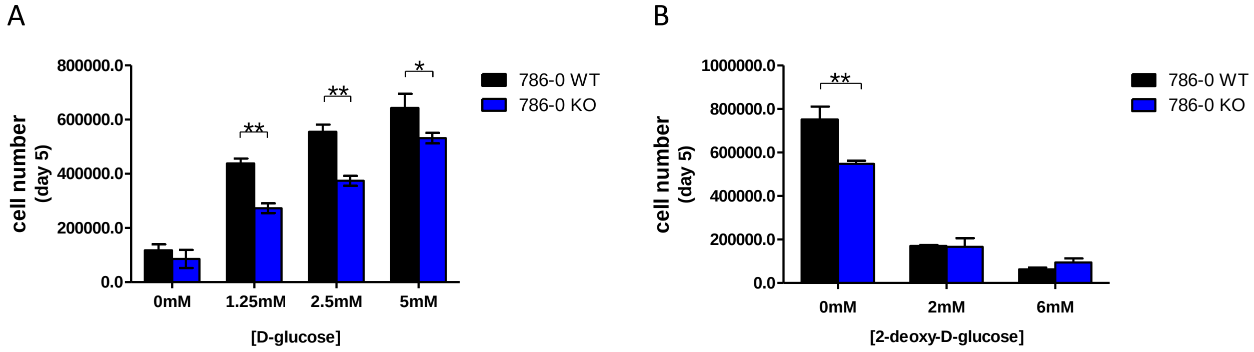

Figure 3.31. 786-0 WT and 786-0 KO cells were cultured in normoxia for 5 days in media with different concentrations of D-glucose (A) or in the presence of 2-DG (B). n=3. * p<0.05, ** p<0.01, *** p<0.001.

Taking into account the important regulation that HIF1α exerts on genes involved in glucose metabolism, the expression of PDK1, PDHA1 and LDHA was analysed by qPCR (Figure 3.32A) and western blot (Figure 3.32B). HIF1α promotes the conversion of glucose to pyruvate and subsequently to lactate, via upregulation LDHA, and it also suppresses metabolism through the Krebs cycle by directly transactivating the gene encoding PDK1. PDK1 will inhibit PDH and thus avoid pyruvate conversion to acetyl-CoA and further entry into the mitochondria. As shown in Figure 3.32A, there were not differences at mRNA level between 786-0 WT and 786-0 KO cells for these genes either in normoxia or hypoxia. The same results were obtained when analysing protein expression (Figure

3.32B). These data suggest that HIF2α is not overtaking HIF1α's role controlling glucose metabolism in 786-0 cells under these conditions.

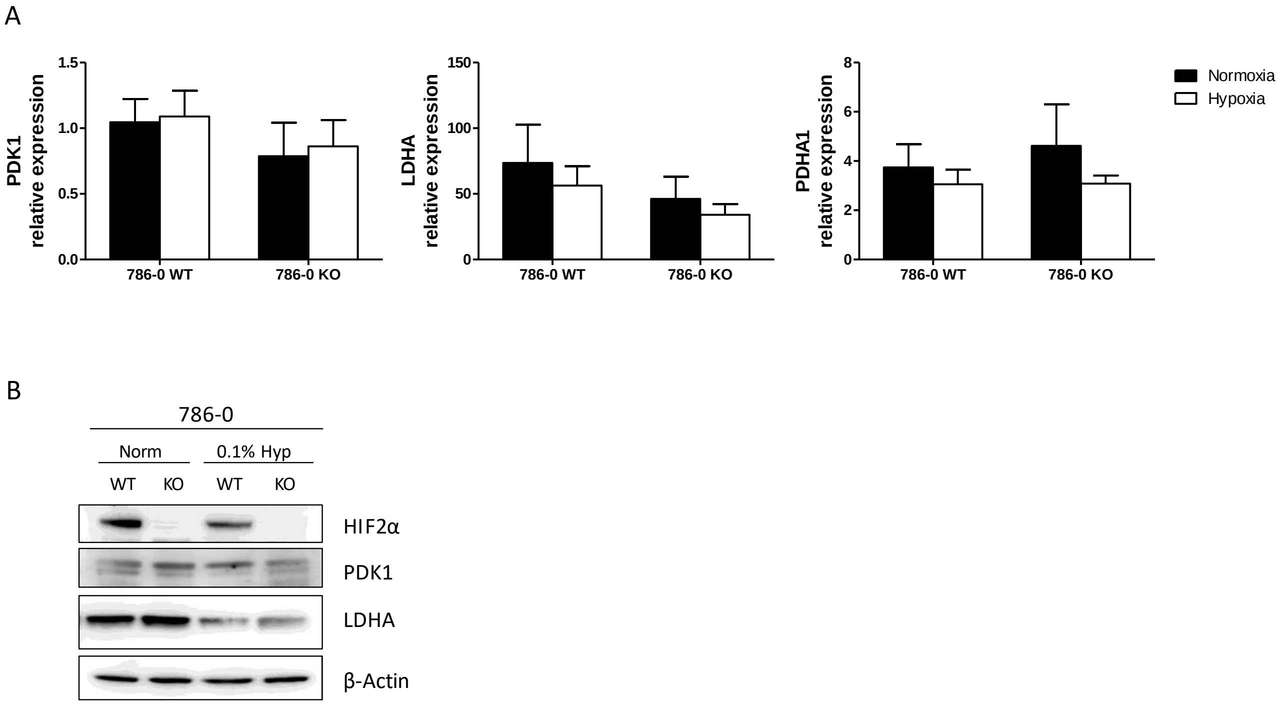

Figure 3.32. A) Relative mRNA expression of *PDK1*, *LDHA* and *PDHA1* in 786-0 WT and 786-0 KO cells cultured in normoxia or 0.1% hypoxia for 48h. n=3. * p<0.05, ** p<0.01, *** p<0.001. B) Protein expression of HIF2α, PDK1 and LDHA in 786-0 WT and 786-0 KO cells cultured in normoxia or 0.1% hypoxia for 48h. n=3.

3.4.6.2. HIF2α's role in lipid metabolism

ccRCC is characterized by its lipid and glycogen-rich cytoplasmic deposits [320] and it has been previously described that HIF2α is an important regulator of lipid storage [318]. Therefore, fatty acid metabolism was also studied in 786-0 cell lines.

No differences were detected between 786-0 WT and 786-0 KO in *CD36* expression, which is involved in fatty acids uptake, but significantly lower expression of *PLIN2* (p<0.05) and hypoxia-inducible gene 2 (*HIG2*) (p<0.05), both genes codifying for proteins covering lipid droplets, was found in 786-0 KO cells (Figure 3.33). This confirms previously published data where HIF2α and PLIN2 expression was positively correlated [318]. Moreover, *CPT1A*, which is involved in the fatty acid transport into the mitochondria to be further used in the β-oxidation, was 3-fold up-regulated in 786-0 KO cells (Figure 3.33). Altogether, this suggests that 786-0 KO cells might have increased β-oxidation, but as the lipid uptake would be the same as 786-0 WT cells, they could be using the fatty acids stored in lipid droplets, followed by a decrease in the amount of those deposits.

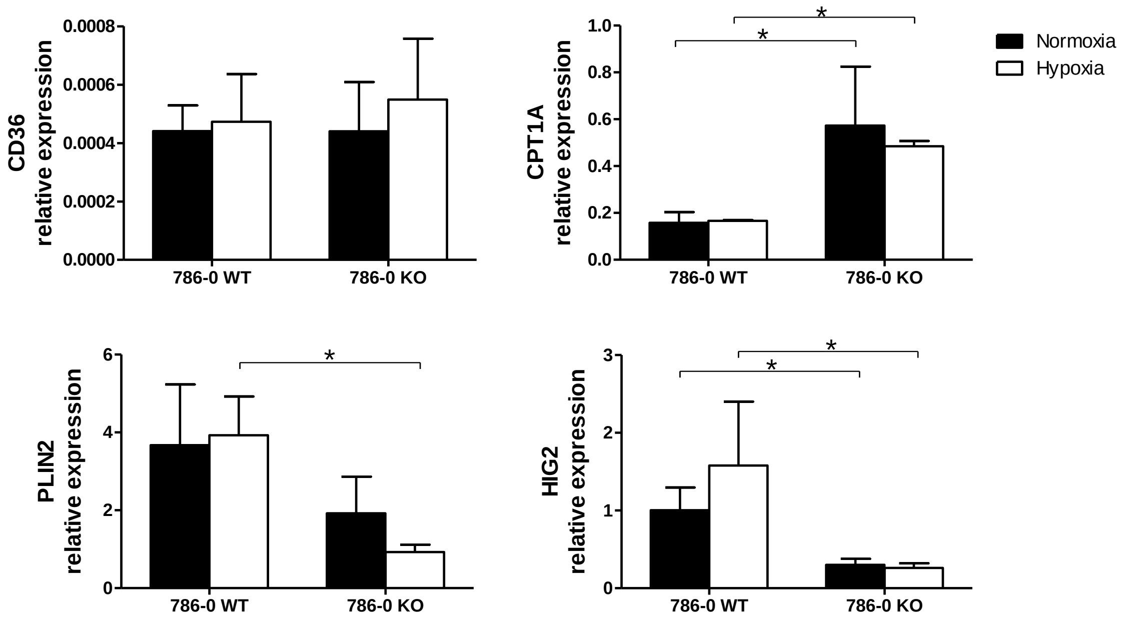

Figure 3.33. Relative expression of *CD36*, *CPT1A*, *PLIN2* and *HIG2* in 786-0 WT and 786-0 KO cells cultured under normoxia or 0.1% hypoxia for 48h. n=3. * $p<0.05$, ** $p<0.01$, *** $p<0.001$.

Lipid droplets are lipid-rich organelles whose main function is the regulation of neutral lipid storage and hydrolysis. They can also provide cholesterol and acyl-glycerols for the membrane formation and suppress the endoplasmic reticulum stress [318]. To further explore lipid droplet content in 786-0 WT and 786-0 KO cells, confocal microscope imaging and flow cytometry was performed. Addition of Oleate-BSA to cell culture induces lipid accumulation, thus it was used as a positive control.

Immunofluorescence images showed lipid accumulation in cells treated with Oleate-BSA, but that pattern was not so strong in non-treated cells (Figure 3.34A). Although 786-0 cells had lipid droplets in their cytoplasm, there were no differences between 786-0 WT and 786-0 KO cells, moreover, the deposits were not clearly defined in any of the cell lines (Figure 3.34A). Even after seeding the cells in hypoxia there was not any enhanced lipid accumulation. However, when analysing lipid droplets by flow cytometry, 786-0 KO cells exhibited 30% more lipids than 786-0 WT ($p<0.01$) and 786-0 KO cells' Nile Red staining level was comparable to that of the positive control (Figure 3.34B). In addition, hypoxia up-regulated the lipid content in both cell lines ranging from 10-30%. Although this result contradicts previously published data in which knocking down HIF2α the lipid droplet content decreased [318], according to the microscope pictures, these cell lines do have lipids, but it seems that they are not contained in droplets. Therefore, the increased fluorescence detected by flow cytometry would be representing spread neutral lipids within the cytoplasm, not the ones stored in droplets.

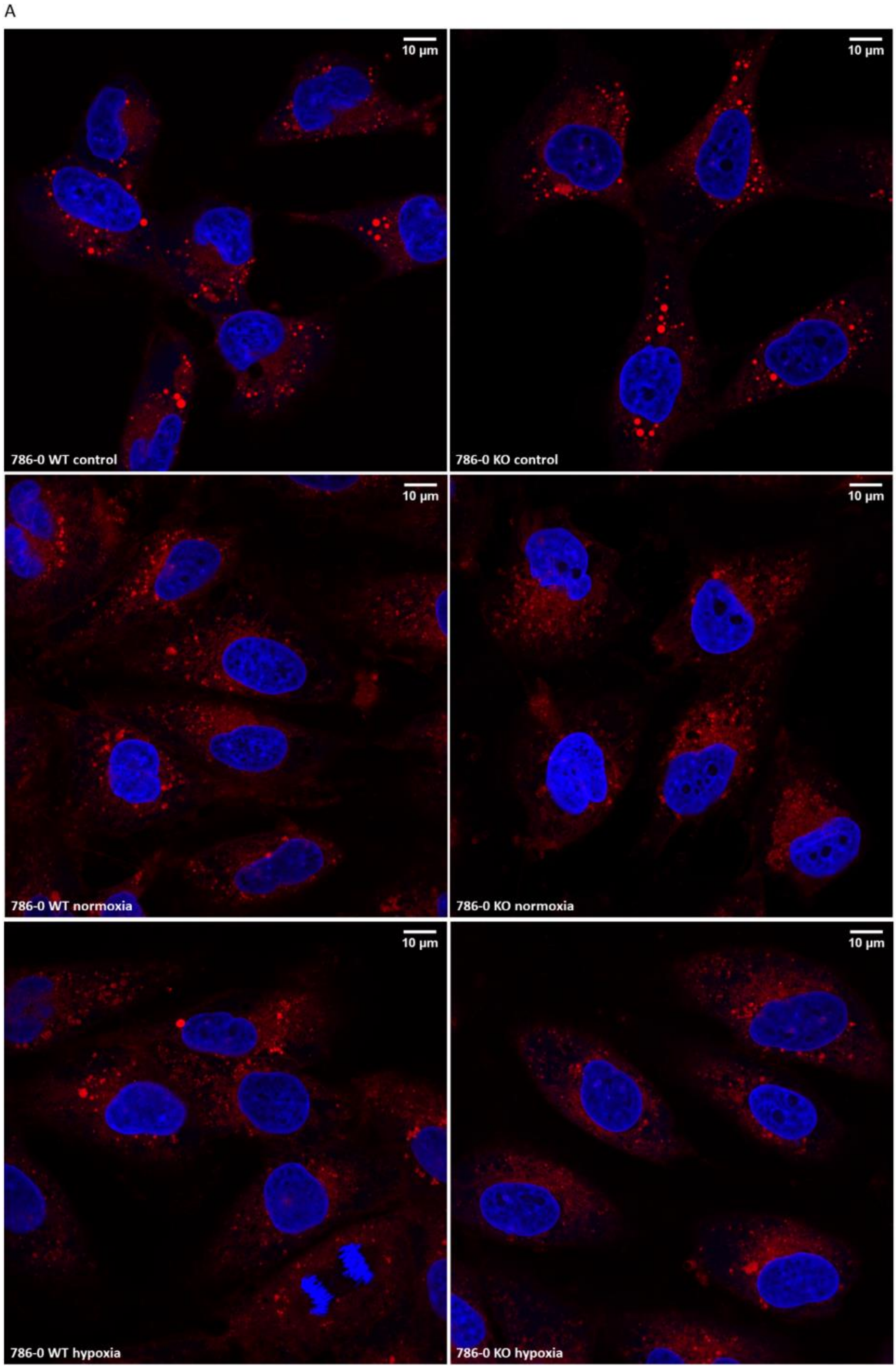
A
10 µm
786-0 WT control
10 µm
786-0 KO control
10 µm
786-0 WT normoxia
10 µm
786-0 KO normoxia
10 µm
786-0 WT hypoxia
10 µm
786-0 KO hypoxia

B

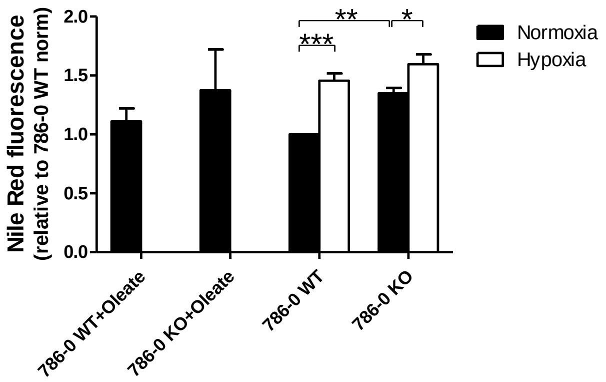

Figure 3.34. A) Immunofluorescence images of Nile Red staining in 786-0 WT and 786-0 KO cells cultured under normoxia or 0.1% hypoxia for 48h. n=3. B) Nile Red fluorescence quantification by flow cytometry in 786-0 WT and 786-0 KO cells cultured under normoxia or 0.1% hypoxia for 48h. n=3. * p<0.05, ** p<0.01, *** p<0.001.

3.4.6.3. HIF2α KO enhances mitochondrial oxidative phosphorylation

HIF2α contribution to the cellular oxygen consumption was also studied. To this end, Seahorse metabolic assay was performed to determine various metabolic features, such as basal respiration, oxygen used for ATP synthesis or maximal respiration of cells, by adding serial drugs which will block different complexes of the mitochondrial oxidative phosphorylation system (OXPHOS) (Figure 3.35).

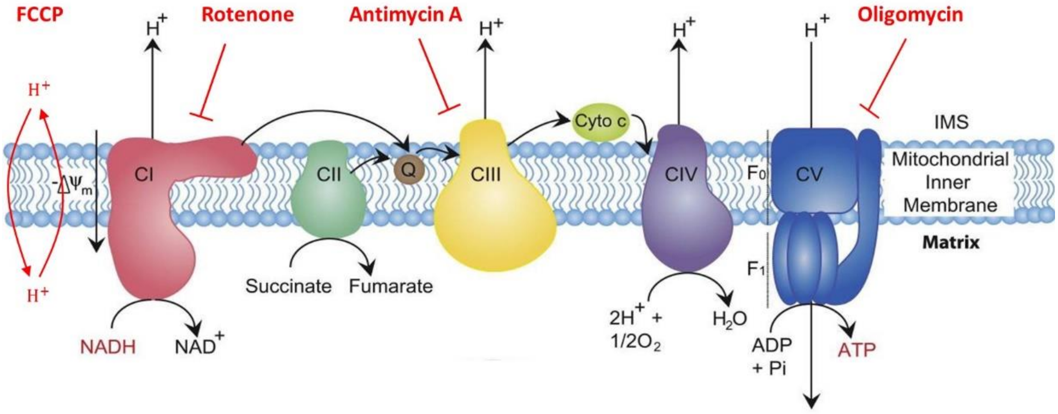
FCCP
Rotenone
Antimycin A
Oligomycin
H+
H+
H+
H+
H+
H+
-ΔΨm
CI
CII
Q
CIII
Cyto c
CIV
Fo
CV
F1
IMS
Mitochondrial Inner Membrane
Matrix
Succinate
Fumarate
NADH
NAD+
2H+ + 1/2O2
H2O
ADP + Pi
ATP

Figure 3.35. Representative picture of the targets of oligomycin, FCCP, rotenone and antimycin A drugs. Modified from [342].

As Figure 3.35 shows, oligomycin was injected to block the ATP synthase complex, thus its injection shows the amount of oxygen used for ATP synthesis beyond the level required to overcome the natural proton leak across the ATP synthase (OCR), which in this case it was not different between 786-0 WT and 786-0 KO cells (Figure 3.36A).

The next added drug was FCCP, which is a proton ionophore that moves protons across lipid bilayers and acts as an uncoupling agent disrupting ATP synthesis by transporting hydrogen ions across the mitochondrial membrane, instead of the proton channel of the ATP synthase. This generates loss of the proton gradient between the mitochondrial matrix and the mitochondrial intermembrane space and loss of the mitochondrial membrane potential. As a result, electron flow across the ETC is increased and oxygen consumption by complex IV reaches the maximum. In addition, loss of mitochondrial membrane potential blocks ATP synthesis by ATP synthase. Therefore, FCCP injection generates an increase in oxygen consumption due to complex IV and in energy consumption due to cells' effort to sustain their energy balance. In this context, 786-0 KO cells presented significantly higher OCR than 786-0 WT cells after FCCP injection ($p<0.001$) (Figure 3.36A). In addition, culturing 786-0 WT cells with PT2385 made them to behave more similarly to 786-0 KO, but not to the same extent, suggesting that HIF2α could block oxygen consumption by the mitochondria. Although the oxygen consumption was increased, ECAR levels kept the same (Figure 3.36B), suggesting that these cells do not rely on glycolysis to maintain their energy levels when energy is highly demanded. Rotenone and antimycin A are ETC inhibitors, and were added to determine the non-mitochondrial respiration. Both 786-0 WT and 786-0 KO cells showed a 2-fold decrease in OCR after Rot/Ant injection, due to impaired mitochondrial function (Figure 3.36A), but no increase in ECAR was observed (Figure 3.36B), further highlighting that glycolysis is not the main energy source of these cells.

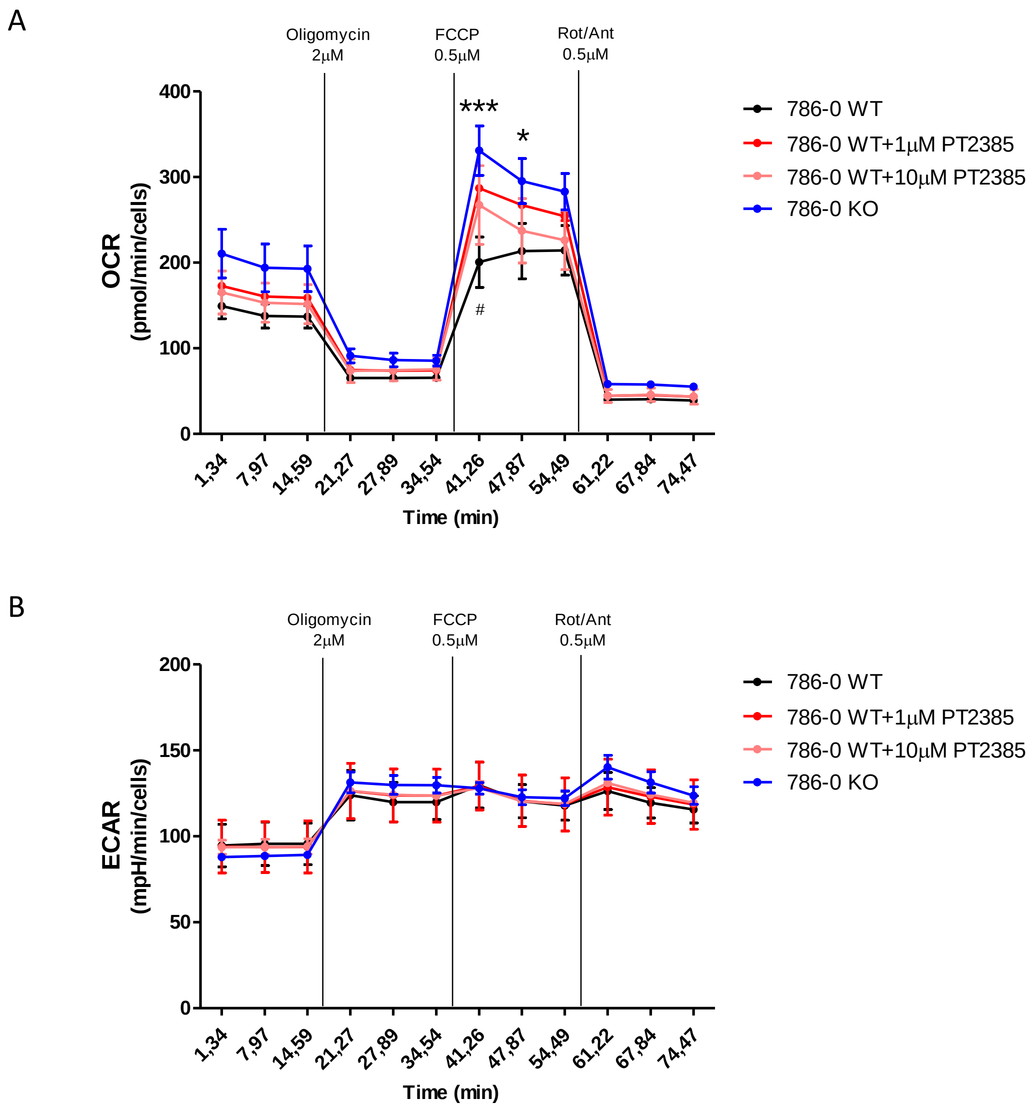

Figure 3.36. OCR (A) and ECAR (B) levels in 786-0 WT cells treated or not with PT2385 and 786-0 KO expressed as a function of time. n=3. * $p<0.05$, ** $p<0.01$, *** $p<0.001$. * represents the comparison between 786-0 WT and 786-0 KO. # represents the comparison between 786-0 WT and 786-0 WT+1μM PT2385.

Regarding RCC4 cell lines, RCC4 VHL basal OCR was 2-fold higher than that of RCC4 WT (Figure 3.37A), due to the faster proliferation rate. Oligomycin injection decreased OCR levels in both cells, being more remarkable in RCC4 VHL, thus showing that the amount of oxygen used for ATP synthesis is high in RCC4 VHL cells. Oligomycin blocks ATP synthase, thus these cells would need another source of energy for ATP production, for instance, glycolysis. That could be happening in RCC4 cells as ECAR levels increased after oligomycin addition (Figure 3.37B). Moreover, after FCCP injection, OCR increased in both RCC4 WT and RCC4 VHL cells by 2- and 3-fold, respectively (Figure 3.37A), showing that mitochondrial membrane potential was lost with FCCP treatment. Similarly to 786-0 cells, OCR incremented but not ECAR (Figure 3.37B), possibly because glycolytic levels in RCC4 cells were already high. Rot/Ant addition dropped OCR levels, because of impaired mitochondrial respiration (Figure 3.37A), but rose ECAR levels in both cell lines (Figure 3.37B). This concomitant increase in ECAR could be due to cells' shift to a more glycolytic state to maintain their energy balance. Here again, if mitochondrial respiration is blocked, RCC4 VHL cells would rely on glycolysis as their source of energy, and having in mind their higher proliferation rate, it could explain that their ECAR levels are higher than RCC4 WT's ($p<0.001$) (Figure 3.37B). PT2385 addition did not affect OCR or ECAR levels in RCC4 cells, suggesting that HIF1α might also be responsible for the observed phenotype.

In general, RCC4 VHL cells mimic 786-0 KO response to a high energy demand after FCCP exposure. This suggests that HIF2α inhibits the mitochondrial oxidative phosphorylation under normal conditions, making the cells obtain their energy from other sources.

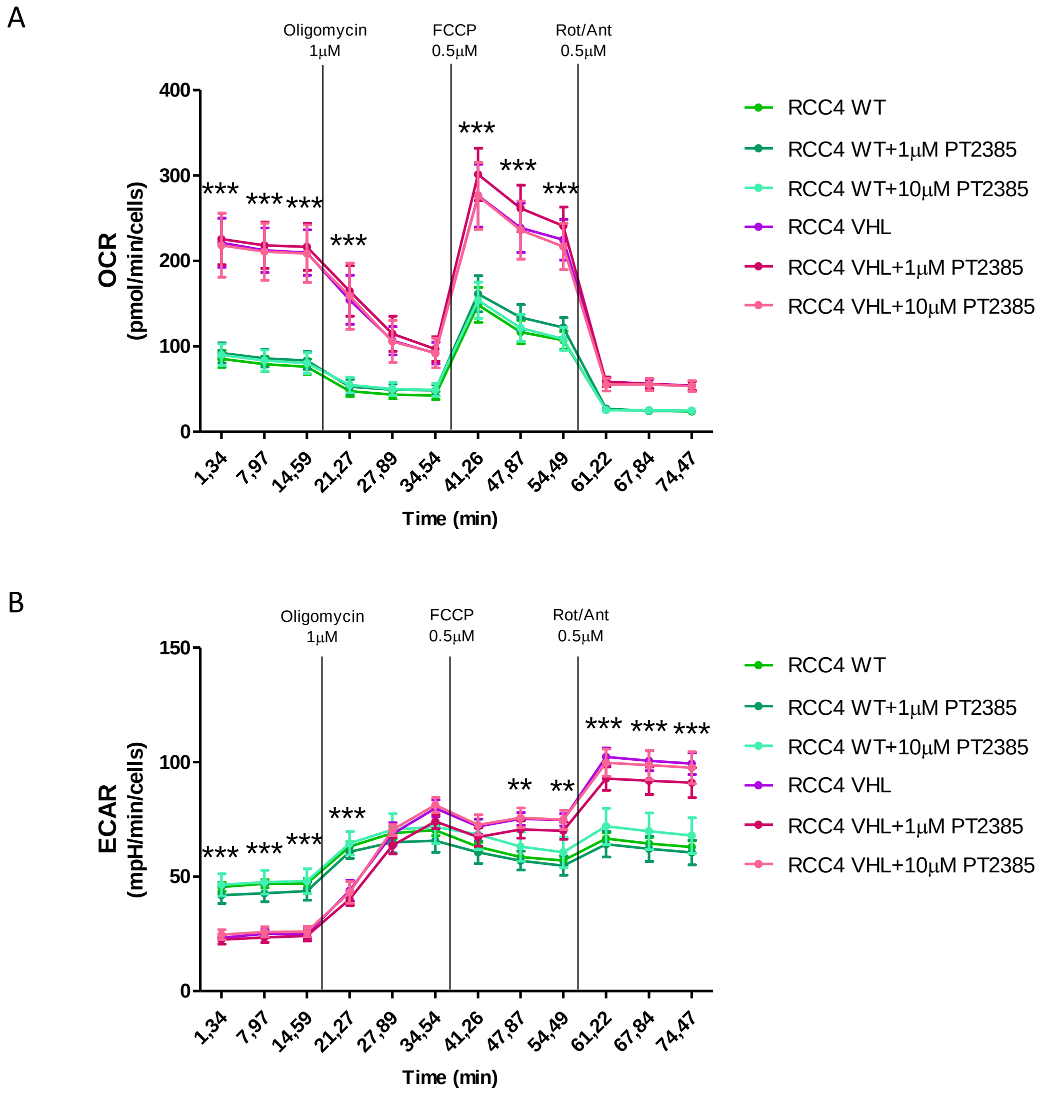

Figure 3.37. OCR (A) and ECAR (B) levels in RCC4 WT and RCC4 VHL cells treated or not with PT2385 expressed as a function of time. n=3. * $p<0.05$, ** $p<0.01$, *** $p<0.001$. * represents the comparison between RCC4 WT and RCC4 VHL.

3.5. Discussion

The successful generation of the HIF2α deficient 786-0 cell line (786-0 KO) allowed the study of this important oncogene in ccRCC development in terms of proliferation, migration, invasion and metabolism, all of which is relevant for the development of new drugs or combination of the existing ones (Table 3.14).

HIF2α effect on 2D cell proliferation

This chapter's results show that HIF2α deficiency does not impair ccRCC cell proliferation when cell confluence is high, whereas it is important for cell proliferation when few cells are in culture, as 786-0 KO cells grew less than 786-0 WT under this condition, both in normoxia and in hypoxia. Similarly, the ability to grow from a single cell was decreased, as they formed less colonies than the parental cell line in clonogenic assays, independently of the oxygen concentration. It has been widely described that HIF2α acts as an oncogene and that it is the tumour driver in ccRCC, rather than HIF1α which acts as a tumour suppressor [125, 126, 231]. In addition, HIF2α can override VHL's suppressive function, whereas HIF1α cannot [126, 343]. In previous reports, a HIF1α or HIF2α variant with full functionality to transactivate the expression of target genes but which escapes VHL degradation was generated. Kondo *et al.* showed that the introduction of this HIF2α variant to VHL-positive 786-0 cells recovered the ability to form tumours in nude mice, showing that HIF2α can bypass VHL tumour suppressor role [126]. Supporting the results presented in this thesis, introduction of HIF2α mutant did not alter 786-0 VHL-positive cells' proliferation *in vitro* [126]. Maranchie *et al.* on the other hand, focused their study on HIF1α, and found that elevated levels of the mutant HIF1α did not cause tumorigenesis in 786-0 VHL-positive cells [126, 343]. Various other studies have shown that HIF2α inhibition does not alter cell proliferation under standard culture conditions [125, 240, 270, 298], whereas when few cells are in culture, such as in a colony formation assay, HIF2α silencing impaired the clonogenic potential of 786-0 cells [93]. Altogether, previously published data and results presented here suggest that HIF2α could confer prosurvival properties to the cells. In line with this idea, Gordan *et al.* found that HIF2α expressing tumours presented enhanced proliferation and resistance to replication stress [231]. Similarly, tumour initiation was demonstrated to rely on HIF2α expression, as precancerous lesions where HIF2α positive, in contrast to normal kidney tissue [278]. Therefore, HIF2α appears to be relevant in both tumour initiation and development. Moreover, the protumoural potential of HIF2α has been long studied *in vivo*, and it has been shown that its genetic silencing impairs tumour development in RCC xenograft mouse models [126, 279, 285, 344], as well as in glioblastoma, colorectal and lung cancer xenografts [345].

This dual behaviour of 786-0 KO cells according to cell confluence could also be explained by the concentration of certain molecules secreted to the media. It was reported that 786-0 cell line secretes EPO, and that by binding to its receptor (EPO-R) expressed in the same cells, promotes cell proliferation in a dose-dependent manner [346]. EPO is known to be a HIF2α target [347-349], therefore, 786-0 KO cells will synthesize less EPO, as shown in this thesis at mRNA level, and consequently will down-regulate the EPO/EPO-R feedback loop possibly reducing the proliferation rate. Moreover, siRNA mediated silencing of EPO-R in ccRCC cell lines led to growth inhibition and decrease invasiveness *in vitro* and *in vivo* [350]. In addition and regarding growth factors, it was demonstrated that HIF2α promoted serum-independent RCC cells' proliferation by activating TGFα/EGFR pathway, as they found that HIF2α was responsible for the increased TGFα levels detected in VHL-negative RCC cells [351]. Moreover, mutant HIF2α was able to induce TGFα overproduction even in VHL-positive cells to levels comparable to those observed in VHL-negative RCC cells [351]. TGFα stimulates cell proliferation via binding to EGFR, but in that study they failed to detect TGFα in the media, implying that TGFα was retained in the cells. However, it is possible to think that 786-0 KO cells synthesize and secrete less TGFα comparing to 786-0 WT, and therefore its extracellular levels are not sufficient enough to induce cell proliferation in the same rate as in the parental cell line.

In this thesis, the HIF2α inhibitor PT2385 was used to pharmacologically mimic HIF2α deficiency. PT2385 avoids the binding affinity of HIF2α to HRE in a dose-dependent manner, but DNA binding is not completely abolished even at saturating concentrations [352]. PT2385 achieved 50% of binding disruption, which was demonstrated as the consequence of partial separation of all HIF2α/ARNT dimers, rather than complete separation of half of the complexes within the cell [352]. In this context and similarly to the genetic silencing, treatment with PT2385 did not inhibit cell proliferation or colony formation at concentrations up to 10µM, neither in normoxia or hypoxia, demonstrating the lack of toxicity of the compound *in vitro*, as previously published [237]. PT2385 addition to cell culture inhibited HIF2α transcriptional activity in a dose-dependent manner, as demonstrated using the HIF2α target genes *VEGFA*, *GLUT1*, *PAI-1* and *EPO*, and previously described for this cell line [237]. Supporting the inhibition of *in vivo* tumour growth achieved by silencing HIF2α using siRNA or shRNA [279, 344], PT2385 has also been proven to inhibit xenograft tumour growth, as well as induce tumour regression in a dose-dependent manner, without causing any adverse effect such as weight loss or behavioural changes [237]. Further supporting PT2385 efficacy, its analogue PT2399 has also been described to repress the expression of HIF2α targets and to induce tumour regression in preclinical mouse models [240]. In that study they found that PT2399 did not alter *in vitro* cell proliferation, but inhibited 786-0 growth in soft agar resembling the impairment of *in vivo* tumour growth, as soft agar clonogenic assay shows anchorage-independent cell growth [353]. Moreover, 786-0 HIF2α KO cells did not form colonies in soft agar [240], also supporting *in vivo* results. Another study showed that PT2399 inhibited HIF2α induced transcription and showed that PT2399 could decrease tumour growth in a ccRCC model [239]. In addition, it has recently been developed the second-generation HIF2α inhibitor PT2977 with the aim of improving PT2385's variable and dose-limited pharmacokinetics (due to the extensive metabolism of PT2385 to its glucuronide metabolite), showing that PT2977 achieved the same effects as PT2385 but at less concentration and doses [354].

Moreover, hypoxia significantly affected the proliferation of both cell lines in the different experiments, showing that even though HIF transcription factors are the most relevant molecules induced under low oxygen conditions, other factors are involved in the resistance to this stress. This is clearly shown in this thesis, as 786-0 cell line does not express HIF1α due to an inactivating mutation in the gene [328].

In contrast, RCC4 cell line showed a different proliferation phenotype compared to 786-0 cells. RCC4 VHL cell line in which both HIF1α and HIF2α are degraded in normoxia (resembling 786-0 KO cell line) proliferated faster and formed more colonies than the HIF-expressing RCC4 WT cell line in normoxia. Moreover, different initial cell densities did not affect RCC4 cells proliferation, as RCC4 VHL divided faster at every tested condition. However, hypoxia had a negative effect in both RCC4 cell lines, being more marked in RCC4 VHL cells, as seen for proliferation and suppression of colony formation.

HIF2α involvement in 3D cell growth

As the physiological characteristics of cells growing in 2D can differ widely from those cells of a 3D culture, spheroid assays were performed to further study the effect of HIF2α deficiency in proliferation in an environment which more closely mimics tumour growth. In this context, 786-0 cells formed compact spheroids, although this compact aggregation was not achieved until day 5 due to the spheroids are stablishing during the first days, as previously seen by using hanging drop cell culture [355]. However, HIF2α absence did not have any effect on the size of the spheroids, whereas it promoted the generation of spheroids with smoother surfaces, as seen for the increased circularity in 786-0 KO spheroids. Supporting this observation, 786-0 cells had been previously described to form very compact and cohesive spheroids, while 786-0 VHL-positive cells produced spheroids that were more loosely aggregated [356]. In this line, treatment with PT2385 markedly augmented spheroid volume and decreased circularity, showing that HIF2α inhibition leads to a less compact structure and more irregular surface, which could be similar to the effect seen by reintroduction of *VHL*. It could be possible that 786-0 KO cells might have acquired additional capacities during the passages to grow as the parental cell line in a spheroid assay, whereas partial and transitory inhibition of HIF2α by PT2385 treatment shows that HIF2α is important to keep cell aggregation within the spheroid. In spite of not detecting differences between the total number of cells in the aggregates, viability of 786-0 KO cells forming the spheroids was lower, suggesting that HIF2α provides protection against the hypoxic microenvironment generated when growing the cells as spheroids. Moreover, PT2385 addition also reduced cell viability, further supporting HIF2α's role in cell survival under hypoxic conditions.

Table 3.14. Summary of 786-0 cells results and comparison with previous publications.

HIF2α inhibition	Result	Reference
Crispr/Cas9	**HIF2α enhances cell proliferation when few cells are in culture**	**Thesis**
siRNA	No alteration in RCC cell proliferation	[125]
shRNA	No alteration in RCC cell proliferation	[270]
siRNA	HIF2α silencing impairs RCC cell clonogenic potential	[93]
PT2385	**PT2385 does not affect cell proliferation or clonogenic potential**	**Thesis**
PT2399	No alteration in *in vitro* RCC cell proliferation	[240]
PT2385	No effect on *in vitro* RCC cell growth	[237]
Crispr/Cas9	**Same spheroid volume but lack of HIF2α generates smoother surfaces**	**Thesis**
VHL^+	Spheroids are more loosely aggregated in 786-0 VHL^+ cells	[356]
Crispr/Cas9	**HIF2α represses *in vitro* cell migration**	**Thesis**
siRNA	HIF2α promotes cell migration in gastric cancer	[357]
siRNA	HIF2α promotes cell migration in head and neck cancer	[358]
Crispr/Cas9	**HIF2α promotes *in vitro* cell invasion**	**Thesis**
siRNA	HIF2α silencing reduces breast cancer cell invasion	[359]
siRNA	HIF2α silencing abolishes pancreatic cancer cell invasion	[360]
Crispr/Cas9	**HIF2α enhances *in vivo* metastasis**	**Thesis**
siRNA	HIF2α promotes lung metastasis in RCC	[361]
Crispr/Cas9	HIF2α activates a metastasis-associated enhancer cluster in RCC	[362]
shRNA	HIF2α promotes lung metastasis in melanoma	[363]
siRNA	HIF2α promotes lymph nodes and lung metastasis in melanoma	[364]
PT2385	Treatment leads to primary tumour regression	[237]
PT2399	Treatment leads to metastasis regression	[240]
Crispr/Cas9	**HIF2α absence decreases *PLIN2* and *HIG2,* but increases *CPT1A***	**Thesis**
shRNA	HIF2α increases PLIN2 expression and lipid accumulation in RCC	[318]
siRNA	HIG2, as HIF1α target, promotes lipid accumulation in ccRCC	[365]
shRNA	HIF-regulated CPT1A repression controls lipid deposition in ccRCC	[320]
Crispr/Cas9	**No decrease in lipid droplets is detected in HIF2α KO cells**	**Thesis**
shRNA	HIF2α expression correlates with lipid content	[318, 320]
Crispr/Cas9	**Hypoxia does not increase lipid droplet quantity by confocal microscopy, but does by flow cytometry**	**Thesis**
siRNA	Hypoxia increases lipid accumulation in breast and glioblastoma cells	[100]
Crispr/Cas9	**HIF2α inhibits mitochondrial respiration**	**Thesis**
PT2385	**Treatment blocks mitochondrial respiration**	**Thesis**
siRNA	HIF2α silencing increases basal OCR and maximal respiratory capacity	[366]
siRNA	HIF2α silencing leads to increase oxidative phosphorylation	[367]

HIF2α role in *in vitro* cell migration and invasion

Regarding the possible role of HIF2α in metastasis, it is well known that it participates and stimulates, together with HIF1α, every step of the metastatic process [104-106]. This dynamic process selects for highly aggressive tumour cells, as they acquire the ability to disseminate from the primary tumour and grow at distant sites [110]. Metastasis is characterised by cellular migration and invasion. In this context, this thesis shows that 786-0 KO cells presented enhanced migration compared to parental cells, in contrast to many other tumour cell lines in which HIF2α promotes cell migration [357, 358, 368]. A study on the migrating border cells of the *Drosophila* ovary showed that the duration of the hypoxic exposure could block or accelerate cell migration [369]. Similarly, they demonstrated that the HIF1α orthologue Sima could either inhibit or promote cell migration in a dose-dependent manner. Therefore, due to the similarity between the fly and human HIF pathways, it possible to suggest that HIF2α may trigger different phenotypes in different human tumour types. It could be also possible that HIF2α transactivates the expression of molecules such as cdc42, which inhibits cell migration in highly metastatic breast cancer cells [370], indirectly impairing cell migration. Supporting HIF2α negative regulation in 786-0 cell migration, treatment of human primary tubular epithelial cells with the PHD inhibitor dimethyloxalyl glycine (DMOG) led to HIF stabilization and resulted in slower migration of tubular epithelial cells [371].

On the contrary, 786-0 KO cells reduced *in vitro* invasion comparing to 786-0 WT. It was described that siRNA silencing of HIF2α in breast cancer cells significantly reduced the invasion ability by inhibiting MMP2 expression [359]. Moreover, high extracellular ATP levels in breast cancer could also stimulate HIF signalling and promote cell invasion both *in vitro* and *in vivo* via HIF2α, rather than HIF1α [372]. They concluded that ATP-induced breast cancer cell invasion was mediated by HIF2α due to the up-regulation of MMP9 and Snail and decrease of E-cadherin expression, all of which was suppressed after HIF2α silencing [372]. Similarly, knocking down HIF2α in pancreatic cancer cells abolished cell invasion by increasing E-cadherin expression and down-regulating the levels of MMP2 and MMP9, all critical for EMT process [360]. However, 786-0 KO cells did not present higher levels of E-cadherin than 786-0 WT, suggesting that invasion is regulated by a different mechanism. Additionally, mice expressing both HIF2α and mutant K-Ras in the lungs developed larger tumours with increase tumour burden, vascularity and local invasion compared to mice expressing only K-Ras [373]. Altogether, HIF2α appears to be an important regulator of cell invasion both *in vitro* and *in vivo.*

Interestingly, treatment of 786-0 WT cells with the HIF2α inhibitor PT2385 did not affect cell migration while it abolished cell invasion in a concentration-dependent manner, but not to the same levels as 786-0 KO cells. On the other hand, silencing of HIF2α did not change the migration or invasion ability of 786-0 cells. This suggests that complete inhibition of HIF2α is required to see an effect on cell migration and invasion, as neither PT2385 nor siRNA suppresses total HIF2α activity, as supported by previous studies [352]. It is remarkable that HIF2α partial blockage has opposing effects depending on the agent used as the inhibiting mechanism is different. PT2385 allosterically binds to HIF2α and thereby prevents the heterodimerization with HIF1β and its subsequent binding to the DNA [235], whereas siRNA binds to complementary mRNA and targets them for degradation in a transitory manner [374]. However, HIF2α silencing was successfully achieved during the whole invasion experiment but at the endpoint (96h), when HIF2α started to express again. These results suggest that the few molecules escaping siRNA silencing might be enough to keep a WT phenotype, even though they are not detectable at protein level. On the other hand, PT2385 treatment clearly shows that DNA binding is not completely abolished by the inhibitor, as previously reported [352], and therefore, an intermediate phenotype is observed.

Migration results are further supported by RCC4 cell line, as RCC4 VHL cells migrated more than RCC4 WT. In this case, not only HIF2α but also HIF1α inhibited cell migration, as seen in the intermediate phenotype generated after PT2385 treatment. RCC4 migratory phenotype observed in this thesis contradicts previous publications. It was reported that RCC4 WT cells, due to *VHL* loss of function, had an increased glutamate release, in addition to the up-regulation of glutamate receptors generated by HIF activity, and that glutamate binding to its receptors stimulated RCC4 cell migration and invasion [375]. Similarly, it has recently been shown that RCC4 WT cells migrated significantly faster than RCC4 VHL cells over 12h [376]. These differences could be due to the use of different techniques as Hu *et al.* used 8 mm-pore Transwell chambers [375] whereas Sumi *et al.* used wells plugged with stoppers for cell seeding [376] instead of the wound healing used in this thesis. Moreover, increased RCC4 VHL migration is in accordance with the enhanced migration observed in the HIF-deficient 786-0 KO cells, suggesting that HIF represses ccRCC cell migration. Nevertheless, further experiments should be performed in other ccRCC cell lines to confirm this. In addition, RCC4 cell lines required more time to close the wound and they barely invaded through the Matrigel®, likely due to the earlier tumour stage they arise from, comparing to 786-0 cells.

HIF2α enhances *in vivo* metastasis

These opposing results between migration and invasion in 786-0 KO cells suggest that HIF2α deficiency leads to increased cell movement, but decreased ability to degrade the ECM and invade and colonize other tissues. This lower invasion could also be due to the lower proliferation starting from few cells, as they could reach a new niche but fail in creating a new tumour. This observation is highly supported by the *in vivo* results, in which 786-0 KO cells failed to generate any metastasis, and by previous reports. In this regard, hypoxia and HIF transcription factors are associated with increased distant metastasis and poor patient outcomes in a variety of cancer types. In RCC, HIF-driven AXL (a member of the TAM family of receptor tyrosine kinases) expression promotes lung metastasis in NOD SCID mice [361]. Moreover, it was described that during renal tumour progression cancer cells potentiate HIF activity by epigenetically modifying metastatic genes, which will later enhance HIF transcriptional activity on those genes and finally promote metastatic progression [377]. Similarly, distal DNA elements called transcriptional enhancers, which are important for the regulation of gene expression, have been identified to promote metastasis in renal cancer [362]. Specifically, in this study they characterized a metastasis-associated enhancer cluster activated by both HIF2α and NF-κB pathway which promoted *in vivo* metastasis via CXCR4. Besides, it has been recently published the prognostic significance of several genes in ccRCC patients [378]. They described that high HIF2α mRNA and protein expression in tumour tissue of patients treated with sunitinib as first-line therapy after nephrectomy was associated with shorter OS and PFS, as well as unfavourable risk factors for cancer recurrence and mortality, showing HIF2α's oncogenic role in ccRCC. Similarly, HIF2α-induced CUB domain-containing protein 1 (CDCP1) expression in melanoma cells promoted lung metastasis in NOD SCID mice [363], whereas in a conditional mouse model of highly metastatic melanoma it was shown that both HIF1α and HIF2α enhanced lymph node and lung metastasis [364]. Silencing of HIFs did not affect *in vitro* cell proliferation, as previously described in this thesis, but it decreased cell invasiveness *in vitro* and abolished metastasis formation *in vivo* [364]. HIF activity can also be enhanced via binding to Y-box protein 1 (YB-1), a DNA and RNA binding protein which regulates transcription, RNA processing and translation [379]. YB-1 was found to be a potent metastatic driver in sarcomas due to its association to *HIF1α* and induction of HIF1α protein expression, leading to HIF1α-mediated *in vivo* metastasis [380]. Regarding breast cancer, hypoxia and HIF1α expression in breast cancer cells enhanced bone metastasis [381], whereas HIF1α deletion or inhibition resulted in delayed tumour growth and decreased lung metastasis [105, 382]. Similarly, HIF2α expression was correlated with reduced recurrence-free and cancer-specific survival in breast cancer patients [383]. Moreover, a meta-analysis revealed strong significant negative associations between HIF2α expression and OS, DFS, DSS, metastasis-free survival and PFS, demonstrating a negative prognostic role of HIF2α in patients suffering from different types of solid tumours [384]. Altogether these studies show that both HIFα subunits can enhance tumour progression and metastasis independent of the tissue of origin.

This thesis has shown that HIF2α expression in 786-0 WT cells promoted metastasis two weeks after cell injection. Mice presented metastasis in the lungs, which are the most common site of metastasis in RCC [385], but also in the mammary fat pad and the brain. Distant metastasis in renal cancer include lungs, lymph nodes, liver, bones and brain [386]. The incidence of brain metastasis is low comparing to other tissues and it has been accounted to be 7-8% in several studies [146, 386, 387], in this thesis 1 out of 10 mice (10%) developed brain metastasis. Brain metastasis occurs with an average interval from nephrectomy of 1-5 years [388-390], likely due to the slow growing nature of RCC. Therefore, although rare events in RCC, brain metastasis occur and are associated with a negative prognosis [391].

Lung metastasis were detected two weeks after tumour cell injection, but they disappeared at week 4 and reappeared 10 weeks later. Spontaneous tumour regression, which is defined as 'partial or complete disappearance of a malignant tumour in the absence of all treatment or in the presence of therapy, which is considered inadequate' [392], is a rare event that can be observed in all types of tumours, but most frequently in RCC. The frequency of spontaneous regression in RCC patients is estimated to be 1% [393]. Spontaneous regression of primary renal tumours can occur [175, 394], but regression of lung metastasis is more common [395-397]. Besides, although with much less frequency, regression of other metastatic sites such as adrenal glands [398], brain, bone and liver [399] have also been reported. As RCC metastasizes quickly, appearance of delayed metastasis is considered a kind of regression [393]. The prognosis of patients exhibiting tumour regression is substantially better than those RCC patients who do not, however, complete regression of metastatic lesions or primary tumour does not imply cure, as demonstrated for one patient who developed brain and lung metastasis 12 years after tumour nephrectomy and complete regression of pulmonary metastasis [176]. Therefore, even though spontaneous regression provides a better outcome, the risk of late recurrence still remains. The primary factors affecting spontaneous regression are tumour cell apoptosis, immune system activation and inhibition of angiogenic molecules present in the tumour microenvironment, moreover, the majority of spontaneous metastasis regression cases have occurred following nephrectomy [337]. Primary tumour resection results in the elimination of growth factors and anti-apoptosis molecules released by the primary tumour, suppressing cancer progression. In addition, during surgery, some cancer cells can disseminate resulting in higher tumour antigen exposure and stimulating a strong antitumour immune response [393]. Spontaneous regression of RCC led to the idea that RCC is a highly immunogenic tumour [179], as the immune system was postulated to be the main responsible for regression [176]. Supporting the immune system's participation, it was shown that a patient with psoriasis and metastatic RCC presented spontaneous regression of pulmonary metastasis after nephrectomy, together with exacerbation of the autoimmune disease [400].

Previous publications show that treatment of mice bearing RCC tumours with the HIF2α inhibitors PT2385 [237] and PT2399 [239, 240] led to primary tumour regression. Moreover, lung metastasis in nude mice were also regressed after PT2399 treatment [240], and they reported that stopping PT2399 treatment for two days allowed tumour growth, which was inhibited again after drug rechallenge.

These studies show that HIF2α promotes primary tumour formation and metastasis, both of which can be avoided by silencing, or as in this thesis, knocking out the expression of HIF2α.

Furthermore, as metastasis reappeared 10 weeks after in 786-0 WT mice, it is possible to think that CSC non-detected by luciferase signal at week 4 persisted and gave rise to metastasis again. CSC are a small population of cancer cells with characteristic of normal stem cells, such as unlimited cell division and multipotency capacity, which will permit the maintenance of the stem cell pool (self-renewal) and give rise to all cell types present in the tumour tissue (multipotency), respectively [401]. This specific cell population is believed to be implicated in tumour progression, metastasis, relapse and poor prognosis. Therefore, elimination of CSC would lead to tumour eradication, while if only one cell is left after the treatment, tumour recurrence is highly probable [402, 403], as CSC are recognized to be the major cause of resistance to therapy. CSC are resistant to current therapies due to their quiescent state, the hypoxic microenvironment in which they reside, the up-regulation of damage response mechanisms and the increased drug efflux potential [404]. HIF2α has been described to participate in CSC population maintenance in several malignancies [405-407], including RCC [408]. Altogether, these results clearly show the spontaneous regression of metastatic lesions occurring in RCC and rise the possibility of metastasis reappearance due to HIF2α-mediated CSC promotion.

HIF2α regulation of cell metabolism

Regarding tumour cell metabolism, cancer cells switch their metabolism from aerobic respiration, in which glucose is completely oxidized through the TCA, to aerobic glycolysis, in which glucose is converted to lactate [409]. This process is known to be mainly driven by HIF1α [98, 271], but it has been reported that HIF2α can also promote it [125, 126, 285]. Therefore, glucose metabolism was analysed in 786-0 WT and 786-0 KO cells. Proliferation increased in a glucose dose-dependent manner in both cell lines. However, 786-0 KO cells presented more difficulties than 786-0 WT to grow, suggesting that HIF2α might confer growth advantages to the parental cell line, such as up-regulating GLUT1 expression, as previously reported [125, 126] and shown in this thesis, to increase glucose uptake. Treatment of the cells with 2-DG on the other hand, impaired proliferation of both cell lines, as it has been previously described for several cancer cell lines [410]. 2-DG is an analogue of glucose which competitively inhibits glucose uptake. It is preferentially captured by tumour cells, but its phosphorylated form (2-DG-P) cannot be further metabolized, thus the ATP and NADPH production from glycolysis and pentose phosphate pathway, respectively, is inhibited [411], and consequently cell proliferation. In 786-0 cells, HIF2α presence did not provide protection against 2-DG, as parental cell proliferation was equally inhibited as 786-0 KO cells. Therefore, even though 786-0 WT cells might uptake more 2-DG due to higher GLUT1 expression, glycolysis impairment by the glucose analogue is the same as in HIF2α KO cells. In addition to not being able to be metabolized, 2-DG-P cannot diffuse to the extracellular media, as the cell membrane is impermeable for it. This 2-DG-P accumulation inside the cell has promoted the development of drugs to image tumour cells based on their high glucose metabolism, such as positron emission tomography (PET) with 2-deoxy-2-[^{18}F]-fluoro-D-glucose (FDG) [412].

Despite that HIF1α is the main driver of the Warburg effect [98, 271], it has been demonstrated that both HIF1α and HIF2α can regulate the expression of the same genes [413]. Moreover, it is known that both HIF transcription factors are expressed under acute hypoxia, but only HIF2α drives chronic hypoxic responses, due to reduce stability of *HIF1α* mRNA [91, 414]. 786-0 cells are considered to be in a chronic hypoxic state due to *VHL* mutation, and they do not express HIF1α due to an inactivating mutation [328]. Therefore, known HIF1α-targeted glycolytic gene expression was evaluated in these cells to see if HIF2α was undertaking HIF1α's glycolytic role. No differences were detected in *PDK1*, *LDHA* or *PDHA1* mRNA expression as well as PDK1 and LDHA protein levels between 786-0 WT and 786-0 KO cells, suggesting that HIF2α is not overtaking HIF1α's control of the glucose metabolism and anaerobic respiration in this cell line, as previously seen by Hu *et al.* [413].

Apart from the glucose metabolism reprogramming, lipid metabolism also undergoes various alterations in ccRCC. Fatty acids are a very important source of energy for cells, as they provide two times more ATP than carbohydrates. Moreover, the NADPH produced from fatty acid oxidation helps cells to counteract oxidative stress [415]. Fatty acids can be incorporated from the extracellular media or obtained from hydrolysed triglycerides stored in lipid droplets, in addition, cells can also induce the anabolic process of *de novo* synthesis [415]. Fatty acids can have many fates, such as being oxidized to obtain energy, form part of the cellular membrane, storage or become signalling molecules [416]. Besides, lipid catabolism depends on oxygen levels. Under hypoxia, fatty acid oxidation is impaired due to HIF-induced inhibition of enzymes involved in fatty acid degradation, such as proliferator-activated receptor-γ coactivator-1α (PGC-1α) and CPT1A [320, 417], therefore, cells accumulate fatty acids in the form of neutral lipids. Neutral lipids are stored in intracellular storage organelles named lipid droplets which consist of a core of neutral lipids (triacylglycerols and sterol esters) surrounded by a monolayer of phospholipids. Although lipid droplet biogenesis is not completely understood, they are thought to be generated from the endoplasmic reticulum [418]. As neutral lipid concentration the in endoplasmic reticulum lumen increases, lipids coalesce forming an oil lens, which upon expansion, starts budding from the endoplasmic reticulum membrane and will finally become an independent organelle [419]. Lipid droplet number, size and composition varies between cells, and even within the cell, and it usually reflects the metabolic state of the cell. It is known that after budding, lipid droplets can expand, via fusion with other lipid droplets, or through transfer of more neutral lipids from the endoplasmic reticulum [420]. In addition to store lipids for metabolic processes and membrane synthesis, lipid droplets protect the cells from lipotoxicity as they can sequester free fatty acids that often act as detergents by disrupting membrane integrity or by being incorporated to lipid species that are cytotoxic at high levels [418]. Similarly, lipid droplets have been reported to confer protection against ROS, as it was shown that oxidative stressors such as hyperoxia, hypoxia or myocardial ischemia resulted in lipid droplet formation [421]. As HIF2α has been described to strongly participate in lipid metabolism in ccRCC [318], various features of this metabolic pathway were analysed in this thesis. HIF2α absence down-regulated mRNA expression of two proteins which cover lipid droplets, *PLIN2* and *HIG2*, whereas *CPT1A* expression, an enzyme regulating fatty acid transport to the mitochondria for β-oxidation, was increased in 786-0 KO cells compared to the parental cell line. It has been described that HIF2α promotes lipid accumulation in ccRCC by increasing PLIN2 expression [318]. Moreover, in this study they showed that HIF2α-driven lipid droplet formation is required for the integrity of the physically and functionally associated endoplasmic reticulum, as *PLIN2* depleted cells suffered from unfolded protein response (UPR). UPR is a stress response pathway activated by the accumulation of misfolded proteins within the endoplasmic reticulum lumen or by exogenous free fatty acids [419]. Lipid droplets serve as temporary depot of proteins destinated for degradation and storage of harmful free fatty acids [422], helping in the maintenance of endoplasmic reticulum homeostasis. Similarly, perturbation of lipid droplet biogenesis also triggers an UPR, possibly due to the aberrant lipid storage that can alter endoplasmic reticulum homeostasis [423]. They concluded that HIF2α-induced PLIN2 is required for lipid droplets formation which will promote endoplasmic reticulum homeostasis and prevent cytotoxic endoplasmic reticulum stress in ccRCC [318]. Similarly, HIG2 has also been described to stimulate intracellular lipid accumulation in cancer [365] and normal cells [424] in a HIF-dependent manner. HIG2 was found to be abundantly expressed in ccRCC and to be a direct and specific HIF1α target [365]. Even though Gimm *et al.* stated that HIG2 was not HIF2α target in 786-0 cells, this thesis results show that at least at mRNA levels, HIF2α does enhance *HIG2* expression, showing that in HIF1α-mutated 786-0 cells HIF2α can transactivate some HIF1α target genes. Moreover, ccRCC is predisposed to lipid deposition rather than lipid catabolism, possibly due to the CPT1A repression mediated by HIFs [320]. CPT1A inhibition avoids fatty acid entry to the mitochondria for further oxidation, and forces fatty acid accumulation in lipid droplets. mRNA expression of *PLIN2, HIG2* and *CPT1A* supports the hypothesis that in the presence of HIF2α, fatty acid β-oxidation is inhibited and, therefore, lipid accumulation increases; whereas after HIF2α depletion, lipid storage is reduced possibly due to an increase in lipid catabolism. Altogether this suggested that fatty acid β-oxidation could be increased in 786-0 KO cells, no via higher fatty acid uptake, as *CD36* expression was similar between cell lines, but by using lipids stored in lipid droplets. However, confocal imaging of the cells did not support this idea, as no differences were detected between cell lines or conditions. Hypoxia-blocked lipid oxidation should lead to an increase in lipid droplet accumulation, as previously reported for breast and glioblastoma cell lines [100]. Both 786-0 WT and 786-0 KO cells appeared to have similar levels of lipids in the cytoplasm, with no differences between normoxia and hypoxia, although the staining was not counted, and the deposits were not as defined as in the positive control. It was published that Nile Red could bind to proteins containing hydrophobic domains, such as low density lipoproteins [425, 426] and also to intracellular membranes [427], in addition to lipids. This could be the reason of the deposit-lack staining pattern. However, when analysing these cells by flow cytometry, Nile Red staining count was higher in hypoxia compared to normoxia, as previously described [100], but also in HIF2α-depleted cells compared to the parental cell line. This contradicts previous publications which show a direct link between HIF2α expression and lipid content [318, 320]. Both studies used shRNA to silence HIF2α and analyse the lipid droplets, whereas here HIF2α was depleted by Crispr/Cas9 technology. Du *et. al* showed that both HIF1α and HIF2α induced lipid droplet formation in RCC4 cells, as silencing of either isoform resulted in a significant decrease, being this inhibition much higher when knocking down both [320]. This double knock down would correspond to 786-0 KO cells, but in contrast to that publication, no dramatic decrease in lipid droplets is reported in this thesis. Furthermore, the increase in the amount of Nile Red fluorescence in 786-0 KO cells detected by flow cytometry suggests that these cells might have more lipids in the cytoplasm than 786-0 WT cells, but as confocal images show, they do not seem to be contained in lipid droplets.

Continuing with the metabolism study, the effect of HIF2α deficiency on oxidative phosphorylation was analysed. In this context, HIF2α blocked mitochondrial oxygen consumption in 786-0 cells, and therefore, mitochondrial respiration. However, no increase in ECAR after FCCP injection in 786-0 KO cells suggests that these cells do not rely on glycolysis to obtain the energy when it is highly demanded, as previously reported [413]. This supports previous results showing that in 786-0 cells HIF2α is not overtaking HIF1α's glycolytic role. PT2385 treatment generated an intermediate phenotype between 786-0 WT and 786-0 KO cells, at every concentration tested. Saturating concentrations (10µM) of the compound were not able to mimic 786-0 KO cells' phenotype, as seen for the invasion assay. Nevertheless, PT2385 shows that HIF2α inhibits mitochondrial respiration in these cells. In agreement with these results, HIF2α knock down significantly increased basal OCR and maximal respiratory capacity in 786-0 cells, in addition to down-regulate the expression of the known HIF2α-targets *GLUT1, VEGFA* and *Cyclin D1* [366]. Moreover, another study showed that HIF2α protein levels were inversely correlated with mitochondrial DNA (mtDNA) content and oxygen consumption in RCC4 cells [428]. Further supporting the inhibitory role of HIF2α in mitochondrial respiration, it was published that the characteristic decrease in oxidative phosphorylation detected in ccRCC could be due to a decrease of the respiratory chain subunits content [315, 326, 367]. Hervouet *et al.* demonstrated that in 786-0 cells the contents of the respiratory chain subunits were increased after siRNA-mediated HIF2α silencing, which would lead to increase electron flux and oxidative phosphorylation. They confirmed that the decreased content of respiratory chain proteins was likely result from post-translational regulation, rather than lower gene expression [367]. It was also reported that the reduced mitochondrial content and mitochondrial respiratory capacity of ccRCC was accompanied by a high degree of glycolysis [429], in contrast to this thesis results, where no increase in ECAR after FCCP treatment suggests that these cells rely on other metabolic pathway rather than glycolysis to obtain the energy. The higher basal OCR and the higher increase in oxygen consumption after the addition of the mitochondrial uncoupler FCCP in 786-0 KO cells suggest that by knocking out HIF2α tumour cells acquire a normal cell-like phenotype, as Nilsson *et al.* had previously shown [429], clearly exhibiting HIF2α's oncogenic function in ccRCC.

The oxidative phosphorylation of RCC4 cell lines further supports the HIF2α-driven mitochondrial impairment of oxygen consumption. Taking into account the high proliferation rate of RCC4 VHL cell line, it is not surprising to see higher basal OCR levels than in RCC4 WT cells, as previously reported [376, 430]. Similarly to 786-0 cells, FCCP treatment increased OCR levels of both RCC4 VHL and RCC4 WT cells, being this increase higher in RCC4 VHL. Even though OCR levels increased, ECAR levels did not change in RCC4 WT cells likely due to the already high glycolytic levels, whereas no increase in RCC4 VHL cells might suggest that these cells rely on other metabolic pathway to obtain the energy. In contrast to 786-0 cells in which PT2385 demonstrated to have an effect on mitochondrial respiration, in RCC4 cells it did not change OCR either ECAR levels, suggesting that in addition to HIF2α, HIF1α is also blocking mitochondrial oxygen use in order to enhance glycolysis. Zhang *et al.* demonstrated that HIF1α activity was necessary for the reduced OCR detected in RCC4 VHL-deficient cells, as silencing of HIF1α resulted in a partial restoration of oxygen consumption [428]. Similarly, LaGory *et al.* demonstrated that VHL-deficient ccRCC cell lines presented decreased mitochondrial content and activity compared to VHL-expressing cells, as seen in this thesis for RCC4 cells. They demonstrated that this was regulated in a HIF-dependent manner, as silencing each subunit rose OCR levels in RCC4 cells [325]. They showed the same phenotype in 786-0 VHL-deficient vs 786-0 VHL-expressing cells. 786-0 VHL-expressing cells could resemble 786-0 KO cells, and the increase in oxygen consumption seen when silencing HIF2α in RCC4 cells could further support the increase in OCR results observed in 786-0 KO cells.

Altogether, these results show that in ccRCC both HIF1α and HIF2α inhibit mitochondrial respiration.

Differences between 786-0 and RCC4 cell lines

The differences between 786-0 and RCC4 cell proliferation can be explained from a metabolic perspective. It was reported that VHL loss of function is related to decrease mtDNA content in RCC cells [431]. This was further confirmed by stable transfection of *VHL* in RCC4 and RCC10 cells, which resulted in an increase in mtDNA content, mitochondrial mass and oxygen consumption [428]. Zhang *et al.* demonstrated that HIF1α gain of function in VHL-negative RCC cells was necessary for the reduced mitochondrial mass and oxygen consumption, as silencing *HIF1α* in RCC4 cells resulted in a partial recovery of mtDNA content and oxygen consumption. They also showed that HIF1α-enhanced activity in RCC4 VHL-negative cells resulted in reduction of mitochondrial metabolism and increase in glucose transport and glycolysis, and that it was mediated by HIF1α-induced down-regulation of c-MYC transcriptional activity [428], as c-MYC has been described to promote mitochondrial biogenesis [432]. Therefore, according to these results, RCC4 VHL cells are likely obtaining the energy from mitochondrial phosphorylation, which provides 36 ATP molecules, in contrast to RCC4 WT cells, which due to the *VHL* mutation and high HIF1α activity, rely on glycolysis [284]. As glycolysis is not as efficient as mitochondrial respiration, because it only generates 2 ATP molecules, RCC4 WT cells would need to consume more glucose than RCC4 VHL cells to support the energy demands, thus finishing earlier the glucose available in the media, and stopping growing. Whereas RCC4 VHL cell line would not need to use as much glucose as RCC4 WT cells to survive and would continue growing. Supporting this theory, it has been reported that RCC4 VHL cells have significantly reduced glucose uptake and glycolytic activity compared to RCC4 WT cells [433].

Hypoxic greater negative effect on RCC4 VHL cell proliferation might also be due to changes in metabolism. RCC4 VHL cells obtain the energy from the mitochondrial oxidative phosphorylation in normoxia as explained before, but under hypoxia, due to the oxygen absence, mitochondrial ETC is not functional and cells switch to glycolysis to obtain energy [284]. This shift to glycolysis will be an additional negative consequence of hypoxic exposure, which together with the direct hypoxic inhibitory effect on proliferation, will significantly decrease RCC4 VHL cell growth. Whereas RCC4 WT cells, as they rely on glycolysis both in normoxia and in hypoxia, the hypoxic inhibitory effect on proliferation is only a consequence of the low oxygen concentration.

Altogether, this thesis chapter shows that HIF2α has an important oncogenic role in ccRCC proliferation, migration, invasion and metabolism. The results presented here suggest that HIF2α should be strongly taken into consideration when targeting ccRCC, as it is involved in many biological aspects promoting tumour development.

3.6. Conclusions

1. Loss of HIF2α in 786-0 cells inhibits 2D cell proliferation when the initial cell number is low, whereas it does not affect 3D cell growth.
2. HIF2α KO enhances migration but inhibits invasion of 786-0 cells *in vitro* and triggers lower metastasis formation *in vivo.*
3. HIF2α alters ccRCC metabolism by inhibiting mitochondrial oxidative phosphorylation.

4. HIF2α conferred resistance to drugs

4.1. Introduction

4.1.1. Repurposing drugs

In oncology, less than 10% of the new drugs succeed from phase I trials to FDA approval. Moreover, the number has been halving every nine years since 1950 [434]. Therefore, it is necessary to try a different approach to discover drugs against malignancies. In this regard, drug repurposing, also called drug repositioning, has gained a lot of interest in the last few years. The 'Repurposing Drugs in Oncology' (ReDO) project is an international collaboration initiated by a group of researchers, clinicians and patient advocates working in the non-profit sector [435]. The aim of the project is to give to well-known and well-characterized non-cancer drugs new uses in oncology, either as individual therapy or in combination with other repurposed drugs [435]. This would reduce drug development time, as pharmacokinetics, bioavailability, toxicities and dosing would be known. However, some drug candidates may be efficacious at much higher doses than the original registrations, with the possibility of toxicities and adverse effects. In those cases, phase I clinical trials might be required to stablish the maximum tolerated dose. Despite that, repurposing drug development takes 3-12 years in contrast to *de novo* developed drugs which can take between 10-17 years of process [436]. In addition, drug repurposing will reduce costs, as most of the repurposed drugs are available as generics.

Drugs must fulfil some criteria in order to be considered as candidates for repurposing [435]:

1) They are well-known drugs with many years of clinical use.
2) The original toxicity profile is good, even at chronic dosing.
3) The mechanism of action is known.
4) They must have strong evidence of success (*in vitro*, *in vivo* and human data).
5) The efficacy in patients is reported.

The first six drugs to be investigated by ReDO were mebendazole (anthelminthic), nitroglycerin (vasodilator), cimetidine (H2-receptor antagonist), clarithromycin (antibiotic), diclofenac (non-steroidal anti-inflammatory) and itraconazole (antifungal). In addition to losartan (angiotensin II receptor antagonist), chloroquine (antimalaria drug), statins (cholesterol synthesis inhibitors) or omeprazole (stomach acid reductor) which are currently under investigation.

4.1.2. Repurposed drugs in RCC

Metastatic RCC patients usually become resistant to current treatment modalities within 1-2 years [141]. In order to prevent and overcome drug resistance, combining therapeutics that target different pathways may appear to be a promising approach but may also increase the adverse effects.

Therefore, it could be beneficial to expand the search to non-cancer drugs which present a safer profile in other diseases. However, due to the high levels of heterogeneity that typify RCC tumours, it has been suggested that individual gene signatures, rather than collective analysis, would be a more useful approach to identify novel therapeutic possibilities [437]. In addition to this, the same authors demonstrated that the identified drug repositioning candidates only targeted cancer cells within the tumour mass [438]. Examples of drugs that have been studied as repurposed drugs for RCC treatment include metfomin, statins and mifepristone.

1) Metformin

Metformin is a drug to treat type 2 diabetes. It decreases hepatic glucose production, intestinal absorption, and improves insulin sensitivity by increasing peripheral glucose uptake [439]. Supporting *in vitro* and *in vivo* assays in which metformin inhibited RCC cell growth, various reports have demonstrated that metformin improves both metastatic and localized RCC patients' outcome [440-442].

2) Statins

Statins are small-molecule inhibitors of the 3-hydroxy-3-methyl-glutaryl-coenzyme A (HMG-CoA) reductase (HMGR). HMGR, anchored in the endoplasmic reticulum membrane, catalyses the conversion of HMG-CoA to mevalonate, and it is the rate limiting enzyme of the cholesterol synthesis pathway (Figure 4.1). It is therefore the major target for drugs blocking this pathway.

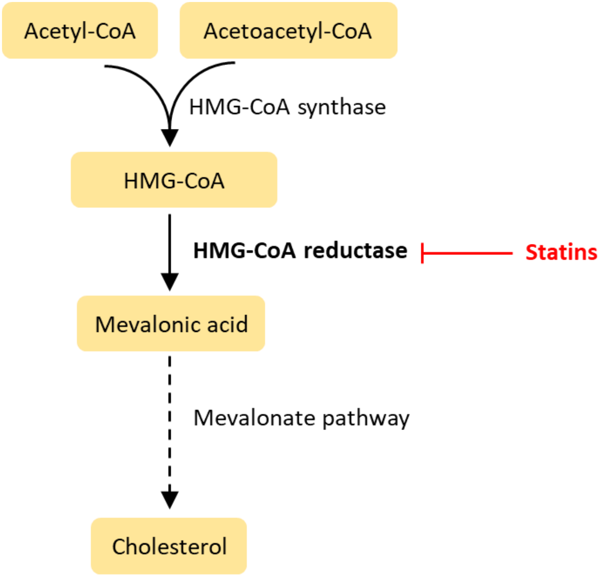

Figure 4.1. Diagram showing the main steps of the mevalonate pathway.

Statins have long been used to reduce cholesterol levels and, therefore, the risk of cardiovascular and cerebrovascular diseases [443]. Besides impairing cholesterol synthesis, they can inhibit other products (e.g. mevalonate and isoprenoids) of the mevalonate pathway too. Statins were first related to cancer in 1991 [444], and subsequently, although controversial, several publications have demonstrated that statins can prevent colorectal [445], breast [446], prostate [447], melanoma [448], leukemia [449] and renal cancer [450, 451], among others, demonstrating the safety and potential utility of repurposing these drugs.

3) Mifepristone

Mifepristone is an antiprogesterone used to end pregnancy by causing the contraction of the uterus. Single agent mifepristone treatment in a metastatic lung cancer patient and a bilateral RCC patient generated a long (5 years for the lung cancer patient and 12 years for the RCC patient) and high-quality survival [452]. In addition, the palliative role of mifepristone in a variety of advanced tumour types, including RCC, has also been described [453].

4.1.3. High-throughput technology

High-throughput screening (HTS) is the automated process of testing a large number of potential biological modulators against a chosen set of defined targets [454]. The primary goal is to identify high quality compounds, called ‘hits’, which affect the target in the desired manner. The best hits are those active at low concentration, as they will provide more specificity and less side effects [454]. Traditional HTS is used to identify a lead compound, rather than a drug, to accelerate drug discovery. From this first identification the compound undergoes further optimization processes where bioavailability, pharmacokinetics, toxicity and specificity are analysed [454].

Cell-based assays, also known as high-content screening (HCS) or high-content analysis (HCA), allow the evaluation of the cytotoxicity, permeability and cellular responses of the tested compounds [455]. Moreover, a variety of different cell lines have been used to predict organ specific toxicity [456].

Despite providing a robust way of testing a wide range of compounds in a short period of time, generated data must be carefully and correctly analysed in order to get reliable results. Many technical, procedural or environmental factors can lead to measurement errors that without correction can significantly restrict the accuracy of the detected hits. The first issue to consider is the spatial system error, defined as differences between wells, which could result from a poorly calibrated apparatus or from environmental variances, such as evaporation in the wells located on the edge of the plate [457]. To avoid spatial system error, positive and negative controls should be placed in wells at both sides of the plate, in addition to not using the edge wells but filling them with media to avoid evaporation.

Moreover, incubating the seeded plates for 1h at RT before placing them in the incubator has been shown to significantly reduce the spatial system error [458].

Technical replicates should also be performed, which after statistical analysis, will show the reliability of the whole process, as well as help determining the threshold value to avoid false positives or false negatives [457]. False positives represent compounds identified as hits but that are not truly active, whereas false negatives are active compounds failed to be identified as a hit. Hits are identified as compounds with high activity or whose responses exceed the fixed threshold value [459]. Therefore, the threshold value will determine the amount of hits, which usually comprise 2% of all tested compounds. A low threshold will result in more hits, and it will also reduce the false negatives, but it will unconditionally increase the probability of obtaining false positives. In contrast, a high threshold generates less hits, as well as less false positives, but it increases the false negatives rate [457]. The threshold is set according to the nature and sensitivity of the HTS to detect an activity. For instance, compounds known to be difficult to generate a detectable effect are analysed with lower threshold values. In this case, false positives will be excluded in the later validation stage.

Any hit obtained from the statistical analysis after the screening needs to be validated, as it is necessary to exclude most false positives as well as stablishing a more detailed effect of the compound. In cell-based assays for compound toxicity analysis for instance, validation assays can be the same viability assay used for the primary screening but including more concentrations of the tested compounds.

4.2. Objectives

The lack of effective treatment for metastatic ccRCC patients has led to drug repurposing. In addition, HIF2α-conferred drug resistance is important given HIF2α's involvement in the progression of the disease. Therefore, the principal aim of this chapter is to identify possible new therapeutic drugs by using HCS technology. The objectives of this chapter are:

1. To identify FDA-approved drugs with different sensitivity between HIF2α-expressing and non-expressing cell lines.
2. To validate the major hits.

4.3. Materials and methods

4.3.1. Pharmacon MicroSource. HCS

In collaboration with Dr Daniel Ebner from the Target Discovery Institute (TDI, Nuffield Department of Medicine, University of Oxford), a HCS of FDA-approved 1600 small compounds (5 Library Plates) was carried out. To this end, the JANUS® Liquid Handler Workstation (PerkinElmer) was used. Firstly, and after optimising the seeding density for each cell line to get 80-90% confluence after 96h, 300 786-0 WT cells and 600 786-0 KO cells per well were seeded in 384-well Black TC-treated plates with Clear Flat Bottom (781091, Greiner) in 75µL of complete DMEM. Seeded plates were kept for 60 min at RT to allow proper cell attachment before placing them in the incubator. 24h later, small compound addition was carried out. Serial dilutions of the 10mM small compound 384-well Library Plates were done in Intermediate Working Stock Plates containing 1.6% DMSO in DMEM to obtain final concentrations of 160µM, 16µM and 1.6µM. Once the compounds were prepared, 5µL of each concentration were added to the cells, getting final concentrations of 10µM, 1µM and 100nM of the compounds per well, respectively. DMSO was added to some wells as a negative control, whereas 100nM and 10nM Gemcitabine (S1714, Selleckchem) were added to other wells as positive controls of the assay. Two replicates per compound concentration and per library plate were prepared, making a total of 30 plates per cell line. Cells were incubated with the compounds for 72h. After this time, cell viability measurement was carried out using Resazurin sodium salt (R7017, Sigma-Aldrich). Briefly, media from seeded plates was removed and replaced with phenol red-free low glucose DMEM (11054020, GIBCO™) supplemented with 4mM glutamine, 10% FBS and 0.1% Resazurin sodium salt. Plates were incubated for 2h at 37ºC before reading in an EnVision plate reader (PerkinElmer) at excitation/emission wavelengths of 560/590nm.

4.3.2. HCS data analysis

To analyse the data, first, the background was subtracted. The lowest reading across all of the plates for one cell line and one library plate (6 plates) was used as background. Then, the quality of the replicates was checked. On the one hand, R^2 and Pearsons' coefficient were calculated to measure the replicate correlation, and on the other hand, Z' were calculated (Equation 4.1) to assess the assay window between the positive and negative controls.

Equation 4.1. Z' standard formula.

$$Z' \text{ standard} = 1 - ((3*(\text{STDEVn}+\text{STDEVp}))/(\text{MEANn}-\text{MEANp}))$$

STDEVn = standard deviation of the negative control (DMSO)

STDEVp = standard deviation of the positive control (100nM or 10nM Gemcitabine)

MEANn = mean of the negative control (DMSO)

MEANp = mean of the positive control (100nM or 10nM Gemcitabine)

Then, plates were normalized by z-score (Equation 4.2).

Equation 4.2. z-score calculation.

$$\text{z-score} = ((\text{MEAN wellR1\&wellR2}) - (\text{MEAN plateR1\&plateR2}))/(\text{STDEV plateR1\&R2})$$

MEAN wellR1&wellR2 = mean of a specific library treated well from replicate 1 and replicate 2 (background subtracted values)

MEAN plateR1&plateR2 = mean of all the library treated wells from replicate 1 and replicate 2

STDEV plateR1&R2 = standard deviation of all the library treated wells from replicate 1 and replicate 2

786-0 WT and 786-0 KO cell lines were compared according to the z-score value. Δ z-score values smaller than -1.96 or bigger than +1.96 correspond to a p-value of <0.05.

Equation 4.3. Δ z-score calculation.

$$\Delta\ \text{z-score} = \text{z-score KO} - \text{z-score WT}$$

Positive values mean that 786-0 KO is less sensitive than 786-0 WT to that compound, whereas negative values mean that 786-0 KO cell line is more sensitive than 786-0 WT (Equation 4.3). Hits were selected based on the Δ z-score value. Statistically significant hits (Δ z-score = <-1.96 or >+1.96) were firstly chosen, followed by those compounds whose Δ z-score was <-1.5 or >+1.5. Selected drugs were further validated by CyQUANT™ Cell Proliferation Assay, as described in ‘Cell Proliferation’ (‘Chapter 3’).

4.3.3. Validation of the Pharmacon screening

In order to validate the results obtained from the HCS, 1000 786-0 WT and 1200 786-0 KO cells were seeded in 96-well black microplates. 24h later, simvastatin (S6196, Sigma-Aldrich), ivermectin (I8898, Sigma-Aldrich), tilorone dihydrochloride (220957, Sigma-Aldrich), nialamide (252999, Sigma-Aldrich), escin (E1378, Sigma-Aldrich), nitazoxanide (N0290, Sigma-Aldrich) or fluvastatin sodium hydrate (SML0038, Sigma-Aldrich) were added at a final concentration of 0.1µM, 0.25µM, 0.5µM, 0.75µM, 1µM, 2.5µM, 5µM, 7.5µM and 10µM. Gemcitabine was also tested at a final concentration of 0.5nM, 1nM, 5nM, 10nM, 50nM and 100nM. The assay was carried out in technical triplicates. Cells were left with the drugs for 5 days, afterwards media was removed and plates were frozen at -80ºC for at least 24h prior to doing CyQUANT™ Cell Proliferation Assay, as previously described.

Further validation of statins was carried out by seeding 1000 786-0 WT, 1200 786-0 KO and 1200 786-0 VHL$^+$ cells in 96-well black microplates. 24h later, simvastatin or fluvastatin was added at 1µM or 2.5µM final concentration, as well as the HIF2α inhibitor PT2385 at a final concentration of 10µM, when specified. After 5 days, media was removed and plates were frozen at -80ºC until CyQUANT™ Cell Proliferation Assay was performed.

4.4. Results

4.4.1. Drug screening validation

With the aim of identifying new possible therapeutic drugs for ccRCC treatment, a drug screening was performed in 786-0 WT and 786-0 KO cells (Figure 4.2). The 1600 small compounds approved by the FDA that were tested included antibacterial, antidiabetic, antifungal, antihypertensive, anti-inflammatory, diuretic, histamine or neurotransmitter-related drugs, among others.

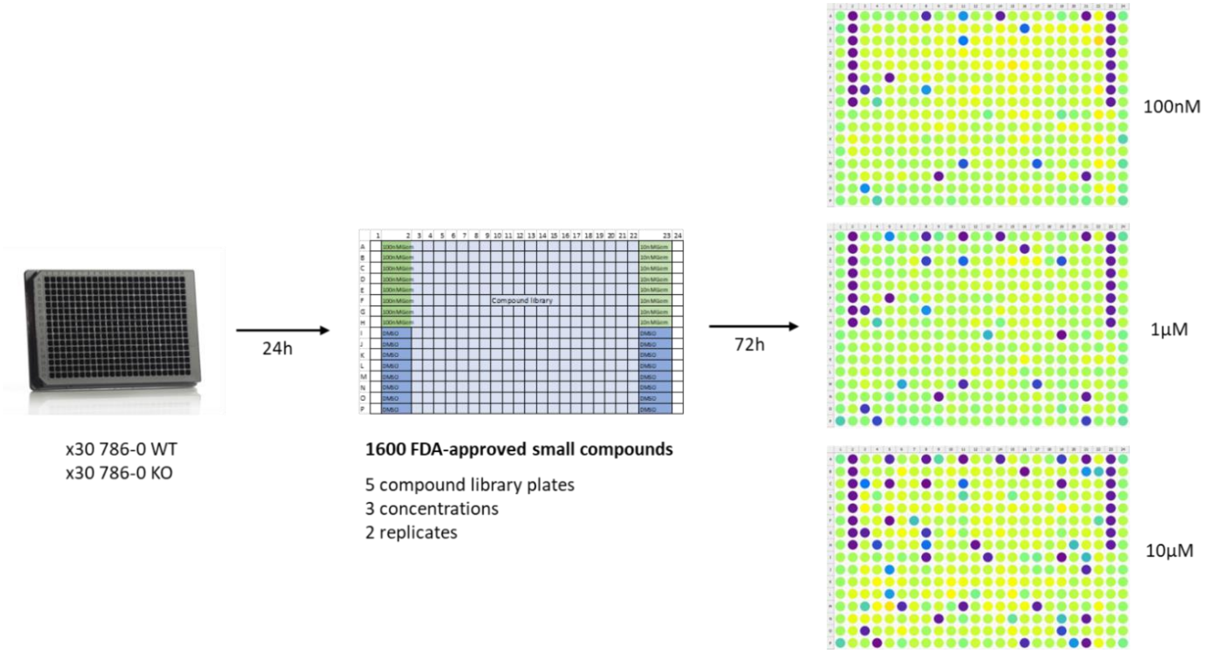
24h
Compound library
72h
100nM
1µM
10µM
x30 786-0 WT
x30 786-0 KO
1600 FDA-approved small compounds
5 compound library plates
3 concentrations
2 replicates

Figure 4.2. Diagram summarizing the drug screening.

13 hits were obtained from this assay. 786-0 KO appeared to be more sensitive than 786-0 WT to nialamide (antidepressive agent), ivermectin (antiparasitic), escin (a saponin inhibitor of edema formation), oxiconazole nitrate (antifungal imidazole), nitaxozanide (antimicrobial), fluvastatin (statin) and simvastatin (statin), as well as to the positive control gemcitabine. Whereas 786-0 WT showed more sensitivity than 786-0 KO to piroctone olamine (antifungal), gramicidin (topical antibacterial), quinestrol (estrogen), sodium nitroprusside (vasodilator), tioxolone (antiseborreic drug) and tilorone (antiviral agent). From these, eight hits were chosen for further validation, but only four (simvastatin, fluvastatin, gemcitabine and nitaxozanide) were successfully validated (Figure 4.3).

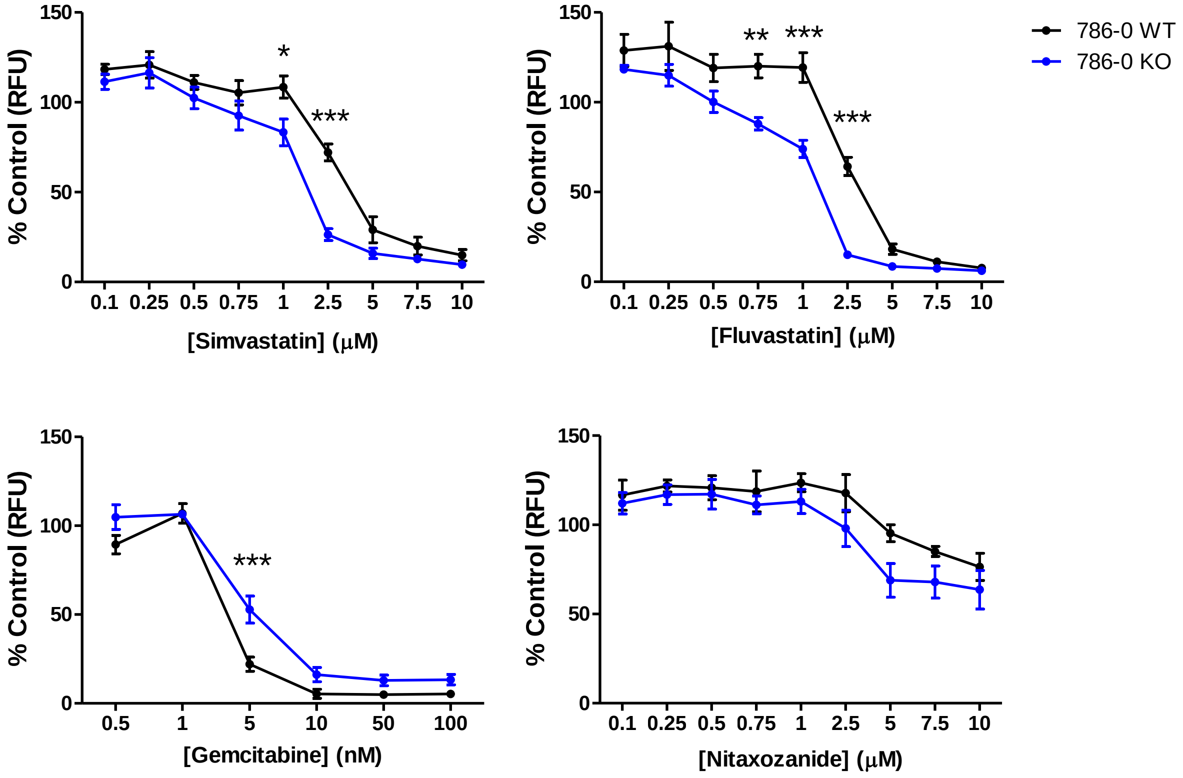

Figure 4.3. Viability of 786-0 WT and 786-0 KO cells treated with simvastatin, fluvastatin, gemcitabine and nitaxozanide during 5 days in normoxia. n=3. * $p<0.05$, ** $p<0.01$, *** $p<0.001$.

As depicted in Figure 4.3 and according to the drug screening, 786-0 KO cells appeared to be significantly more sensitive than 786-0 WT for simvastatin, fluvastatin and nitaxozanide, whereas they were more resistant for gemcitabine.

4.4.2. HIF2α confers resistance to statins

Due to the importance of HIF2α in lipid metabolism and to further explore its involvement in the cholesterol pathway, a siRNA approach was used to strengthen the results obtained with the KO and rule out possible off-target effects due to clonal selectivity. In addition to this, it has recently been published that treatment with statins is lethal for *VHL* defective ccRCC cell lines and that this effect is dependent on HIF signalling [460]. Therefore, 786-0 cell line stably expressing *VHL* gene (786-0 VHL^{+}) was included in the assays.

786-0 VHL^{+} cells, like 786-0 WT and 786-0 KO cells, do not express HIF1α due to an inactivating mutation on the gene [328]. However, they do not express HIF2α in normoxia as a consequence of VHL-mediated degradation, whereas they do express HIF2α in hypoxia, as observed in Figure 4.4.

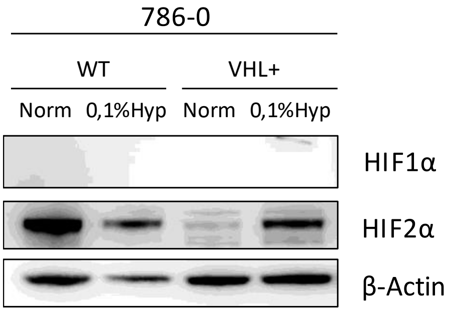

Figure 4.4. Western blot of 786-0 WT and 786-0 VHL$^+$ cells cultured under normoxia or 0.1% hypoxia for 48h. n=3.

Confirming previous results, 786-0 KO cells were more sensitive than 786-0 WT cells to statin treatment ($p<0.05$), and this effect was concentration-dependent (Figure 4.5). As described in 'Chapter 3', PT2385 addition did not further inhibit cell proliferation, showing that it does not synergize with statins. Supporting previously reported data [460], the sensitivity was mediated by HIF2α signalling, as the siRNA approach gave the same results as the KO. However, in contrast to that study, VHL-expressing cells were not more resistant than 786-0 *VHL* mutated cells (786-0 WT and 786-0 KO), moreover, 786-0 VHL$^+$ cells presented no differences in proliferation compared to 786-0 WT cells ($p>0.05$), suggesting that the effect is exclusively mediated by HIF2α absence.

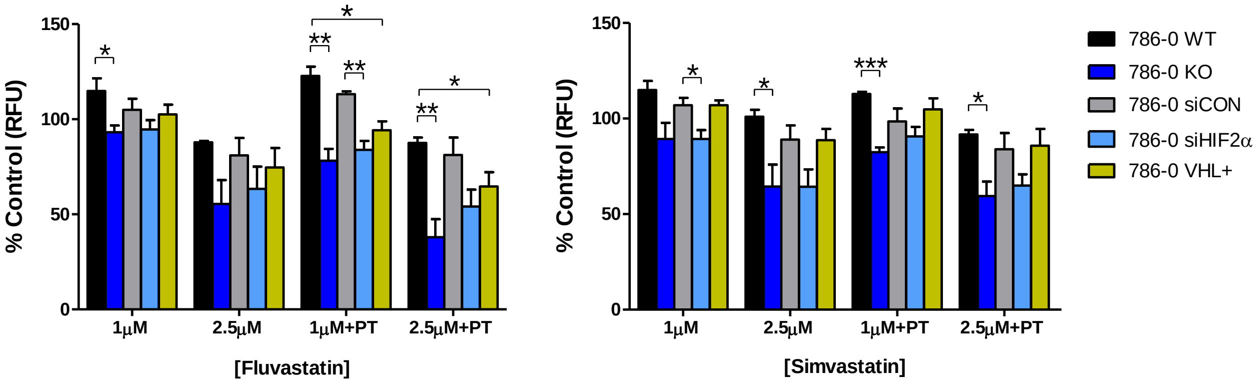

Figure 4.5. Viability of 786-0 WT, 786-0 KO, 786-0 WT transfected with siRNA control (siCON) or siRNA for HIF2α (siHIF2α) and 786-0 VHL$^+$ cells treated with 1μM or 2.5μM fluvastatin or simvastatin +/- 10μM PT2385 (PT) during 5 days in normoxia. n=3. * $p<0.05$, ** $p<0.01$, *** $p<0.001$.

4.5. Discussion

Statins impair tumour progression acting at various steps of the tumour development. They can stop tumour cell growth via blocking cholesterol synthesis, the major structural component of cell membranes, as well as by inhibiting new blood vessel formation [461]. Statins have also been described to induce tumour cell apoptosis [447] and repress metastasis by inhibiting cell migration and invasion, as they can reduce MMP and transcription factors (e.g. NF-κB) levels [462, 463].

This thesis results show that the statins fluvastatin and simvastatin significantly impair proliferation of 786-0 HIF2α deficient cells. Although both are successfully being used to lower cholesterol levels, fluvastatin is a synthetic hydrophilic statin, whereas simvastatin is a natural lipophilic statin obtained from *Aspergillus terreus* [464]. In addition, fluvastatin bioavailability is approximately 24%, but is more easily removed from the body, whereas less than 5% of administrated simvastatin enters in the circulation and has an active effect [464]. Supporting the proliferation results, there are some studies showing that the treatment of ccRCC cell lines with statins inhibits cell growth. It was previously reported that fluvastatin suppressed 786-0 *VHL*-mutated cell growth and induced apoptosis in a dose-dependent manner [465]. The authors showed that the effects were mediated by the inhibition of mTOR pathway. Similarly, Fang *et al.* found that simvastatin inhibited ccRCC cell proliferation and mobility *in vitro* and that it reduced tumour growth in a xenograft mouse model via targeting mTOR pathway [450]. mTOR pathway involvement in ccRCC progression led to the development of drugs targeting mTOR, such as temsirolimus and everolimus. These studies suggest that repurposing statins for ccRCC treatment could be considered as these drugs are well-known and they act via blocking the signalling of an already target of ccRCC treatment. Further supporting mTOR pathway involvement in statin treatment, another study showed that combination of fluvastatin with AICAR (5-aminoimidazole-4-carboxamide ribose), which is the pharmacological activator of the mTOR inhibitor AMP-activated kinase (AMPK), resulted in enhancement growth inhibition [466].

In addition to this, statin treatment appeared to be lethal for *VHL* defective ccRCC cell lines through a HIF-dependent mechanism [460]. They show that lethality was mediated by overactivation of HIFs after *VHL* loss. These authors also described that fluvastatin treatment delayed tumour initiation and tumour growth *in vivo*, and that it was able to promote tumour regression. However, in this thesis statin treatment did not show differences between VHL-expressing and no-expressing cells, whereas it demonstrated that 786-0 KO cells were more sensitive than 786-0 WT, suggesting that HIF2α signalling provides resistance to both tested statins, in contrast to the study of Thompson *et al.* [460].

This thesis results, together with the aforementioned studies and others using different statins [467, 468], support that statins could be a new ccRCC treatment option. HIF2α conferred protection against statins suggests that one way of repurposing these drugs could be via combination treatment with HIF2α antagonists. Even though no differences in proliferation were detected after addition of PT2385 *in vitro*, previously published data on HIF2α antagonists [237, 239] suggests that it might have a synergetic effect *in vivo*. However, the discrepancy in results between Thompson *et al.* [460] and this thesis shows that more investigation needs to be done to stablish the role of HIFs in mediating treatment responses.

786-0 cells different sensitivity to statins was detected at a concentration between 0.5-5µM. In line with this observation, most *in vitro* studies on statins are performed using concentrations 1000-fold higher (1-50µM) than the ones found in human plasma (1-15nM) [469]. Besides, it has been reported that statin-induced adverse effects are dose-dependent, and mainly comprise muscle symptoms [470]. Therefore, in order to get advantage of the pleiotropic effects of statins identified *in vitro*, statin bioavailability needs to be improved so that the anticancer effect can be achieved at lower doses, avoiding this way the adverse effects.

Altogether, these results show that statins are promising agents for ccRCC treatment but, more *in vivo* work is needed to stablish the correct dose and determine which patients could benefit, as well as studies to address statin’s anticancer mechanism of action and absorption rates.

4.6. Conclusions

1. HCS is a promising and reliable strategy for drug repurposing.
2. HIF2α deficient 786-0 cells are more sensitive than 786-0 WT to statin treatment.

5. Type I IFN pathway regulation in hypoxia

5.1. Introduction

5.1.1. Interferons

Interferons (IFNs) comprise a family of cytokines first described in 1957 [471]. The name was originally due to their ability to inhibit (interfere with) viral replication within cells. It is now known that IFNs mediate a broad range of processes, not just antiviral action, including regulation of cell survival and tumour growth and modulation of the immune system's response [472].

Based on the receptor through which they signal, IFNs are classified as one of three types: type I, type II and type III [473]. In humans and mice, there are 17 different type I IFNs including 13 IFNα subtypes, IFNβ, IFNε, IFNκ and IFNω. In contrast, type II and type III IFNs consist of a single member each, IFNγ and IFNλ, respectively. Nevertheless, all IFNs are involved in the innate response against pathogenic infection upon detection of microbial products, known as pathogen-associated molecular patterns (PAMPs), such as genetic material, viral glycoproteins or bacterial lipopolysaccharides (LPS), via pattern-recognition receptors (PRRs) [474-476], leading to production and secretion of IFNs to activate an immune response against the infection in multiple cell types. These cytokines can exert direct antimicrobial response by inhibiting pathogen replication and inducing cell death of infected cells or can act in a paracrine manner in non-infected adjacent cells promoting them to produce an array of genes called interferon-stimulated genes (ISGs) to prevent pathogen spread [477].

5.1.2. IFN pathway

5.1.2.1. Early phase

The PRRs are located in various cellular compartments so that they can detect different parts of the pathogen during the course of the infection. They are mainly classified into two groups, either cytosolic PRRs or transmembrane PRRs. Cytosolic PRRs include the ubiquitously-expressed retinoic acid-inducible gene I (RIG-I) and melanoma differentiation-associated gene 5 (MDA5) for double-strand RNA (dsRNA) sensing, and the cyclic GMP-AMP (cGAMP) synthase (cGAS), DExD/Hbox helicase 41 (DDX41), DNA-dependent activator of IFN-regulatory factors (DAI, also known as ZBP1) and interferon-γ-inducible factor 16 (IFI16) for double-strand DNA (dsDNA) sensing. In contrast, transmembrane PRRs comprised of Toll-like receptor (TLR) family members are limited to specialized cells such as macrophages and DC (Figure 5.1).

1) Cytosolic PRRs

RIG-I and MDA5 are both caspase recruitment domain (CARD)-containing RNA helicases able to recognize dsRNA. RIG-I is activated by short dsRNA molecules, whereas MDA5 recognizes long (>2kb) dsRNAs. Both dsRNA forms can arise from the genetic material of a dsRNA virus, or alternatively can be generated by single-strand RNA (ssRNA) viral replication in the cell [478, 479]. Interaction of either of the PRRs with viral RNA induces unwinding of the dsRNA and conformational changes to RIG-I and MDA5 that expose the CARD-containing domains, which in turn interact with the CARD-containing domain of IFNβ promoter stimulator-1 (IPS-1) [480], also known as mitochondrial antiviral-signalling protein (MAVS), which is located in the mitochondrial membrane. This leads to TANK binding kinase 1 (TBK1) activation via TRAF3 and to inducible IκB kinase (Iκκ) activation via TRAF6. TBK1 is essential for the phosphorylation of IRF3 and IRF7 [481, 482], whereas the contribution of Iκκ to the cytosolic pathway is minor, although it also phosphorylates IRF3 and IRF7 [483]. Phosphorylation of IRF3 and IRF7 promotes the formation of homo and heterodimers. These dimers induce the expression of chemokines, inflammatory cytokines and IFNβ after their translocation to the nucleus [484-486].

Various receptors have been described to be involved in dsDNA sensing in the cytosol. For example, once dsDNA is bound, DDX41 [487], IFI16 [488] and DAI [489] can directly bind to the stimulator of interferon genes (STING) adaptor protein that resides in the endoplasmic reticulum of the cell [490]. STING in turn translocates to signalling compartments via the Golgi apparatus [491], where it associates with TBK1 and activates IRF3 by phosphorylation [492]. NF-κB is also activated by dsDNA sensing, and appears to collaborate with IRF3 to induce type I IFN gene expression [493]. On the contrary, cGAS undergoes conformational changes after binding to dsDNA [494], inducing its catalytic activity to generate the second messenger cGAMP, which will bind to and activate STING [495, 496].

2) Transmembrane PRRs

TLR family members offer a broad coverage to detect almost every pathogen, as they can recognize many different forms of genetic material and also extracellular components, leading to IFN pathway activation. For instance, TLR3 recognizes dsRNA, whilst TLR7 and TLR8 detect ssRNA [497] and TLR9 identifies unmethylated CpG islands [498], in addition to TLR4 that binds to LPS present in the membrane of Gram-negative bacteria [499]. TLRs that bind genetic material are located in the endosomal compartment, whereas TLR4 signals from the cell surface. Upon recognition of foreign material, TLRs recruit adaptor proteins through their Toll-IL-1 receptor (TIR) domain, such as myeloid differentiation primary response gene 88 (MyD88), TIR domain-containing adaptor protein (TIRAP), TIR domain containing adaptor-inducing IFN (TRIF) and the TRIF-related adaptor molecule (TRAM) [500]. Signalling can be categorized into two pathways: MyD88 pathway (signals coming from TRL7, TLR8 and TLR9) or TRIF pathway (after TLR3 and TLR4 activation) [501].

After the activation of their specific adaptors, cytosolic and membrane PRR pathways converge. MyD88 interacts with IRAK-1, IRAK-4 and TRAF6 to finally trigger IRF7 activation [502, 503], whereas TRIF and TRAM adaptor proteins activate TBK1 and Iκκ [483, 504] via TRAF3 [505] to promote the phosphorylation of IRF3 rather than IRF7, in contrast to RIG-I and MDA5 pathway [506]. Phosphorylated IRF3 (pIRF3) will dimerize and translocate to the nucleus to induce the expression of type I IFN genes [483].

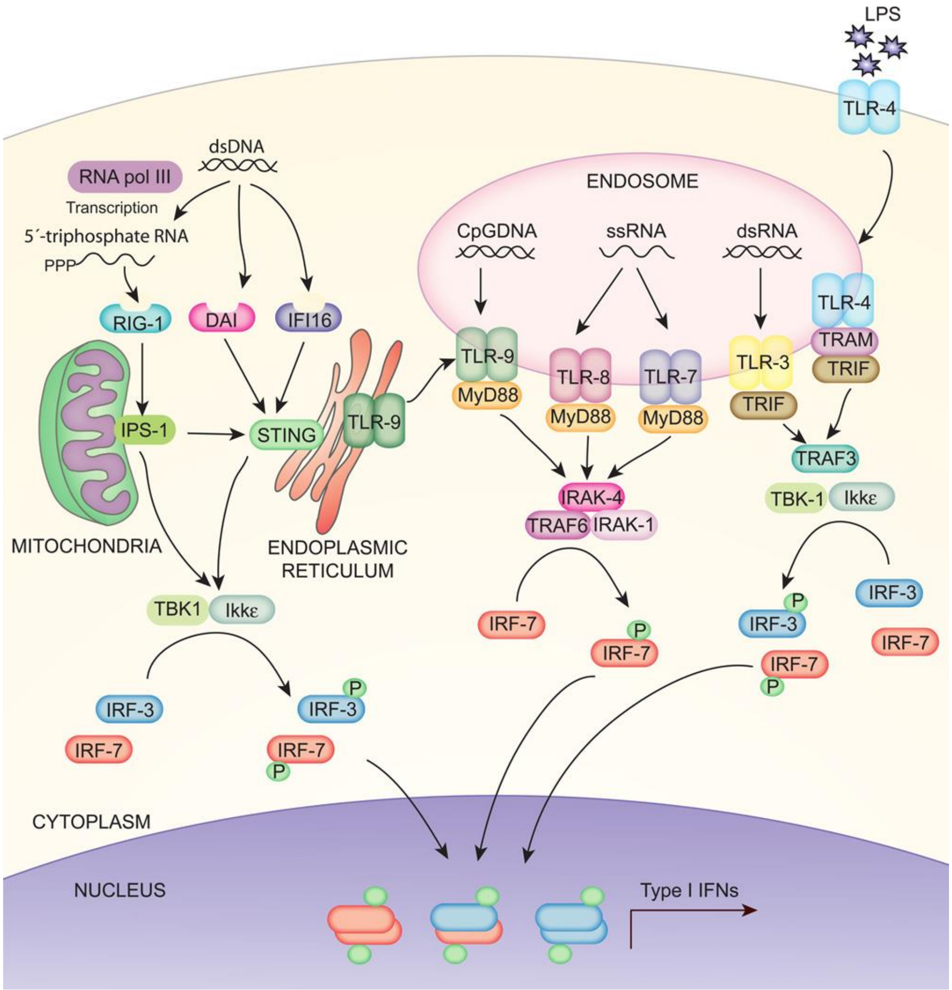
LPS
TLR-4
dsDNA
RNA pol III
Transcription
5´-triphosphate RNA
PPP
ENDOSOME
CpGDNA
ssRNA
dsRNA
RIG-1
DAI
IFI16
TLR-4
TRAM
TRIF
TLR-9
MyD88
TLR-8
MyD88
TLR-7
MyD88
TLR-3
TRIF
IPS-1
STING
TLR-9
TRAF3
IRAK-4
TRAF6
IRAK-1
TBK-1
Ikkε
MITOCHONDRIA
ENDOPLASMIC RETICULUM
TBK1
Ikkε
IRF-7
P
IRF-7
P
IRF-3
IRF-3
IRF-7
P
IRF-7
IRF-3
P
IRF-3
IRF-7
P
CYTOPLASM
NUCLEUS
Type I IFNs

Figure 5.1. Main intracellular pathways leading to type I IFN production [507].

5.1.2.2. Late phase

Infected cells produce high amounts of IFNs to fight against the infection. Type I IFNs initiate their signalling via binding to IFNα receptor (IFNAR), found on the surface of all nucleated cells (Figure 5.2). All type I IFNs bind to this heterodimeric receptor formed by the subunits IFNAR1 and IFNAR2 [473, 508].

IFNAR1 is considered the ‘signal transduction’ chain, whereas IFNAR2 is more likely to be the high affinity binding chain of the receptor. On engagement, the intracellular domains of IFNAR1 and IFNAR2 move together, as do their associated signalling adaptors, tyrosine kinase 2 (TKY2) and Janus kinase 1 (JAK1) [473]. TKY2 and JAK1 are then activated by reciprocal phosphorylation [509], and they phosphorylate tyrosine residues on the receptor that will act as docking sites for the signal transducer and activator of transcription (STAT) proteins [510]. Recruited STAT proteins are phosphorylated by JAK and other kinases, leading to their dissociation from the receptor, activation and dimerization [510].

The canonical signalling cascade involves STAT1 and STAT2. These two transcription factors form a ternary complex called interferon-stimulated gene factor 3 (ISGF3) with interferon-regulatory factor 9 (IRF9) (Figure 5.2). ISGF3 complex translocate to the nucleus, where it binds to a DNA sequence motif known as interferon-stimulated response elements (ISREs) [510]. In addition to ISGF3, type I IFNs also promote the formation of STAT1 and STAT3 homo or heterodimers. In this case, the dimers bind to a different sequence called gamma-activated sequence (GAS) [511]. STAT2/IRF9 complex, in the absence of STAT1, can also be generated [512]. Moreover, type I IFNs can activate downstream signalling though STAT-independent pathways such as p38 and extracellular signal regulated kinase (ERK) [472]. All these pathways will finally activate the transcription of ISGs involved in different mechanisms to restrain pathogens.

Most ISG-encoded proteins contribute to immune-stimulatory and antiviral effects. Moreover, PRRs, JAKs and STATs are also ISGs, therefore reinforcing IFN signalling. Some ISGs, such as IFIT proteins, IRF9, MX1 or MX2 have direct antiviral activity [513]. While various ISGs function as chemo-attractants to lymphocytes and monocytes, others have pro-apoptotic effects, such as TRAILS, Fas/FasL or ISG12. Moreover, some ISGs control the magnitude of the IFN response. USP18 is an ISG involved in the negative regulation of IFN signalling by decreasing the stability of IFN-IFNAR binding [514] or removing ISG15 from its substrates [515]. While the interferon-inducible isoform of Adenosine Deaminase Acting on RNA (ADAR-p150) edits RNA duplexes in self mRNAs by deaminating adenosines into inosines to prevent aberrant activation of the IFN pathway [516].

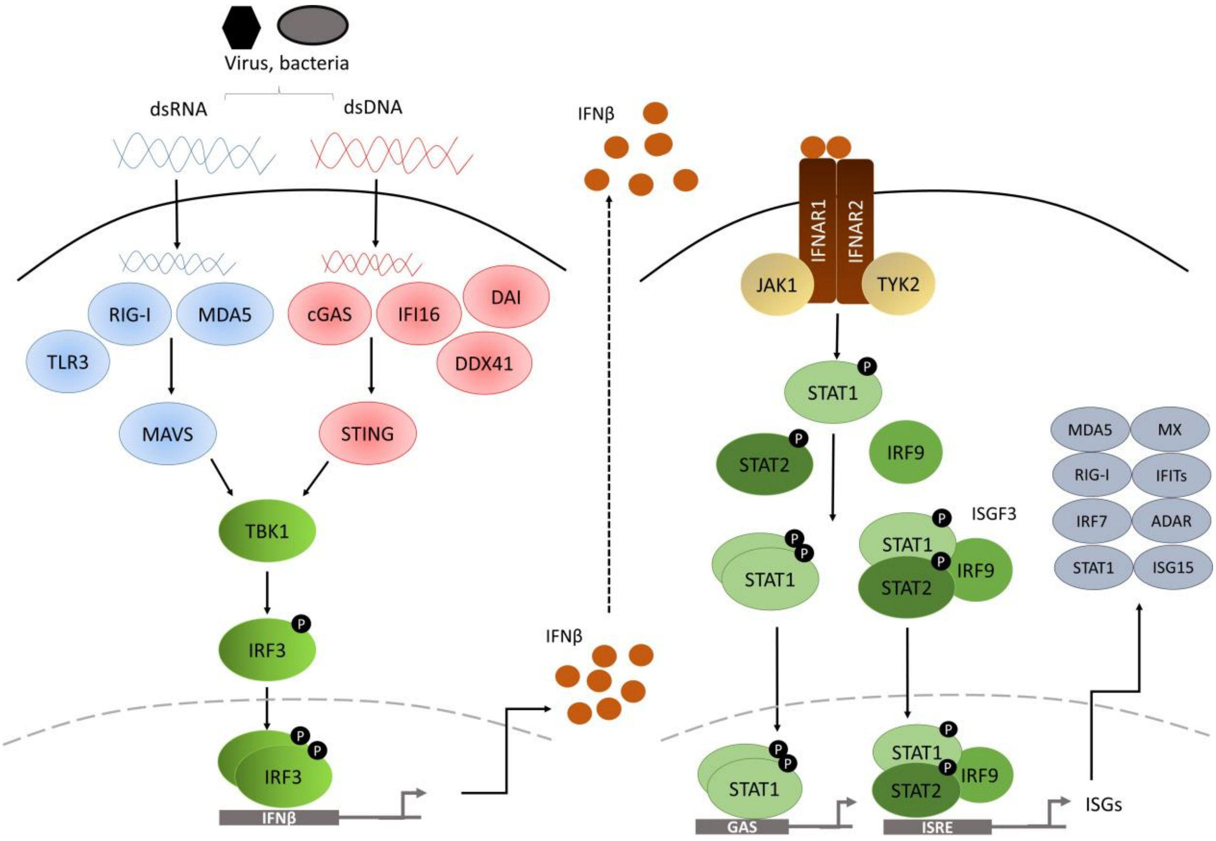
Virus, bacteria
dsRNA
dsDNA
RIG-I
MDA5
TLR3
cGAS
IFI16
DAI
DDX41
MAVS
STING
TBK1
IRF3
P
IFNβ
IFNAR1
IFNAR2
JAK1
TYK2
STAT1
STAT2
IRF9
ISGF3
GAS
ISRE
ISGs
MDA5
MX
RIG-I
IFITs
IRF7
ADAR
STAT1
ISG15

Figure 5.2. Diagram showing the type I IFN pathway. Modified from [517].

5.1.3. IFNs and cancer

Type I IFNs can be produced in the absence of infection [518], such as in the presence of DNA from apoptotic cells [519], non-removed nucleic acids [520] and autoimmune disease antibodies [521]. It has also been demonstrated that *Lactobacillus acidophilus* from the gut microbiota is able to stimulate high production of IFNβ in DC [522], suggesting that the basal IFN production plays a role in the homeostasis of mucosal organs.

In 1909 Paul Ehrlich first proposed that the immune system could recognize and eliminate tumour cells [523]. However, this was not widely accepted and given the name of 'cancer immunosurveillance' until the late 50s [524, 525]. The first experiments to test this hypothesis in the 1970s were not successful as they were carried out on mice that were only partially immunodeficient and the knowledge about the immune system was limited [526]. In the 1990s, endogenous IFNγ was demonstrated to protect the host against transplanted, chemically induced and spontaneous tumour growth [527-529]. It was also observed that mice lacking perforin were more susceptible to 3-methylcholanthrene (MCA)-induced tumour formation [530]. Perforin is a pore-forming protein found in the granules of CTLs and NK cells.

These granules also contain the serine protease granzyme. Upon degranulation, perforin binds to the targets cell's membrane and forms pores to allow the passive diffusion of granzyme, which in turn will induce tumour cell apoptosis [531]. Experiments with mice lacking the recombinase activating gene (RAG)-2, and thus lacking lymphocytes T, B and NK T cells, further demonstrated that tumour development in mice was controlled by the immune system, as RAG-2 deficient mice were more sensitive to MCA-induced sarcomas [532].

Nevertheless, it was noted that tumour formation still occurs in individuals that are immunocompetent, suggesting that tumour cells are able to escape the immune system pressure [533]. This idea arose from the observation that tumours from immunocompetent and immunodeficient hosts have different immunogenic properties [25]. Tumours developed in mice with an intact immune system formed progressively growing tumours when transplanted into immunocompetent recipients, whereas tumours originated in the absence of an immune system were rejected when transplanted into immunocompetent hosts, but grew in immunodeficient hosts [532, 534]. This suggested that the immune system performs an 'editing' process on tumour cells. It can eliminate highly immunogenic tumour cells, but less immunogenic cells can escape the deletion phase and generate tumours poorly recognized by the immune system [25]. Therefore, the immune system provides protection against tumour development, but it can also promote tumour growth by selecting tumour cells with low immunogenicity. This dual effect made to refine the cancer immunosurveillance hypothesis, which was further renamed as 'cancer immunoediting' [532, 533].

Apart from the host's ability to produce IFNγ, tumour cell responsiveness to IFNγ is also important for a successful antitumour immune response. Tumour cells insensitive to IFNγ due to a mutant IFNγ receptor (IFNGR1), grew more aggressively when transplanted into a wild type host [527], but when those cells were made responsive again by complementation with a wild type IFNGR1, they became highly immunogenic and failed to form tumours in the recipients [528]. Similarly, it was observed that several highly immunogenic and poorly tumourigenic sarcomas from RAG-2 deficient mice [532] were converted into poorly immunogenic, and thus highly tumourigenic, when rendered insensitive to IFNγ. These observations suggest that IFNγ production both by tumour cells and tumour host is relevant for an adequate immunosurveillance.

Although type I IFNs were thought to be mainly antiviral agents, their importance as immunomodulators has become clear. In the 1960s, it was demonstrated that tumour-bearing mice had a better outcome when treated with type I IFNs [535, 536]. Although these studies showed the antitumour potential of type I IFNs, it was not until 1981 when the role of endogenously produced type I IFNs was assessed. When mice challenged with tumour cells were treated with serum containing anti-IFN specific antibodies, they developed bigger tumours and had decreased survival comparing to mice treated with control serum [537, 538]. In a similar way, endogenously produced type I IFN was required to protect the host against transplanted and primary carcinogen-induced tumour growth [135]. This study also showed that in contrast to IFNγ, type I IFNs do not require tumour cell responsiveness to exert the antitumour immune response. They found that in spite of being insensitive to IFNα/β, 4 of 11 IFNAR1-deficient MCA-induced sarcomas were rejected when transplanted into wild type recipients [135]. Moreover, some IFNAR1-deficient sarcomas that grew in wild type recipients were not converted into highly immunogenic, non-growing tumours when IFNAR1 expression was restored. Besides, sarcoma cells from mice lacking IFNAR1 and IFNGR1 were only rejected when sensitivity to IFNγ was restored, not to type I IFN. On the other hand, they found that IFNα/β sensitivity in hematopoietic cells of the host was required for an antitumour immune response [135].

5.1.3.1. Cancer immunoediting

The editing process that the immune system performs in tumours can be divided into three phases: elimination, equilibrium and escape [533] (Figure 5.3). It is known that tumour cells and immune cells interact during the whole process of tumour formation and that these interactions are mediated by endogenously produced type I and type II IFNs. Type I IFNs are known to activate DC [539], to increase macrophages' and NK cells' cytotoxicity, to induce the production of IL-15, which is critical for the proliferation and maintenance of NK cells and CTLs [540], and to increase the production of stromal angiostatic molecules to block new vessel formation [541].

1) Elimination phase

The elimination phase, also termed protection, is the first step in the cancer immunoediting. If successfully performed, it will eradicate the developing tumour and the immunoediting process will not progress to subsequent phases [25].

In this phase, both the innate and adaptive immune system recognize cancer cells and kill them. The antitumour immune response starts when cells of the innate immune system detect that a tumour is growing. As a result, the disruption of the tissue surrounding the tumour generates pro-inflammatory molecules that together with chemokines secreted by tumour cells [542] act as danger signals for the immune system [543]. Once immune cells reach the tumour mass, they need to distinguish between normal self-cells and transformed self-cells. This is achieved by recognising tumour-cell-expressed ligands for the NK cell receptor Natural killer group 2 member D (NKG2D), which are induced by genotoxic stress, the generated inflammation or the transformation process itself [544], or tumour-specific antigens presented by antigen presenting cells [545].

This recognition process leads to chemokine and cytokine production at the tumour site. Released IFNs induce the production of more chemokines, which will attract more immune cells to the tumour and will in turn produce more cytokines, and therefore the signal will be amplified [25]. The massive release of molecules will activate different processes, including antiproliferative [546], pro-apoptotic [547] and angiostatic [548] processes to kill tumour cells. The main two cell populations recruited by type I IFNs are NK cells and CTLs. As tumour cell death generates tumour-cell antigens, the adaptive immune system will start to take part in the immunoediting process.

2) Equilibrium phase

This is a subclinical phase in which the tumour persists, but it is prevented from expanding due to the presence of the immune system. It is probably the longest phase, and can even take years to occur in humans [549]. The immune system is able to contain any tumour cell variant that has not been killed in the previous phase, but it is not able to completely remove the tumour. Furthermore, during this phase, new tumour cell variants arise that display reduced immunogenicity (i.e. more resistant to the immune attack) [25].

3) Escape phase

The escape phase is the tumour progression phase. It is the result of immune exhaustion or inhibition, or the consequence of the emerged new cell population's ability to bypass the immune pressure. Tumour cells can impede an antitumour immune response either through the production of immunosuppressive cytokines (TGFβ and IL-10) or via T cells with immunosuppressive activities (Treg cells) [25]. New tumour cells might have also been submitted to alterations that make them unrecognizable by immune cells or that allow them to avoid immune destruction [528]. These poorly immunogenic cells will be able to grow and generate a clinically detectable tumour [1, 25].

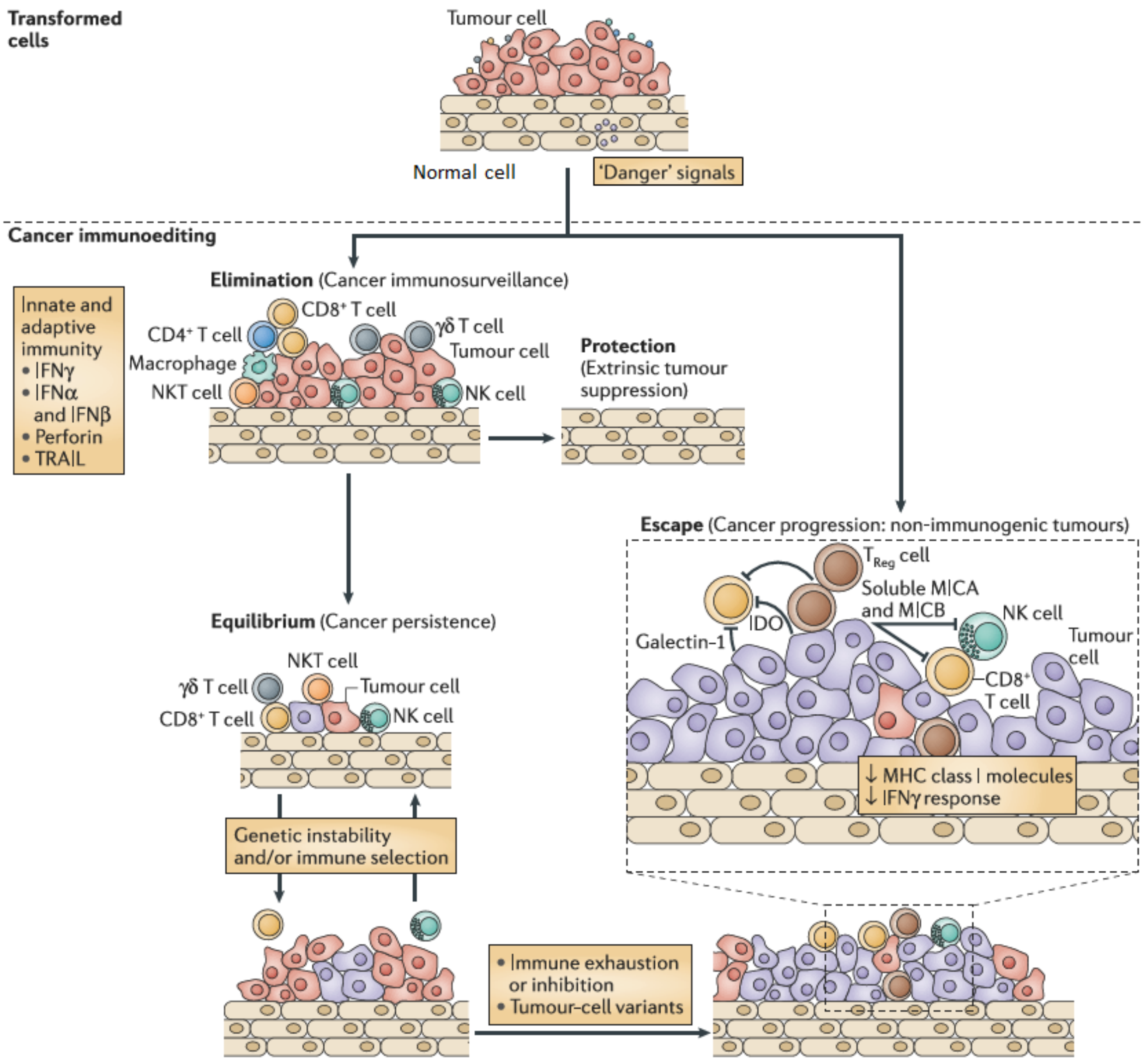
Transformed cells
Tumour cell
Normal cell
'Danger' signals
Cancer immunoediting
Elimination (Cancer immunosurveillance)
Innate and adaptive immunity
• IFNγ
• IFNα and IFNβ
• Perforin
• TRAIL
CD8+ T cell
CD4+ T cell
γδ T cell
Tumour cell
Macrophage
NKT cell
NK cell
Protection (Extrinsic tumour suppression)
Escape (Cancer progression: non-immunogenic tumours)
TReg cell
Soluble MICA and MICB
NK cell
IDO
Galectin-1
Tumour cell
CD8+ T cell
↓ MHC class I molecules
↓ IFNγ response
Equilibrium (Cancer persistence)
NKT cell
γδ T cell
Tumour cell
CD8+ T cell
NK cell
Genetic instability and/or immune selection
• Immune exhaustion or inhibition
• Tumour-cell variants

Figure 5.3. Cancer immunoediting process. Modified from [545].

5.1.3.2. IFNs and anticancer therapies

It is well established that type I IFNs are key components in the success of many of the current anticancer modalities including radiotherapy, chemotherapy, immunotherapy and oncolytic viruses [127], through promotion of direct (tumour cell inhibition) and indirect (antitumour immune response) effects [550]. Indirect effects, recently termed 'immunogenic cell death' (ICD), arise as a consequence of the release of nucleic acids or proteins from dying tumour cells that can activate immune cells [550].

Regarding radiotherapy, it has long been known that the host immune system determines the efficiency of the treatment [551]. It was demonstrated that type I IFN production by myeloid cells and IFN detection by tumour cells after radiotherapy was essential to eradicate the tumour in a mouse melanoma model, as mice lacking IFNAR1 were unresponsive to IFNβ [552]. Another study showed that radiation-induced type I IFNs recruited lymphocytes at the tumour site (ICD) and that exogenously administrated IFNα enhanced radiotherapy efficacy [553]. Furthermore, it has been demonstrated that radiation-mediated antitumour immunity in immunogenic tumours requires a functional cytosolic DNA-sensing pathway in DC, which subsequently triggers a type I IFN signalling response in those cells essential for CTLs activation [554].

As with radiotherapy, the anticancer effects of chemotherapy, which were long thought to be mediated only by direct tumour cell killing, are now realised to be due in part at least, to the induction of ICD, thereby involving the immune system in the process. Injection of mice with tumour cells pretreated with doxorubicin prevented *in vivo* tumour growth [555]. Chemotherapeutic agents used in the clinic such as anthracyclines (e.g. doxorubicin, epirubicin, mitoxantrone, bleomycin) or oxaliplatin have been demonstrated to induce ICD, via IFN signalling [556]. For successful treatment, anthracyclines must be able to induce the release of type I IFNs in both tumour and immune cells so that an antitumour adaptive immune response against tumour-cell antigens can be activated [557]. This study also showed that IFNAR1 expression in cancer cells is important for the activity of anthracyclines, as administration of an IFNAR1 neutralizing antibody abolished the therapeutic activity of the drugs. Moreover, a type I IFN-related gene signature in patients with breast carcinoma treated with anthracycline-based chemotherapy was able to predict clinical responses to the treatment [557]. As an example, chemotherapy up-regulated the levels of MX1 and its high levels were associated with better OS in those patients.

Immunotherapy has gained a lot of interest in the last few years, mainly because of the development of immune checkpoint inhibitors. By blocking immune checkpoints, the level of T cell activation can be controlled, thus avoiding excessive inflammation and promoting self-tolerance [558]. The two main targets are CTLA-4 and PD-1, both expressed by activated T cells. CTLA-4 controls T cell activation by competing with its homologous T cell costimulatory receptor (CD28) in the binding to their ligands. Both molecules bind to CD80 and CD86 (also called B7-1 and B7-2) expressed by antigen-presenting cells, but CTLA-4 transmits an inhibitory signal to T cells, whereas CD28 transmits a stimulatory signal. Thus full activation of T cells requires binding of CD28 to CD80 and CD86, but in tumours, CTLA-4 is frequently up-regulated, as a consequence of T cell exhaustion due to long time exposure to tumour cells [558]. Similar to CTLA-4, PD-1 regulates T cell activation by binding to PD-L1 and PD-L2 expressed in infiltrating inflammatory cells and tumour cells. Cancer cells overexpress PD-L1 which blocks T cell activation and finally dampens the antitumour immune response [559]. In this regard, antibodies against immune checkpoint modulators can restore the effector T cell functions and the antitumour immune response.

Despite existing approved monoclonal antibodies targeting both CTLA-4 and PD-1 for the treatment of lung cancer, RCC and melanoma, among other, the efficacy remains low [560, 561]. These therapies rely on the increase of immune responses, and given the importance of type I IFNs in the maturation, survival and activation of most immune cells [135], it is likely that a functional IFN pathway is necessary to achieve success with these therapies. Consistent with this idea, Zaretsky *et al.* demonstrated that melanoma patients that underwent relapse after treatment with the PD-1 inhibitor pembrolizumab had loss-of-function mutations in genes encoding JAK1 and JAK2 [562]. On the other hand, defects in IFNγ signalling led to resistance to PD-1 and CTLA-4 blockage [563], whereas lung tumours resistant to anti-PD-1 therapy presented mutations in IFNAR2 and IFNγ signalling pathway [564].

Oncolytic virus therapy is based on the ability of modified virus to specifically target tumour cells, whilst not affecting healthy cells. In contrast to other therapies, oncolytic virus therapy requires a defective IFN signalling to succeed, since viruses are susceptible to IFN-mediated antiviral activity. *Herpes simplex virus* (HSV) could destroy murine breast tumour cells unable to produce and respond to IFNs [565]. In the same way, cancer cell sensitivity to *Vesicular stomatitis virus* (VSV) induced cell death was increased after knocking down or blocking IFNAR [566], IRF5 and IRF7 [567], thus providing evidence for the requirement of a defective IFN pathway.

5.1.3.3. Negative regulation of IFN signalling

Although an intact IFN signalling is required for antiviral activity, in the immunoediting process and for the success of many anticancer therapies, an excessive IFN response can have detrimental effects. Indeed, many immune disorders such as chronic infection or autoimmune diseases are associated with deregulated IFN signalling. Upon infection, the IFN pathway must be rapidly activated for an acute response, but afterwards, it should be weakened to avoid tissue damage. However, if the IFN signalling persists, it in turn will be harmful as it acquires immunosuppressive features that promote persistent viral infection [568, 569].

Likewise, chronic IFN signalling has been found in systemic lupus erythematosus (SLE) patients [570]. SLE is characterized by excess apoptosis and tissue damage, and decrease clearance of apoptotic bodies, which results in an excess of autoantigens. The number of immune cells loading self-derived nucleic acids is considerably increased, thus inducing high type I IFN levels which contribute to the disease, promoting both autoimmunity and inflammation [571].

It is therefore important to control IFN signalling to prevent toxicity. Moreover, in some cases the negative regulation of the pathway could be the main reason for the resistance to some therapies.

There are negative regulation activities at nearly every stage of the pathway: receptor, signal transduction and IRF level.

1) Receptor level

The gene encoding for IFNAR2 can undergo alternative splicing and generate a truncated form of the receptor incapable of signalling [508], or alternatively a soluble form [572]. For some cytokines, the soluble form of the receptor inhibits the signalling, but this has not been demonstrated for type I IFNs yet. It has also been suggested that ADAM17 protease could be involved in the generation of this soluble form [573].

Regarding IFNAR1, it can be ubiquitinated, endocytosed and later degraded in the lysosomes [574]. After ligand binding and formation of the ternary complex, IFNAR1 is phosphorylated. Phosphorylation of two serine residues in the 'destruction motif' of the cytoplasmic tail attracts Skp1-Cullin1-F-box protein β transducin repeat-containing protein (SCFβ-Trcp) E3 ubiquitin ligase, which will ubiquitinate IFNAR1 and lead it to degradation [574]. Moreover, in the absence of ligand binding or receptor chain ubiquitination, IFNAR1 remains in the cell membrane [575]. But upon ligand binding, the adaptor protein TYK2 is phosphorylated and the endocytic domain of IFNAR1 that it was masking gets exposed [576], triggering receptor endocytosis. Furthermore, ubiquitination of IFNAR1 promotes its interaction with the adaptin protein 2 (AP2)-clathrin complex that is required for the internalization of IFNAR1 [575]. This means that both ubiquitination and endocytosis processes co-operate in the degradation of the receptor. The level of endocytosis and receptor degradation correlates with the degree of signal [577]. High IFNAR1 levels in the cell membrane and high and tightly binding of type I IFNs to the receptor will strongly promote IFNAR1 degradation, whereas low type I IFN concentration or low affinity IFN binding will not have a big effect on the receptor levels. It has also been shown that although the receptor is internalized, it can continue signalling from endosomes [578].

2) Signal transduction level

TKY2/JAK1-STAT axis is a potential target for some dephosphorylation proteins known as suppressors of cytokine signalling (SOCS). These proteins can bind to phospho-tyrosine residues in receptors, to TYK2 or to JAK kinases and target them for degradation in the proteasome. Among the 7 members of the family, SOCS1 and SOCS3 are involved in the type I IFN signalling. It was shown that up-regulation of both proteins could inhibit STAT1 phosphorylation [579], whereas silencing of *SOCS3* [579] or *SOCS1* [580] made tumour cells more sensitive to type I IFNs. TYK2 dephosphorylation by SOCS1 reduced IFN response, on the one hand as a consequence of blocking TYK2 activity, and on the other hand, due to the negative impact on IFNAR1 cell surface expression, which is stabilized by TYK2 [581]. In addition to cancer, it was shown that that unrestricted type I IFN signalling, due to a lack of SOCS1, induced inflammation and was potentially lethal in mice [582], highlighting the importance of a regulated IFN signalling.

Apart from SOCS proteins, epigenetic modification of JAK1 [583] or STAT ubiquitination [584] makes cells unresponsive to IFNα. Similar to ubiquitin conjugation, there are some ubiquitin-like molecules, such as ISG15, that can be linked to substrates by E3 ligases, through a process called ISGylation [585]. But in contrast to ubiquitination, this process promotes the signalling. It has been demonstrated that USP18 can remove ISG15 from both JAK1 and STAT1, and in this way down-regulate the pathway [586].

3) IRF level

It is known that many ISGs participate in the negative regulation of the pathway. One example is ISG56, also called IFIT1, whose overexpression resulted in the inhibition of IRF3 activation, NF-κB activation and IFNβ production [587]. Furthermore, some members of the tripartite motif (TRIM) family of E3 ubiquitin ligases can target several members of the IFN pathway, such as TBK1, Iκκβ, IRF3, IRF7 and NF-κB, for degradation [588]. Another IFN-induced protein is the guanylate binding protein 4 (GBP4), which by binding to IRF7, avoids its association with TRAF6, thus reducing its phosphorylation and activity [589].

5.1.4. Hypoxia and the immune system

As mentioned before, one of the hallmarks of cancer is immune evasion [1]. It is well known that hypoxia generates an immunosuppressive microenvironment within the tumour by impeding the homing of immune effector cells and by blocking their activity. It has also been reported that hypoxic regions in the tumour are infiltrated by high levels of immunosuppressive cells, such as MDSC, tumour-associated macrophages (TAM) and Treg cells [119, 590]:

1) Myeloid-derived suppressor cells (MDSC)

MDSC are a heterogeneous population of immature myeloid cells which contribute to immunosuppression through different mechanisms [591]. Tumour-derived factors, such as VEGFA, promote MDSC accumulation in the tumour and in secondary lymph organs, where they can induce T cell anergy, block $CD8^+$ T cell activity and promote Treg cell proliferation [592]. A further contribution of hypoxia to the immunosuppressive microenvironment is the attraction of MDSC to the tumour and their stimulation to inhibit T cells' and NK cells' antitumour activity. Hypoxia also promotes MDSC differentiation to TAM [593].

2) Tumour-associated macrophages (TAM)

Cancer cells can secrete many cytokines that recruit monocytes to the tumour and differentiate them into TAM. TAM can further differentiate and acquire a more pro-inflammatory phenotype (M1) or a pro-angiogenic and immune evasive phenotype (M2). TAM infiltrating tumours are associated with a M2 phenotype [594] and are mainly located in hypoxic areas [595], where they have been found to suppress T cell function [596] and to promote tumour growth by inducing angiogenesis via VEGFA [597] and through matrix remodelling via the up-regulation of MMP7 expression [598]. Moreover, cleavage of Fas ligand by MMP7 in adjacent tumour cells makes those cells less responsive to lysis by NK cells and T cells [599], thus promoting the hypoxic immunosuppressive environment.

3) Lymphocytes

Lymphocytes include NK cells, T cells and B cells. While NK cells function in the innate immune response, T cells and B cells are part of the adaptive immune response, by promoting cell-mediated cytotoxicity or antibody-driven humoral response, respectively. Treg cells on the other hand, are a specialized group of T cells that suppress immune response by inhibiting T cell proliferation and cytokine production, thereby maintaining homeostasis and self-tolerance [600].

It is well known that hypoxia significantly reduces lymphocyte proliferation directly [601]. But it can also inhibit T cell proliferation in an indirect manner. Hypoxia promotes the generation of TGFβ [602] and CCL28 [603] by tumour cells, which in turn up-regulate Treg cells, and therefore inhibit effector T cells. Consequently, it has been observed that the presence and activity of T cells in hypoxic regions is also reduced *in vivo* [604]. Moreover, it was reported lower presence of T cells and NK cells in hypoxic areas in lung and dermal tumours [605] and in prostatic tumours [606]. In both studies, immune cell infiltration increased when hypoxic areas were reduced by respiratory hyperoxia [605] or the hypoxia-activated prodrug evofosfamide (TH-302) [606], respectively. Hypoxic TGFβ production can also decrease NKG2D receptor levels on NK cells, thus reducing tumour cell recognition by NK cells [607].

4) Dendritic cells (DC)

DC are antigen-presenting cells, thus their main function is to process antigens and present them to resting T cells, thereby connecting innate and adaptive immunity [608]. Under hypoxia, DC express less differentiation and maturation markers, such as CD40, CD80 or CD86, and several reports have proven that hypoxia-stimulated factors like VEGFA inhibit the maturation and function of DC [609].

5) Other factors

Apart from the specific effect of hypoxia on immune cells, several other molecules contribute to the immunosuppressive environment generated under low oxygen levels. It is well known that hypoxia can lead to immune evasion by up-regulating immune checkpoint inhibitor molecules in tumour cells [610], such as CD47, PD-L1 and major histocompatibility complex, class I, G (HLA-G). Furthermore, under hypoxic conditions, PD-L1 expression is also up-regulated in MDSC [611] and DC [612], negatively regulating T cell antitumour function.

Hypoxia-induced autophagy is another mechanism by which tumour cells can escape NK cell-mediated killing [613]. Through autophagy, granzyme B can be selectively degraded, allowing tumour cells to bypass NK cell mediated apoptosis [614].

Major histocompatibility complex class I chain related (MIC) molecules, one family of NKG2D receptor ligands, are not usually expressed in benign cells, but are up-regulated in many tumour cells [615]. This would effectively lead to NK and T cell mediated immunosurveillance. However, hypoxic cancer cells secrete MIC ligands (soluble MIC) to down-regulate and degrade NKG2D receptor on T cells [616] and avoid immune activity.

As a consequence of the metabolic switch to glycolysis that tumour cells undergo under hypoxic conditions, acid lactic levels in the extracellular media increase considerably. Recent data highlights the role of lactate as a ‘signalling molecule’ promoting the escape of the immune surveillance of hypoxic tumour cells [617]. Lactate can attenuate the cytotoxic activity of CTLs [618] and NK cells [619], impede the differentiation and activation of DC [620, 621] and recruit MDSC to the tumour [619]. Moreover, it has recently been published that high lactate levels inhibit type I IFN signalling via binding to MAVS adaptor protein [622].

Adenosine is also an important extracellular metabolite that accumulates in hypoxic tumours. Hypoxia up-regulates the expression of CD39 and CD73, enzymes involved in the nucleotide metabolism, on tumour cells, as well as A2A adenosine receptor (A2AR) on immune cells [623]. Extracellular adenosine signals through A2AR on immune cells, such as T cells, NK cells and DC, and inhibits their activity [624]. Treg cells express high levels of CD39 and CD73, and they are able to produce and secrete adenosine, contributing to the immune evasion [625].

5.1.5. Mitochondria and the type I IFN signalling

5.1.5.1. Mitochondria description

Mitochondria are highly specialized organelles present in almost all eukaryotic cells. Their main function is the production of energy through OXPHOS, but they also participate in calcium signalling, regulation of cellular metabolism and programmed cellular death [626].

Mitochondria originated from energy-producing α-bacteria through an endosymbiotic process. Those bacteria were engulfed by archezoan cells and finally became part of the cell [627]. Consequently, these organelles maintain some characteristics of their prokaryotic ancestor, such as the double membrane, an independent genome and the energy-producing activity. mtDNA is a closed-circular, dsDNA molecule of about 16.6kb [628], and in mammalian cells, each organelle normally contains several identical copies, known as homoplasmy. However, due to the oxidative environment and the increased replication, mtDNA mutations are quite frequent, leading to the co-existence of different mtDNA molecules within a mitochondrion (heteroplasmy) [629].

The strands can be distinguished by the nucleotide composition, which results in different buoyant densities in denaturing caesium chloride gradients [630]. The heavy strand (H-strand) is guanine rich, whereas the light strand (L-strand) is cytosine rich. mtDNA contains 37 genes, 28 in the H-strand and 7 in the L-strand. The H-strand encodes information for 2 ribosomal RNA (rRNA), 14 transfer RNA (tRNA) and 12 polypeptides, whereas the L-strand only codifies for 8 tRNA and a single polypeptide (Figure 5.4). The 13 proteins are constituents of the OXPHOS located in the mitochondrial inner membrane [631]. mtDNA is highly efficient, as the genes lack introns and intergenic sequences are barely present [628].

mtDNA replication and transcription starts in the only non-coding region of the molecule, the displacement loop (D-loop) [628]. The D-loop contains the site for mtDNA replication initiation (origin of H-strand synthesis, OH) and the transcription initiation sites, two for the H-strand (ITH1 and ITH2) and one for the L-strand (ITL). ITH2 is used less frequently than ITH1. Although the 22 tRNAs encoded in the mtDNA are sufficient to translate the 13 mitochondrial protein genes, mitochondrial replication and transcription processes depend on nuclear encoded factors [632].

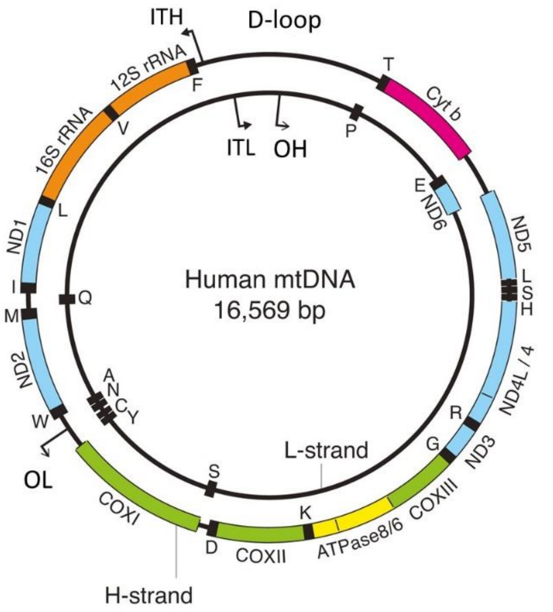

Figure 5.4. Map of the human mitochondrial genome. Modified from [633].

5.1.5.2. Mitochondria as immunogenic organelles

The efficiency of the immune system to trigger an immune response against the invading pathogen relies on the recognition of PAMPs, and the capacity to distinguish between self and non-self structures using several mechanisms, such as recognition of specific pathogen nucleic acid structures or labelling self-nucleic acids (methylation of the RNA) [634]. Interestingly, it has been reported that misplaced self-molecules can also activate immune responses [543]. Under stress conditions, cells release molecules called damage-associated molecular patterns (DAMPs) or alarmins to the extracellular space, which will act as stress signals. Similar to PAMPs, DAMPs are recognized by PRRs and activate an immune response.

As a result of their endosymbiotic origin, mitochondria are highly immunogenic organelles [627], which generate a number of DAMPs as they keep some bacterial-like characteristics capable of triggering an immune response [635]. To prevent the leak of mitochondrial pro-inflammatory molecules to the cytosol, cells undergo autophagy, but in major stress conditions, this system is overwhelmed and mitochondrial DAMPs are released. Mitochondrial DAMPs comprise (Figure 5.5): ATP, succinate, cardiolipin, N-formylpeptides, mitochondrial transcription factor A (TFAM), cytochrome-c, mtDNA and mitochondrial RNA (mtRNA):

1) ATP

ATP constitutes the main energy source for most cellular processes, but when found in the extracellular media, it plays a key role in cell signalling. Moreover, under stress conditions, ATP is secreted from various cell types to alert the immune system of tissue damage [636].

2) Succinate

Succinate is a metabolic intermediate of the TCA generated in the mitochondria. In addition to its role in the production of energy, it can also act as a DAMP and induce an inflammatory response when released [637].

3) Cardiolipin

Cardiolipin is a lipid dimer localized in the mitochondrial inner membrane. It is important in mitochondrial respiration, protein import or mitochondria biogenesis [638, 639]. Cardiolipin is also found in bacterial membranes. When exposed to the extracellular media, it stimulates T cells [640] and it can also induce an inflammatory immune response by binding to inflammasomes [641].

4) N-formylpeptides

Bacteria need to add a formyl group to methionine to initiate protein synthesis. Similarly, mitochondria also add a formyl group to methionine to translate mRNAs transcribed from mtDNA [642]. Those N-formyl peptides are potent chemoattractant for immune cells [643], thus when sensed, they trigger an immune response.

5) TFAM

TFAM is essential for mtDNA packing and therefore, its maintenance. It regulates mtDNA transcription initiation and copy number [644]. It has been reported that TFAM can induce an inflammatory response in the extracellular media, both alone [645] or in combination with other mitochondrial DAMPs such as N-formyl peptides [646] or mtDNA [647].

6) Cytochrome-c

Cytochrome-c resides in the inner mitochondrial membrane, where it transports electrons between respiratory complexes III and IV. It is usually released to the cytosol to induce cell apoptosis, and some studies have shown that subsequent release to the extracellular media induces an inflammatory response headed by immune cells [648].

7) mtDNA

mtDNA has some features that can activate an immune response, including its circular structure, methylated CpG motifs, as well as oxidative damage. Extracellular mtDNA binds to TRL9, which recognizes unmethylated or low methylated CpG motifs in the DNA, a characteristic of bacterial [649] and viral [650] DNA, and subsequently induces an immune response [651]. mtDNA can also drive an inflammatory response in the cytosol, via binding to inflammasomes [652] or through the cGAS-STING pathway [653]. A side effect of mitochondrial respiration is the generation of ROS, which can oxidize mtDNA, making it further immunogenic [654, 655].

8) mtRNA

Like mtDNA, mtRNA is another potent DAMP able to trigger an immune response. In 2015, Krüger *et al.* found that a specific segment of the mitochondrial single-strand rRNA was recognized by TLR8 and that it could stimulate peripheral blood mononuclear cells (PBMCs) in a MyD88-dependent manner and induce an inflammatory response [656]. Subsequently, Dhir *et al*. found that dsRNA originating from the mtDNA transcription could trigger type I IFN response when released to the cytoplasm [657].

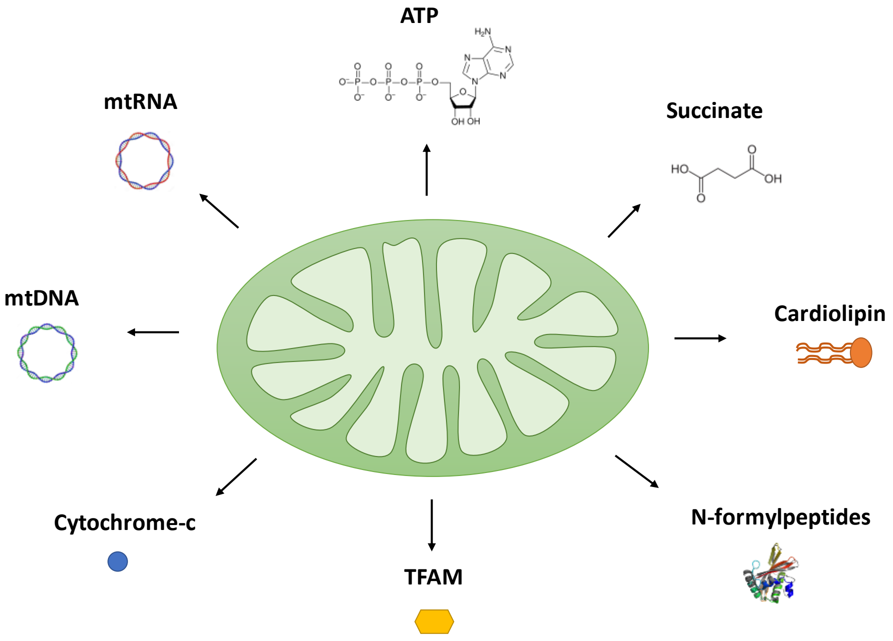

Figure 5.5. Mitochondrial DAMPs.

5.1.5.3. Mitophagy

Autophagy is the process through which cells discard unwanted cellular material, including misfolded proteins or protein aggregates, damage organelles (mitochondria, endoplasmic reticulum, peroxisomes), nuclear components, lipid droplets and even intracellular pathogens. A double membrane structure called autophagosome encloses the cellular contents and fuses with lysosomes for material degradation. The origin of the autophagosome membrane remains unknown, although it has been suggested to be generated from the endoplasmic reticulum [658], Golgi apparatus [659], mitochondria [660] or the plasma membrane [661]. After fusion with the lysosome and subsequent cargo degradation, breakdown products (e.g. amino acids, fatty acids or carbohydrates) are released to the cytoplasm and recycled for energy generation or macromolecule synthesis [662]. Stress conditions such as nutrient (e.g. amino acids, growth factor or glucose [663, 664]) or oxygen deprivation [665] have been reported to trigger autophagy.

Mitochondria are important organelles for cells, not only because they are the principal site of ATP production, but also because other important metabolic processes such as fatty acid degradation, iron metabolism, urea cycle and calcium storage take place in them [666]. Therefore, cells exert a quality and quantity control over mitochondria. Damaged or unwanted mitochondria are removed by a specific autophagic process called mitophagy [667].

BNIP3 and Nix are pro-apoptotic proteins localized in the outer mitochondrial membrane, which participate in mitophagy processes. Both BNIP3 [668, 669] and Nix [670, 671] recruit the autophagosome to mitochondria via direct binding to the microtubule-associated protein 1 light chain 3 (LC3) present in the autophagosomal membrane, triggering this way mitochondria degradation.

Mitophagy takes place under physiological processes, such as red blood cell maturation, and pathological events, such as cancer. Several groups have shown that Nix deficiency leads to anemia and developmental disorder in erythroid maturation, due to the lack of mitochondria clearance [672, 673]. Similarly, BNIP3 and Nix KO mice displayed accumulation of dysfunctional mitochondria [674]. In an oncology context, tumour cells' mitochondria are severely affected by the usual hypoxic conditions present within the tumour mass. During hypoxia, oxidative phosphorylation is decreased, cytochrome c oxidase (complex IV) cannot transport electrons because of the lack of oxygen and ROS levels increase [675], causing mitochondrial oxidative damage and mitochondrial dysfunction. Moreover, it has been shown that under hypoxia nitric oxide (NO) levels also increase [676], further inhibiting cytochrome c oxidase activity [677]. On the other hand, hypoxia affects mitochondrial calcium flux [678, 679], mitochondrial morphology [680] and membrane potential [681]. All these events lead to altered mitochondria which need to be removed in a controlled way, because they are a source of DAMPs which can trigger an immune response. It has been shown that hypoxic cancer cells induce mitophagy via Nix in glioblastoma [682]. Similarly, cardiac cells were found to induce mitophagy to protect from hypoxia/reoxygenation injury [683]. Therefore, under hypoxic conditions, cells perform protective mitophagy via BNIP3 and Nix induction in a HIF-dependent manner [317, 684].

In addition to dysfunctional mitochondria removal and suppression of mitochondrial biogenesis [685, 686], hypoxia has also been reported to stimulate mitochondria biogenesis via nitric oxide synthase (NOS) [687] and PGC-1α [688]. This suggests that under hypoxia, cells develop a tight control on mitochondria number and quality to maintain homeostasis between the energy demand and mitochondria functionality.

5.2. Objectives

Hypoxia is one of the main characteristics of solid tumours which generates an immunosuppressive environment and it is linked to chemotherapy and radiotherapy resistance. The latter treatments are less effective under low oxygen levels, or they rely on an intact immune response. Determining new mechanisms by which hypoxia and immune response are connected would allow the generation of drugs to enhance immune system's response under hypoxia, and therefore trigger an efficient antitumour immune response. Thus, the main objective of this chapter is to investigate the regulation of the type I IFN pathway by hypoxia. The aims are:

1. To determine the expression of the type I IFN pathway members under hypoxic condition in different cell types, both at basal level and upon signalling activation.
2. To study the presence of endogenous DAMPs (mitochondrial dsRNA) under hypoxia and its link to the type I IFN pathway.

5.3. Materials and methods

5.3.1. Cell culture

5.3.1.1. Breast cancer cell lines

The breast cancer cell lines MCF7, T47D, BT474, MDA-MB-231, MDA-MB-453, MDA-MB-468, HCC1187 and HCC1806 were obtained from ATCC®, whereas the MCF7 parental (MCF7 WT) and MCF7 HIF1α KO (MCF7 KO) cell line were kindly donated by Dr Dimitrios Anastasiou and Dr Fiona Grimm (Francis Crick Institute, UK). Regarding the estrogen receptor (ER), progesterone receptor (PR) and human epidermal growth factor receptor 2 (HER2) status, these cell lines can be classified as ER+, HER2+ or triple negative (TN) as shown in Table 5.1. All breast cell lines were cultured in low glucose DMEM supplemented with 10% FBS. Mycoplasma contamination was checked every three months.

Table 5.1. Breast cancer cell line classification according to hormone receptor status.

Cell line	ER	PR	HER2	Classification
MCF7	+	+	-	ER+
T47D	+	+	-	ER+
BT474	+	+	+	HER2+
MDA-MB-231	-	-	-	TN
MDA-MB-453	-	-	-	TN
MDA-MB-468	-	-	-	TN
HCC1187	-	-	-	TN
HCC1806	-	-	-	TN

5.3.1.2. Osteosarcoma cell lines

143B osteosarcoma cell line and mtDNA lacking 143B cells (Rho zero cells) were a kind gift of Dr Karl Morten (University of Oxford, UK).

143B cell line was grown in high glucose (4.5g/L) DMEM (41966052, Gibco™) supplemented with 10% FBS. 143B is a thymidine kinase deficient (TK^{-}) cell line and consequently it has the nucleotide synthesis pathway disrupted. As mtDNA replication is independent from genomic DNA replication it needs constant supply of dNTPs, which are either imported from the cytosol or synthesized in the mitochondria by salvage enzymes [689]. Salvage pathways consist on the reutilization of nucleosides or bases arising from DNA or RNA degradation. In mammalian cells, salvage pathways rely on kinases to convert nucleosides into nucleotides [690]. The first step is carried out by thymidine kinase 1 (TK1) and deoxycytidine kinase (dCK) in the cytosol and thymidine kinase 2 (TK2) and deoxyguanosine kinase (dGK) in the mitochondria [691]. As a result of TK deficiency, in 143B cells the salvage pathway of pyrimidines is lost. Since the synthesis of DNA precursors is affected, this cell line has been used for long to generate mtDNA depleted cells (also called Rho zero, ρ0) to study mitochondrial disorders [692].

Rho zero cells were generated by treating 143B cells with 10µM 2',3'-dideoxycytidine (ddC, D5782, Sigma-Aldrich) for 10 days. mtDNA depletion leads, on the one hand, to no oxidative phosphorylation, as none of the members of the ETC are synthesized, and on the other hand, to pyrimidine synthesis impairment due to dysfunction of dihydrooratate dehydrogenase, an enzyme involved in pyrimidine synthesis located in the mitochondrial inner membrane, which requires mitochondrial electron transport for normal function [693]. In addition, human Rho zero cells have a growth requirement for pyruvate [692, 694]. The way to overcome these issues is to supplement with pyruvate and uridine the Rho zero cell culture media [692, 694], consequently, this cell line was grown in high glucose DMEM supplemented with 50µg/mL uridine (A15227, Alfa Aesar) and 10% FBS.

U2OS mTUNE osteosarcoma cell lines were kindly donated by Dr Christian Frezza (University of Cambridge, UK). Three isogenic cell lines with different levels of heteroplasmy of the mtDNA were used: mTUNE M7, M45 and M80 [695]. These cell lines were grown in low glucose DMEM supplemented with 10% FBS and tested for mycoplasma contamination routinely.

5.3.1.3. Kidney cancer cell line

HEK293 kidney cancer cell line stably expressing the IFNβ promoter/luciferase (HEK293 P125) was obtained from Dr Jan Rehwinkel (University of Oxford, UK). This cell line was cultured in low glucose DMEM supplemented with 10% FBS.

5.3.1.4. Non-tumour cell lines

HUVEC (Human Umbilical Vein Endothelial cells) were purchased to Lonza and grown in EGM™-2 Endothelial Cell Growth Medium-2 (CC-3162, Lonza) for no longer than seven passages. Human fibroblasts and HKC8 (a non-transformed proximal renal tubular cell line) were cultured in low glucose DMEM supplemented with 10% FBS. They were mycoplasma tested every three 3 months.

All cell lines were authenticated during the course of this project.

5.3.2. Cell treatments

MCF7 cells were seeded in normoxia or 0.1% hypoxia and treated for 48h with the following mitochondria targeting drugs: the vacuolar protein sorting 34 (Vps34) inhibitor SAR405 (16979, Cayman Chemical) at 5µM final concentration, chloramphenicol (C0378, Sigma-Aldrich) at 200µM final concentration, mubritinib (S-2216, Selleckchem) at 100nM final concentration, ABT-737 (sc-207242, Santa Cruz Biotechonology) at 5µM final concentration, metformin (D150959, Sigma-Aldrich) at 2mM final concentration or gamitrinib-triphenylphosphonium (G-TPP, HY-102007, MedChemExpress) at 5µM final concentration.

5.3.3. Cell transfection

5.3.3.1. Transfection of polyinosinic-polycytidylic acid

Transfection of polyinosinic-polycytidylic acid (poly I:C, P1530, Sigma-Aldrich) was performed in 1mL Opti-MEM™ I Reduced Serum Medium in the last 6h of the experiment. MCF7 cells were transfected with 20µg/mL poly I:C, 786-0 cells with 0.5µg/mL and due to the toxicity of poly I:C and hypoxic stress, MCF7 WT and MCF7 KO cells were transfected with 0.5µg/mL whereas fibroblast were transfected with 0.1µg/mL. Briefly, two different tubes were made, 500µL Opti-MEM™ I Reduced Serum Medium were mix with poly I:C (Mix A), and 500µL Opti-MEM™ I Reduced Serum Medium were mixed with 5µL Lipofectamine™ 2000 Transfection Reagent (11668027, Invitrogen™) (Mix B). After 5 min at RT, 500µL Mix B were added to Mix A, and kept for 20 min at RT. Cell media was replaced with 1mL transfection media (Mix A+B) and 6h later cells were processed. In parallel, control wells were subjected to the same procedure with Lipofectamine™ 2000 Transfection Reagent only.

5.3.3.2. Transfection of siRNA for BNIP3

Cells were transfected with 5nM siRNA for BNIP3 (siBNIP3, Dharmacon™) or 20nM siRNA control (siCON, Dharmacon™) (Table 5.2) in 1mL Opti-MEM™ I Reduced Serum Medium. MCF7 cells were seeded in 6-well plates and 24h later transfection was performed. Mix A was prepared by mixing 500µL Opti-MEM™ I Reduced Serum Medium and siRNA (siCON or siBNIP3), whereas Mix B was prepared by mixing 500µL Opti-MEM™ I Reduced Serum Medium and 5µL Lipofectamine™ 2000 Transfection Reagent. Both mixes were kept 5 min at RT. Then, 500µL Mix B were added to Mix A, and wait for 20 min. Cell culture media was replaced with 1mL transfection mix and 6h later 20% FBS was added. The following day media was replaced with complete DMEM and cells were placed into 0.1% hypoxia for 48h.

Table 5.2. siCON and siBNIP3 sequences. TT* overhangs.

siRNA	Sequence (5'-3')
siCON	ACGACACGCAGGUCGUCAUTT*
siBNIP3	UCGCAGACACCACAAGAUA
	GAACUGCACUUCAGCAAUA
	GGAAAGAAGUUGAAAGCAU
	ACACGAGCGUCAUGAAGAA

5.3.4. Lactate measurement

1x10^5 MCF7 WT and MCF7 KO cells were seeded in normoxia and 0.1% hypoxia for 48h. After that time, 1mL media was removed and centrifuged at 300g for 5 min at RT. Supernatant was stored at -80ºC until used. Cells were trypsinized and counted for further data normalization. Lactate concentration was measured using Lactate Reagent Set (2864, Instruchemie). Briefly, lactate standards were prepared by serial dilutions from the Lactate Stock Standard (4.44mM). NAD Mixture was prepared by mixing Lactate NAD Reagent, 2mL Lactate Buffer Reagent, 4mL MilliQ water and 100µL Lactate LDH Reagent. Reaction was performed in a 96-well plate by adding 10µL supernatant or lactate standard and 290µL NAD Mixture, in triplicate. After mixing and incubating the plate 15 min at 37ºC, absorbance was measured at 340nm.

The procedure utilizes LDHA enzyme, which catalyses the conversion of lactate to pyruvate by reducing NAD. In the presence of excess NAD and hydrazine (present in Lactate Buffer Reagent), substantially all lactate is converted to pyruvate. The increase in absorbance due to reduction of NAD to NADH indicates the amount of lactate originally present in the sample.

5.3.5. IFNβ promoter assay

HEK293 P125 reporter cells (stably expressing the IFNβ promoter/luciferase region [696]) kindly given by Dr Jan Rehwinkel were used to detect immunostimulatory RNAs present in normoxia or hypoxia treated cells. For this assay, 4x10^4 HEK293 P125 cells per well were seeded in 96-well plates. The following day, cells were pretreated with 30U/mL of recombinant IFN-A/D (I4401, Sigma-Aldrich). 24h after of incubation, fresh media was added and cells were transfected with 100ng of RNA per well using Lipofectamine™ 2000 Transfection Reagent. Briefly, 100ng RNA were mixed with 9µL Opti-MEM™ I Reduced Serum Medium per well, and incubate for 5 min at RT. In parallel, 0.5µL Lipofectamine™ 2000 Transfection Reagent were diluted in 9µL Opti-MEM™ I Reduced Serum Medium per well and incubated for 5 min too. Then both solutions were mixed and incubated for 20 min at RT. After this time, 18µL of RNA:Lipofectamine complex were added dropwise per well. As positive controls, 1ng of the MDA5 ligand V-EMCV-RNA (RNA from the *Encephalomyocarditis virus*) or RIG-I ligand IVT-RNA (*in vitro* transcripts-RNA) were included (gift from Dr Jan Rehwinkel) [696]. 24h after transfection, ONE-Glo™ Luciferase Assay (E6110, Promega) was performed. Media was removed and 100µL OneGlo reagent was added per well. Plates were incubated for 3 min in the darkness. Afterwards, the solution was mixed by pipetting and 70µL were transferred to a white plate (436111, Thermo Fisher Scientific™) and read on a FluorOPTIMA luminometer.

5.3.6. Mitochondria extraction

Mitochondria were isolated from MCF7 cells seeded in normoxia or 0.1% hypoxia for 48h using Mitochondria Isolation Kit for Cultured Cells (89874, Thermo Fisher Scientific™), and following manufacturer's instructions. First, cells were trypsinized and spun down by centrifuging at 300g for 5 min at RT. Supernatant was removed and 800µL Mitochondria Isolation Reagent A was added to each sample and vortexed. After 2 min incubation on ice, 10µL Mitochondria Isolation Reagent B was added and samples were incubated on ice for 5 min, vortexing every minute. Afterwards, 800µL Mitochondria Isolation Reagent C was added and mixed by inverting the tubes several times. Samples were centrifuged at 700g for 10 min at 4ºC. Supernatants were transferred to a new tube a further centrifuged at 3000g for 15 min at 4ºC to obtain a more purified fraction of mitochondria, with less lysosomal and peroxisomal contaminants. Supernatants (cytosolic fractions) were transferred to a new tube and frozen at -80ºC. Pellets containing the mitochondria were further processed by addition of 500µL Mitochondria Isolation Reagent C and centrifuging 12000g for 5 min at 4ºC. Supernatant was discarded and RNA from the mitochondria was extracted using Tri Reagent®, following the protocol previously explained. 200µL of the cytosolic fraction were also used to extract RNA.

5.3.7. Immunofluorescence

5.3.7.1. Immunofluorescence for dsRNA

Cells were plated on borosilicate glass coverslips and cultured in normoxia or 0.1% hypoxia for 48h. Prior to fixation, mitochondria were stained with MitoTracker™ Deep Red (M22426, Thermo Fisher Scientific™) at 200nM final concentration for 1h. After, cells were washed once with PBS and fixed in 4% PFA for 8 min at RT. Then, cells were washed with PBS and permeabilized with PBS containing 0.1% Triton X-100 (T8787, Sigma-Aldrich) for 20 min at RT. Cells were washed with 0.1M glycine (G7126, Sigma-Aldrich) for 10 min at RT to neutralize the remaining PFA. After washing three times with PBS, cells were incubated for 60 min with PBS containing 1% BSA and 10% normal goat serum (ab7481, Abcam) (block solution). Cells were incubated overnight at 4ºC in a humidified chamber with J2 primary antibody at 1:200 and rhodamine phalloidin (R415, Invitrogen™) at 1:40 concentration in block solution. Cells were washed three times with PBS prior to incubation with goat anti-mouse IgG conjugated with Alexa Fluor 488 (R37120, Invitrogen™) secondary antibody at 1:500 and Hoechst 33342 (H3570, Invitrogen™) at 1:1000 concentration in block solution for 1h at RT. After washing three times with PBS, coverslips were mounted with Vectashield® Mounting Medium for Flourescence without DAPI and sealed with nail polish.

5.3.7.2. Immunofluorescence dsRNA image analysis

Slides were imaged in a Zeiss 880 Inverted confocal microscope (Zeiss) using a ZEN fluorescence microscopy system (Zeiss) and a 63x Plan-Apochromat objective. Laser properties, acquisition mode and detectors were manually adjusted for each experiment.

Images were analysed using Fiji Image J software. Specific macros were created by Dr Ulrike Schulze and Dr Dominic Waithe (University of Oxford, UK) for the analysis:

1- Combine_ROI: this macro translates the drawings performed on the images to define the cell and the nucleus into ‘cell’, ‘nucleus’ and ‘cytoplasm’.
2- Measure_intensity: this macro measures the total intensity of the selected channel in the cytoplasm of the cell. We can include a threshold value to avoid background signal.

First, the image was divided into the different channels (Figure 5.6A). Using Fiji Image J ROI Manager tool, the cell and the nucleus of each cell to be analysed was defined (Figure 5.6B). Combine_ROI was run and the generated file was saved for further analysis. Once defined the cell, nucleus and cytoplasm, Measure_intensity macro was run in the channel corresponding to J2 staining. This was first run in the secondary antibody control images (cells incubated with the secondary antibody but not with the primary antibody) to know the background signal of the secondary antibody. A mean of the intensity values obtained in the control images was used as the threshold value for the images to be analysed. Then, J2 antibody staining intensity was measured in a minimum of 40 cells per condition with the previously defined threshold value.

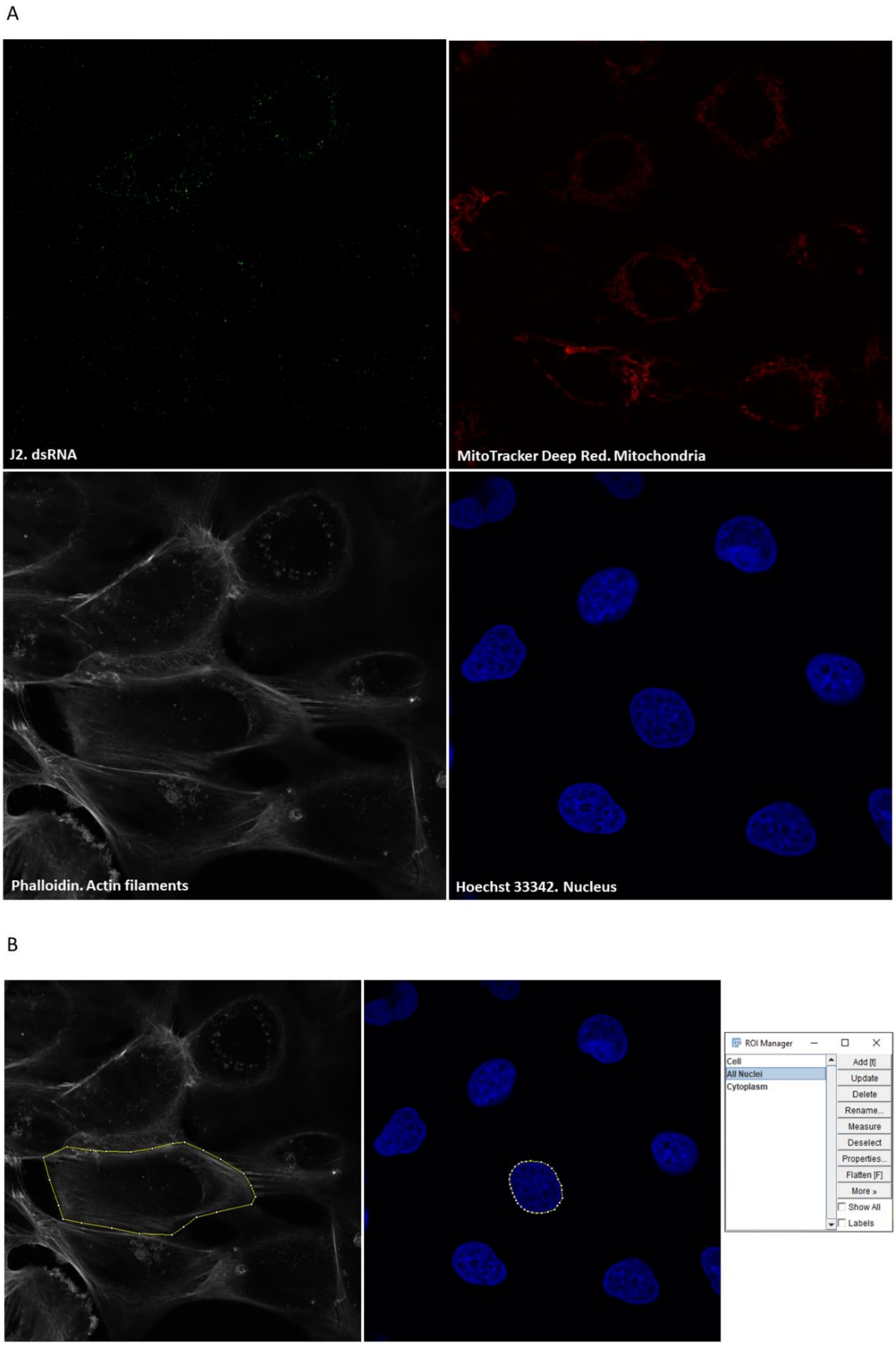
A
J2. dsRNA
MitoTracker Deep Red. Mitochondria
Phalloidin. Actin filaments
Hoechst 33342. Nucleus
B
ROI Manager
Cell
All Nuclei
Cytoplasm
Add [t]
Update
Delete
Rename...
Measure
Deselect
Properties...
Flatten [F]
More »
Show All
Labels

Figure 5.6. A) Immunofluorescence image divided into the different channels corresponding to dsRNA, mitochondria, actin filaments and nucleus. B) Drawing of the cell shape and the nucleus.

5.3.7.3. Immunofluorescence for mitophagy

$2x10^4$ MCF7 cells were seeded in 24-well glass-bottom SensoPlate™ (662892, Greiner) for 48h. 1h prior to imaging, media was removed and replaced with complete DMEM containing 50nM LysoTracker™ Red DND-99 (L7528, Invitrogen™) and 100nM MitoTracker™ Green FM (M7514, Invitrogen™). Then, media was removed and replaced with fresh media. Living cells were imaged in a Zeiss 880 Inverted confocal microscope (Zeiss) using a ZEN fluorescence microscopy system (Zeiss) and a 63x Plan-Apochromat objective. Laser properties, acquisition mode and detectors were manually adjusted for each experiment.

5.4. Results

5.4.1. Hypoxia causes a down-regulation of the type I IFN pathway at basal levels

In order to investigate the effect of hypoxia on the type I IFN pathway, MCF7 cells were cultured under normoxia, 1% hypoxia and 0.1% hypoxia for 48h. Hypoxia was observed to down-regulate IFN pathway members of early and late phase both at mRNA (Figure 5.7A) and protein (Figure 5.7B) levels. Moreover, this effect was oxygen concentration-dependent, as 0.1% hypoxia caused a greater down-regulation than 1% hypoxia.

At mRNA level, the effect was noticeable from the dsRNA sensors RIG-I and MDA5 (encoded by *DDX58* and *IFIH1*, respectively), the adaptor *MAVS* and the transcription factors *IRF3* and *IRF7* which trigger cytokine and IFNβ production. 0.1% hypoxia generated 30-50% of suppression in the expression of these genes. Similarly, levels of molecules involved in the late phase of the IFN response, such as *STAT1* and *STAT2* signal transducers and the ISG *ADAR-p150*, displayed the same phenomenon ($p<0.001$).

At protein level, hypoxia lowered the activation of RIG-I, IRF7, STAT1 and ADAR-p150. Constitutive levels of ADAR-p110, on the other hand, did not change under hypoxia (Figure 5.7B). Taking into account that activation of the type I IFN pathway is mediated through phosphorylation of STAT1 and STAT2, STAT1 protein phosphorylation status at serine position 727 (Ser727) was checked (Figure 5.7B). Less phosphorylation in hypoxia confirmed that the type I IFN pathway in hypoxia was not as active as in normoxia.

Consistent observations were made in a panel of six further breast cancer cell lines containing representatives of ER+ (T47D), HER2+ (BT474) and TN (MDA-MB-231, MDA-MB-468, MDA-MB-453 and HCC1187) cell lines. In general, down-regulation ranging between 20-60% of suppression of the type I IFN pathway was observed in all of these cell lines under hypoxic conditions. However, TN cell lines seemed to be more resistant to the hypoxic inhibitory effect, showing a lower or no down-regulation of some genes, such as *DDX58*, *IRF3* or *MX1* ($p>0.05$) (Figure 5.7C).

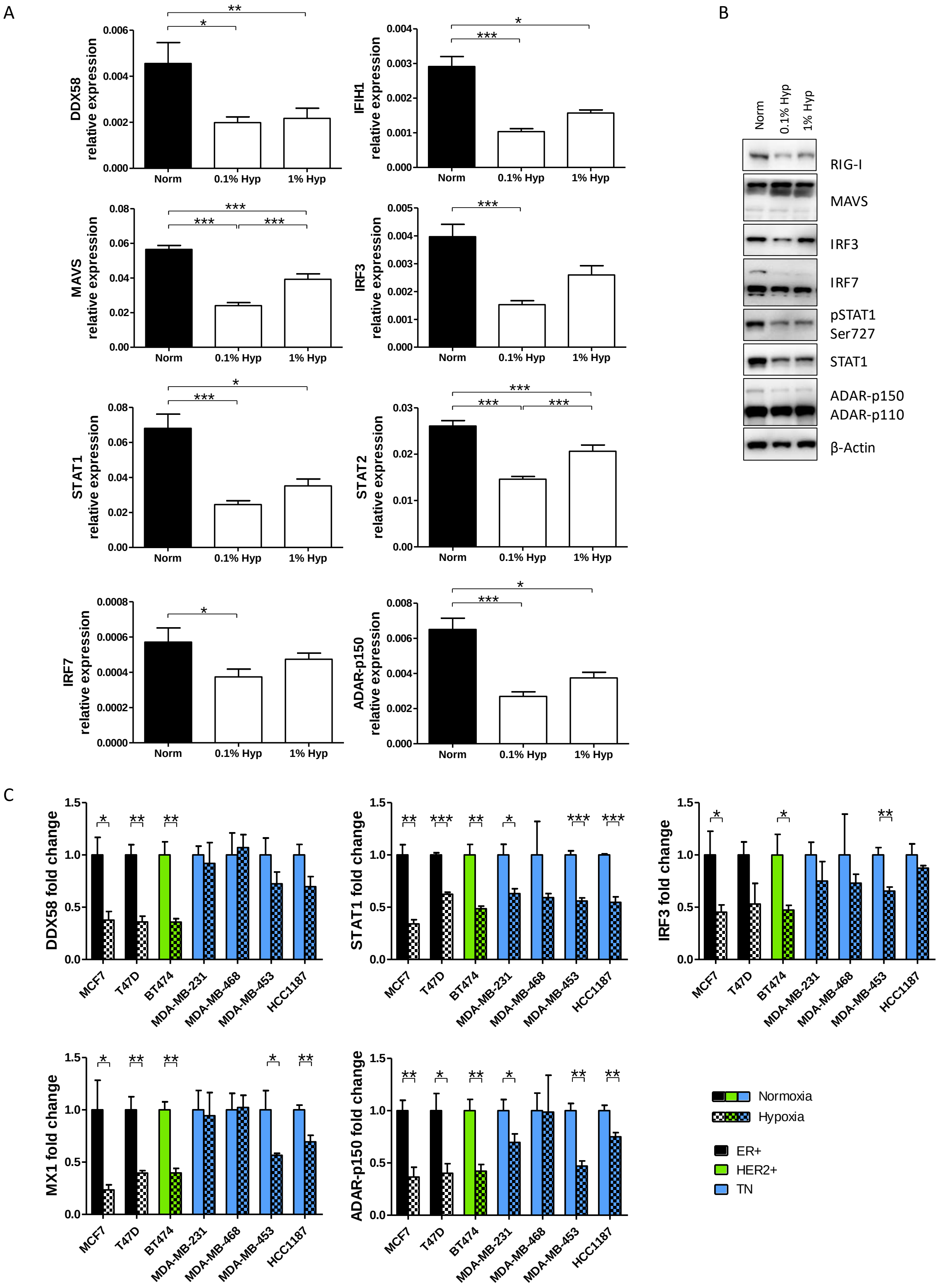

Figure 5.7. A) mRNA and B) protein levels of different genes involved in the type I IFN pathway in MCF7 cells cultured in normoxia, 0.1% hypoxia or 1% hypoxia for 48h. n=3. C) mRNA expression of genes of the type I IFN pathway in different breast cancer cell lines cultured in normoxia or 0.1% hypoxia for 24h. n=10. * p<0.05, ** p<0.01, *** p<0.001.

5.4.2. Reoxygenation after hypoxia leads to recovery of the type I IFN pathway

To explore the inhibitory effect of hypoxia during the 48h of hypoxic exposure, a time course experiment in 0.1% hypoxia was performed. MCF7 cells were cultured in hypoxia for 4h, 8h, 16h, 24h or 48h and mRNA (Figure 5.8A) and protein (Figure 5.8B) levels of members of the type I IFN pathway were analysed.

As depicted in Figure 5.8A, mRNA down-regulation started after 4h of hypoxia exposure for *IRF3* and *ADAR-p150* ($p<0.05$) genes, whereas 8h were required for *DDX58*, *IFIH1*, *MAVS* and *STAT1*. Hypoxia induced suppression ranged from 30-50% and varied between genes. Nevertheless, the down-regulation was more pronounced by 16h under hypoxic conditions, as it inhibited the expression of every gene by more than 50%. Beyond 16h there was little or no reduction in mRNA levels.

In contrast, down-regulation was not noticeable at the protein level until 48h (Figure 5.8B), suggesting that the repression occurs first at transcription level and consequently, it affects protein expression.

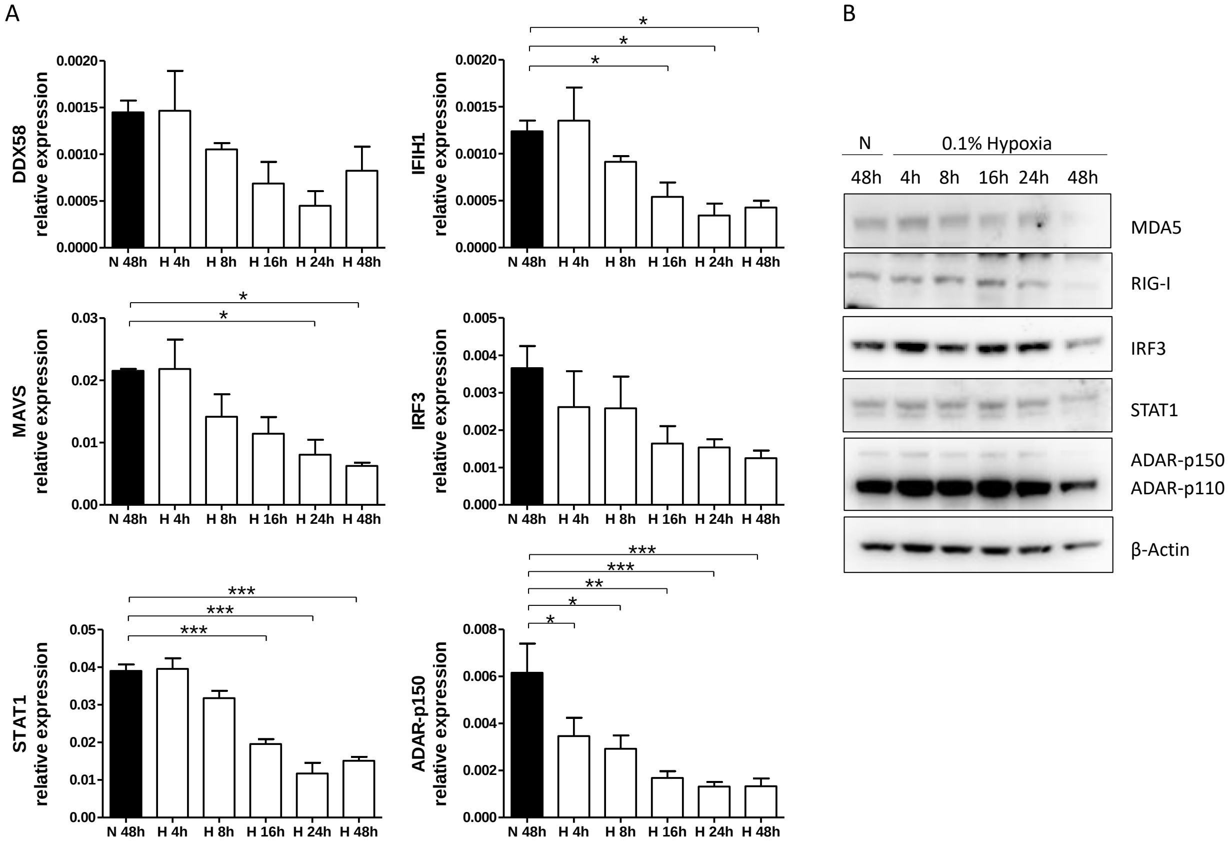

Figure 5.8. Expression of various genes involved in the type I IFN pathway at mRNA (A) and protein (B) level in MCF7 cells cultured in normoxia for 48h or 0.1% hypoxia for 4h, 8h, 16, 24h and 48h. n=3. * $p<0.05$, ** $p<0.01$, *** $p<0.001$.

To further explore the differences between mRNA and protein levels in response to oxygen, reoxygenation experiments were performed. MCF7 cells were incubated either in normoxia or 0.1% hypoxia for 48h and subsequently reoxygenated for 8h, 16h or 24h. As shown in Figure 5.9A, reoxygenation caused a gradual increase in the expression of the tested genes at mRNA level after 8h. Consistent with previous results (Figure 5.7), hypoxia induced a down-regulation of the pathway at protein level, but reoxygenation up to 24h was not able to reverse this effect except for RIG-I (Figure 5.9B). These results further support the idea that RNA responds more rapidly than protein to oxygen tension.

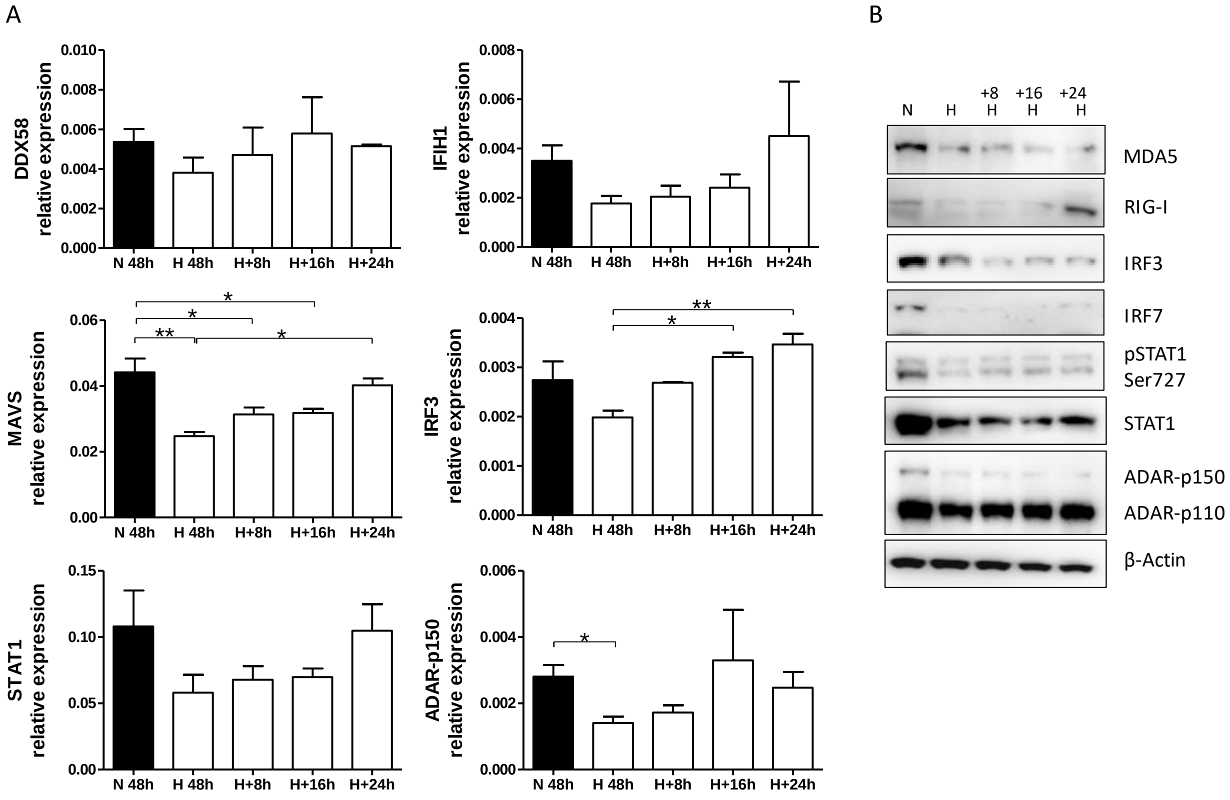

Figure 5.9. A) qPCR data showing the relative expression of *DDX58*, *IFIH1*, *MAVS*, *IRF3*, *STAT1* and *ADAR-p150* in MCF7 cells cultured in normoxia or subjected to reoxygenation for up to 24h. n=3. * p<0.05, ** p<0.01, *** p<0.001. B) Western blot results of the expression of the same genes at protein level in MCF7 cells cultured in normoxia for 48h or hypoxia for 48h plus reoxygenation for 8h, 16h and 24h. n=3.

5.4.3. Hypoxia down-regulates the type I IFN pathway stimulated with a dsRNA mimic

In order to check if the down-regulation induced by hypoxia at basal levels would persist upon activation of the IFN pathway, MCF7 cells were cultured in either normoxia or 0.1% hypoxia for 48h and transfected with the synthetic analogue of dsRNA poly I:C in the last 6h of the incubation. The addition of poly I:C to the cells activated the pathway as reflected by phosphorylation in STAT1 and IRF3 (pSTAT1-Ser727 and pIRF3-Ser386, respectively) (Figure 5.10A), in a dose-dependent manner. However, the level of type I IFN pathway activation was lower under hypoxia, as poly I:C induced expression of pSTAT1 and pIRF3 was down-regulated. Hypoxia also caused lower expression levels of MDA5, RIG-I, IRF3 and IRF7, as found previously without the addition of poly I:C.

Various breast cancer cell lines with different hormone receptor status were also tested for poly I:C pathway induction. Despite poly I:C activated the type I IFN pathway in all ER+ (Figure 5.10A), HER2+ (Figure 5.10B) and TN (Figure 5.10C) cell lines, hypoxia caused lower induction, as demonstrated by less pIRF3 and pSTAT1 protein levels (Figure 5.10). The expression of MDA5 and RIG-I receptors, as well as STAT1 and IRF7 transcription factors, was diminished under low oxygen concentrations, showing that the lower type I IFN response in hypoxia is a general effect on breast cancer cell lines.

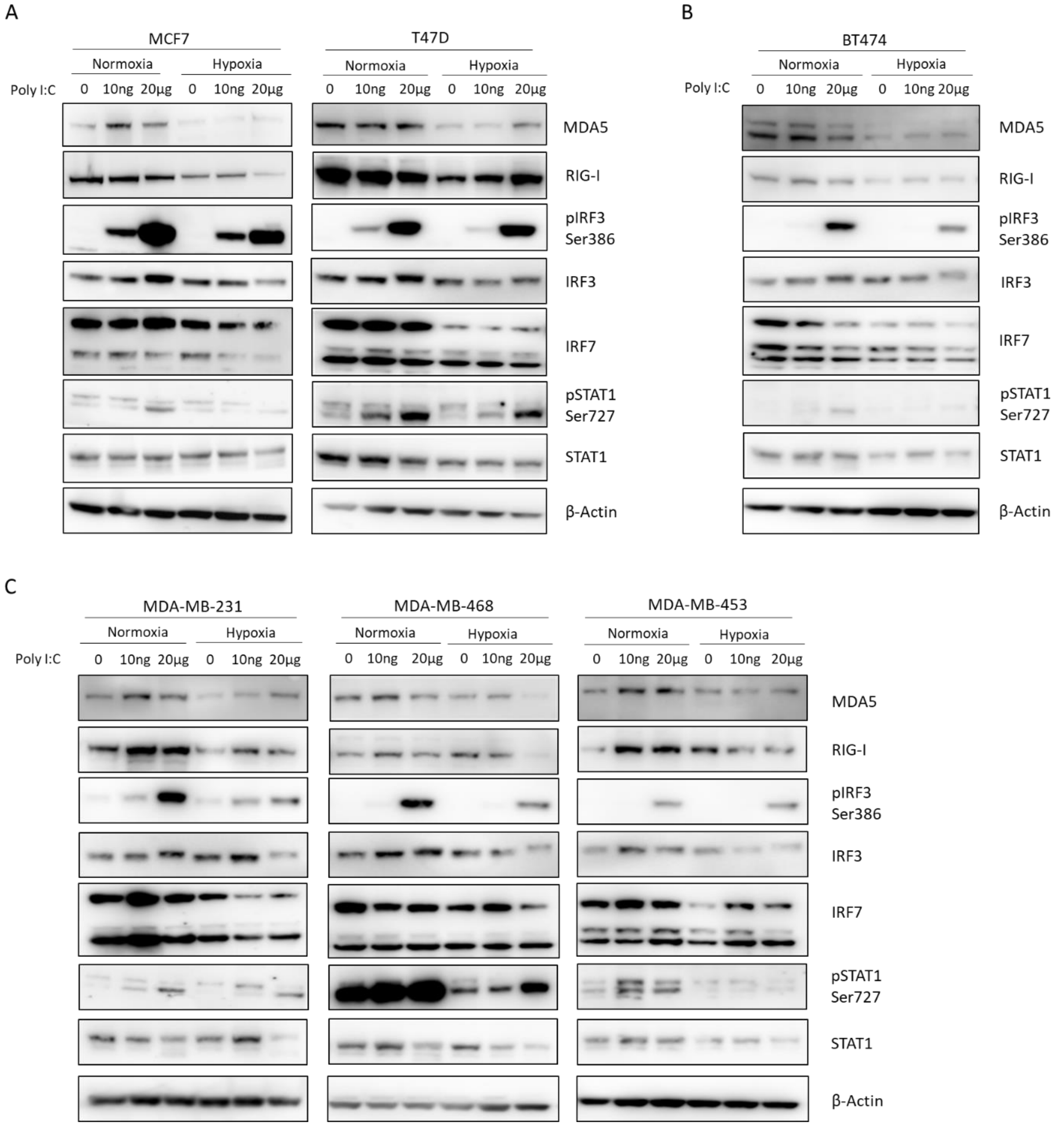
A
MCF7
T47D
Normoxia
Hypoxia
Normoxia
Hypoxia
Poly I:C
0 10ng 20µg 0 10ng 20µg
0 10ng 20µg 0 10ng 20µg
MDA5
RIG-I
pIRF3 Ser386
IRF3
IRF7
pSTAT1 Ser727
STAT1
β-Actin
B
BT474
Normoxia
Hypoxia
Poly I:C
0 10ng 20µg 0 10ng 20µg
MDA5
RIG-I
pIRF3 Ser386
IRF3
IRF7
pSTAT1 Ser727
STAT1
β-Actin
C
MDA-MB-231
MDA-MB-468
MDA-MB-453
Normoxia
Hypoxia
Normoxia
Hypoxia
Normoxia
Hypoxia
Poly I:C
0 10ng 20µg 0 10ng 20µg
0 10ng 20µg 0 10ng 20µg
0 10ng 20µg 0 10ng 20µg
MDA5
RIG-I
pIRF3 Ser386
IRF3
IRF7
pSTAT1 Ser727
STAT1
β-Actin

Figure 5.10. Type I IFN pathway activation by poly I:C in ER+ (A; MCF7 and T47D), HER2+ (B; BT474) and TN (C; MDA-MB-231, MDA-MB-468 and MDA-MB-453) breast cancer cells. Cell were cultured in normoxia or hypoxia for 48h and transfected with poly I:C in the last 6h. n=3.

Other cell lines from normal tissue such as HKC8 and fibroblasts were assessed to explore the pathway in a non-tumour environment. Poly I:C stimulated the pathway, as seen by an increase in MDA5, RIG-I, pIRF3 and pSTAT1-Tyr701 levels (Figure 5.11). Consistent with the tumour cell lines, hypoxia reduced that induction. In both cell lines pIRF3 levels were lower in hypoxia, whereas IRF3 levels increased in HKC8 but did not change in fibroblasts. This shows that under hypoxia, most IRF3 molecules are not phosphorylated.

These results further suggest that type I IFN pathway down-regulation in hypoxia is a general feature of both cancer and normal cells from different tissues.

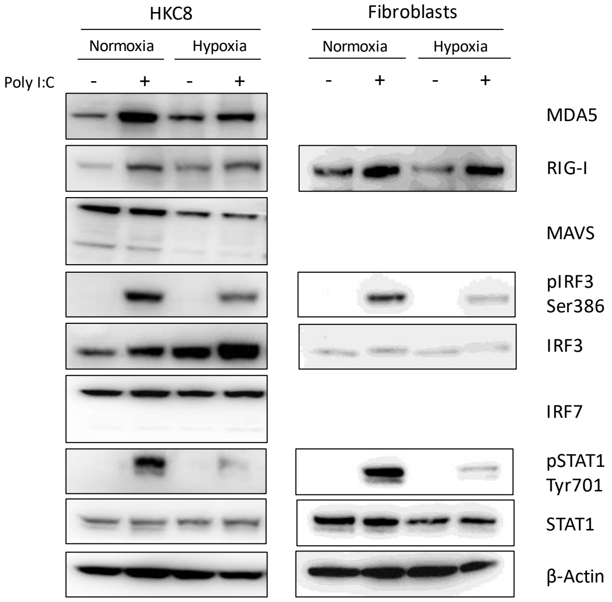

Figure 5.11. Type I IFN pathway activation upon poly I:C stimulation during 6h in HKC8 cells and fibroblasts cultured in normoxia or 0.1% hypoxia for 48h. n=3.

5.4.4. HIF1α and HIF2α role in the type I IFN pathway

As hypoxia down-regulated the pathway in both cancer and normal tissues of different origin, the role of the main hypoxia transcription factors, HIF1α and HIF2α, was studied to further investigate the mechanisms underlying this phenomenon.

5.4.4.1. Type I IFN pathway is partially dependent on HIF1α

To study the role of HIF1α in the type I IFN pathway, MCF7 WT and MCF7 KO cells were used. MCF7 cells were treated with the dsRNA mimic poly I:C to stimulate the pathway in normoxia and hypoxia. Poly I:C induced RIG-I, IRF3, pIRF3, IRF7 and pSTAT1 expression in both cell lines under normoxia. This induction was higher in MCF7 KO cells, with the exception of pSTAT1, which was induced but at lower levels than in MCF7 WT cells. The effect of poly I:C was attenuated in hypoxia for all the above proteins to similar residual levels in both cell lines, thus excluding HIF1α as the main responsible for the down-regulation (Figure 5.12A). Interestingly, RIG-I and STAT1 levels were higher in MCF7 KO than in MCF7 WT cells, supporting a partial role of HIF1α in suppressing them. However, in hypoxia RIG-I and STAT1 levels were reduced in both cell lines, suggesting a HIF1α-independent mechanism to further regulate them.

The expression of the type I IFN receptors responsible for the late phase of the pathway after IFNβ binding, *IFNAR1* and *IFNAR2*, was also determined (Figure 5.12B). Both subunits were significantly down-regulated in MCF7 WT cells in hypoxia compared to normoxia ($p<0.05$ and $p<0.001$, respectively). Interestingly, MCF7 KO cells showed 30-50% lower levels of both receptors in normoxia than MCF7 WT cells ($p<0.01$), and the levels were comparable to those of hypoxic MCF7 WT cells. Moreover, hypoxia did not cause any further down-regulation on the expression of *IFNAR1* and *IFNAR2* in MCF7 KO cells. This result shows that HIF1α is unlikely to explain the down-regulation seeing in MCF7 WT cells in hypoxia, further suggesting a complex mechanism in which HIF1α has a basal role increasing responsiveness to poly I:C, but the effect of hypoxia down-regulating many IFN genes still persists.

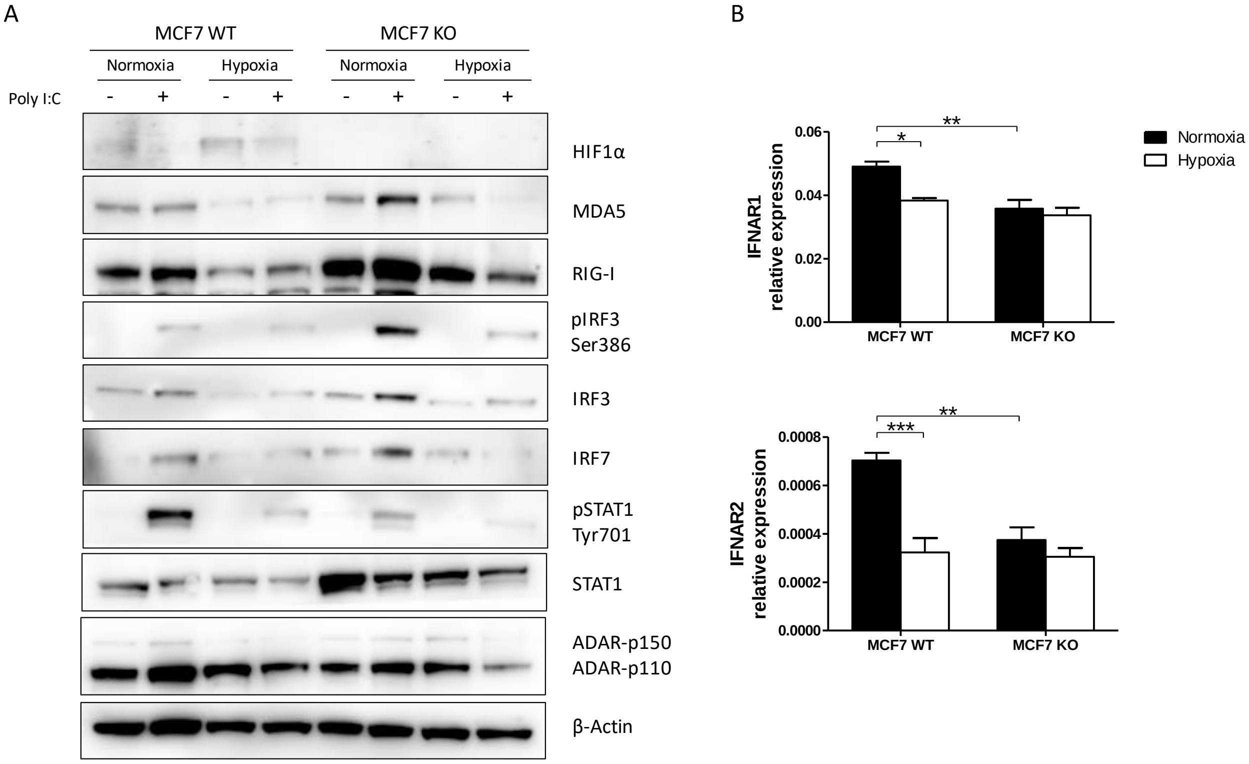

Figure 5.12. A) Protein expression of various genes of the type I IFN pathway in MCF7 WT and MCF7 KO cells cultured in normoxia or 0.1% hypoxia for 48h and stimulated with poly I:C. n=3. B) *IFNAR1* and *IFNAR2* mRNA expression in MCF7 WT and MCF7 KO cells cultured in normoxia or 0.1% hypoxia for 48h. n=3. * $p<0.05$, ** $p<0.01$, *** $p<0.001$.

In addition to this, some ISGs associated with chronic antiviral response such *IFIH1*, *MX1* or *STAT1* can be transcribed by unphosphorylated STAT1, an effect driven by higher IRF9 expression [697]. MCF7 KO cells showed higher STAT1 than MCF7 WT cells (Figure 5.12A) and IRF9 expression at protein level was also higher in MCF7 KO cells (Figure 5.13A). This increase in IRF9 levels was associated with significantly higher ISG expression even in hypoxia compared to MCF7 WT cells ($p<0.001$) (Figure 5.13B). MCF7 KO cells presented between 2- and 6-fold increased expression of *DDX58*, *IFIH1*, *STAT1* and *ADAR-p150* in normoxia and hypoxia compared to MCF7 WT cells, showing that HIF1α is repressing the expression of these genes. However, hypoxic MCF7 KO cells had lower ISG levels than normoxic MCF7 KO (p<0.001). These results show that HIF1α up-regulation in hypoxia is partly responsible for the type I IFN pathway down-regulation achieved under low oxygen levels, but that other HIF1α-independent mechanisms are likely contributing to the observed decrease.

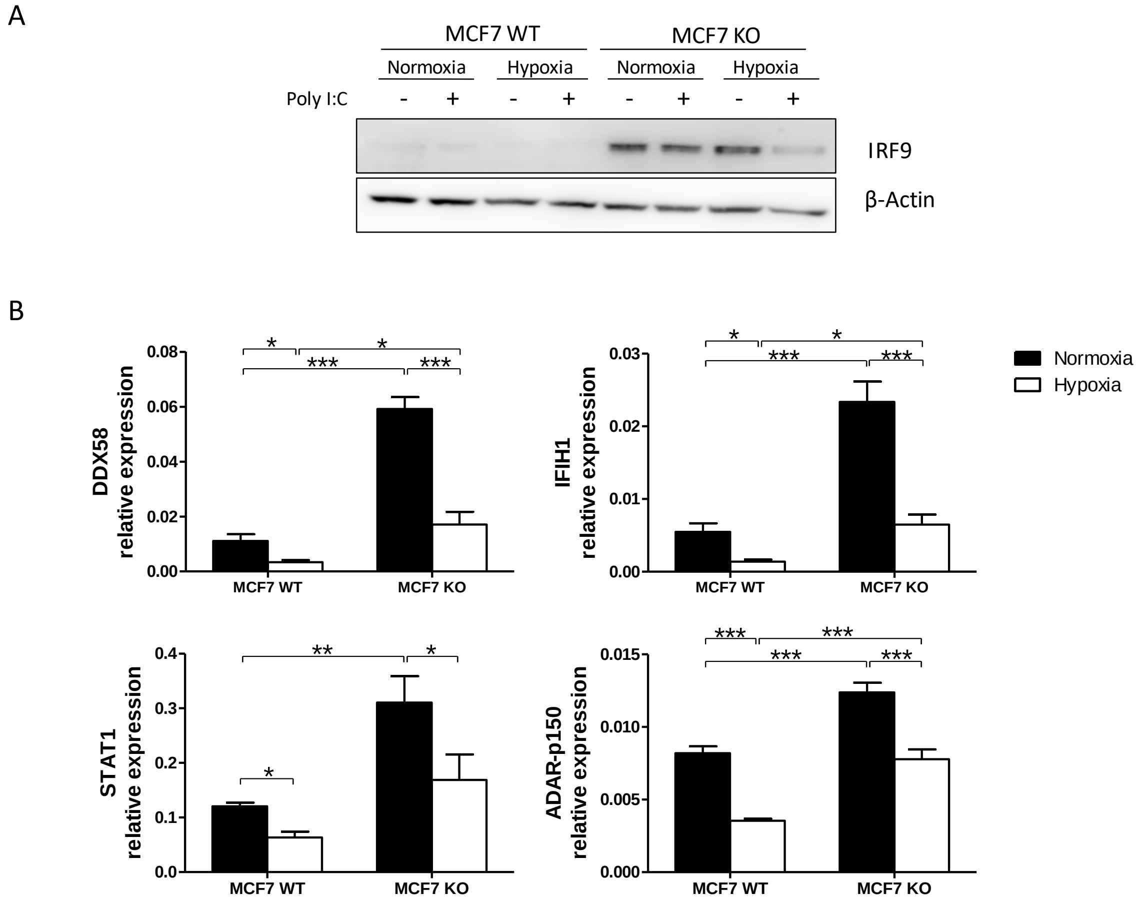

Figure 5.13. A) IRF9 protein expression in MCF7 WT and MCF7 KO cells cultured in normoxia or 0.1% hypoxia for 48h. n=3. B) Some ISGs mRNA expression levels in MCF7 WT and MCF7 KO cells cultured in normoxia or 0.1% hypoxia for 48h. n=3. * p<0.05, ** p<0.01, *** p<0.001.

5.4.4.2. Hypoxic lactate levels inhibit the type I IFN pathway

Recently, it has been described that lactate is an important metabolite responsible for the type I IFN signalling inhibition by directly binding to MAVS adaptor protein [622]. Furthermore, the lactate generated during the metabolic switch to glycolysis that tumour cells undergo in hypoxia act as a 'signalling molecule' to promote tumour escape from the immune system [617]. In MCF7 cells, hypoxia exposure induced 5-fold increase in lactate production in both MCF7 WT and MCF7 KO cells (Figure

5.14), showing that high lactate levels in hypoxia could be promoting the immunosuppressive environment. In addition, there were no differences between cell lines, supporting the hypothesis that hypoxia-induced type I IFN pathway inhibition is not exclusively dependent on HIF1α.

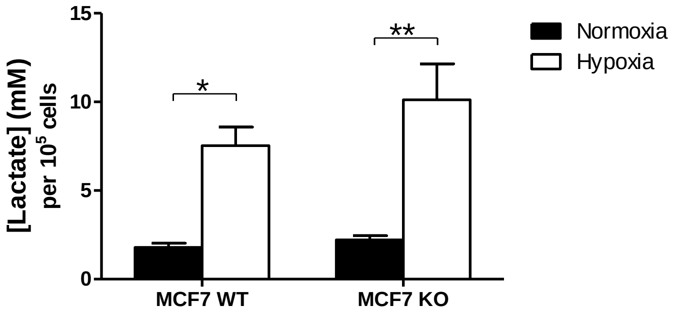

Figure 5.14. Lactate concentration (mM) per 10^5 cells in the supernatant of MCF7 WT and MCF7 KO cells cultured in normoxia or 0.1% hypoxia for 48h. n=3. * $p<0.05$, ** $p<0.01$, *** $p<0.001$.

5.4.4.3. Type I IFN pathway and HIF2α

HIF1α's partial involvement in the regulation of the type I IFN pathway, suggests that other mechanisms than HIF1α might participate in the observed hypoxic down-regulation, e.g. HIF2α. In order to study HIF2α involvement in the regulation of the type I IFN pathway, 786-0 and RCC4 ccRCC cell lines (described in 'Chapter 3') were used, as it is well-described the oncogenic role of HIF2α in ccRCC [125].

In 786-0 cells, poly I:C induced pIRF3 and pSTAT1 expression in both cell lines, while no changes were observed for MDA5, RIG-I, IRF3 or STAT1 (Figure 5.15A). STAT1 normoxic levels were similar in both cell lines, due to HIF1α is not expressed in none of them. Hypoxia led to the down-regulation of MDA5, RIG-I, pIRF3, IRF3, pSTAT1, STAT1 and ADAR-p150 upon poly I:C transfection both in 786-0 WT and 786-0 KO cells, showing that in spite of HIF1α and HIF2α deficiency hypoxia still suppresses the type I IFN response.

In RCC4 cell line, poly I:C treatment strongly induced the dsRNA receptors levels in normoxia (Figure 5.15B). This shows that high HIF1α/HIF2α was not enough to reduce normoxic RCC4 WT levels to those observed in hypoxia. MDA5 and RIG-I levels were further down-regulated in both cell lines in hypoxia, suggesting that the down-regulation occurs through other mechanisms than HIF-mediated. Poly I:C treatment did not generate changes in IRF3 levels, but did induce pIRF3 expression in both cell lines. As it occurred in MCF7 KO cells, STAT1 basal levels were much higher in RCC4 VHL than in RCC4 WT cells in normoxia, which fits with the suppressive role of HIF1α on STAT1. In this model, poly I:C transfection increased pSTAT1 and decreased STAT1 levels, and this was achieved to a greater extent in RCC4 VHL cells, pointing to a role of HIF1α and HIF2α in suppressing phosphorylation.

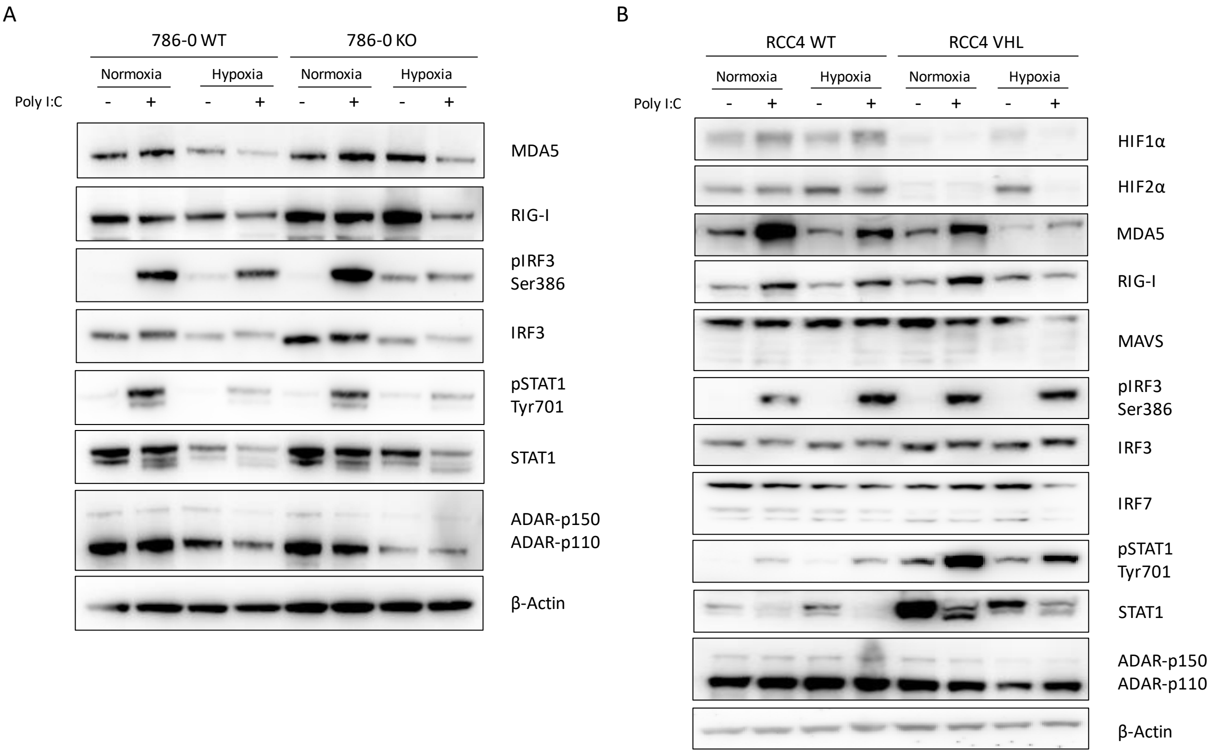
A
786-0 WT
786-0 KO
Normoxia
Hypoxia
Normoxia
Hypoxia
Poly I:C
- + - + - + - +
MDA5
RIG-I
pIRF3 Ser386
IRF3
pSTAT1 Tyr701
STAT1
ADAR-p150
ADAR-p110
β-Actin
B
RCC4 WT
RCC4 VHL
Normoxia
Hypoxia
Normoxia
Hypoxia
Poly I:C
- + - + - + - +
HIF1α
HIF2α
MDA5
RIG-I
MAVS
pIRF3 Ser386
IRF3
IRF7
pSTAT1 Tyr701
STAT1
ADAR-p150
ADAR-p110
β-Actin

Figure 5.15. Protein levels of type I IFN pathway members in A) 786-0 WT and 786-0 KO cells and B) RCC4 WT and RCC4 VHL cells cultured in normoxia or 0.1% hypoxia for 48h and transfected with poly I:C in the last 6h of the exposure. n=3.

In general, and despite the differences observed between cell lines (Table 5.3), there is a partial role of HIF1α and HIF2α in regulating some members of the pathway, but more importantly, hypoxia causes a HIF-independent down-regulation of the type I IFN pathway.

Table 5.3. Summary of the western blot results of each cell line.

Cell line	Poly I:C induced changes	Hypoxia induced changes upon poly I:C transfection	STAT1 basal levels
MCF7 WT	up RIG-I, pIRF3, IRF3, IRF7 and pSTAT1.	down MDA5, RIG-I, pIRF3, IRF3, IRF7 and pSTAT1.	higher in MCF7 KO
MCF7 KO	up MDA5, RIG-I, pIRF3, IRF3, IRF7 and pSTAT1.	down MDA5, RIG-I, pIRF3, IRF3, IRF7 and pSTAT1.	
786-0 WT	up pIRF3 and pSTAT1.	down MDA5, RIG-I, pIRF3, IRF3, pSTAT1, STAT1 and ADAR-p150.	equal in both cell lines
786-0 KO	up pIRF3 and pSTAT1.	down MDA5, RIG-I, pIRF3, IRF3, pSTAT1, STAT1 and ADAR-p150.	
RCC4 WT	up MDA5, RIG-I, pIRF3 and pSTAT1.	down MDA5 and RIG-I.	higher in RCC4 VHL
RCC4 VHL	up MDA5, RIG-I, pIRF3 and pSTAT1.	down MDA5, RIG-I and pSTAT1.	

5.4.5. Hypoxic total RNA causes lower IFNβ induction

In order to determine how the endogenous type I IFN pathway is down-regulated under hypoxia, the ability of total RNA extracted from cells cultured in normoxia or hypoxia for 48h to activate the IFNβ promoter was analysed, using the IFNβ promoter assay [696]. Briefly, this assay consists on transfecting RNA into a HEK293 cell line stably expressing a luciferase reporter linked to the IFNβ promoter (HEK293 P125) and measuring the luciferase activity 24h later (Figure 5.16A). HEK293 P125 wild type (P125 WT) and various KO for different members of the pathway, such as MDA5 (P125 MDA5 KO), RIG-I (P125 RIG-I KO) and MAVS (P125 MAVS KO) were used. As depicted in Figure 5.16B, both MDA5 KO and MAVS KO led to lower IFNβ promoter stimulation under normoxia ($p<0.001$), whereas RIG-I absence minimally changed the luciferase intensity. RIG-I selectively binds short dsRNA while MDA5 binds long dsRNA (>2kb) [698], thus these results suggest that most of the signalling is induced by long dsRNA molecules within the cells, a signal almost lost under both 0.1% and 1% hypoxia (Figure 5.16B), further confirming that IFNβ promoter stimulation is inhibited in low oxygen conditions.

Moreover, poly I:C, previously demonstrated to activate the type I IFN pathway (Figure 5.10), is a synthetic MDA5 ligand thus, type I IFN pathway could be activated by endogenous long dsRNA molecules. Therefore, to analyse which RNA species from the total RNA were responsible for the induction of the IFNβ promoter, RNA from normoxic and hypoxic MCF7 cells was treated with different RNAses and the MDA5 ligand V-EMCV, only containing dsRNA, was used as a positive control (Figure 5.16C). RNAse III treatment (specific for dsRNA) completely abolished normoxic ($p<0.05$), hypoxic ($p<0.01$) and V-EMCV RNA ($p<0.01$) induced IFNβ promoter activity, whereas RNAse A (specific for ssRNA) treatment did not affect luciferase signal (p>0.05). These results show that endogenous dsRNA is responsible for IFNβ promoter activation, rather than ssRNA.

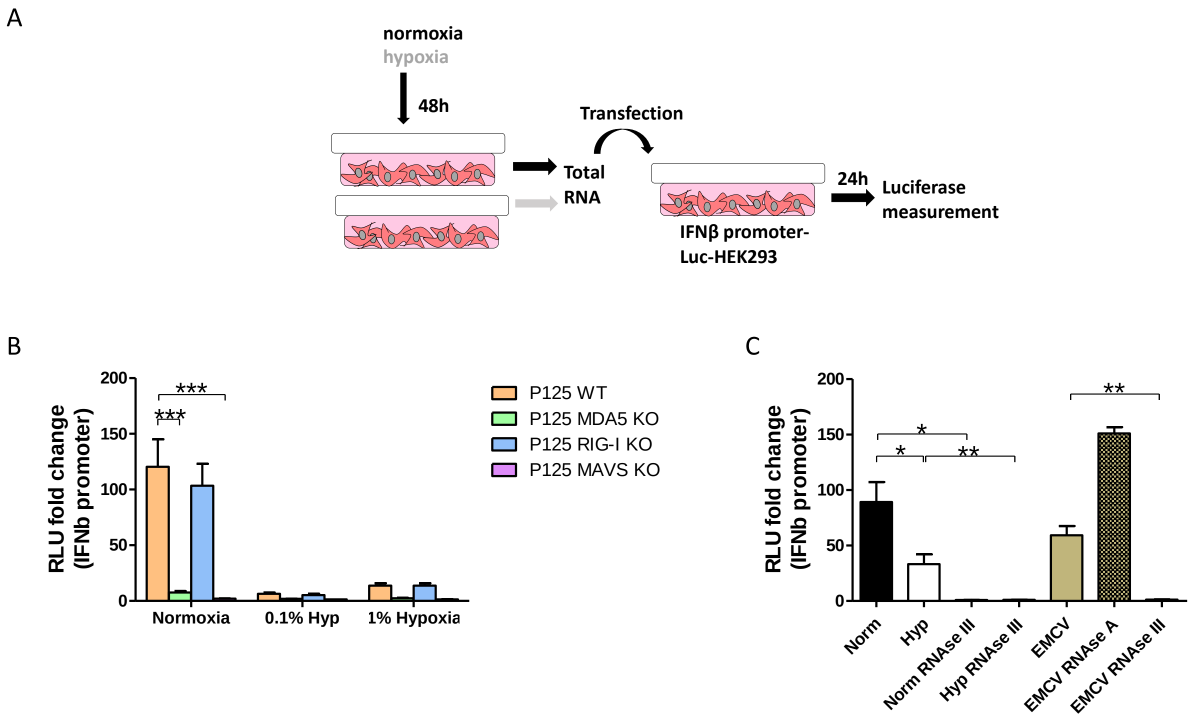

Figure 5.16. A) IFNβ promoter assay diagram. B) IFNβ promoter activation in HEK293 P125 WT and in different KO cultured in normoxia and hypoxia (0.1% and 1%) for 48h. C) IFNβ promoter activation by RNA from MCF7 cells cultured in normoxia or 0.1% hypoxia and treated with RNAses specific for different RNAs. n=3. * p<0.05, ** p<0.01, *** p<0.001.

As 0.1% hypoxia showed stronger effect on the inhibition of IFNβ promoter activity compared to 1% hypoxia, subsequent experiments were performed under 0.1% hypoxic conditions. To investigate the timeline when hypoxia triggered this effect, a time course of 4h, 8h, 16h, 24h and 48h was performed in MCF7 cells. As shown in Figure 5.17A, just after 4h in hypoxia IFNβ activation was suppressed by 45%, and this was maintained until 48h. To further study the ability of cells to recover from the hypoxic stress, a time course of reoxygenation after hypoxia was performed. For this, MCF7 cells were cultured in hypoxia for 48h and afterwards in normoxia for 15 min, 30 min, 1h, 2h, 4h, 8h, 16h and 24h. Reoxygenation caused a gradual recovery of the IFNβ promoter stimulation, from the initial 60% of suppression to reaching almost normoxic basal levels at 24h (Figure 5.17B).

A panel of breast cancer cell lines with different receptor status were used to rule out a cell line dependent effect of hypoxia in MCF7 cells. In all tested cell lines, hypoxic RNA caused an average of 2-fold reduction in IFNβ promoter stimulation (Figure 5.17C), suggesting a general effect of hypoxia.

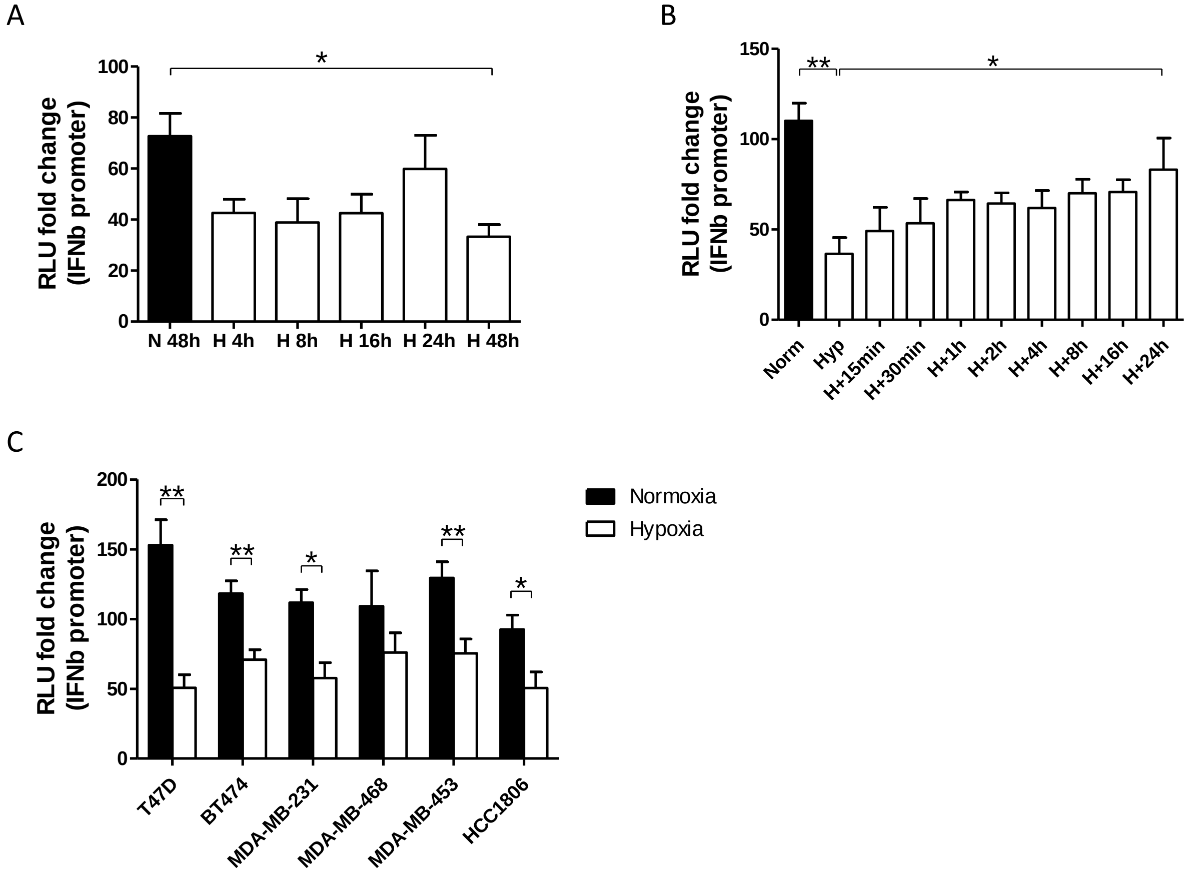

Figure 5.17. A) IFNβ promoter activation by RNA from MCF7 cells cultured in normoxia (N) for 48h or 0.1% hypoxia (H) for 4h, 8h, 16h, 24h or 48h. B) IFNβ promoter stimulation by RNA from MCF7 cells cultured in normoxia or 0.1% hypoxia for 48h plus reoxygenation up to 24h. C) Induction of IFNβ promoter by RNA from a panel of breast cancer cell lines cultured in normoxia or 0.1% hypoxia for 48h. n=3. * $p<0.05$, ** $p<0.01$, *** $p<0.001$.

As it was previously observed that the down-regulation of the type I IFN pathway was independent of HIF1α and HIF2α, to further check HIF-independency in the hypoxic inhibition of IFNβ promoter activation, RNA extracted from 786-0 WT and 786-0 KO, and RCC4 WT and RCC4 VHL cells seeded in normoxia or hypoxia was tested. Hypoxic RNA triggered 50-85% lower IFNβ promoter activation in both cell lines and all tested genotypes (Figure 5.18), confirming the HIF-independent effect. However, 786-0 KO cells had 2-fold higher IFNβ promoter stimulation under normoxia compared to parental 786-0 WT cells ($p<0.01$), suggesting a possible effect of HIF2α in suppressing IFNβ induction, although minimal compared to the effect of hypoxia ($p<0.001$).

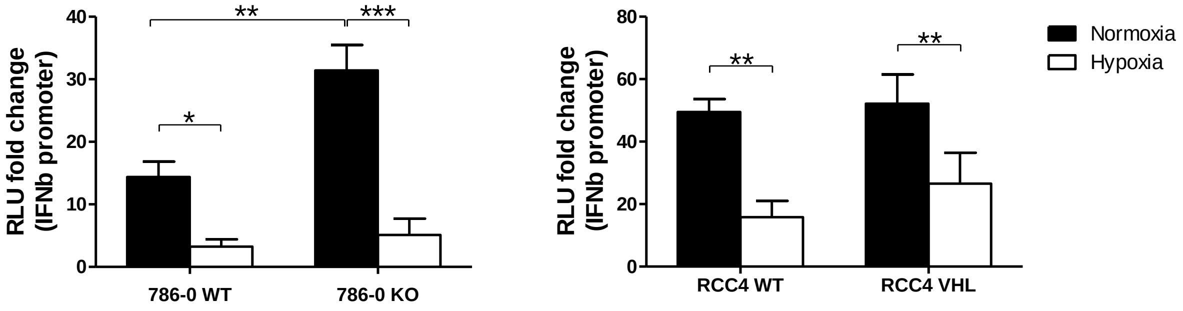

Figure 5.18. IFNβ promoter activation by RNA from ccRCC cell lines (786-0 and RCC4) cultured in normoxia and 0.1% hypoxia for 48h. n=3. * p<0.05, ** p<0.01, *** p<0.001.

To test if this effect was also present in non-tumour cells, endothelial cells (HUVEC) and fibroblasts were studied as well. As observed with tumour cells, hypoxic RNA significantly reduced the activation of IFNβ promoter, as it suppressed the activation by 80%. (Figure 5.19).

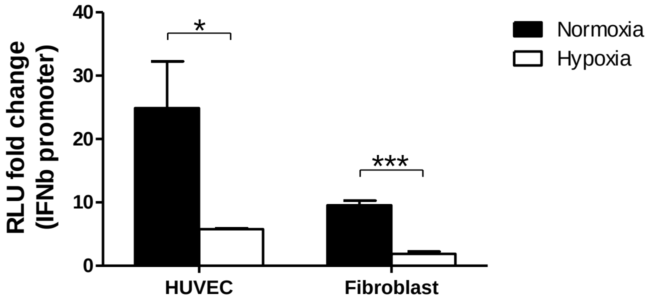

Figure 5.19. Ability of normoxic and hypoxic RNA from non-tumour cells to induce IFNβ promoter. n=3. * p<0.05, ** p<0.01, *** p<0.001.

5.4.6. Imaging of dsRNA levels under hypoxia

IFNβ promoter assay showed that hypoxic dsRNA was not able to stimulate IFNβ promoter to the same levels as normoxic dsRNA, suggesting lower presence of dsRNA species in hypoxia. Therefore, to confirm this down-regulation of dsRNA levels in hypoxia, fluorescence microscopy was performed using the J2 antibody, which is widely used to specifically detect dsRNA [699]. As depicted in Figure 5.20A, MCF7 cells showed a substantial variability of dsRNA intensity between individual cells, but in general, dsRNA staining was significantly lower in hypoxic MCF7 cells (p<0.001). This down-regulation was time-dependent (Figure 5.20B), and significant after 16h in hypoxia (p<0.001), fitting previously observed expression data for type I IFN genes (Figure 5.8A). To confirm HIF1α and HIF2α independency in the hypoxia-induced inhibition of the IFNβ promoter stimulation, 786-0 WT and 786-0 KO cells were analysed. Both cell lines had significantly lower dsRNA levels under hypoxia ($p<0.001$) (Figure 5.20C), but in contrast to the higher IFNβ promoter activation in normoxia, 786-0 KO cells presented less dsRNA intensity than 786-0 WT. Comparing to MCF7 cells, the variability between cells was still present, but to a lower extent.

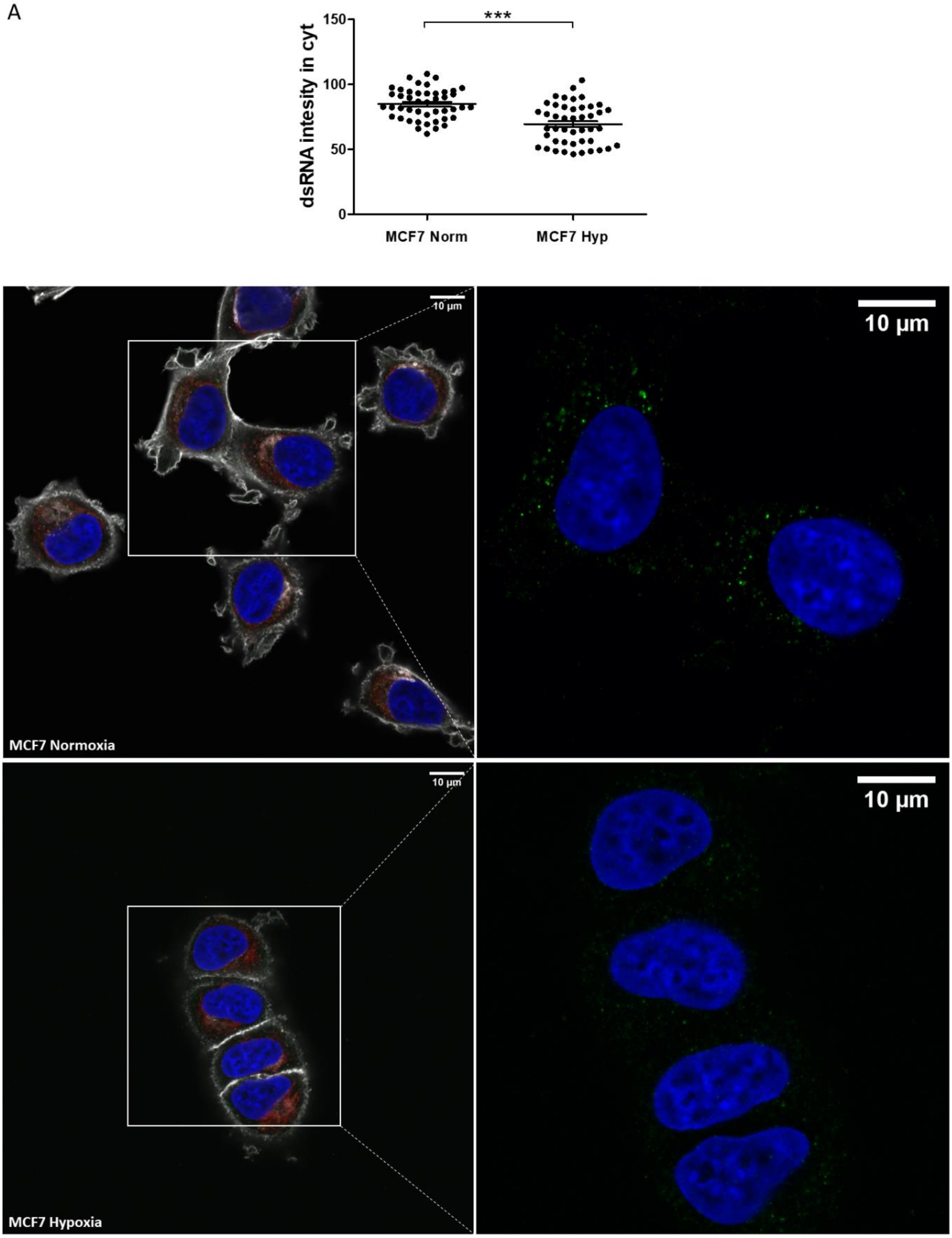
A
dsRNA intesity in cyt
150
100
50
0
***
MCF7 Norm
MCF7 Hyp
10 µm
10 µm
MCF7 Normoxia
10 µm
10 µm
MCF7 Hypoxia

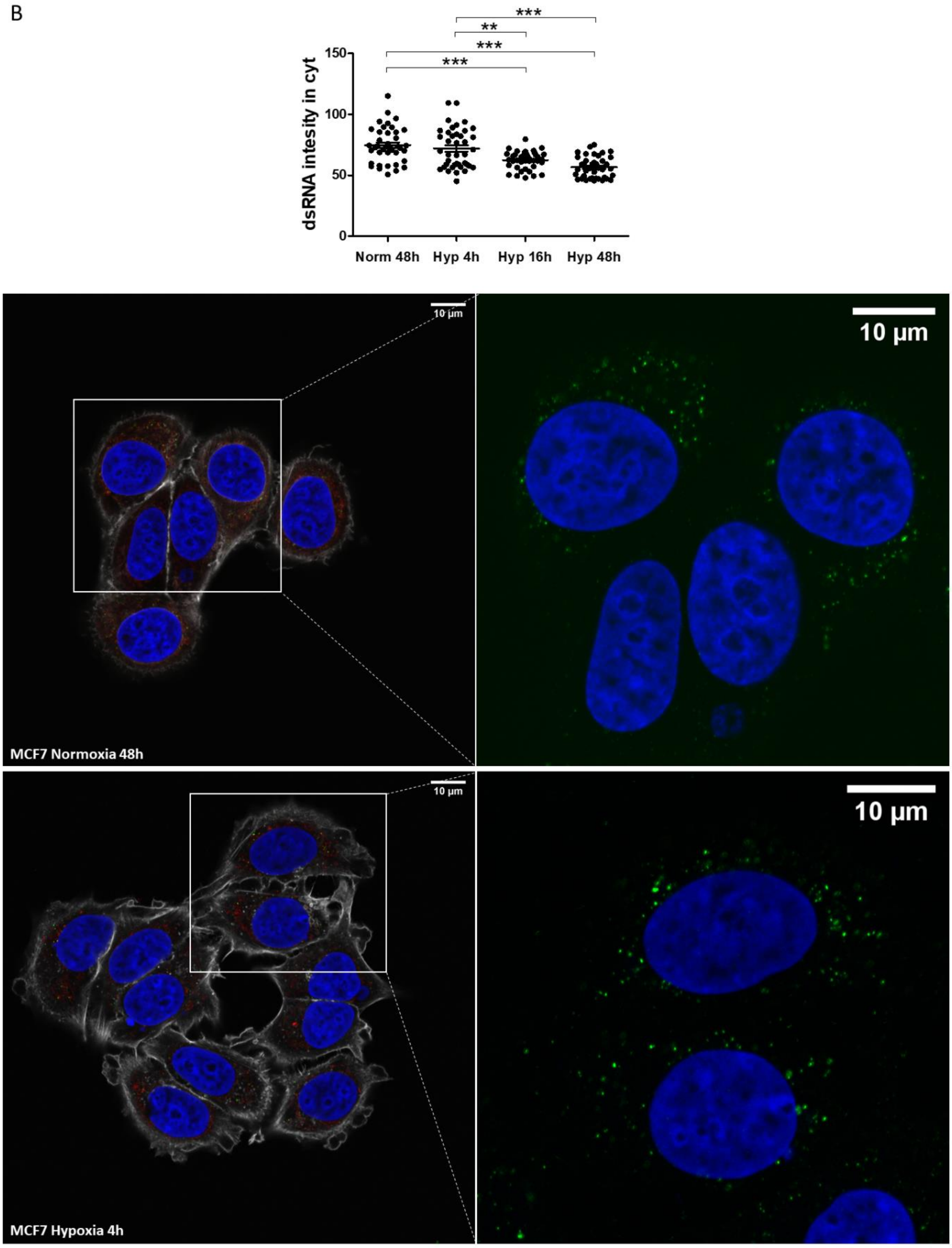
B
***
**
***
***
dsRNA intesity in cyt
150
100
50
0
Norm 48h
Hyp 4h
Hyp 16h
Hyp 48h
10 µm
10 µm
MCF7 Normoxia 48h
10 µm
10 µm
MCF7 Hypoxia 4h

(Figure continued in next page)

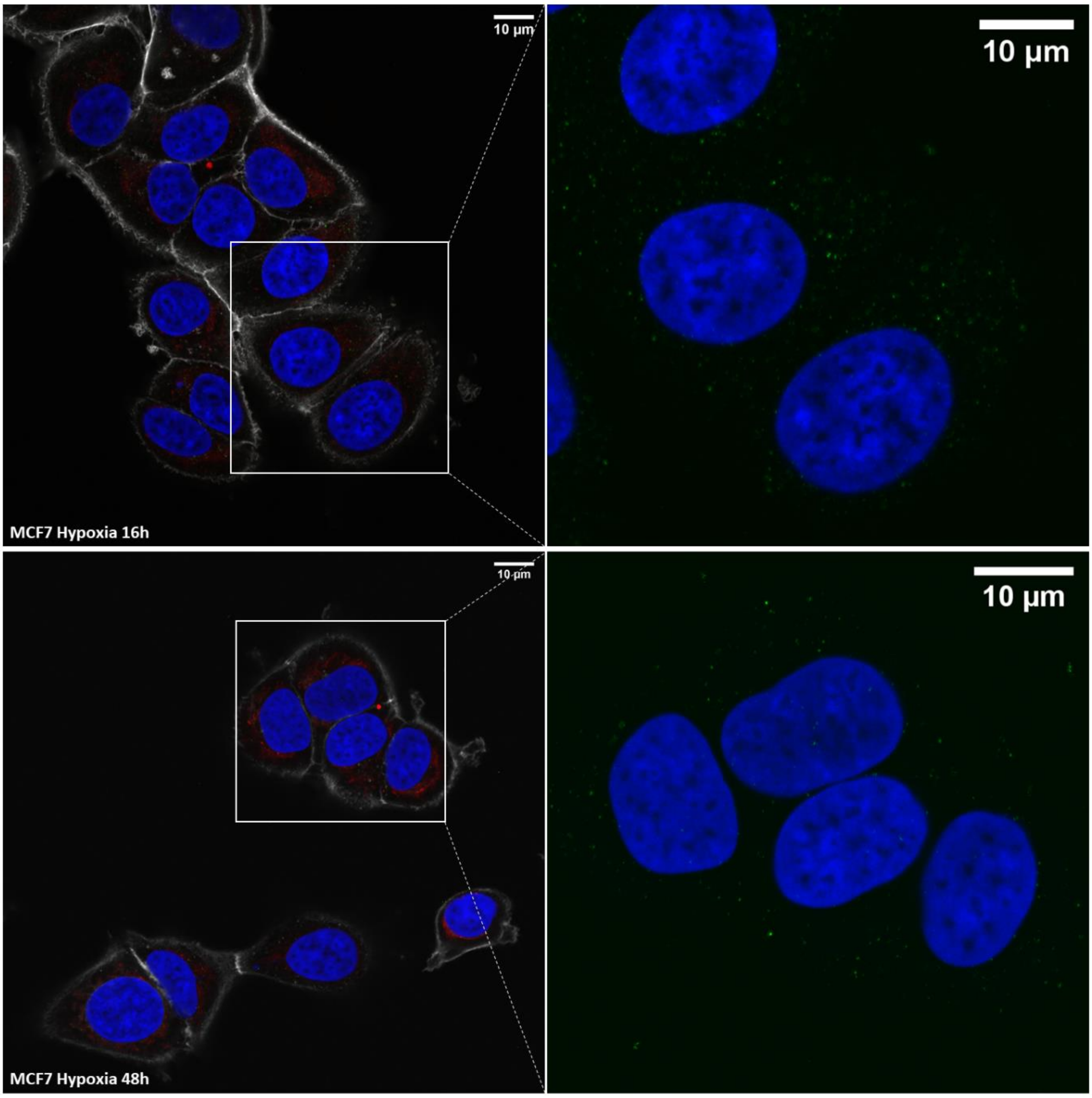
10 µm
10 µm
MCF7 Hypoxia 16h
10 µm
10 µm
MCF7 Hypoxia 48h

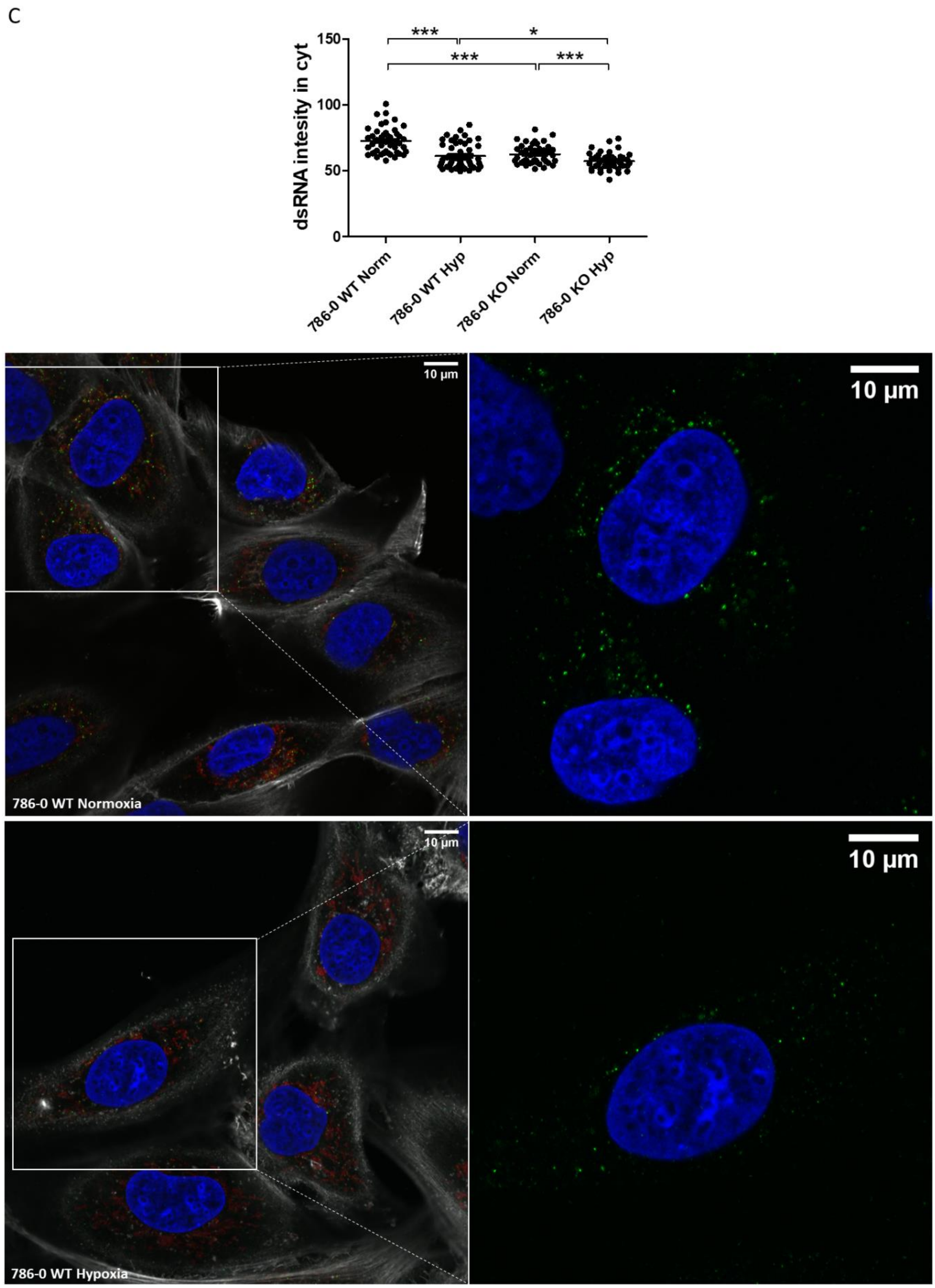
C
dsRNA intesity in cyt
150
100
50
0
***
*
***
***
786-0 WT Norm
786-0 WT Hyp
786-0 KO Norm
786-0 KO Hyp
10 µm
10 µm
786-0 WT Normoxia
10 µm
10 µm
786-0 WT Hypoxia

(Figure continued in next page)

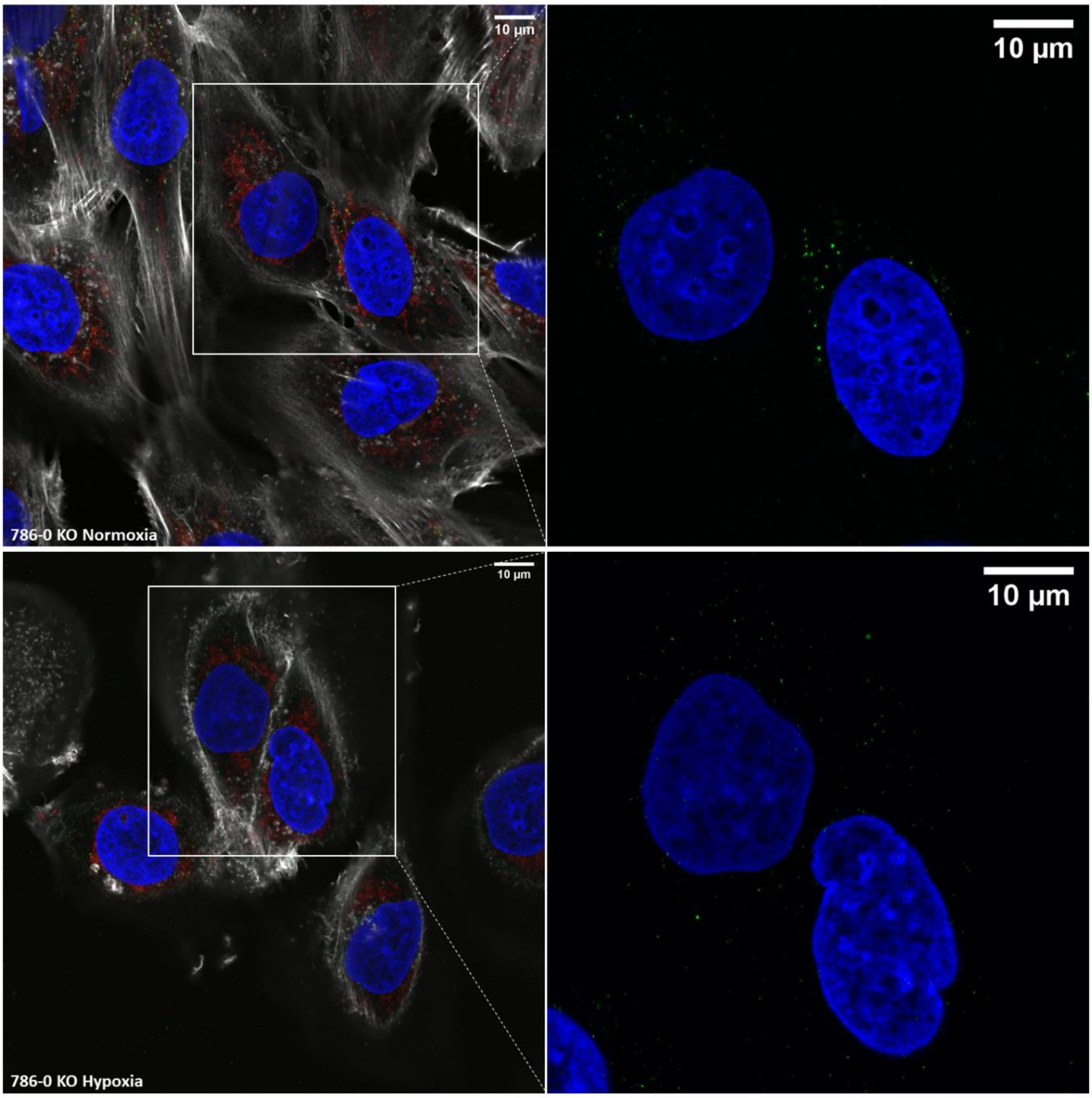

Figure 5.20. Fluorescence microscopy images of MCF7 WT cells cultured in normoxia or 0.1% hypoxia for 48h (A), MCF7 WT cells cultured in normoxia for 48h or 0.1% hypoxia for 4h, 16h and 48h (B) and of 786-0 WT and 786-0 KO cells cultured in normoxia or 0.1% hypoxia for 48h (C). Cells were stained with Hoechst 33342 for the nucleus (blue), MitoTracker™ Deep Red for the mitochondria (red), J2 for the dsRNA (green) and rhodamine phalloidin for actin filaments (white). n=3. * $p<0.05$, ** $p<0.01$, *** $p<0.001$.

5.4.7. mtDNA and effect of mutation status on dsRNA in hypoxia

It has been recently reported that 99% of endogenous dsRNA originates from mitochondrial transcription [657]. Therefore, 143B Rho zero (Rho zero) osteosarcoma cell line lacking mtDNA was tested to confirm dsRNA staining.

In 143B cells the synthesis of nucleotides is affected due to the lack of TK enzymes (as explained in 'Materials and methods'). Therefore, this cell line is usually used to generate Rho zero cells [692]. Rho zero cells were first generated by applying ethidium bromide [694], but apart from the loss of mtDNA, mutagenic effects in the nuclear genome were also recorded [700]. Since then, the nucleoside analogue ddC has been more frequently used to successfully deplete mtDNA, as dideoxycytidine triphosphate (ddCTP), the nucleotide derivate from ddC, is a potent inhibitor of the mitochondrial DNA gamma polymerase, thereby blocking mtDNA synthesis [701] without generating any side effects [702].

A

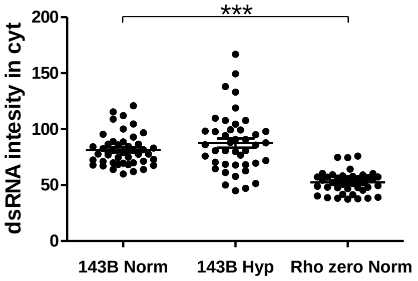

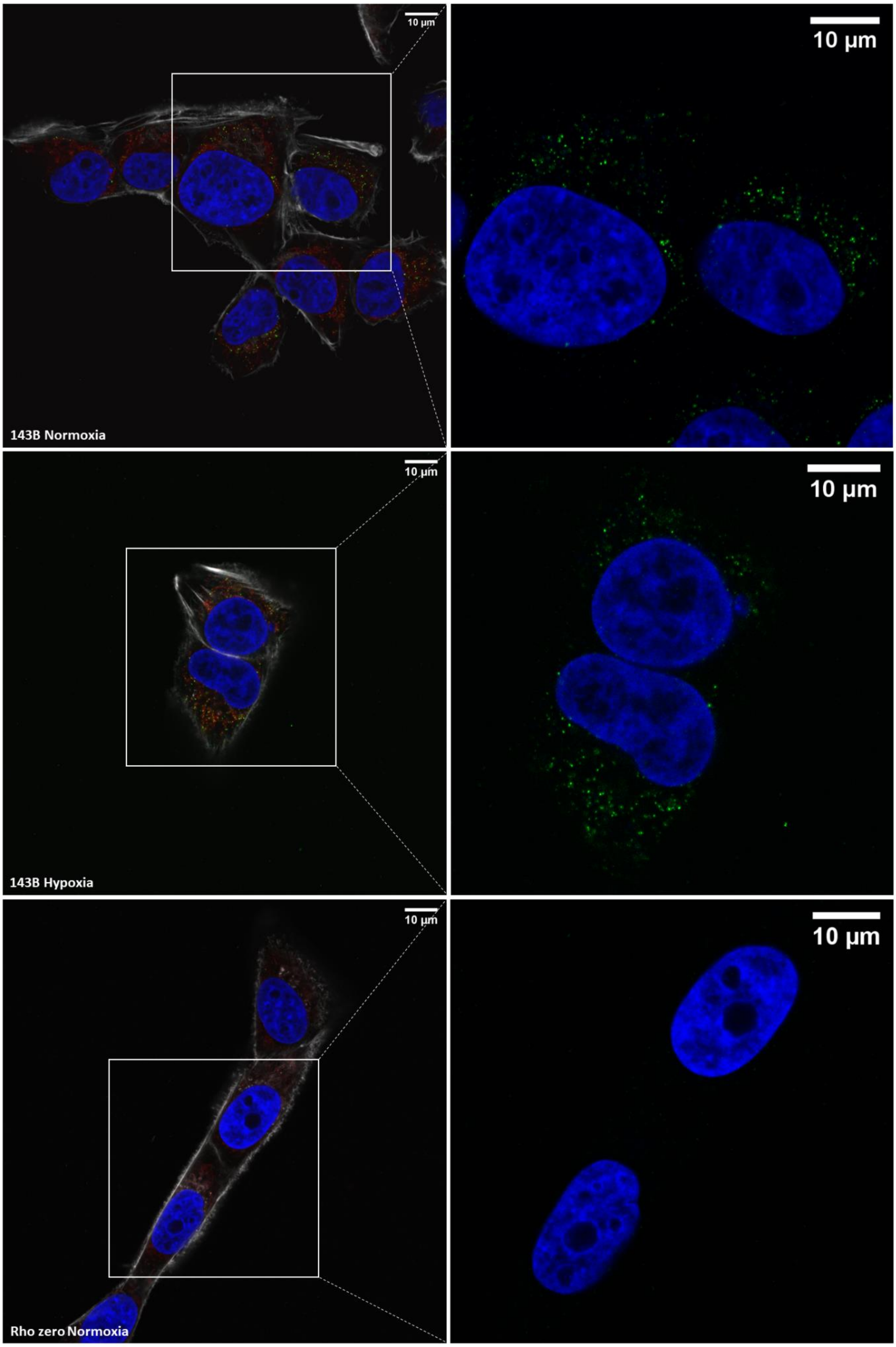
10 µm
10 µm
143B Normoxia
10 µm
10 µm
143B Hypoxia
10 µm
10 µm
Rho zero Normoxia

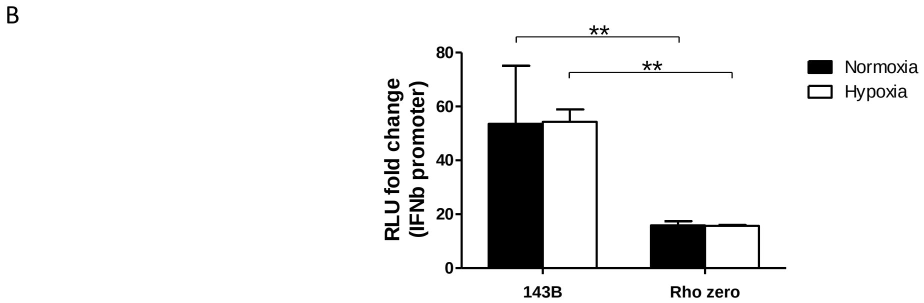

Figure 5.21. A) Fluorescence microscopy images of 143B parental and Rho zero cell lines cultured in normoxia and in 0.1% hypoxia for 48h. Cells were stained with Hoechst 33342 for the nucleus (blue), MitoTracker™ Deep Red for the mitochondria (red), J2 for the dsRNA (green) and rhodamine phalloidin for actin filaments (white). n=3. B) IFNβ promoter assay of 143B parental and Rho zero cell lines cultured in normoxia and in 0.1% hypoxia for 48h. n=3. * $p<0.05$, ** $p<0.01$, *** $p<0.001$.

Significantly lower dsRNA staining was detected in the mtDNA depleted Rho zero cell line than in the parental 143B ($p<0.001$) (Figure 5.21A), as well as 70% less luciferase activation ($p<0.01$) (Figure 5.21B). This strongly reinforces the idea that mitochondrial dsRNA (mtdsRNA) is responsible for the IFNβ promoter activation and that the inhibition achieved in hypoxia is due to lower dsRNA levels. There was no difference between normoxia and hypoxia in the parental 143B cell line, either in the dsRNA staining (Figure 5.21A) or in the IFNβ promoter assay (Figure 5.21B). This was the only cell line among the all tested in which hypoxia did not down-regulate the type I IFN pathway.

To explore if different degrees of mtDNA mutation could affect the amount of dsRNA and consequently the IFNβ promoter stimulation, U2OS mTUNE osteosarcoma cell line was used. mtDNA mutation leads to dysfunctional mitochondria and impaired metabolism in this organelle. One of the main issues when studying metabolic dysfunction is the difficulty assessing the direct consequences of dysregulated mitochondrial metabolism and the indirect effects caused by mitochondrial defects. To overcome this issue, specific elimination of mtDNA using mitochondrially targeted zinc-finger nucleases (mtZFNs) has recently been used to generate isogenic cell lines [695]. Using this editing technology, U2OS TUNE osteosarcoma cells harbouring different degrees (7%, 45% or 80%) of heteroplasmy for the mtDNA mutation m8993T>G were created (U2OS mTUNE M7, M45 and M80) [695]. This mutation results in a defect in the ATP6 subunit of the ATP synthase and is responsible for several genetic diseases. Using these cell lines, it is possible to asses if mtDNA mutation or impaired mitochondrial metabolism has an effect on mtdsRNA release under hypoxia, or if hypoxia down-regulation of dsRNA levels is independent of this.

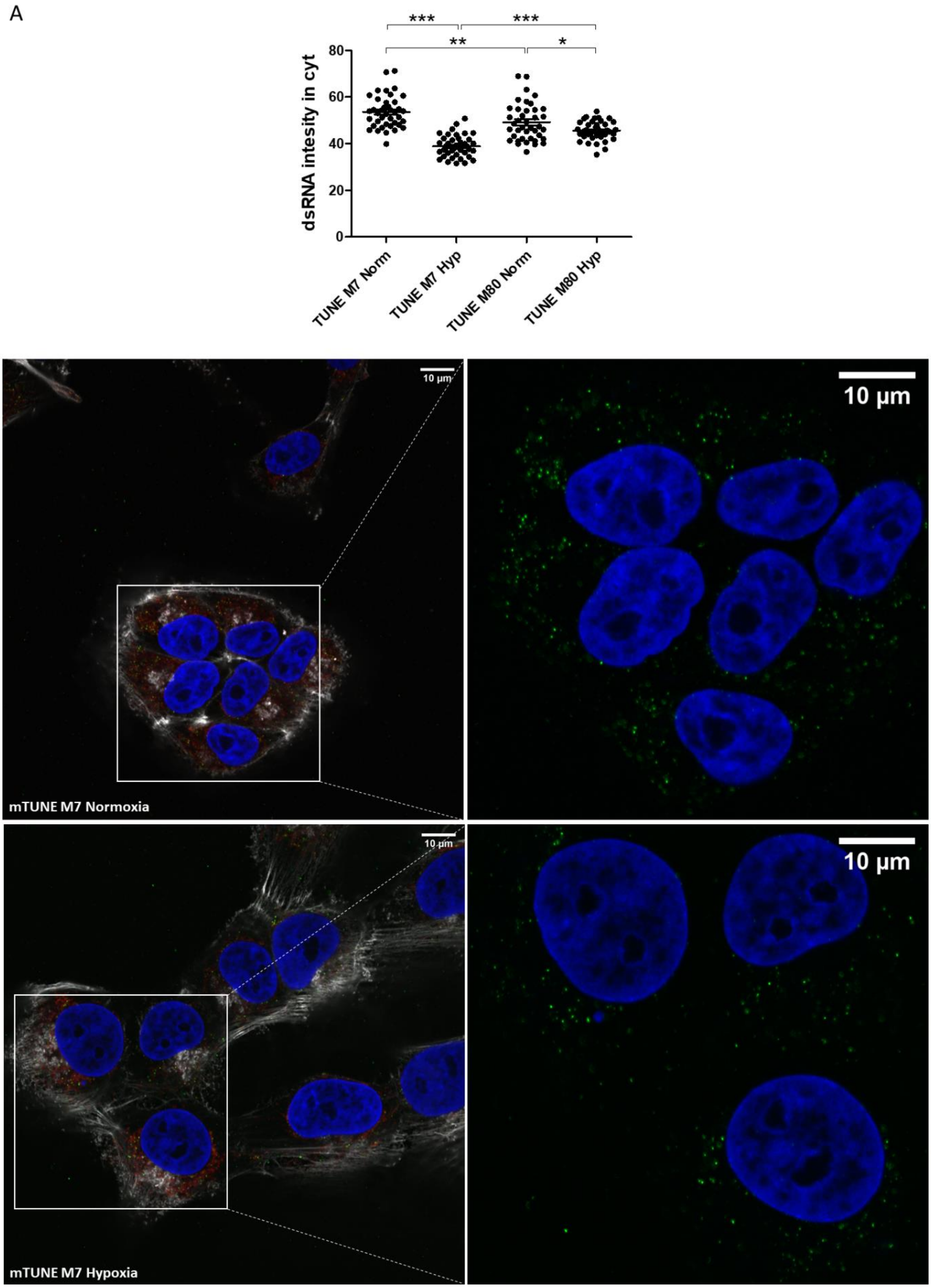

(Figure continued in next page)

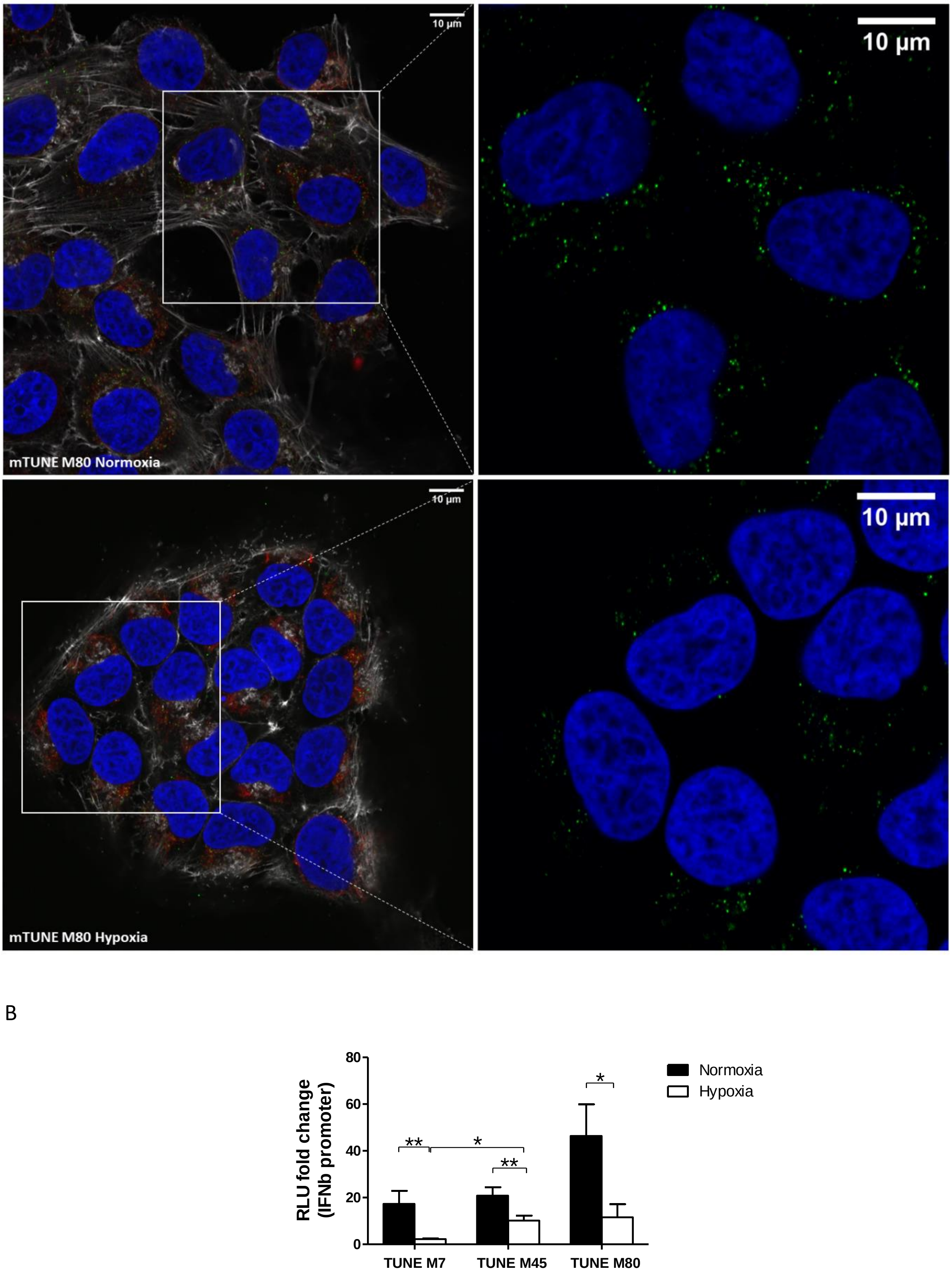
10 µm
mTUNE M80 Normoxia
10 µm
10 µm
mTUNE M80 Hypoxia
10 µm
B
RLU fold change (IFNb promoter)
80
60
40
20
0
TUNE M7
TUNE M45
TUNE M80
**
*
**
*
Normoxia
Hypoxia

Figure 5.22. A) Fluorescence microscopy images of U2OS mTUNE cell lines cultured in normoxia and in 0.1% hypoxia for 48h. Cells were stained with Hoechst 33342 for the nucleus (blue), MitoTracker™ Deep Red for the mitochondria (red), J2 for the dsRNA (green) and rhodamine phalloidin for actin filaments (white). n=3. B) IFNβ promoter assay of U2OS mTUNE cell lines cultured in normoxia and in 0.1% hypoxia for 48h. n=3. * $p<0.05$, ** $p<0.01$, *** $p<0.001$.

Hypoxia decreased dsRNA levels in all mTUNE cell lines independently of the mutation level (TUNE M7 $p<0.001$, TUNE M80 $p<0.05$) (Figure 5.22A) and significantly suppressed IFNβ promoter activation in 50-90% (Figure 5.22B). Moreover, the basal IFNβ promoter stimulation levels were similar in mTUNE M7 and mTUNE M45 cell lines (Figure 5.22B), as were their metabolic profiles [695], but 2-fold higher in mTUNE M80. However, dsRNA staining was lower in mTUNE M80 in the cytoplasm ($p<0.01$). Nevertheless, hypoxia exerted considerably greater effect, thus showing that mtdsRNA down-regulation in hypoxia is independent of mtDNA degree of mutation.

As Dhir *et al.* [657] showed, when enzymes involved in mtdsRNA degradation are inhibited, such as polyribonucleotide nucleotidyltransferase 1 (PNPT1) and RNA helicase SUV3, mtdsRNA accumulates in the cytoplasm and triggers an IFN response. Therefore, the expression of these two enzymes was tested in 786-0 and mTUNE cells cultured in normoxia and different levels of hypoxia (Figure 5.23). Neither PNPT1 nor SUV3 expression was higher in hypoxia in any of the tested cell lines, suggesting that lower dsRNA in hypoxia is not due to an increase in the turnover machinery.

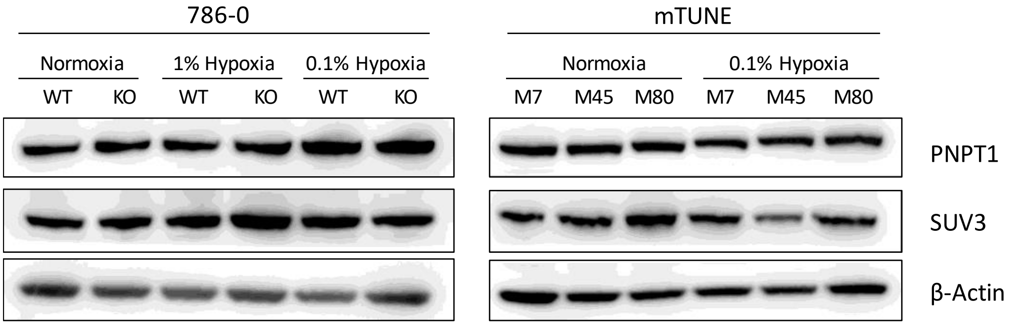

Figure 5.23. 786-0 WT, 786-0 KO and U2OS mTUNE cells were cultured in normoxia or hypoxia for 48h and protein levels of PNPT1 and SUV3 were analysed. n=3.

5.4.8. Hypoxia negatively regulates mtDNA transcription

As the enzymes involved in the mtdsRNA degradation were not affected by hypoxia, lower mtDNA transcription under hypoxia could explain the lower presence of mtdsRNA. To test this hypothesis, the expression of genes encoded by the nuclear genome whose final product acts in the mitochondria (*SHMT2*, *POLRMT*, *TFAM* and *TFB1M*) and mitochondrial encoded genes as positive controls (*12S*, *ND3*, *ATP6* and *CYTB*) was analysed. Among the nuclear genes, key genes involved in mitochondrial transcription were chosen such as the mitochondrial serine hydroxymethyltransferase (*SHMT2*), involved in the first step in mitochondrial one-carbon metabolism cleaving serine to glycine, mitochondrial RNA polymerase (*POLRMT*) which catalyses mtDNA transcription, *TFAM* which associates and stabilizes mtDNA and regulates mtDNA transcription as it is required for efficient promoter recognition by POLRMT, and mitochondrial transcription factor B1 (*TFB1M*) which interacts with POLRMT and TFAM during mtDNA transcription. Regarding the selected mitochondrial encoded genes, expression of the rRNA 12S, the ND3 subunit of the NADH dehydrogenase (complex I), the ATP6 subunit of the ATP synthase and cytochrome B (*CYTB*) were studied.

Both nuclear and mitochondrial encoded genes were down-regulated in MCF7 cells cultured in 0.1% hypoxia (Figure 5.24). Most of the tested genes showed 20-50% lower expression after only 4h in hypoxia (*SHMT2*, *POLRMT*, *TFAM*, *ND3*, *ATP6* and *CYTB*), but it was not significant for all until 16h of hypoxia exposure, when in achieved more than 50% suppression, in accordance with previous results where 16h in hypoxia was the decisive time point to down-regulate the type I IFN pathway (Figure 5.8). These results show that hypoxia decreases transcription of both nuclear encoded genes involved in mitochondrial transcription and mitochondrial encoded genes, supporting the hypothesis that mtdsRNA resulting from mitochondrial transcription could be lower in hypoxia.

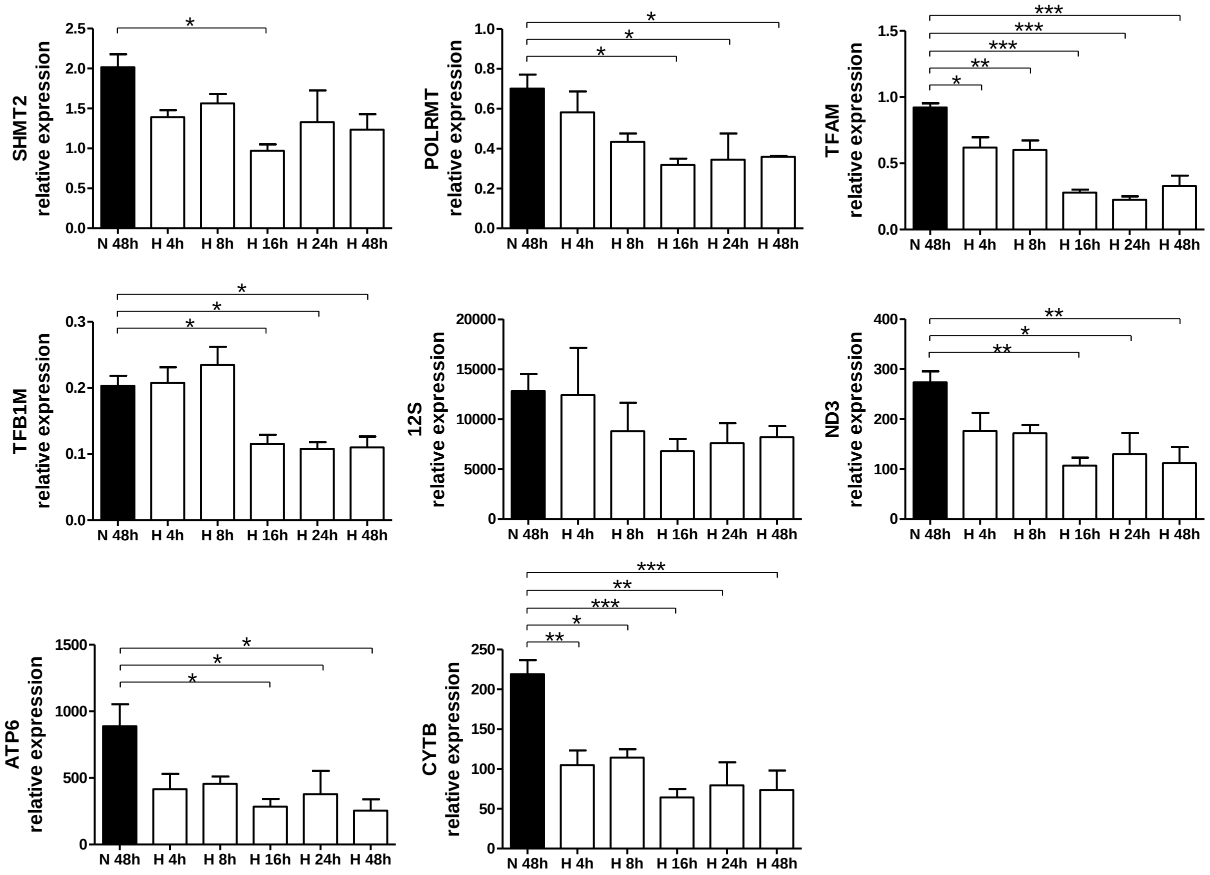

Figure 5.24. mRNA expression of nuclear and mitochondrial encoded genes in MCF7 cells cultured in normoxia (N) for 48h or 0.1% hypoxia (H) for 4h, 8h, 16h, 24h and 48h. n=3. * p<0.05, ** p<0.01, *** p<0.001.

To determine the role of HIF2α in the regulation of these genes, 786-0 WT and 786-0 KO cells were studied. Hypoxia exposure did not change nuclear or mitochondrial encoded gene expression in 786-0 WT cells, except for the 2-fold increase seen in *POLRMT* and *TFB1M*. In regard to 786-0 KO cells, hypoxia decreased in more than 50% mitochondrial encoded gene expression, but did not generate any differences in nuclear encoded genes (Figure 5.25). Moreover, as the expression of *12S*, *ND3* and *ATP6* was 50% higher in hypoxic 786-0 WT than in 786-0 KO cells, HIF2α could be involved in the mtRNA transcription in hypoxia.

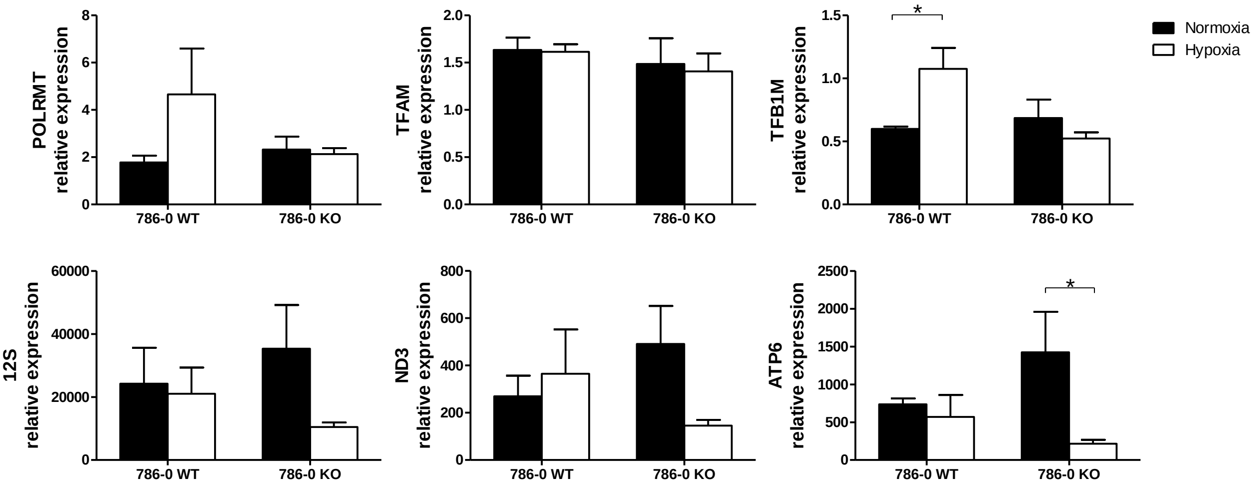

Figure 5.25. Relative expression of *POLRMT*, *TFAM*, *TFB1M*, *12S*, *ND3* and *ATP6* in 786-0 WT and 786-0 KO cells cultured in normoxia or 0.1% hypoxia for 48h. n=3. * $p<0.05$, ** $p<0.01$, *** $p<0.001$.

It was described that HIF2α could enhance c-MYC transcriptional activity [92] and that c-MYC increased the expression of POLRMT, thereby increasing mtDNA transcription levels [703]. These studies suggested that in 786-0 KO cells, hypoxia down-regulated mitochondrial gene expression was due to the fact that the HIF2α/c-MYC/POLRMT axis is not functioning. Expression of c-MYC in 786-0 cells showed that c-MYC was down-regulated in 786-0 KO cells in hypoxia at mRNA level comparing to 786-0 WT (Figure 5.26A), even though the effect was not significant, whereas no differences were seen at protein level (Figure 5.26B). This shows that total c-MYC protein expression is not changed in hypoxia or between cell lines, however, the amount of c-MYC in the nucleus or in the cytoplasm was not evaluated in these experiments. Therefore, the possibility of lower mitochondrial transcription in 786-0 KO hypoxic cells could still be due to lower c-MYC transcriptional activity.

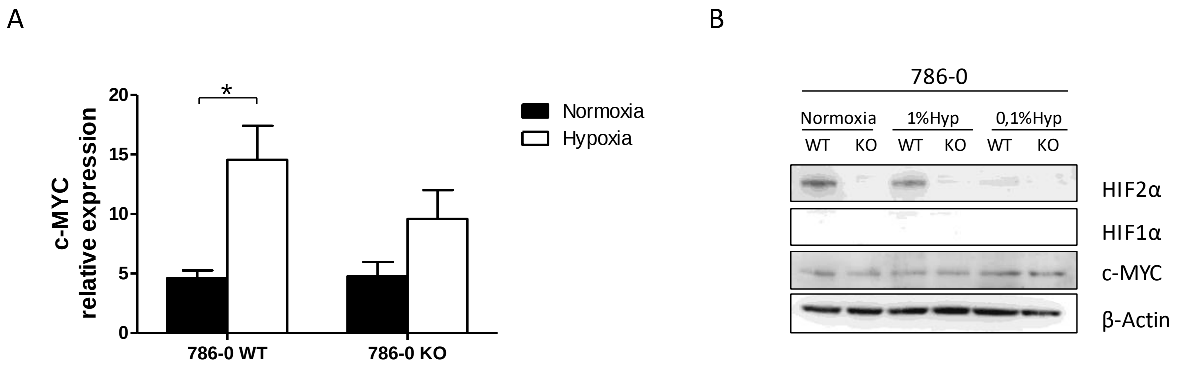

Figure 5.26. A) *c-MYC* mRNA expression in 786-0 WT and 786-0 KO cells cultured in normoxia or 0.1% hypoxia for 48h. n=3. * $p<0.05$, ** $p<0.01$, *** $p<0.001$. B) c-MYC, HIF1α and HIF2α protein expression in 786-0 WT and 786-0 KO cells cultured in normoxia or hypoxia (1% or 0.1%) for 48h. n=3.

The expression of *POLRMT*, *TFAM* and *TFB1M* and some mitochondrial encoded genes was also determined in 143B and Rho zero cells (Figure 5.27A) and in U2OS mTUNE cells (Figure 5.27B). 143B cell line did not present differences in the expression of any of the analysed genes between normoxia and hypoxia, further showing that this cell line is quite resistant to hypoxic conditions (Figure 5.27A). On the other hand, as in the parental cell line, Rho zero cells presented similar levels of nuclear encoded genes between normoxia and hypoxia. But as expected, *12S*, *ND3* and *ATP6* mitochondrial genes were absent in Rho zero cells (Figure 5.27A).

In mTUNE M7 cells the expression of *POLRMT* and *TFAM* was inhibited in hypoxia ($p<0.001$), as well as the mitochondrial genes *ND3* and *ATP6* (Figure 5.27B), ranging from 20-80% suppression, suggesting that in this cell line the presence of lower dsRNA levels in hypoxia could be due to less mtDNA transcription. On the other hand, mTUNE M80 cells showed 2-fold less *POLRMT*, *TFAM* and *TFB1M* expression than mTUNE M7 in normoxia, which involves lower mitochondrial gene expression (Figure 5.27B). However, hypoxia did not affect the expression of nuclear encoded genes involved in mtDNA transcription or mitochondrial encoded genes in mTUNE M80 cells ($p>0.05$), except for *TFAM* ($p<0.01$). These differences between isogenic cell lines suggest that there is a more complex regulation of mtdsRNA, arising from the degree of mutation in *ATP6*, although it still decreases in both cell lines in hypoxia.

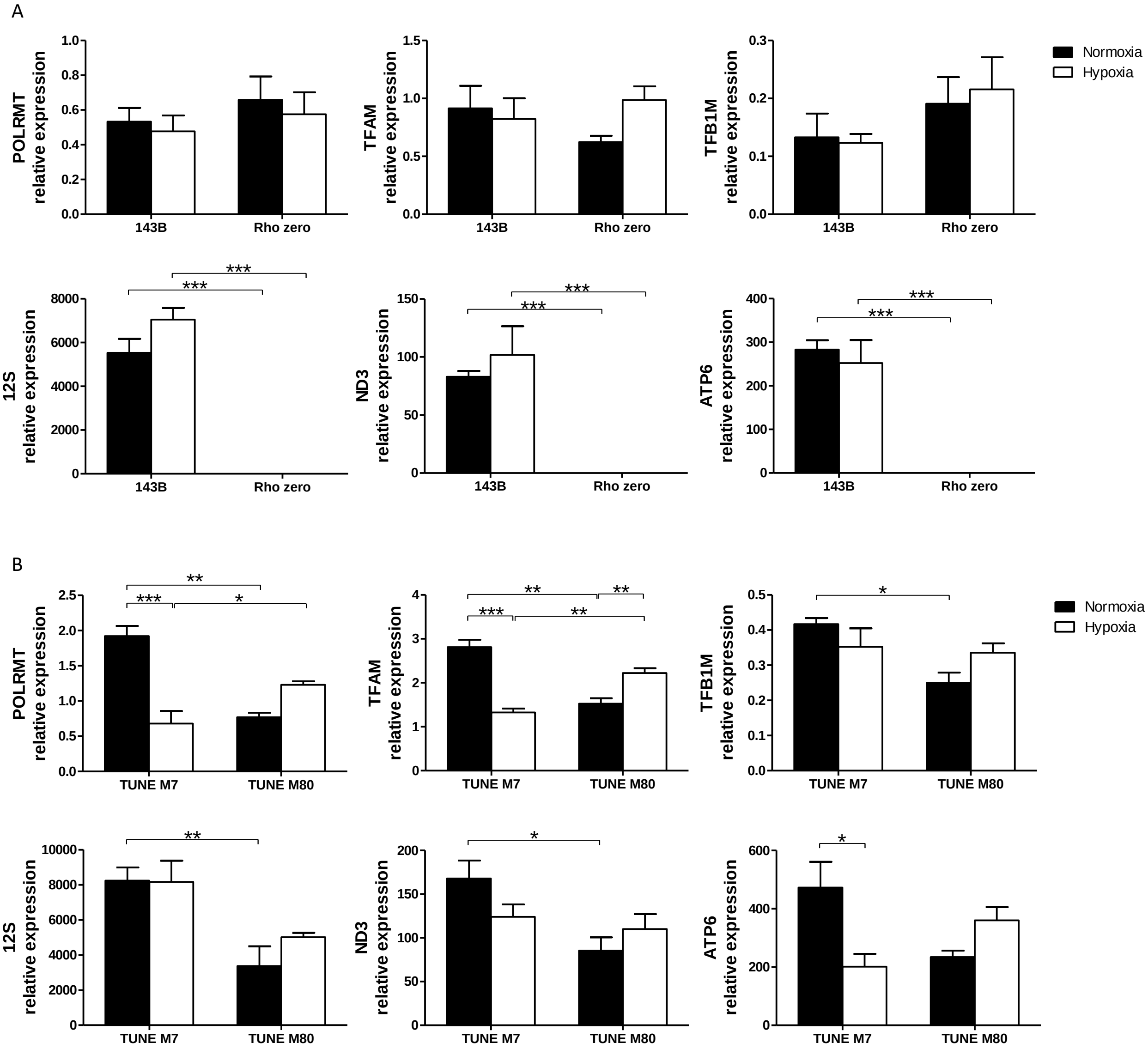

Figure 5.27. Relative expression of *POLRMT*, *TFAM*, *TFB1M*, *12S*, *ND3* and *ATP6* in 143B and Rho zero cells (A) and in U2OS mTUNE M7 and M80 cells (B) cultured in normoxia or 0.1% hypoxia for 48h. n=3. * p<0.05, ** p<0.01, *** p<0.001.

5.4.9. Hypoxia negatively regulates mitochondrial ribosomal protein expression

In 2015, a proteomics study revealed that in hypoxia, various mitochondrial ribosomal proteins (MRPs) involved in mtRNA translation were down-regulated [704]. Therefore, the expression of mRNA coding for some members of the MRP family was analysed. As shown in Figure 5.28A, in MCF7 cells MRP expression levels were 20-50% decreased in hypoxia, being significant at 16h of hypoxia (p<0.01). Hypoxia also down-regulated MRP expression in 786-0 WT and 786-0 KO cells by 10-50% (Figure 5.28B), pointing again to a HIF1α and HIF2α independent mechanism.

Altogether, these data suggest that hypoxia inhibits mtDNA transcription and therefore mtdsRNA production leading to type I IFN pathway activation. Furthermore, inhibition of mtRNA translation may also prevent cells from transcribing mtDNA.

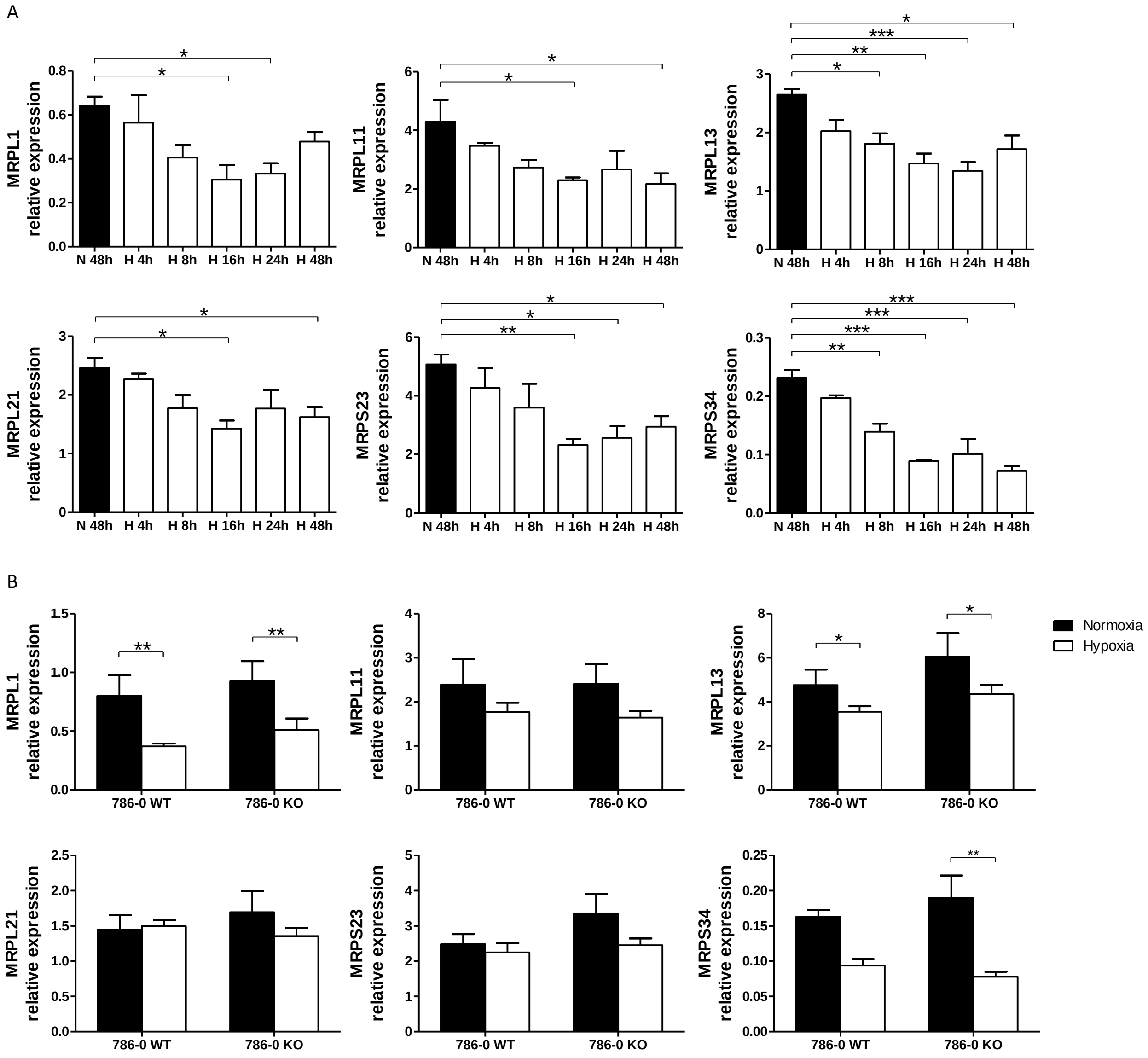

Figure 5.28. A) MRP relative expression in MCF7 cells cultured in normoxia (N) for 48h or 0.1% hypoxia (H) for 4h, 8h, 16h, 24h and 48h. n=3. B) MRP relative expression in 786-0 WT and 786-0 KO cells cultured in normoxia or 0.1% hypoxia for 48h. n=5. * $p<0.05$, ** $p<0.01$, *** $p<0.001$.

5.4.10. mtRNA is responsible for IFNβ promoter induction

Despite the differences between cell lines, it is clear that hypoxia down-regulates both the type I IFN pathway (expression and IFNβ promoter activation) and mtdsRNA levels. To confirm that mtdsRNA induced the type I IFN pathway, MCF7 cells were cultured in normoxia or 0.1% hypoxia for 48h, and their intact mitochondria were isolated. Firstly, effective mitochondria isolation was confirmed by analysing the expression of known nuclear and mitochondrial encoded genes in both fractions (Figure 5.29A). Nuclear gene expression was detected both in the cytosolic and mitochondrial fractions, suggesting that the mitochondrial fraction could be slightly contaminated with mRNA from the cytoplasm. Nevertheless, the expression of mitochondrial encoded genes was significantly higher in the mitochondrial fraction (ranging from 6- to 9-fold) and present only in small amounts in the cytosolic fraction. Interestingly, hypoxia decreased mitochondrial gene expression levels in the mitochondrial fraction in 50%, whereas it down-regulated the nuclear encoded gene expression but not significantly.

To further confirm that dsRNA originated in the mitochondria was responsible for the type I IFN pathway down-regulation under hypoxia, IFNβ promoter assay was performed using mtRNA and cytosolic RNA. As shown in Figure 5.29B, IFNβ promoter was strongly activated by mtRNA, rather than cytosolic RNA ($p<0.001$). Importantly, RNA isolated from hypoxic mitochondria caused a significantly lower induction ($p<0.001$), compared to normoxic mtRNA. These results support the hypothesis that the type I IFN pathway down-regulation under hypoxia is due to lower dsRNA levels arising from the mitochondria possibly due to lower mtDNA transcription in hypoxia.

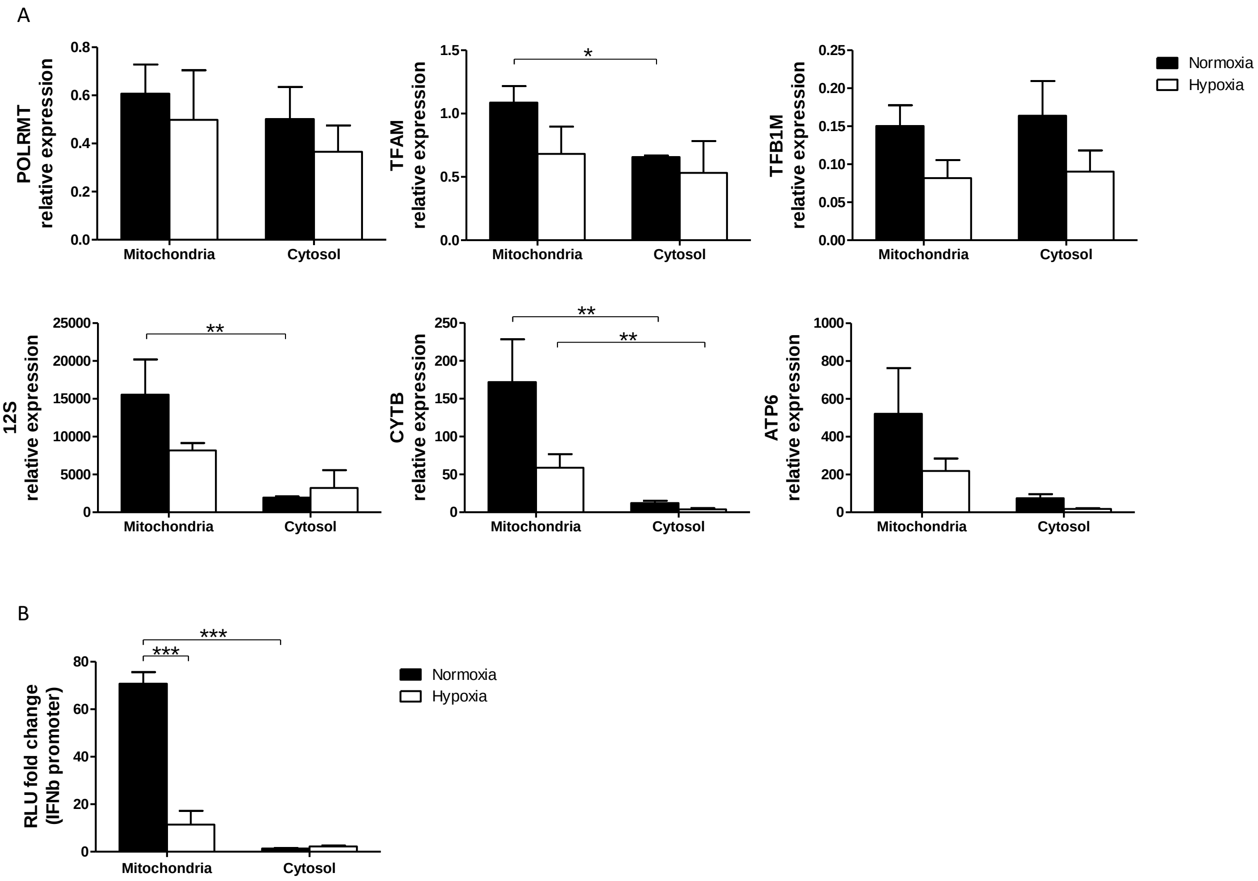

Figure 5.29. A) Relative expression of nuclear and mitochondrial encoded genes in mitochondrial and cytosolic fractions of MCF7 cells cultured in normoxia or 0.1% hypoxia for 48h. B) IFNβ promoter stimulation by mtRNA or cytosolic RNA extracted from MCF7 cells cultured in normoxia or 0.1% hypoxia for 48h. n=3. * $p<0.05$, ** $p<0.01$, *** $p<0.001$.

5.4.11. Lower mtRNA in hypoxia is not due to increase mitophagy

It is known that mitochondria are damaged in hypoxia [675] and that their morphology and membrane potential changes, rendering them non-functional [680, 681]. Consequently, cells remove those unwanted mitochondria by specialized autophagy (mitophagy). In order to check if the down-regulation of mtdsRNA in hypoxia was due to less mitochondria within the cell, mitophagy was analysed by knocking down one of the main genes involved in this process, *BNIP3*. The expression of *BNIP3* and various ISGs (*DDX58*, *MX1*, *IFIT1*, *IFIT2*, *ADAR-p150* and *ISG15*) was analysed in MCF7 cells silenced for BNIP3 (siBNIP3) and seeded in normoxia or 0.1% hypoxia for 48h. As shown in Figure 5.30A, *BNIP3* was successfully silenced in MCF7 cells, as no induction was detected in hypoxia. There were no differences in ISG expression between MCF7 cells transfected with a control siRNA (siCON) and MCF7 siBNIP3 in hypoxia (Figure 5.30B), suggesting that BNIP3 presence does not interfere in the type I IFN signalling.

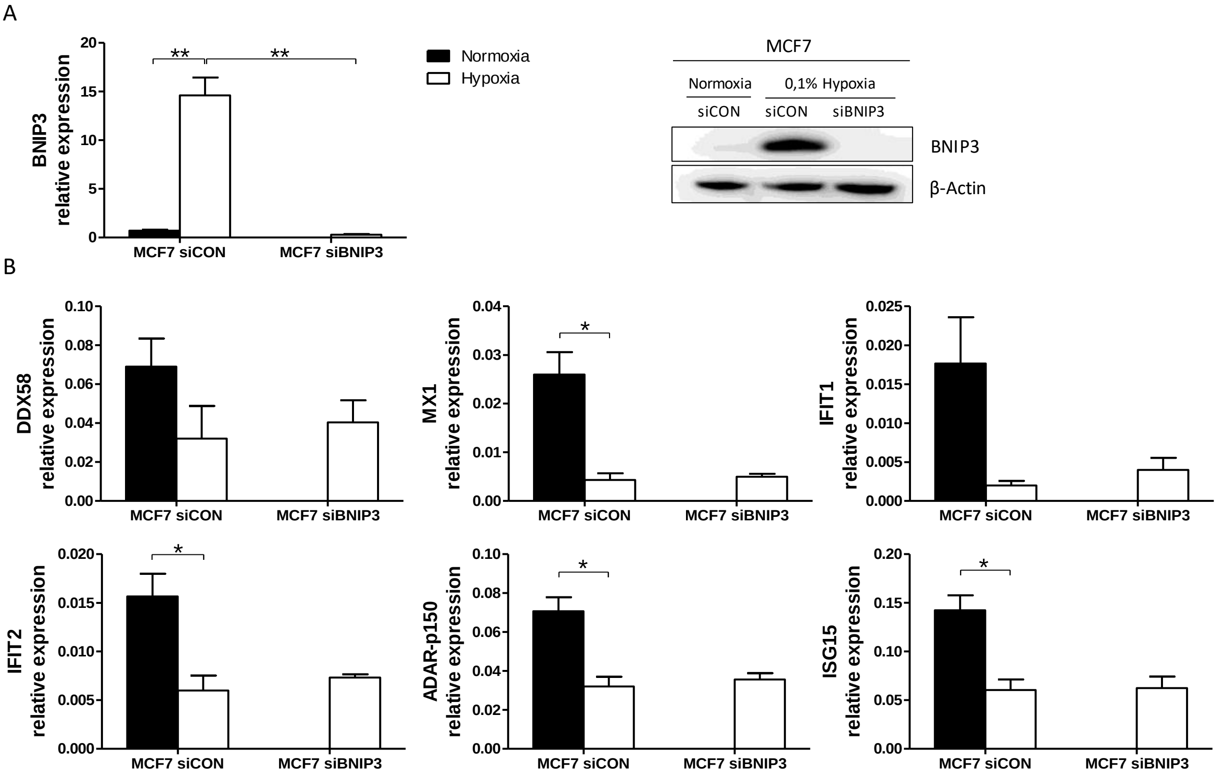

Figure 5.30. mRNA and protein expression of BNIP3 (A) and several ISGs (B) in MCF7 cells silenced with a siRNA control (siCON) or siRNA for BNIP3 (siBNIP3) and cultured in normoxia or 0.1% hypoxia for 48h. n=3. * p<0.05, ** p<0.01, *** p<0.001.

This was further confirmed by the IFNβ promoter assay, in which hypoxia-induced inhibition in the activation of the reporter was not recovered upon silencing *BNIP3* (Figure 5.31). This result strengthens the hypothesis that lower type I IFN activation in hypoxia is not due to an increase in mitophagy, which would be degrading the mtRNA.

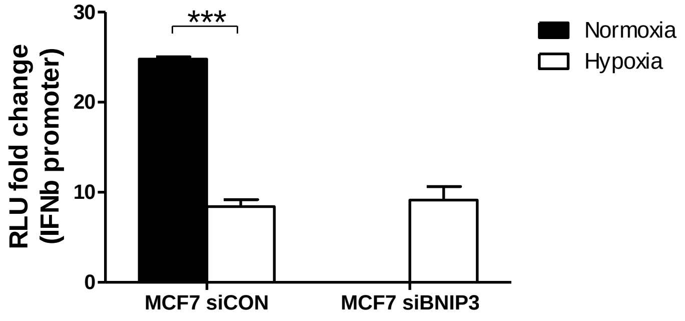

Figure 5.31. IFNβ promoter activation by RNA from MCF7 cells transfected with siCON or siBNIP3 and cultured in normoxia and 0.1% hypoxia for 48h. n=3. * p<0.05, ** p<0.01, *** p<0.001.

In order to see how hypoxia was affecting mitochondria, live cell immunofluorescence imaging was performed. MCF7 cells were cultured in normoxia and 0.1% hypoxia for 48h and 1h previous to imaging, cells were stained with a mitochondrial and a lysosomal dye, as explained in 'Immunofluorescence for mitophagy' section. Figure 5.32 shows that in hypoxia there was not mitophagy, as no colocalization of both markers was detected. As previously reported [680], these pictures clearly exhibit that mitochondria shape changes under low oxygen conditions. It was published that the metabolic stress cells undergo under hypoxia-reoxygenation resulted in the appearance of shorter mitochondria and a decrease in fusion activity [705]. Moreover, in hypoxia mitochondria took an elongated structure and they seemed to surround the nucleus (Figure 5.32). Supporting this observation, it was found that 72h exposure to 1% hypoxia induced perinuclear localization of mitochondria in HeLa and U2OS cells [706], whereas another study showed that pulmonary artery endothelial cell exposure to hypoxia resulted in the perinuclear clustering of mitochondria [707]. Moreover, hypoxia caused a time-dependent movement of mitochondria from the periphery of the cell to the nuclear region, mediated by dynein motor protein [708].

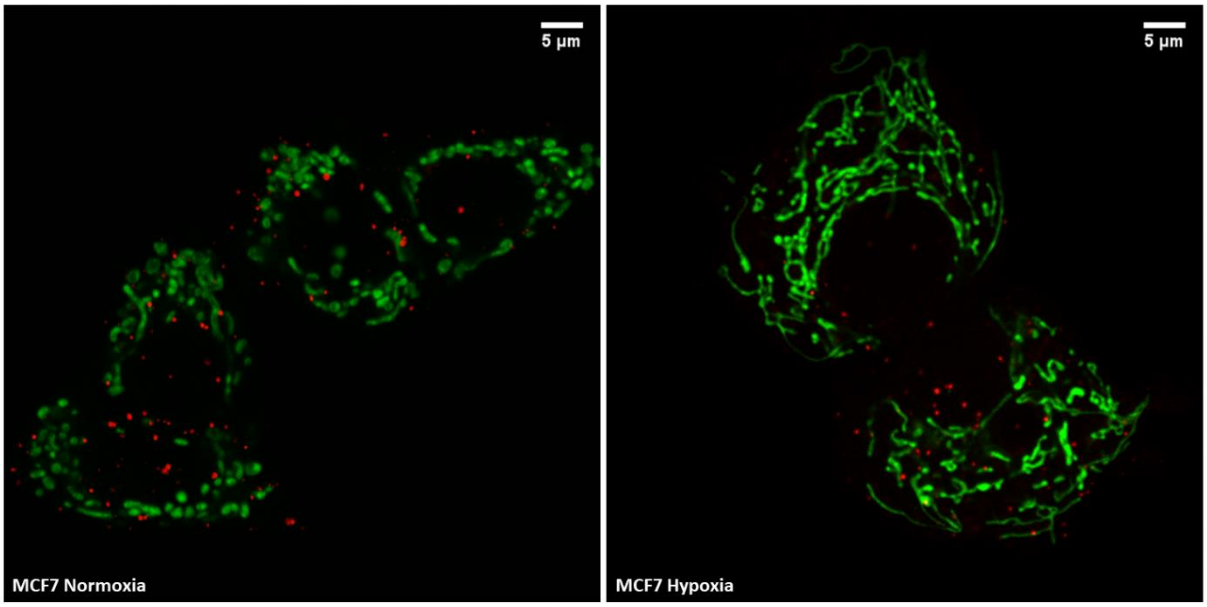

Figure 5.32. Living cell immunofluorescence imaging of MCF7 cells cultured in normoxia or 0.1% hypoxia for 48h. Mitochondria were stained using MitoTracker™ Green FM and lysosomes were stained with LysoTracker™ Red DND-99. n=3.

5.4.12. Effect of mitochondria-targeting drugs in dsRNA levels

As mitochondria are the main source of dsRNA in the cells [657], the effect of different drugs targeting mitochondria was assessed in MCF7 cells. Chloramphenicol inhibits mitochondrial protein synthesis via binding to the 50S subunit of the 70S ribosome found in the mitochondria, in contrast to the 80S ribosome present in the cytosol. ABT-737 and G-TPP both induce cell apoptosis and mitophagy. ABT-737 is a BCL2 apoptosis regulator (BCL2) inhibitor, thus it will induce cell apoptosis by inhibiting the anti-apoptotic molecule BCL2, as well as mitophagy. Similarly, G-TPP accumulates in the mitochondria of tumour cells and by inhibiting the heat shock protein 90 (Hsp90) promotes cell apoptosis. On the other hand, mubritinib and metformin decrease mitochondrial respiration by inhibiting ETC complex I, and the Vps34 inhibitor SAR405 alters vesicle trafficking and inhibits autophagy by blocking autophagosome formation. IFNβ promoter assay revealed that only mubritinib and G-TPP treatment were able to decrease by 4- and 2-fold, respectively, IFNβ promoter stimulation under normoxia (Figure 5.33). Furthermore, hypoxia was not able to further inhibit IFNβ promoter activity in MCF7 cells treated with these two drugs.

These results suggest that the type I IFN down-regulation detected in hypoxia is not due to reduced respiration alone as metformin, a complex I inhibitor, did not affect the assay. However, mubritinib, which also targets complex I [709], is also known to inhibit HER2 [710]. It was shown that HER2 inhibition by trastuzumab increased the expression of pro-apoptotic proteins, which induced the opening of mitochondrial permeability transition pores, ROS production and mitochondrial dysfunction due to loss of mitochondrial membrane potential [711]. Therefore, HER2 inhibition by mubritinib could be further contributing to mitochondria dysfunctionality and the consequent lower dsRNA synthesis, even though in the context of acute myeloid leukaemia mubritinib inhibition of mitochondrial respiration was not mediated by HER2 [709]. Furthermore, it was shown that successful anti-HER2 monoclonal antibody treatment in breast cancer required type I and type II IFNs, therefore, mubritinib treatment in hypoxia is likely not showing any effect due to the down-regulation of the type I IFN pathway generated by hypoxia [712]. A drug that had a more extensive effect on the mitochondria (G-TPP), potentially affecting protein folding, reduced IFNβ promoter activation to a baseline equal to that in hypoxia. G-TPP specifically inhibits the mitochondrial protein-folding chaperone Hsp90, generating unfolding protein stress in the mitochondria [713]. Therefore, G-TPP induced lower IFNβ promoter activation might be due to increase mitochondrial stress. As Hsp90 stabilizes proteins involved in cancer cell survival, Hsp90 inhibitors are potent drugs for anticancer treatment. G-TPP has also been described to induce mitophagy [714], but as previously demonstrated in this thesis (Figure 5.32), it is not likely to be the mechanism for lower dsRNA and thus decrease IFNβ promoter stimulation. Overall, despite mubritinib and G-TPP inhibition of IFNβ promoter stimulation, hypoxia seems to have a greater effect, as it could down-regulate the activation after every treatment.

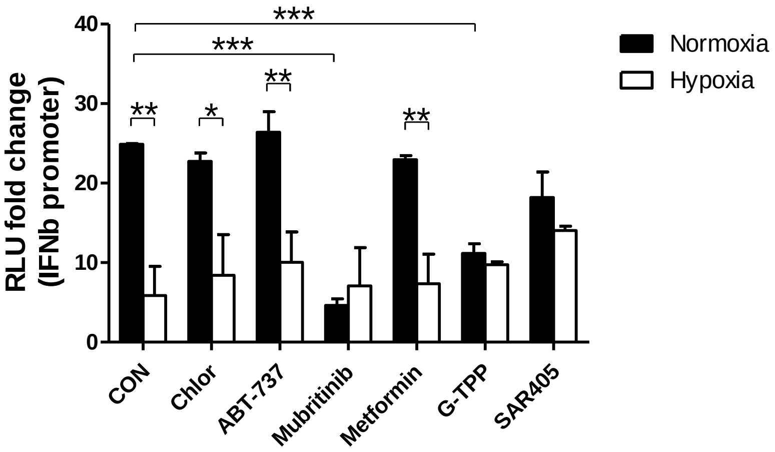

Figure 5.33. IFNβ promoter assay using RNA from MCF7 cells cultured in normoxia or 0.1% hypoxia and treated with DMSO as control (CON), chloramphenicol (Chlor), ABT-737, mubritinib, metformin, G-TPP and SAR405 for 48h. n=3. * $p<0.05$, ** $p<0.01$, *** $p<0.001$.

5.5. Discussion

Hanahan and Weinberg described in 2000 that one of the mechanisms by which tumours progress is through immune evasion [1]. This is achieved by impeding the homing of effector immune cells (T cells and NK cells) and promoting the recruitment of immunosuppressive cells such as MDSC, TAM and Treg cells, among other mechanisms. In addition to this, hypoxia is one of the main characteristics of solid tumours and it has been related to an immunosuppressive environment within the tumour.

Hypoxic regulation of the type I IFN pathway

In this thesis, a new mechanism of hypoxic immunosuppression through the down-regulation of the type I IFN pathway is described. This happened at oxygen levels commonly found in tumours, even in cases of most severe hypoxia (1% and 0.1%) [715]. Hypoxic-dependent down-regulation of the type I IFN pathway was seen for members of both early and late phase. At mRNA level, the down-regulation was significant as soon as 16h under hypoxia, whereas it took 48h to observe the down-regulation at protein level. Hypoxia generally inhibits gene transcription, apart from the subset of genes whose expression increases dramatically in a HIF-dependent manner. In addition, hypoxia also impairs cap-dependent protein synthesis mainly via blocking the initiation step of the mRNA translation [716, 717]. As protein synthesis is a highly energy demanding process, it is believed that cells reduce mRNA translation in low oxygen conditions to avoid energy consumption and promote cell survival [718]. Moreover, it was shown that lack of ATP in hypoxia affected protein synthesis [719, 720].

On the other hand, reoxygenation gradually reversed hypoxic inhibitory effect, taking 24h to recover normoxic levels again at mRNA level, but not at protein, except for RIG-I, whose expression was higher than in normoxia. Supporting these results, it was reported that suppression of mRNA translation in hypoxia could be rescued by supplementation of glucose or reoxygenation [721], enhancing protein synthesis rates above normal values in some cases. This effect has been attributed to high ATP levels, due to still functional glycolysis and the reactivation of mitochondrial respiration [722]. In contrast to a neuro-inflammatory model of ischemia-reperfusion in which IFNα and IFNβ levels increased after 2h and 24h reperfusion, respectively, above basal levels [723], or a hepatic ischemia-reperfusion model in which ADAR1 mRNA and protein levels were significantly higher at 6h of reperfusion [724], there was not any up-regulation above normoxic values after reoxygenation in MCF7 cells, neither an overshoot during the process.

Altogether, these results suggest that hypoxia has a greater effect on the type I pathway transcription than translation, as mRNA decreases more quickly in hypoxia and it recovers faster than protein after reoxygenation. This points to a stabilization of mRNA or to *de novo* transcription during the reoxygenation phase, which will be later translated into protein level changes, rather than protein degradation.

Furthermore, hypoxia lowered poly I:C induced activation of the type I IFN pathway in various cancer and non-transformed cell lines, suggesting that hypoxia in different tissues decreases the basal expression of this pathway limiting the IFN response when an activator is detected.

However, it is also possible that endogenous activators of the pathway are also affected by hypoxia leading to lower stimulation and immune response. In this context, lack of type I IFNs in the tumour microenvironment will result in no activation of DC [539] and reduction of macrophages’ and NK cells’ cytotoxicity, further contributing to hypoxia-induced immunosuppressive environment and finally allowing tumour growth. It was published that in lung and dermal tumours respiratory hyperoxia induced tumour regression by reducing the extracellular adenosine concentration, resulting in increased T cell and NK cell infiltration and activity, as well as reduced Treg cell-mediated immune response suppression in the tumour mass [605]. Another study showed that using the hypoxia-activated prodrug evofosfamide (TH-302, which alkylates DNA inducing intrastrand and interstrand crosslinks and thus, leading to apoptosis of hypoxic tumour cells [725]) hypoxia-generated immunosuppression diminished, as infiltration of T cells in formerly hypoxic areas was restored [606]. Moreover, TH-302 treatment reduced immunosuppressive myeloid cell population (TAM and MDSC) and their activity in the tumours, in addition to lower the ability of this tumour regions to recruit immature myeloid cells from the stroma and induce their differentiation. These two studies support the reoxygenation results showing that the type I IFN pathway is recovered.

HIF1α and HIF2α involvement in the hypoxic inhibition of the type I IFN pathway

This thesis also showed that hypoxia-induced down-regulation of the type I IFN pathway is independent of HIF1α, although some members such as RIG-I and STAT1 were up-regulated by HIF1α deletion, as observed in MCF7 KO cells. To further support HIF1α independent mechanism, MCF7 KO cells presented the same mRNA levels of *IFNAR1* and *IFNAR2* as MCF7 WT cells in hypoxia, showing that HIF1α is not the main responsible for the hypoxic inhibition of the pathway. Supporting this data, a previous study showed that 2% hypoxia reduced RIG-I and MDA5 protein expression in malignant murine and human cells in a HIF1α-dependent manner, even after treating the cells with the type I IFN activator 5’-triphosphate RNA (3pRNA), whereas non-malignant or primary cells presented similar levels both in normoxia and hypoxia [726]. In line with this thesis results, they also detected lower *IFNAR* levels in hypoxia, and stated that RIG-I requires a functional receptor to respond to stimulus. In addition to this, another work found that *RIG-I* gene presented a HRE in the regulatory region, and that RIG-I expression was up-regulated in human muscle cells in hypoxia [727]. Moreover, it was previously reported that some ISGs, such as *IFIH1* or *STAT1*, which are associated to chronic antiviral response, can be transcribed by unphosphorylated STAT1, as high IRF9 expression drives their transcription [697]. MCF7 KO cells showed up-regulation of IRF9 and higher levels than parental MCF7 cells of some ISGs such as *DDX58*, *IFIH1*, *ADAR-p150* and *STAT1*. However, hypoxia again decreased their expression showing that despite the partial role of HIF1α in the inhibition of the expression of these genes, hypoxic suppression is still present.

It has also been described that the lactate in the extracellular media contributes to hypoxia-induced immunosuppression [617], in part via inhibition of the type I IFN signalling [622]. In this case, high lactate levels were detected in the supernatant of hypoxic cells, with no differences between parental and HIF1α-deficient cells. The high lactate levels detected in the supernatant of MCF7 hypoxic cells could explain the observed HIF1α-independent suppression of the type I IFN pathway. It is well known that HIF1α is the main responsible for the shift to aerobic glycolysis observed in hypoxia, but as previously described [728], other factors such as HIF2α can enhance LDHA expression and the consequent conversion of pyruvate to lactate. However, HIF2α does not seem to play an important role in the type I IFN down-regulation either, as observed in 786-0 and RCC4 cells, as hypoxia was able to lower the expression of several members of the pathway, independently of HIF2α expression.

Supporting HIF-independent down-regulation of the type I IFN pathway, it has been described that the chromatin modifications generated under low oxygen conditions can both trigger activation and repression of selected genes [729]. Johnson *et al.* found that the transcription inhibition generated by hypoxia was HIF1α-independent. After 24h or 48h exposure to 0.2% hypoxia, total RNA transcription was repressed 42% and 65%, respectively, while mRNA synthesis was blocked 22% and 51%, respectively. They also found that during hypoxia, histones were subjected to modifications associated with transcriptional activation (H3K9ac and H3K4me3) and repression (H3K9/27me2 and H3K27me3) in a HIF-independent manner, as well as nucleosome location changes [729]. This work suggests that hypoxia can trigger chromatin and histone modifications to regulate gene transcription. Similarly, a recent paper showed that 1h of hypoxia induced a rapid and HIF-independent increase in H3 histone methylation, particularly in the transcription activation related H3K4me3 and H3K36me3 marks that affected type I IFN pathway [730]. They reported that this increase in histone methylation was due to reduced activity of several dioxygenases of the Jumonji-C (JmjC) domain containing histone demethylase family, specifically KDM5A, which are not active in the absence of oxygen as it occurs with PHDs, therefore histone methylation is not abolished. Batie *et al*. showed that after reoxygenation, histone methylation marks returned to normoxic levels, supporting the hypothesis that hypoxia-induced increase in histone methylation was due to lack of JmjC enzymes' activity [730]. Overall, these studies suggest that hypoxia could down-regulate the expression of type I IFN genes in first instance by modifying chromatin access or by lowering the presence of transcription activation markers due to decreased activity of JmjC enzymes.

mtdsRNA induces type I IFN response

On the other hand, endogenous dsRNA was responsible for the type I IFN pathway induction, rather than other RNA forms in the cells. This was determined by IFNβ promoter activation, which was not able to generate any response upon treatment with the dsRNA-specific RNAse III. As expected, hypoxia lowered the activation of the IFNβ promoter as soon as 4h of exposure, while reoxygenation after hypoxia caused a gradual recovery to normoxic levels. Moreover, this hypoxia repressive effect was independent of HIF1α and HIF2α as it occurred with the exogenous dsRNA poly I:C, and it was present in cancerous and primary cells.

Among the endogenous dsRNA, specifically mtdsRNA triggered IFNβ promoter stimulation via MDA5/MAVS and not RIG-I/MAVS sensing pathway. This data is supported by a recent publication in which it was reported that 99% of the total dsRNA within the cell originates from the mtDNA transcription [657]. Due to the close circular structure, mtDNA transcription is bidirectional and it generates overlapping symmetrical transcripts [731, 732], which if released to the cytoplasm can induce a potent immune response. To avoid this, cells have several mechanisms to regulate mtdsRNA levels, such as the mtdsRNA degrading enzymes SUV3 and PNPT1. Total RNA turnover regulates gene expression as well as potentially toxic RNA-processing by-products and it is known to be spatially organized in foci called P-bodies within the cytoplasm of eukaryotic cells [733]. Similarly, mtdsRNA is also subjected to degradation in distinct foci of the mitochondria (named D-foci) by the PNPase-SUV3 complex called mitochondrial degradosome [734]. Moreover, formation of this complex is necessary for mtdsRNA turnover and probably avoids the generation of potentially deleterious dsRNA molecules which could trigger an immune response. Borowski *et al.* first demonstrated that PNPT1 is the mitochondrial RNAse which by associating with SUV3 helicase forms a complex indispensable for the spatially organized mtdsRNA degradation [734]. Later on, Dhir *et al.* showed that loss of either SUV3 or PNPT1 leads to mtdsRNA accumulation, its release to the cytoplasm and consequent increase in the type I IFN response [657].

Oligoadenylate synthetase (OAS)/RNAse L pathway has also been described to be involved in dsRNA sensing [735]. Upon detection of dsRNA, IFN-inducible OAS enzymes produce 2'-5'-oligoadenylates which activate RNAse L to cleave all cellular RNAs. On the other hand, in addition to its tumour suppressor role, p53 is also an ISG which appears to avoid the generation of transcripts capable of inducing a type I IFN immune response [736]. It has recently been published that in the absence of p53, a strong immunogenic mtdsRNA is produced in mouse embryonic fibroblasts (MEFs) which can induce a potent immune response in recipient cells [737]. RNA sequencing studies in this study revealed that *p53* mutant MEFs had higher amount of differentially expressed mitochondrial genes and of genes involved in immune response, such as *ifnα* and *ifnβ*, compared to wild type. They also observed that *oas3* gene was highly expressed in *p53* mutant MEFs, and concluded that the mtdsRNA generated by the OAS/RNAse L system triggered the immune response, as silencing RNAse L in *p53* mutant MEFs avoided the immune stimulation caused by endogenous mtdsRNA. Overall, this study showed that p53-OAS/RNAse L system is another mechanism by which cells remove immunogenic mtdsRNA to prevent self-nucleic acid from inducing an immune response [737].

Hypoxic effect on mtDNA transcription

However, this thesis has shown that hypoxia did not affect the levels of SUV3 or PNPT1, suggesting that the lower mtdsRNA detected in hypoxia was not due to increased degradation, but could be due to decreased mitochondrial transcription. The expression of both nuclear encoded genes involved in mitochondrial transcription and mitochondrial encoded genes were down-regulated in hypoxia. This down-regulation was significant for all tested genes after 16h in hypoxia at mRNA level, as seen for the type I IFN inhibition as well, and showed that hypoxia blocks transcription both in the nucleus and in the mitochondria. However, the protein expression of the genes was not tested. In addition to the transcriptional blockade, and as previously published at protein level [704], hypoxia decreased the expression of MRPs in a time-dependent manner, being again 16h the decisive timepoint. Supporting this data, it was reported that mRNAs encoding for ribosomal proteins were more sensitive to the translational repression of hypoxia than the majority of mRNAs [720]. Moreover, dsRNA staining was significantly lower at 16h under hypoxia in MCF7 cells. Altogether, this data shows that under hypoxia, specifically from 16h onwards, mtdsRNA quantity is significantly lower in all tested cell lines (except for 143B) by dsRNA staining, probably due to transcriptional repression. Therefore, hypoxia could down-regulate the type I IFN pathway by decreasing general transcription which would affect the IFN pathway itself, and by inhibiting mtdsRNA formation which could stimulate IFN response under low oxygen conditions.

mtdsRNA down-regulation in hypoxia was HIF1α and HIF2α independent as less dsRNA staining was detected in both 786-0 WT and 786-0 KO cells. Nevertheless, hypoxia did not lower mitochondrial or nuclear gene expression in the parental cell line, whereas it did down-regulate mitochondrial encoded genes in HIF2α KO cells. This suggests that HIF2α has a relevant role in mtDNA transcription. Supporting this hypothesis, it was described a HIF2α/c-MYC/POLRMT axis in which HIF2α promoted c-MYC transcriptional activity [92] and c-MYC transcription factor induced *POLRMT* expression [703], therefore increasing mtdsRNA levels and possibly avoiding hypoxia induced down-regulation, as seen in 786-0 WT cells. Thus, as this axis could be lost in 786-0 KO cells as a consequence of HIF2α deletion, hypoxia could still inhibit mitochondrial encoded gene´s transcription due to less POLRMT levels. Even though no differences at total protein level were detected by western blot, protein levels in the nucleus or cytosol were not analysed. MRP expression was also HIF-independent, as most of them were down-regulated in hypoxia, suggesting that impairment in mtDNA transcription could directly affect mitochondrial translation later on, similar to the translation-mediated transcription attenuation detected in bacteria [738].

mtDNA lack or mutation effect in the type I IFN signalling regulation

Given the importance of mtDNA in the type I IFN pathway, cell lines lacking mtDNA or harbouring specific mtDNA mutations were analysed. 143B cell line was the only one in which hypoxia did not down-regulate IFNβ promoter stimulation, dsRNA levels or mtDNA transcription, among the all tested, showing that this cell line is highly resistant to low oxygen concentrations. As a positive control, the mtDNA depleted 143B Rho zero cell line was used, and as expected, no mtdsRNA was detected, either IFNβ promoter activation or mitochondrial encoded gene expression. Few studies have described the behaviour of 143B cells under hypoxia. It was published that <1% hypoxia slightly slowed down 143B cells' proliferation rate compared to normoxia [739], but it did not impair it. Similarly, another study showed that 143B cell's proliferation was inhibited between 5-0% hypoxia in a concentration-dependent manner [740]. Another work in various osteosarcoma cell lines determined that the effect of hypoxia, acidosis and interstitial fluid pressure, all of which influence tumour progression, had a greater effect if combined [741]. In spite of not including 143B cell line, this study suggests that hypoxia alone may not be sufficient to generate an effect on 143B cells, thus behaving in the same way as in normoxia. Similarly, the hypoxia-induced decrease in the amount of mtdsRNA or IFNβ promoter stimulation was not affected by the degree of mutation in *ATP6* gene, as observed in mTUNE cells. However, mTUNE M80 cells, which presented 80% of heteroplasmy, presented higher basal IFNβ promoter activity than the other isogenic cell lines, possibly due to the increase mutation level which might make the cell to recognize it as non-self and induce an immune response. Moreover, hypoxia down-regulated the expression of nuclear and mitochondrial encoded genes in mTUNE M7 cells, suggesting that lower mtdsRNA levels could be due to less transcription, however, this was not observed for mTUNE M80 cells. In fact, mTUNE M80 cells did not present significant differences between normoxia and hypoxia for the aforementioned genes, although the expression of all seemed to be slightly increased in low oxygen conditions. Moreover, normoxic levels of these genes were lower in mTUNE M80 cells compared to mTUNE M7, suggesting that the lower dsRNA staining detected under this condition could be due to less mtDNA transcription. These results could show that the degree of m8993T>G mutation in *ATP6* gene influences mtDNA transcription in mTUNE cells and could suggest a more complex regulation of mtdsRNA, although there is no previous link between this mutation and mtDNA transcription. However, it was recently published that the degree of mutation was negatively correlated with OCR, ETC components and activity and mitochondrial metabolites such as citrate, aspartate and malate, whereas a positive correlation was found with ECAR, lactate secretion and the glycolytic metabolites phosphoenolpyruvate and pyruvate [695]. All these features correspond to an increase glycolysis proportional to the degree of mutation, and they found that mitochondrial dysfunction triggered cytosolic reductive carboxylation too [695]. Therefore, mTUNE M80 cells might have lower mtDNA transcription in basal conditions to avoid the generation of a non-functional ATP synthase which will not generate enough ATP to cover cell's energy demands.

Mitophagy and the type I IFN pathway

mtdsRNA content could also be reduced by enhancement of mitophagy under hypoxia. In order to prevent the accumulation of non-healthy or dysfunctional mitochondria, cells trigger this specific programmed cell death, which has been described to be induced under hypoxia to avoid the generation of DAMPs and the consequent immune response [665]. It was reported that both PTEN-induced putative kinase 1 (PINK1) and Parkin (PRKN) participate in the removal of damaged mitochondria. PINK1 is constitutively degraded when mitochondrial membrane potential is adequate, but under stress conditions which induce loss of mitochondrial membrane potential, PINK1 is stabilized and accumulates in the organelle [742]. From there, it recruits cytosolic Parkin to start the removal of damaged mitochondria [742, 743]. Supporting the role of mitophagy in the regulation of the type I IFN, it was recently published that *Pink*$^{-/-}$ and *Prkn*$^{-/-}$ mice in which mitophagy is deficient, presented higher serum concentrations of several interleukins and IFNβ, in addition to increase mtDNA circulating levels [744]. The authors concluded that in the absence of PINK1 or Parkin, type I IFN response to mitochondrial stress was induced through STING signalling. Therefore, this study suggests that decrease mtRNA and IFN response under hypoxia could be due to increased mitophagy. However, in this thesis, successful knock down of the important mitophagy gene *BNIP3* did not revert the hypoxia-induced down-regulation of known ISGs or IFNβ promoter activation, suggesting that BNIP3-mediated mitophagy is not the reason for the lower mtdsRNA levels detected in hypoxia. Moreover, live cell imaging of mitochondria and lysosomes further support this result, as no colocalization was observed either in normoxia or hypoxia. As previously described [680], mitochondria shape changed under low oxygen stress conditions and they appeared to locate closer to the nucleus. It is known that mitochondria protect from stress conditions such as starvation, UV radiation or oxidative stress by changing their morphology and acquiring a more elongated shape. In this regard, it has been reported that mitochondrial fission arrest caused by hypoxia, results in elongated interconnected organelles in murine brain tissue [745], which could be a cellular survival mechanism under those stress conditions.

In contrast, but still supporting the data, hypoxia-induced mitophagy requires previous mitochondria fragmentation, and therefore less elongated morphology [746]. It was also reported that cardiomyocytes exposed to hypoxia and low glucose conditions, to simulate ischemia, presented increased mitochondrial fission [747]. These studies show that mitochondria are tightly regulated under hypoxia in a very complex way, which may vary from one cell line to another and depend on each cell's energy demands. Moreover, drugs targeting the mitochondria did not affect IFNβ promoter stimulation, except for mubritinib and G-TPP, which caused a down-regulation that reached hypoxic levels. The effect of these two drugs was no additive to the hypoxia-induced down-regulation, as IFNβ promoter stimulation under hypoxia was equal to that in normoxia. This suggests that low oxygen concentration has a greater effect in lowering the IFNβ promoter activation than any of the tested mitochondria-targeting drugs.

Implications of the type I IFN signalling inhibition

Tumour hypoxia is known to create resistance to radiation treatments, as oxygen is essential for ROS formation to kill cancer cells [748, 749], and to chemotherapy, by up-regulating the expression of anti-apoptotic and prosurvival genes [750]. In addition to that, hypoxia generates an immunosuppressive microenvironment in the tumour mass which allows tumour cell growth and immune evasion. Similarly, adequate type I IFN signalling is responsible for the success of therapies such as radiotherapy, chemotherapy or immunotherapy [127]. Therefore, lower type I IFN signalling under hypoxia is likely to reduce the success of various anticancer treatments. Furthermore, it is demonstrated in this thesis that hypoxia inhibits mtdsRNA formation, leading to decrease IFNβ promoter activity and thus, to lower the type I IFN response. It has been reported that in tumour types such as bladder, breast, esophageal, head and neck, kidney and liver the amount of mtDNA was significantly lower than in the paired adjacent normal tissue, and it was associated with shorter patient survival [751].

Altogether, this thesis chapter shows that hypoxia induces down-regulation of the type I IFN pathway at basal level as a consequence of lower transcription, but also endogenous activators such as mtdsRNA are reduced under hypoxia, possibly contributing to the radiotherapy and chemotherapy resistance observed in advanced tumours containing hypoxic areas, as these therapies rely on an intact type I IFN response [550]. This suggests that future treatments should consider not only the immunosuppressive role of hypoxia on the tumour mass but also the cause, developing for instance, drugs that promote mtdsRNA formation under hypoxia to enhance type I IFN signalling, or drugs which directly activate the pathway.

5.6. Conclusions

1. Hypoxia down-regulates the type I IFN pathway at basal levels and upon stimulation with poly I:C treatment in a HIF-independent manner in both normal and tumour cell lines.
2. Reoxygenation after hypoxia promotes type I IFN pathway recovery.
3. Type I IFN pathway is activated by endogenous dsRNA originating in the mitochondria which is down-regulated under hypoxia, in both normal and tumour cell lines, independently of HIF1α/HIF2α and mtDNA mutation levels.
4. Down-regulation of mtdsRNA levels in hypoxia is probably due to inhibition of mtDNA transcription and not as a consequence of increased mtdsRNA degradation or mitophagy.

6. General summary

This thesis has demonstrated the role of HIF2α in ccRCC oncogenesis, as previously reported [125, 126]. HIF2α appeared to be implicated in both primary tumour initiation and later metastasis, as HIF2α KO cells were unable to grow from single cells or invade other tissues. In addition, HIF2α demonstrated to have opposing roles in cell migration and invasion. Even so, all results pointed to that in ccRCC HIF2α plays a crucial role in the progression of the disease, showing that the already ongoing clinical trials targeting HIF2α could provide new therapeutic strategies for patients. In addition, this thesis has also proven that HIF2α confers resistance to the lipid-lowering drugs statins. Even though no increase effect was detected by the addition of the HIF2α antagonist PT2385 to statin treatment *in vitro*, it is still possible that the combined therapy has a synergetic effect in humans.

On the other hand, it has been previously reported that one of the main characteristics of solid tumours, hypoxia, creates an immunosuppressive environment in the tumour [25], helping in the progression of the disease. This thesis has demonstrated that oxygen tension is crucial for the degree of the type I IFN pathway basal expression and later activation, suggesting that hypoxia-induced down-regulation of the type I IFN pathway might contribute to the resistance of different therapeutic strategies, such as radiotherapy, chemotherapy or immunotherapy [127]. Interestingly, this hypoxic effect is independent of HIF transcription factors, as well as cell malignancy, as type I IFN signalling inhibition was detected in both *VHL* mutated and non-mutated cancer cell lines and in non-tumour cells, suggesting that hypoxia inhibits this pathway in every cell type. In addition, although not investigated in this thesis, an active type I IFN pathway is required for immune cell maturation and activity [135]. Altogether, these results suggest that previous treatment with drugs reducing tumour hypoxia could be beneficial to increase the type I IFN pathway in both tumour and infiltrating immune cells, and therefore, the efficacy of later therapies.

Moreover, this thesis further shows that the levels of mtdsRNA, previously reported to activate the type I IFN pathway [657], are considerably lower under hypoxia. The results point to a decrease in mtDNA transcription, as previously reported in genomic DNA [729], and suggest that the combined use of drugs targeting hypoxia and drugs increasing the degree of mtdsRNA could be useful to increase the type I IFN pathway expression and activation which is required for the success of many treatments.

Overall, this thesis shows that hypoxia and HIF transcription factors are key molecules in different tumour backgrounds and that in order to create successful therapies, it is necessary to have a wider view of the tumour itself, taking into account secondary mechanisms responsible for the disease.

7. Summary in Spanish

7.1. Introducción general

El cáncer es una enfermedad heterogénea que puede surgir en cualquier tipo celular. En el año 2000 Hanahan y Weinberg propusieron que todos los tumores tenían unas características comunes [1]: 1) independencia de las señales de crecimiento, 2) insensibilidad a las señales de inhibición de crecimiento, 3) evasión de apoptosis, 4) capacidad de replicación ilimitada, 5) angiogénesis y 6) invasión y metástasis. En 2011, incluyeron a estas características: inestabilidad genómica, inflamación protumoral, reprogramación del metabolismo y evasión del sistema inmune [2].

La hipoxia es una de las características más importantes de los tumores sólidos. En condiciones de baja concentración de oxígeno, las células tumorales activan una serie de respuestas para hacer frente a este estrés y poder sobrevivir, la mayoría de ellas mediada por los factores de transcripción inducibles por hipoxia HIF (HIF1α, HIF2α y HIF3α) [31]. La actividad de HIF está regulada por diversos factores, siendo el oxígeno el más importante. En condiciones normales, la subunidad α es hidroxilada por las enzimas prolil hidroxilasas (PHDs) [43, 44], permitiendo la unión del complejo E3 ubiquitina ligasa von Hippel Lindau (VHL) que estimulará su degradación proteosomal. Sin embargo, en condiciones de hipoxia las PHDs no están activas, por lo que la subunidad α puede translocarse al núcleo celular, dimerizar con la subunidad β y promover la transcripción de genes para hacer frente a la escasez de oxígeno y promover el desarrollo tumoral [752].

7.2. Estudio de HIF2α en carcinoma renal

7.2.1. Introducción

En este sentido, el carcinoma renal de células claras (ccRCC por su abreviatura del inglés *clear cell Renal Cell Carcinoma*) es un modelo de estudio importante ya que el 80% de los casos presentan el gen *VHL* inactivado bien por mutación o metilación [252, 253], dando lugar a que los factores de transcripción HIF no sean degradados. En ccRCC, HIF1α y HIF2α tienen diferentes funciones en el desarrollo del tumor, mientras que HIF1α se ha descrito como un factor supresor de tumores que atenúa el crecimiento de las células tumorales, HIF2α es considerado un estimulador de la progresión tumoral [125, 126]. El análisis inmunohistoquímico de muestras de riñón de pacientes con la enfermedad VHL mostró que se pueden detectar ambas isoformas en lesiones pretumorales, mientras que células tubulares normales de riñón carecen de la expresión de HIF2α [278]. Es más, otro estudio demostró que se pueden distinguir tres subtipos ccRCC: los que presentan *VHL* intacto, y dentro de los que tienen *VHL* inactivado, los que expresan HIF1α y HIF2α y los que solo expresan HIF2α [231]. En este estudio vieron que los tumores que sólo expresaban HIF2α eran los que tenían peor pronóstico y un mayor índice de proliferación, al igual que demostraron otras investigaciones [93, 283].

Por otro lado, ccRCC se caracteriza por ser altamente vascular y presentar elevados niveles de lípidos y glicógeno en las células. A medida que el tumor aumenta de tamaño, se genera un gradiente de oxígeno dentro de la masa tumoral que crea regiones hipóxicas e incluso anóxicas. Como consecuencia, varios tipos tumorales, incluyendo ccRCC, promueven la creación de nuevos vasos sanguíneos a partir de los existentes, proceso denominado angiogénesis, principalmente mediante la vía de señalización de HIF [94, 291], para obtener los nutrientes y el oxígeno necesario. De la misma forma, estas células hipóxicas alteran también su metabolismo, tal es el efecto en ccRCC que este tipo tumoral se ha clasificado como ‘enfermedad metabólica’ durante mucho tiempo [210, 299]. En condiciones de normoxia, las células metabolizan la glucosa mediante el ciclo de Krebs y producen energía en la mitocondria. Sin embargo, las células tumorales reconducen la glucosa hasta la producción de ácido láctico, incluso en presencia de oxígeno, proceso conocido como ‘efecto Warburg’ [21]. HIF1α es el principal factor que estimula este cambio [98, 271], aunque se ha descrito que HIF2α también participa [125, 126, 285]. Además de alteraciones en el metabolismo de la glucosa, ccRCC también presenta cambios en el metabolismo lipídico. Las células de ccRCC acumulan gotas lipídicas en su citosol, probablemente como consecuencia de la inhibición del catabolismo lipídico mediado por HIF [320]. Se ha descrito que las gotas lipídicas, además de acumular lípidos en su interior, protegen a las células del estrés del retículo endoplasmático y promueven la progresión de ccRCC [318]. En cáncer de mama y glioblastoma, estos depósitos estimulan la supervivencia celular después de periodos de hipoxia y reoxigenación [100]. Es más, la inhibición tanto de HIF1α como de HIF2α reduce la cantidad de gotas lipídicas in ccRCC [318, 320, 321].

7.2.2. Resultados

7.2.2.1. Papel de HIF2α en la proliferación celular

Tras haber confirmado el éxito en la generación de la línea de ccRCC 786-0 deficiente en HIF2α (786-0 KO), se procedió a investigar cómo difería de la línea parental 786-0 *wild type* (786-0 WT) a nivel de proliferación en 2-dimensiones (2D) y 3-dimensiones (3D). Cuando la densidad celular inicial era elevada, la proliferación de ambas líneas celulares fue similar, mientras que a baja densidad (250, 500 y 1000 células) las células 786-0 KO proliferaron menos que las 786-0 WT. Este mismo efecto se pudo observar en ensayos de formación de colonias, donde las 786-0 KO formaron 40% menos de colonias que las 786-0 WT. Así mismo, independientemente del número inicial de células, la hipoxia afectó negativamente la proliferación de ambas líneas celulares, tal y como se observó en ambos ensayos. Sin embargo, la adición del antagonista de HIF2α PT2385 no alteró el crecimiento celular *in vitro*, tal y como se había visto previamente [237]. Respecto al crecimiento en 3D, no se detectó un aumento de volumen de las esferas a lo largo del tiempo, no obstante, las 786-0 KO formaron esferas más redondas que las 786-0 WT, y a pesar de tener un número similar de células totales, el porcentaje de viabilidad fue inferior, mostrado que la carencia de HIF2α sí afecta a la proliferación cuando las células se encuentran en un ambiente hipóxico más similar al que se encuentra en los tumores. En este caso, la adición de PT2385 generó unas esferas menos compactas y, por tanto, de mayor volumen.

Dado que solo se obtuvo un clon tras el Crispr/Cas9, se empleó la línea celular RCC4, también de carcinoma renal, para apoyar los resultados de esta tesis y excluir un posible efecto clonal. La línea RCC4 WT que contiene el gen *VHL* mutado y por tanto expresa HIF1α y HIF2α en normoxia e hipoxia proliferó significativamente menos que la línea RCC4 VHL, la cual sí expresa el gen *VHL* y, por consiguiente, solo expresa HIF1α y HIF2α en hipoxia. Del mismo modo, RCC4 WT formó menor número de colonias que RCC4 VHL. Estos resultados se oponen al fenotipo identificado en las 786-0, donde las 786-0 KO proliferaron menos. Sin embargo, el hecho de que las RCC4 WT sí expresen HIF1α podría estar implicado en el resultado, desde un punto de vista metabólico.

7.2.2.2. La deleción de HIF2α promueve la migración e inhibe la invasión celular *in vitro*

Conocida la implicación de HIF en la promoción de la transición epitelio-mesenquimal (EMT) que las células experimentan durante el desarrollo tumoral, se realizaron estudios de migración e invasión celular. Las células 786-0 KO mostraron una mayor migración, pero menor invasión que las 786-0 WT. En la misma línea, las células RCC4 WT migraron menos, mostrando la implicación de HIF2α. Sin embargo, la línea celular RCC4 no mostró capacidad de invasión, probablemente debido al temprano estadio tumoral del que proceden. Por otro lado, la inhibición transitoria de HIF2α mediante ARN de silenciamiento (siRNA) no generó ningún cambio ni en la migración ni en la invasión celular, mientras que la adición de PT2385 al cultivo no alteró la migración de las 786-0 WT, pero sí inhibió su invasión de manera dosis-dependiente.

7.2.2.3. HIF2α estimula metástasis *in vivo*

Tal y como se observó *in vitro*, las células 786-0 KO fueron incapaces de generar metástasis *in vivo* tras ser inyectadas en ratones inmunosuprimidos. Los ratones inyectados con las células 786-0 WT desarrollaron metástasis en pulmón, cerebro y en el tejido adiposo de la glándula mamaria. Las metástasis en pulmones fueron detectadas dos semanas tras la inyección de las células tumorales, aunque desaparecieron en la semana 4 para volver a aparecer 10 semanas más tarde, sugiriendo que los bajos niveles de macrófagos y células NK (de la abreviatura del inglés *natural killer*) presentes en los ratones son suficientes para la regresión de las metástasis.

7.2.2.4. La deleción de HIF2α altera el metabolismo celular

La regulación de la expresión de ciertos genes es exclusiva de un factor, mientras que hay otros genes que pueden ser regulados por HIF1α y HIF2α [413]. En este sentido, en las células 786-0, HIF2α no promovió la activación de *PDK1*, *PDHA1* y *LDHA*, genes implicados en el metabolismo de la glucosa principalmente regulados por HIF1α, demostrando que en esta línea celular HIF2α no reemplaza el papel de HIF1α que no es funcional [328].

Respecto al metabolismo lipídico, en las células 786-0 KO la expresión a nivel de ARN de *PLIN2* y *HIG2* fue significativamente menor que en las 786-0 WT, mientras que los niveles de *CPT1A* fueron mayores. Estos datos sugieren que en ausencia de HIF2α, las células 786-0 KO disminuyen la cantidad de gotas lipídicas en su citosol promoviendo la β-oxidación de los ácidos grasos retenidos en ellas, obteniendo así la energía necesaria para seguir con el curso de la enfermedad. Sin embargo, por inmunofluorescencia no se detectaron diferencias en la cantidad de gotas lipídicas, mientras que por citometría de flujo las 786-0 KO presentaron mayores niveles de fluorescencia que las parentales.

Por último, las células 786-0 KO presentaron mayor OCR (abreviatura del inglés *oxygen consumption rate*) que las células 786-0 WT tras la adición del ionóforo FCCP, sugiriendo que HIF2α podría estar inhibiendo la respiración mitocondrial. La adición de PT2385 al cultivo celular aumento los niveles de OCR de las células, pero sin llegar a los valores de las 786-0 KO, de la misma forma, las RCC4 VHL también mostraron mayor consumo de oxígeno que las RCC4 WT, respaldando la inhibición ejercida por HIF2α en la respiración mitocondrial.

7.2.3. Discusión

Los resultados muestran que la deficiencia de HIF2α no afecta a la proliferación de ccRCC cuando la confluencia es elevada, pero sí cuando el número inicial de células es bajo. Estos resultados se respaldan con previos estudios donde vieron que la inhibición de HIF2α no altera la proliferación celular en condiciones de cultivo estándar [125, 240, 270, 298], pero sí en ensayos de formación de colonias [93]. De manera similar, se ha descrito que la inhibición farmacológica de HIF2α mediante PT2385 [237], PT2399 [240] o PT2977 [354] no afecta a la proliferación celular *in vitro*, tal y como se vio en esta tesis, pero sí inhibe el crecimiento tumoral *in vivo.* En lo que respecta al crecimiento en 3D, se observó que las 786-0 forman esferas muy compactas, mientras que las células 786-0 que expresan VHL (786-0 VHL$^+$) producen esferoides un poco más laxos [356], tal y como se detectó al añadir PT2385. Es posible que las 786-0 KO hayan adquirido capacidades adicionales a lo largo de los pasajes para crecer como la línea parental, mientras que la inhibición transitoria y parcial de HIF2α por PT2385 muestra que HIF2α es importante para mantener las células agregadas en las esferas.

La incapacidad de las células 786-0 KO para invadir tanto *in vitro* como *in vivo* muestra el papel que ejerce HIF2α en la progresión tumoral. Es posible que HIF2α esté inhibiendo la migración celular, tal y como se vio en un estudio donde dependiendo de la duración de la hipoxia HIF1α podía promover o inhibir la migración [369], pero los resultados de esta tesis muestran que HIF2α es estrictamente necesario para colonizar otros tejidos, primero, en el proceso de invasión, y posteriormente, en la proliferación. Por un lado, las células requirieron de HIF2α para poder invadir a través del Matrigel y, por otro lado, cuando la densidad celular era baja, como ocurre al inicio de las metástasis, las células 786-0 KO presentaron dificultades para crecer. Del mismo modo, las 786-0 KO fueron incapaces de formar metástasis, tal y como se había descrito previamente [361, 377]. Las metástasis en los pulmones aparecieron dos semanas después de la inyección de las células tumorales, pero estas desaparecieron para volver a aparecer 10 semanas más tarde, tal y como se ha observado en algunos pacientes de RCC [176]. Los primeros indicios de remisión de metástasis tras la realización de nefrectomías dieron lugar a la idea de que RCC es un tipo tumoral muy inmunogénico [179], ya que se postuló que el sistema inmune era el principal responsable [176]. Diversos estudios enfatizan la involucración de HIF2α en la regresión tumoral, ya que el empleo de los inhibidores de HIF2α PT2385 [237] y PT2399 [239, 240] dio lugar a la regresión tumoral, y en caso de PT2399, también de metástasis.

En línea con los resultados de esta tesis, se ha descrito que HIF2α no regula la respiración aeróbica en la línea celular 786-0 [413], mientras que parece que sí está involucrado en el metabolismo lipídico. Estudios previos demostraron la relación directa entre HIF2α y las gotas lipídicas, así como la importancia de estas últimas para la progresión tumoral [318, 320]. No obstante, en esta tesis no se pudieron observar mayores acúmulos de gotas lipídicas en las 786-0 WT, en comparación con las 786-0 KO. Además, las 786-0 KO presentaron mayores niveles de fluorescencia para Nile Red, el cual se une a las gotas lipídicas. Estos resultados sugieren que las células 786-0 KO pueden contener más lípidos en el citosol que las 786-0 WT, pero que estos no se encuentran acumulados en gotas lipídicas. Por otro lado, tal y como se había descrito previamente [366, 428], HIF2α inhibió la respiración mitocondrial en las células 786-0 y RCC4, redirigiendo el metabolismo celular.

7.2.4. Conclusiones

1. HIF2α es importante para la proliferación celular en 2D cuando el numero inicial de células es bajo, mientras que no afecta a la proliferación en 3D.
2. La ausencia de HIF2α promueve la migración, pero inhibe la invasión *in vitro* y reduce las metástasis *in vivo.*
3. HIF2α altera el metabolismo inhibiendo la respiración mitocondrial.

7.3. Resistencia a drogas mediada por HIF2α

7.3.1. Introducción

En oncología menos del 10% de las nuevas drogas que pasan los estudios de fase I llegan a ser aprobadas por la FDA (abreviatura del inglés *Food and Drug Administration*), y el número ha ido bajando desde 1950 [434]. Por eso, se está empleando un enfoque distinto en el desarrollo de nuevas terapias, denominado 'reutilización de drogas' (término en inglés *drug repurposing*) [435], que se basa en dar nuevas aplicaciones en oncología a drogas no oncológicas ya conocidas y caracterizadas. Esto reduce el tiempo de desarrollo de las drogas, ya que la farmacocinética, biodisponibilidad y toxicidad es conocida. No obstante, en ciertos casos es necesario ajustar la dosis y por tanto estudios de fase I son necesarios [436]. En este sentido, se han estudiado tres drogas para su uso en RCC: la metformina [440-442], actualmente empleada en el tratamiento de la diabetes tipo 2, las estatinas [450, 451], inhibidoras de la 3-hidroxi-3-metilglutaril-coenzima A reductasa (HMG-CoA reductasa), enzima clave en la síntesis del colesterol, y la mifepristona [453], empleada para dar fin al embarazo.

7.3.2. Resultados

Con la idea de identificar nuevas drogas para el tratamiento de ccRCC en las que HIF2α estuviera implicado se testaron 1600 drogas aprobadas por la FDA en las líneas 786-0 WT y 786-0 KO. Entre ellas, las estatinas fluvastatina y simvastatina mostraron diferencias significativas entre las líneas celulares, tal y como se validó posteriormente. Se observó que HIF2α proporcionaba resistencia a ambas drogas, independientemente del estado el gen *VHL.*

7.3.3. Discusión

Las estatinas inhiben la progresión tumoral a varios niveles, desde el bloqueo de la síntesis de colesterol, que es el principal componente de las membranas celulares, hasta la inhibición de la formación de nuevos vasos sanguíneos [461]. Las células 786-0 KO mostraron mayor sensibilidad al tratamiento con simvastatina y fluvastatina, tal y como se había descrito previamente [450, 465]. Ambos estudios determinaron que el modo de acción de las estatinas implicaba la vía de mTOR, una ruta actualmente diana en el tratamiento de ccRCC, por lo que la utilización de las estatinas en ccRCC es prometedora, aunque requiere de más estudios.

7.3.4. Conclusiones

1. La línea celular carente de HIF2α es más sensible que la 786-0 WT al tratamiento con estatinas.

7.4. Regulación de la vía del interferón tipo I

7.4.1. Introducción

Los interferones (IFNs) son un conjunto de citoquinas que se clasifican en tres tipos: tipo I, tipo II y tipo III [473]. En humanos, los de tipo I constan de 13 subtipos de IFNα, IFNβ, IFNε, IFNκ e IFNω. Mientras que los de tipo II y tipo III contienen un único miembro, IFNγ e IFNλ, respectivamente. Estas citoquinas están involucradas en la respuesta inmune del organismo contra agentes patógenos, ya que tras la detección de los agentes infecciosos (el material genético o los polisacáridos presentes en la membrana) conocidos como PAMPs (del inglés *pathogen-associated molecular patterns*), por unos receptores celulares denominados PRRs (del inglés *pattern-recognition receptors*) [474-476], las células producen y secretan IFNs para activar una respuesta inmune contra el agente infeccioso. Los IFNs pueden inducir la muerte de la célula infectada, o pueden actuar de forma paracrina sobre células no infectadas estimulándolas a producir una batería de genes denominados ISGs (del inglés *IFN-stimulated genes*) para prevenir la propagación de la infección [477].

Dentro de los PRRs citosólicos se encuentran RIG-I (del inglés *retinoic acid-inducible gene I*) y MDA5 (abreviatura del inglés *melanoma differentiation-associated gene 5*) que detectan ARN de doble cadena (dsRNA), además de cGAS (del inglés *cyclic GMP-AMP (cGAMP) synthase*), DDX41 (del inglés *DExD/Hbox helicase 41*), DAI (abreviatura de inglés *DNA-dependent activator of IFN-regulatory factors*) e IFI16 (del inglés *IFN-γ-inducible factor 16*) que identifican ADN de doble cadena (dsDNA). Los PRRs transmembrana están formados por la familia de receptores TLR (del inglés *Toll-like receptor*). Independientemente de la localización de los receptores, después de interaccionar con el agente patógeno, estos activan la vía del IFN. La señal comienza en los receptores y a través de proteínas adaptadoras, finaliza con la fosforilación de IRF3 e IRF7, que tras formar dímeros inducirán la expresión de quimioquinas, citoquinas inflamatorias e IFNβ [484-486]. Los IFNs secretados se unen a los receptores IFNAR presentes en células no infectadas, y a través de moléculas adaptadoras y trasmisoras de la señal, generarán la formación de complejos específicos capaces de translocarse al núcleo y promover la activación de ISGs [510].

Es conocido que la hipoxia genera un ambiente inmunosupresor dentro del tumor, ya que impide la estabilización de células inmunes efectoras y bloquea su actividad. Es más, en regiones hipóxicas la cantidad de células inmunosupresoras como MDSC (del inglés *myeloid-derived supressor cells*), TAM (abreviatura del inglés *tumour-associated macrophages*) y células Treg (del inglés *regulatory T cells*) es elevada [119, 590], lo cual conlleva a la evasión del sistema inmune y por tanto facilita el crecimiento tumoral [1]. Sin embargo, el efecto de la hipoxia en la vía del IFN tipo I aún no se ha estudiado.

Por otro lado, se ha descrito que las mitocondrias son orgánulos altamente inmunogénicos debido a su origen bacteriano [627]. El dsRNA procedente de la transcripción del ADN mitocondrial (mtDNA), por ejemplo, se identificó en 2018 como un potente estimulador de la vía del IFN tipo I si era liberado al citosol [657]. Las células por tanto llevan un control estricto de las mitocondrias, bien para evitar la activación del sistema inmune por moléculas propias o bien para asegurar la total capacidad celular de producir energía, ya que la mitocondria es el principal orgánulo de síntesis de energía [626]. La mitofagia, o la autofagia mitocondrial, es el principal mecanismo por el que las células eliminan las mitocondrias no funcionales [667].

En este capítulo se describe el efecto de la hipoxia sobre la vía del IFN tipo I y la involucración del dsRNA mitocondrial en el proceso.

7.4.2. Resultados

7.4.2.1. La hipoxia disminuye la activación de la vía del IFN tipo I

La hipoxia generó una disminución en la activación de la vía del IFN tipo I tanto en condiciones basales como después de haber sido estimulada con el análogo de dsRNA poly I:C (del inglés *polyinosinic-polycytidylic acid*). La inhibición se observó a nivel de ARN y proteína en diferentes moléculas de la ruta, pero notablemente en los niveles de fosforilación de STAT1 e IRF3, y fue dependiente de oxígeno, ya que 0.1% de hipoxia generó mayor inhibición que 1%. Además, la reoxigenación celular tras la exposición a hipoxia permitió a las células recuperar la activación de la ruta de manera gradual. Esta inhibición ejercida por hipoxia mostró ser parcialmente independiente de HIF1α y HIF2α. Algunos miembros de la ruta como RIG-I y STAT1 sí mostraron estar inhibidos por HIF1α, aunque la exposición a hipoxia también los inhibió, mostrando que el efecto hipóxico es independiente del ejercido por HIF1α. HIF2α, sin embargo, no pareció estar involucrado en la regulación de la vía del IFN tipo I, ya que la inhibición hipóxica se pudo detectar tanto en células que expresaban HIF2α como en células que no.

7.4.2.2. El ARN total procedente de células hipóxicas disminuye la activación del promotor de IFNβ

Empleando el ensayo de activación del promotor de IFNβ, se observó que la mayor parte de la señalización era inducida por dsRNA. La activación disminuyó notablemente al utilizar ARN de células hipóxicas, del mismo modo que se recuperó al emplear ARN procedente de células sometidas a reoxigenación. En este ensayo también se observó que la inhibición ejercida por hipoxia no dependía de HIF1α y HIF2α, ya que independientemente de la expresión de HIF1α y HIF2α el ARN procedente de células hipóxicas generó menor activación del promotor de IFNβ.

7.4.2.3. Los niveles de dsRNA en hipoxia son más bajos que en normoxia debido a una menor transcripción del mtDNA

El ensayo de estimulación del promotor de IFNβ sugirió que los niveles de dsRNA en hipoxia eran inferiores a los de normoxia, tal y como se comprobó mediante inmunofluorescencia. Los menores niveles de dsRNA en hipoxia no fueron consecuencia de una mayor degradación, ya que la expresión de las enzimas PNPT1 (del inglés *polyribonucleotide nucleotidyltransferase 1*) y de la ARN helicasa SUV3 no incrementó en hipoxia. No obstante, sí se observaron menores niveles de ARN de moléculas involucradas en la transcripción del mtDNA en condiciones de hipoxia, sugiriendo que la menor cantidad de dsRNA en hipoxia puede deberse a una menor transcripción del mtDNA. Además, se detectó que los niveles de ARN de genes que codifican proteínas ribosómicas mitocondriales (MRP) era menor en hipoxia que en normoxia, sugiriendo también que una posterior disminución en la traducción puede prevenir a la célula de sintetizar ARN. Asimismo, se descartó la mitofagia como posible causa de la menor cantidad de dsRNA mitocondrial en hipoxia.

7.4.2.4. El dsRNA mitocondrial activa al promotor de IFNβ

Dado que la hipoxia disminuyó la vía del IFN tipo I y la transcripción del mtDNA, se investigó si los menores niveles de dsRNA mitocondrial eran la causa de la menor activación de la vía de IFN tipo I. El ARN procedente de la mitocondria y no el del citosol fue el que activó al promotor de IFNβ, activación que se disminuyó notablemente cuando el ARN empleado procedía de células hipóxicas.

7.4.3. Discusión

En esta tesis se describe un nuevo mecanismo de inmunosupresión ejercido por hipoxia, a través de la regulación negativa de la vía del IFN tipo I. En general, la hipoxia inhibe la transcripción génica, a excepción de los genes activados mediante HIF, y la síntesis proteica, ya que es un proceso que requiere mucha energía [716, 717]. En esta tesis se detectaron menos niveles de ARN y proteína de miembros de la vía del IFN tipo I en condiciones de hipoxia. Además, al exponer las células a normoxia después de haber sido sometidas a hipoxia, se revertió el efecto inducido por hipoxia de manera gradual, tal y como se había descrito previamente [721]. Es más, el efecto negativo de hipoxia mostró ser parcialmente independiente de la expresión de HIF1α, incluso después de haber activado la vía del IFN tipo I con poly I:C. Un estudio detectó el mismo efecto al someter las células a 2% de hipoxia después de haberlas tratado con el activador de la vía del IFN tipo I 3pRNA [726]. Apoyando la diferencia entre hipoxia y HIF, se descubrió que la inhibición transcripcional generada por hipoxia era independiente de HIF1α, pero que dependía de modificaciones producidas en la cromatina [729], sugiriendo que la hipoxia induce modificaciones en el material genético y en las histonas y modula así la expresión génica.

Por otro lado, el dsRNA procedente de la mitocondria promovió la activación del promotor de IFNβ, dato respaldado por un estudio que muestra que el 99% del dsRNA celular se origina en la mitocondria [657]. Si este dsRNA es liberado al citosol, puede desencadenar la activación de una respuesta inmune, ya que la célula lo identifica como extranjero [657]. Para evitar esta activación inmune, las células tienen diversos mecanismos que degradan el dsRNA, como son las enzimas PNPT1 y SUV3 [734]. Sin embargo, en esta tesis la reducción en los niveles de dsRNA mitocondrial en hipoxia no se debió a un incremento en su degradación, ni tampoco fue consecuencia de una mayor mitofagia, que eliminaría mitocondrias hipóxicas no funcionales [665]. Los resultados de esta tesis apuntan a una menor transcripción del mtDNA en condiciones de hipoxia, similar a la inhibición de la transcripción nuclear, que llevaría a la disminución de los niveles de dsRNA celulares, tal y como se detectó por inmunofluorescencia, y menor estimulación de la vía del IFN tipo I.

La hipoxia genera un ambiente inmunosupresor dentro de la masa tumoral que permite el crecimiento tumoral y promueve la evasión del sistema inmune. Además, se conoce que el éxito de muchos tratamientos oncológicos requieren que la vía del IFN tipo I sea funcional [127]. Por lo que la disminución de la activación de esta vía en condiciones de hipoxia puede generar un impacto negativo en el tratamiento, además del ya generado por la hipoxia. Los resultados presentados en esta tesis sugieren que futuros tratamientos deberían considerar no sólo el efecto inmunosupresor de la hipoxia, si no también tener en cuenta las causas de esa inmunosupresión, como puede ser una menor transcripción del mtDNA.

7.4.4. Conclusiones

1. La hipoxia inhibe la vía del IFN tipo I en condiciones basales y tras la estimulación con poly I:C independientemente de HIF1α/HIF2α.
2. La vía del IFN tipo I es activada por el dsRNA originado en la mitocondria, cuyos niveles disminuyen en hipoxia debido a una reducción en la transcripción, y no debido a una mayor degradación o mitofagia.

8. References

1. Hanahan, D. and R.A. Weinberg, *The hallmarks of cancer.* Cell, 2000. **100**(1): p. 57-70.
2. Hanahan, D. and R.A. Weinberg, *Hallmarks of cancer: the next generation.* Cell, 2011. **144**(5): p. 646-74.
3. Fedi, P., S. Tronick, and S. Aaronson, *Growth factors.* Cancer medicine, 1997: p. 41-64.
4. Giancotti, F.G. and E. Ruoslahti, *Integrin signaling.* Science, 1999. **285**(5430): p. 1028-32.
5. Medema, R.H. and J.L. Bos, *The role of p21ras in receptor tyrosine kinase signaling.* Crit Rev Oncog, 1993. **4**(6): p. 615-61.
6. Weinberg, R.A., *The retinoblastoma protein and cell cycle control.* Cell, 1995. **81**(3): p. 323-30.
7. Fynan, T.M. and M. Reiss, *Resistance to inhibition of cell growth by transforming growth factor-beta and its role in oncogenesis.* Crit Rev Oncog, 1993. **4**(5): p. 493-540.
8. Evan, G. and T. Littlewood, *A matter of life and cell death.* Science, 1998. **281**(5381): p. 1317-22.
9. Hayflick, L., *Mortality and immortality at the cellular level. A review.* Biochemistry (Mosc), 1997. **62**(11): p. 1180-90.
10. Blasco, M.A., *Telomeres and human disease: ageing, cancer and beyond.* Nat Rev Genet, 2005. **6**(8): p. 611-22.
11. Hanahan, D. and J. Folkman, *Patterns and emerging mechanisms of the angiogenic switch during tumorigenesis.* Cell, 1996. **86**(3): p. 353-64.
12. Whitelock, J.M., et al., *The degradation of human endothelial cell-derived perlecan and release of bound basic fibroblast growth factor by stromelysin, collagenase, plasmin, and heparanases.* J Biol Chem, 1996. **271**(17): p. 10079-86.
13. Valastyan, S. and R.A. Weinberg, *Tumor metastasis: molecular insights and evolving paradigms.* Cell, 2011. **147**(2): p. 275-92.
14. Coussens, L.M. and Z. Werb, *Matrix metalloproteinases and the development of cancer.* Chem Biol, 1996. **3**(11): p. 895-904.
15. Varner, J.A. and D.A. Cheresh, *Integrins and cancer.* Curr Opin Cell Biol, 1996. **8**(5): p. 724-30.
16. Lengauer, C., K.W. Kinzler, and B. Vogelstein, *Genetic instabilities in human cancers.* Nature, 1998. **396**(6712): p. 643-9.
17. Levine, A.J., *p53, the cellular gatekeeper for growth and division.* Cell, 1997. **88**(3): p. 323-31.
18. DeNardo, D.G., P. Andreu, and L.M. Coussens, *Interactions between lymphocytes and myeloid cells regulate pro- versus anti-tumor immunity.* Cancer Metastasis Rev, 2010. **29**(2): p. 309-16.
19. Grivennikov, S.I., F.R. Greten, and M. Karin, *Immunity, inflammation, and cancer.* Cell, 2010. **140**(6): p. 883-99.
20. Qian, B.Z. and J.W. Pollard, *Macrophage diversity enhances tumor progression and metastasis.* Cell, 2010. **141**(1): p. 39-51.
21. Warburg, O., *On the origin of cancer cells.* Science, 1956. **123**(3191): p. 309-14.
22. Feron, O., *Pyruvate into lactate and back: from the Warburg effect to symbiotic energy fuel exchange in cancer cells.* Radiother Oncol, 2009. **92**(3): p. 329-33.
23. Kennedy, K.M. and M.W. Dewhirst, *Tumor metabolism of lactate: the influence and therapeutic potential for MCT and CD147 regulation.* Future Oncol, 2010. **6**(1): p. 127-48.
24. Semenza, G.L., *Tumor metabolism: cancer cells give and take lactate.* J Clin Invest, 2008. **118**(12): p. 3835-7.
25. Dunn, G.P., L.J. Old, and R.D. Schreiber, *The three Es of cancer immunoediting.* Annu Rev Immunol, 2004. **22**: p. 329-60.
26. Buchbinder, E.I. and A. Desai, *CTLA-4 and PD-1 Pathways: Similarities, Differences, and Implications of Their Inhibition.* Am J Clin Oncol, 2016. **39**(1): p. 98-106.
27. Shields, J.D., et al., *Induction of lymphoidlike stroma and immune escape by tumors that express the chemokine CCL21.* Science, 2010. **328**(5979): p. 749-52.
28. Yang, L., Y. Pang, and H.L. Moses, *TGF-beta and immune cells: an important regulatory axis in the tumor microenvironment and progression.* Trends Immunol, 2010. **31**(6): p. 220-7.
29. Mougiakakos, D., et al., *Regulatory T cells in cancer.* Adv Cancer Res, 2010. **107**: p. 57-117.
30. Ostrand-Rosenberg, S. and P. Sinha, *Myeloid-derived suppressor cells: linking inflammation and cancer.* J Immunol, 2009. **182**(8): p. 4499-506.
31. Semenza, G.L. and G.L. Wang, *A nuclear factor induced by hypoxia via de novo protein synthesis binds to the human erythropoietin gene enhancer at a site required for transcriptional activation.* Mol Cell Biol, 1992. **12**(12): p. 5447-54.
32. Tian, H., S.L. McKnight, and D.W. Russell, *Endothelial PAS domain protein 1 (EPAS1), a transcription factor selectively expressed in endothelial cells.* Genes Dev, 1997. **11**(1): p. 72-82.
33. Wang, G.L., et al., *Hypoxia-inducible factor 1 is a basic-helix-loop-helix-PAS heterodimer regulated by cellular O2 tension.* Proc Natl Acad Sci U S A, 1995. **92**(12): p. 5510-4.
34. Bertout, J.A., S.A. Patel, and M.C. Simon, *The impact of O2 availability on human cancer.* Nat Rev Cancer, 2008. **8**(12): p. 967-75.

35. Ema, M., et al., *A novel bHLH-PAS factor with close sequence similarity to hypoxia-inducible factor 1alpha regulates the VEGF expression and is potentially involved in lung and vascular development.* Proc Natl Acad Sci U S A, 1997. **94**(9): p. 4273-8.
36. Gu, Y.Z., et al., *Molecular characterization and chromosomal localization of a third alpha-class hypoxia inducible factor subunit, HIF3alpha.* Gene Expr, 1998. **7**(3): p. 205-13.
37. Makino, Y., et al., *Inhibitory PAS domain protein (IPAS) is a hypoxia-inducible splicing variant of the hypoxia-inducible factor-3alpha locus.* J Biol Chem, 2002. **277**(36): p. 32405-8.
38. Hara, S., et al., *Expression and characterization of hypoxia-inducible factor (HIF)-3alpha in human kidney: suppression of HIF-mediated gene expression by HIF-3alpha.* Biochem Biophys Res Commun, 2001. **287**(4): p. 808-13.
39. Dengler, V.L., M. Galbraith, and J.M. Espinosa, *Transcriptional regulation by hypoxia inducible factors.* Crit Rev Biochem Mol Biol, 2014. **49**(1): p. 1-15.
40. Hu, C.J., et al., *The N-terminal transactivation domain confers target gene specificity of hypoxia-inducible factors HIF-1alpha and HIF-2alpha.* Mol Biol Cell, 2007. **18**(11): p. 4528-42.
41. Huang, L.E., et al., *Regulation of hypoxia-inducible factor 1alpha is mediated by an O2-dependent degradation domain via the ubiquitin-proteasome pathway.* Proc Natl Acad Sci U S A, 1998. **95**(14): p. 7987-92.
42. Jiang, B.H., et al., *Transactivation and inhibitory domains of hypoxia-inducible factor 1alpha. Modulation of transcriptional activity by oxygen tension.* J Biol Chem, 1997. **272**(31): p. 19253-60.
43. Appelhoff, R.J., et al., *Differential function of the prolyl hydroxylases PHD1, PHD2, and PHD3 in the regulation of hypoxia-inducible factor.* J Biol Chem, 2004. **279**(37): p. 38458-65.
44. Berra, E., et al., *HIF prolyl-hydroxylase 2 is the key oxygen sensor setting low steady-state levels of HIF-1alpha in normoxia.* Embo j, 2003. **22**(16): p. 4082-90.
45. Ohh, M., et al., *Ubiquitination of hypoxia-inducible factor requires direct binding to the beta-domain of the von Hippel-Lindau protein.* Nat Cell Biol, 2000. **2**(7): p. 423-7.
46. Latif, F., et al., *Identification of the von Hippel-Lindau disease tumor suppressor gene.* Science, 1993. **260**(5112): p. 1317-20.
47. Kuznetsova, A.V., et al., *von Hippel-Lindau protein binds hyperphosphorylated large subunit of RNA polymerase II through a proline hydroxylation motif and targets it for ubiquitination.* Proc Natl Acad Sci U S A, 2003. **100**(5): p. 2706-11.
48. Okuda, H., et al., *Direct interaction of the beta-domain of VHL tumor suppressor protein with the regulatory domain of atypical PKC isotypes.* Biochem Biophys Res Commun, 1999. **263**(2): p. 491-7.
49. Grosfeld, A., et al., *Interaction of hydroxylated collagen IV with the von hippel-lindau tumor suppressor.* J Biol Chem, 2007. **282**(18): p. 13264-9.
50. Ohh, M., et al., *The von Hippel-Lindau tumor suppressor protein is required for proper assembly of an extracellular fibronectin matrix.* Mol Cell, 1998. **1**(7): p. 959-68.
51. Schermer, B., et al., *The von Hippel-Lindau tumor suppressor protein controls ciliogenesis by orienting microtubule growth.* J Cell Biol, 2006. **175**(4): p. 547-54.
52. Ohh, M., et al., *Synthetic peptides define critical contacts between elongin C, elongin B, and the von Hippel-Lindau protein.* J Clin Invest, 1999. **104**(11): p. 1583-91.
53. Kamura, T., et al., *Rbx1, a component of the VHL tumor suppressor complex and SCF ubiquitin ligase.* Science, 1999. **284**(5414): p. 657-61.
54. Pause, A., et al., *The von Hippel-Lindau tumor-suppressor gene product forms a stable complex with human CUL-2, a member of the Cdc53 family of proteins.* Proc Natl Acad Sci U S A, 1997. **94**(6): p. 2156-61.
55. Boyer, R., *Posttranslational modification of proteins: Expanding nature's inventory. Christopher T. Walsh, Roberts & Company Publishers, Greenwood Village, CO, 2005, 576 pp., ISBN 0-9747077-3-2, $98.00.* Biochemistry and Molecular Biology Education, 2006. **34**(6): p. 461-462.
56. Cardote, T.A.F., M.S. Gadd, and A. Ciulli, *Crystal Structure of the Cul2-Rbx1-EloBC-VHL Ubiquitin Ligase Complex.* Structure, 2017. **25**(6): p. 901-911.e3.
57. Lando, D., et al., *FIH-1 is an asparaginyl hydroxylase enzyme that regulates the transcriptional activity of hypoxia-inducible factor.* Genes Dev, 2002. **16**(12): p. 1466-71.
58. Mahon, P.C., K. Hirota, and G.L. Semenza, *FIH-1: a novel protein that interacts with HIF-1alpha and VHL to mediate repression of HIF-1 transcriptional activity.* Genes Dev, 2001. **15**(20): p. 2675-86.
59. Klimova, T. and N.S. Chandel, *Mitochondrial complex III regulates hypoxic activation of HIF.* Cell Death Differ, 2008. **15**(4): p. 660-6.
60. Waypa, G.B., et al., *Hypoxia triggers subcellular compartmental redox signaling in vascular smooth muscle cells.* Circ Res, 2010. **106**(3): p. 526-35.

61. Ivan, M., et al., *HIFalpha targeted for VHL-mediated destruction by proline hydroxylation: implications for O2 sensing.* Science, 2001. **292**(5516): p. 464-8.
62. Salnikow, K., et al., *Regulation of hypoxia-inducible genes by ETS1 transcription factor.* Carcinogenesis, 2008. **29**(8): p. 1493-9.
63. Laughner, E., et al., *HER2 (neu) signaling increases the rate of hypoxia-inducible factor 1alpha (HIF-1alpha) synthesis: novel mechanism for HIF-1-mediated vascular endothelial growth factor expression.* Mol Cell Biol, 2001. **21**(12): p. 3995-4004.
64. Lu, H., R.A. Forbes, and A. Verma, *Hypoxia-inducible factor 1 activation by aerobic glycolysis implicates the Warburg effect in carcinogenesis.* J Biol Chem, 2002. **277**(26): p. 23111-5.
65. Koh, M.Y., B.G. Darnay, and G. Powis, *Hypoxia-associated factor, a novel E3-ubiquitin ligase, binds and ubiquitinates hypoxia-inducible factor 1alpha, leading to its oxygen-independent degradation.* Mol Cell Biol, 2008. **28**(23): p. 7081-95.
66. Luo, W., et al., *Hsp70 and CHIP selectively mediate ubiquitination and degradation of hypoxia-inducible factor (HIF)-1alpha but Not HIF-2alpha.* J Biol Chem, 2010. **285**(6): p. 3651-63.
67. Richard, D.E., et al., *p42/p44 mitogen-activated protein kinases phosphorylate hypoxia-inducible factor 1alpha (HIF-1alpha) and enhance the transcriptional activity of HIF-1.* J Biol Chem, 1999. **274**(46): p. 32631-7.
68. Kalousi, A., et al., *Casein kinase 1 regulates human hypoxia-inducible factor HIF-1.* J Cell Sci, 2010. **123**(Pt 17): p. 2976-86.
69. Geng, H., et al., *HIF1alpha protein stability is increased by acetylation at lysine 709.* J Biol Chem, 2012. **287**(42): p. 35496-505.
70. Mole, D.R., et al., *Genome-wide association of hypoxia-inducible factor (HIF)-1alpha and HIF-2alpha DNA binding with expression profiling of hypoxia-inducible transcripts.* J Biol Chem, 2009. **284**(25): p. 16767-75.
71. Schodel, J., D.R. Mole, and P.J. Ratcliffe, *Pan-genomic binding of hypoxia-inducible transcription factors.* Biol Chem, 2013. **394**(4): p. 507-17.
72. Schodel, J., et al., *High-resolution genome-wide mapping of HIF-binding sites by ChIP-seq.* Blood, 2011. **117**(23): p. e207-17.
73. Villar, D., et al., *Cooperativity of stress-responsive transcription factors in core hypoxia-inducible factor binding regions.* PLoS One, 2012. **7**(9): p. e45708.
74. Pawlus, M.R., L. Wang, and C.J. Hu, *STAT3 and HIF1alpha cooperatively activate HIF1 target genes in MDA-MB-231 and RCC4 cells.* Oncogene, 2014. **33**(13): p. 1670-9.
75. Arany, Z., et al., *An essential role for p300/CBP in the cellular response to hypoxia.* Proc Natl Acad Sci U S A, 1996. **93**(23): p. 12969-73.
76. Bedford, D.C., et al., *Target gene context influences the transcriptional requirement for the KAT3 family of CBP and p300 histone acetyltransferases.* Epigenetics, 2010. **5**(1): p. 9-15.
77. Carrero, P., et al., *Redox-regulated recruitment of the transcriptional coactivators CREB-binding protein and SRC-1 to hypoxia-inducible factor 1alpha.* Mol Cell Biol, 2000. **20**(1): p. 402-15.
78. Ebert, B.L. and H.F. Bunn, *Regulation of transcription by hypoxia requires a multiprotein complex that includes hypoxia-inducible factor 1, an adjacent transcription factor, and p300/CREB binding protein.* Mol Cell Biol, 1998. **18**(7): p. 4089-96.
79. Luo, W., et al., *Pyruvate kinase M2 is a PHD3-stimulated coactivator for hypoxia-inducible factor 1.* Cell, 2011. **145**(5): p. 732-44.
80. Galbraith, M.D., et al., *HIF1A employs CDK8-mediator to stimulate RNAPII elongation in response to hypoxia.* Cell, 2013. **153**(6): p. 1327-39.
81. Kenneth, N.S., et al., *SWI/SNF regulates the cellular response to hypoxia.* J Biol Chem, 2009. **284**(7): p. 4123-31.
82. Beischlag, T.V., et al., *Recruitment of thyroid hormone receptor/retinoblastoma-interacting protein 230 by the aryl hydrocarbon receptor nuclear translocator is required for the transcriptional response to both dioxin and hypoxia.* J Biol Chem, 2004. **279**(52): p. 54620-8.
83. Kim, J.H. and M.R. Stallcup, *Role of the coiled-coil coactivator (CoCoA) in aryl hydrocarbon receptor-mediated transcription.* J Biol Chem, 2004. **279**(48): p. 49842-8.
84. Freedman, S.J., et al., *Structural basis for negative regulation of hypoxia-inducible factor-1alpha by CITED2.* Nat Struct Biol, 2003. **10**(7): p. 504-12.
85. Yoon, H., et al., *CITED2 controls the hypoxic signaling by snatching p300 from the two distinct activation domains of HIF-1alpha.* Biochim Biophys Acta, 2011. **1813**(12): p. 2008-16.
86. Zhong, L., et al., *The histone deacetylase Sirt6 regulates glucose homeostasis via Hif1alpha.* Cell, 2010. **140**(2): p. 280-93.

87. Lim, J.H., et al., *Sirtuin 1 modulates cellular responses to hypoxia by deacetylating hypoxia-inducible factor 1alpha.* Mol Cell, 2010. **38**(6): p. 864-78.
88. Dioum, E.M., et al., *HIF-2alpha-haploinsufficient mice have blunted retinal neovascularization due to impaired expression of a proangiogenic gene battery.* Invest Ophthalmol Vis Sci, 2008. **49**(6): p. 2714-20.
89. Xia, X. and A.L. Kung, *Preferential binding of HIF-1 to transcriptionally active loci determines cell-type specific response to hypoxia.* Genome Biol, 2009. **10**(10): p. R113.
90. Koh, M.Y., et al., *The hypoxia-associated factor switches cells from HIF-1alpha- to HIF-2alpha-dependent signaling promoting stem cell characteristics, aggressive tumor growth and invasion.* Cancer Res, 2011. **71**(11): p. 4015-27.
91. Koh, M.Y. and G. Powis, *Passing the baton: the HIF switch.* Trends Biochem Sci, 2012. **37**(9): p. 364-72.
92. Gordan, J.D., et al., *HIF-2alpha promotes hypoxic cell proliferation by enhancing c-myc transcriptional activity.* Cancer Cell, 2007. **11**(4): p. 335-47.
93. Bertout, J.A., et al., *HIF2alpha inhibition promotes p53 pathway activity, tumor cell death, and radiation responses.* Proc Natl Acad Sci U S A, 2009. **106**(34): p. 14391-6.
94. Rey, S. and G.L. Semenza, *Hypoxia-inducible factor-1-dependent mechanisms of vascularization and vascular remodelling.* Cardiovasc Res, 2010. **86**(2): p. 236-42.
95. Du, R., et al., *HIF1alpha induces the recruitment of bone marrow-derived vascular modulatory cells to regulate tumor angiogenesis and invasion.* Cancer Cell, 2008. **13**(3): p. 206-20.
96. Lee, K., et al., *Anthracycline chemotherapy inhibits HIF-1 transcriptional activity and tumor-induced mobilization of circulating angiogenic cells.* Proc Natl Acad Sci U S A, 2009. **106**(7): p. 2353-8.
97. Carmeliet, P. and R.K. Jain, *Principles and mechanisms of vessel normalization for cancer and other angiogenic diseases.* Nat Rev Drug Discov, 2011. **10**(6): p. 417-27.
98. Semenza, G.L., *Regulation of metabolism by hypoxia-inducible factor 1.* Cold Spring Harb Symp Quant Biol, 2011. **76**: p. 347-53.
99. Semenza, G.L., *HIF-1 mediates metabolic responses to intratumoral hypoxia and oncogenic mutations.* J Clin Invest, 2013. **123**(9): p. 3664-71.
100. Bensaad, K., et al., *Fatty acid uptake and lipid storage induced by HIF-1alpha contribute to cell growth and survival after hypoxia-reoxygenation.* Cell Rep, 2014. **9**(1): p. 349-365.
101. Metallo, C.M., et al., *Reductive glutamine metabolism by IDH1 mediates lipogenesis under hypoxia.* Nature, 2011. **481**(7381): p. 380-4.
102. Ye, J., et al., *Serine catabolism regulates mitochondrial redox control during hypoxia.* Cancer Discov, 2014. **4**(12): p. 1406-17.
103. Pescador, N., et al., *Hypoxia promotes glycogen accumulation through hypoxia inducible factor (HIF)-mediated induction of glycogen synthase 1.* PLoS One, 2010. **5**(3): p. e9644.
104. Wong, C.C., et al., *Inhibitors of hypoxia-inducible factor 1 block breast cancer metastatic niche formation and lung metastasis.* J Mol Med (Berl), 2012. **90**(7): p. 803-15.
105. Zhang, H., et al., *HIF-1-dependent expression of angiopoietin-like 4 and L1CAM mediates vascular metastasis of hypoxic breast cancer cells to the lungs.* Oncogene, 2012. **31**(14): p. 1757-70.
106. Schito, L., et al., *Hypoxia-inducible factor 1-dependent expression of platelet-derived growth factor B promotes lymphatic metastasis of hypoxic breast cancer cells.* Proc Natl Acad Sci U S A, 2012. **109**(40): p. E2707-16.
107. Gilkes, D.M. and G.L. Semenza, *Role of hypoxia-inducible factors in breast cancer metastasis.* Future Oncol, 2013. **9**(11): p. 1623-36.
108. Lamouille, S., J. Xu, and R. Derynck, *Molecular mechanisms of epithelial-mesenchymal transition.* Nat Rev Mol Cell Biol, 2014. **15**(3): p. 178-96.
109. Jin, F., et al., *New insight into the SDF-1/CXCR4 axis in a breast carcinoma model: hypoxia-induced endothelial SDF-1 and tumor cell CXCR4 are required for tumor cell intravasation.* Mol Cancer Res, 2012. **10**(8): p. 1021-31.
110. Rankin, E.B. and A.J. Giaccia, *Hypoxic control of metastasis.* Science, 2016. **352**(6282): p. 175-80.
111. Rohwer, N., et al., *Hypoxia-inducible factor 1alpha mediates anoikis resistance via suppression of alpha5 integrin.* Cancer Res, 2008. **68**(24): p. 10113-20.
112. Psaila, B. and D. Lyden, *The metastatic niche: adapting the foreign soil.* Nat Rev Cancer, 2009. **9**(4): p. 285-93.
113. Cox, T.R., et al., *The hypoxic cancer secretome induces pre-metastatic bone lesions through lysyl oxidase.* Nature, 2015. **522**(7554): p. 106-110.
114. Erler, J.T., et al., *Hypoxia-induced lysyl oxidase is a critical mediator of bone marrow cell recruitment to form the premetastatic niche.* Cancer Cell, 2009. **15**(1): p. 35-44.
115. Zhang, H., et al., *HIF-1 regulates CD47 expression in breast cancer cells to promote evasion of phagocytosis and maintenance of cancer stem cells.* Proc Natl Acad Sci U S A, 2015. **112**(45): p. E6215-23.

116. Barsoum, I.B., et al., *A mechanism of hypoxia-mediated escape from adaptive immunity in cancer cells.* Cancer Res, 2014. **74**(3): p. 665-74.
117. Topalian, S.L., C.G. Drake, and D.M. Pardoll, *Immune checkpoint blockade: a common denominator approach to cancer therapy.* Cancer Cell, 2015. **27**(4): p. 450-61.
118. Hatfield, S.M., et al., *Systemic oxygenation weakens the hypoxia and hypoxia inducible factor 1alpha-dependent and extracellular adenosine-mediated tumor protection.* J Mol Med (Berl), 2014. **92**(12): p. 1283-92.
119. Noman, M.Z., et al., *Hypoxia: a key player in antitumor immune response. A Review in the Theme: Cellular Responses to Hypoxia.* Am J Physiol Cell Physiol, 2015. **309**(9): p. C569-79.
120. Chang, C.H., et al., *Metabolic Competition in the Tumor Microenvironment Is a Driver of Cancer Progression.* Cell, 2015. **162**(6): p. 1229-41.
121. Ho, P.C., et al., *Phosphoenolpyruvate Is a Metabolic Checkpoint of Anti-tumor T Cell Responses.* Cell, 2015. **162**(6): p. 1217-28.
122. Herr, B., et al., *The supernatant of apoptotic cells causes transcriptional activation of hypoxia-inducible factor-1alpha in macrophages via sphingosine-1-phosphate and transforming growth factor-beta.* Blood, 2009. **114**(10): p. 2140-8.
123. Jochmanova, I., et al., *Hypoxia-inducible factor signaling in pheochromocytoma: turning the rudder in the right direction.* J Natl Cancer Inst, 2013. **105**(17): p. 1270-83.
124. Schodel, J., et al., *Hypoxia, Hypoxia-inducible Transcription Factors, and Renal Cancer.* Eur Urol, 2016. **69**(4): p. 646-657.
125. Raval, R.R., et al., *Contrasting properties of hypoxia-inducible factor 1 (HIF-1) and HIF-2 in von Hippel-Lindau-associated renal cell carcinoma.* Mol Cell Biol, 2005. **25**(13): p. 5675-86.
126. Kondo, K., et al., *Inhibition of HIF is necessary for tumor suppression by the von Hippel-Lindau protein.* Cancer Cell, 2002. **1**(3): p. 237-46.
127. Zitvogel, L., et al., *Type I interferons in anticancer immunity.* Nat Rev Immunol, 2015. **15**(7): p. 405-14.
128. Tarhini, A.A., H. Gogas, and J.M. Kirkwood, *IFN-alpha in the treatment of melanoma.* J Immunol, 2012. **189**(8): p. 3789-93.
129. Ardizzoni, A., et al., *Combination chemotherapy and interferon alpha 2b in the treatment of advanced non-small-cell lung cancer. The Italian Lung Cancer Task Force (FONICAP).* Am J Clin Oncol, 1991. **14**(2): p. 120-3.
130. Lawrence, M.S., et al., *Mutational heterogeneity in cancer and the search for new cancer-associated genes.* Nature, 2013. **499**(7457): p. 214-218.
131. Topalian, S.L., et al., *Safety, activity, and immune correlates of anti-PD-1 antibody in cancer.* N Engl J Med, 2012. **366**(26): p. 2443-54.
132. Brahmer, J.R., et al., *Phase I study of single-agent anti-programmed death-1 (MDX-1106) in refractory solid tumors: safety, clinical activity, pharmacodynamics, and immunologic correlates.* J Clin Oncol, 2010. **28**(19): p. 3167-75.
133. Liang, Y., et al., *Targeting IFNα to tumor by anti-PD-L1 creates feedforward antitumor responses to overcome checkpoint blockade resistance.* Nature Communications, 2018. **9**(1): p. 4586.
134. Garcia-Diaz, A., et al., *Interferon Receptor Signaling Pathways Regulating PD-L1 and PD-L2 Expression.* Cell Rep, 2017. **19**(6): p. 1189-1201.
135. Dunn, G.P., et al., *A critical function for type I interferons in cancer immunoediting.* Nat Immunol, 2005. **6**(7): p. 722-9.
136. Karakashev, S.V. and M.J. Reginato, *Progress toward overcoming hypoxia-induced resistance to solid tumor therapy.* Cancer Manag Res, 2015. **7**: p. 253-64.
137. Capitanio, U., et al., *Epidemiology of Renal Cell Carcinoma.* Eur Urol, 2019. **75**(1): p. 74-84.
138. Bray, F., et al., *Global cancer statistics 2018: GLOBOCAN estimates of incidence and mortality worldwide for 36 cancers in 185 countries.* CA Cancer J Clin, 2018. **68**(6): p. 394-424.
139. Escudier, B., et al., *Renal cell carcinoma: ESMO Clinical Practice Guidelines for diagnosis, treatment and follow-up.* Ann Oncol, 2014. **25 Suppl 3**: p. iii49-56.
140. Board, C.N.E. *Kidney Cancer: Statistics*. 2019.
141. Capitanio, U. and F. Montorsi, *Renal cancer.* Lancet, 2016. **387**(10021): p. 894-906.
142. Lopez-Beltran, A., et al., *2004 WHO classification of the renal tumors of the adults.* Eur Urol, 2006. **49**(5): p. 798-805.
143. Srigley, J.R., et al., *The International Society of Urological Pathology (ISUP) Vancouver Classification of Renal Neoplasia.* Am J Surg Pathol, 2013. **37**(10): p. 1469-89.
144. Shinagare, A.B., et al., *Genitourinary imaging: part 2, role of imaging in medical management of advanced renal cell carcinoma.* AJR Am J Roentgenol, 2012. **199**(5): p. W554-64.
145. Edge, S.B. and C.C. Compton, *The American Joint Committee on Cancer: the 7th edition of the AJCC cancer staging manual and the future of TNM.* Ann Surg Oncol, 2010. **17**(6): p. 1471-4.
146. Bianchi, M., et al., *Distribution of metastatic sites in renal cell carcinoma: a population-based analysis.* Ann Oncol, 2012. **23**(4): p. 973-80.

147. http://www.urology.com.sg/kidney-health/kidney-cancer/.

148. Dunnick, N.R., *Renal cell carcinoma: staging and surveillance.* Abdom Radiol (NY), 2016. **41**(6): p. 1079-85.

149. Cheng, L., et al., *Molecular and cytogenetic insights into the pathogenesis, classification, differential diagnosis, and prognosis of renal epithelial neoplasms.* Hum Pathol, 2009. **40**(1): p. 10-29.

150. Pavlovich, C.P., L.S. Schmidt, and J.L. Phillips, *The genetic basis of renal cell carcinoma.* Urol Clin North Am, 2003. **30**(3): p. 437-54, vii.

151. Wettersten, H.I., et al., *Metabolic reprogramming in clear cell renal cell carcinoma.* Nat Rev Nephrol, 2017. **13**(7): p. 410-419.

152. Escudier, B., et al., *Randomized phase II trial of first-line treatment with sorafenib versus interferon Alfa-2a in patients with metastatic renal cell carcinoma.* J Clin Oncol, 2009. **27**(8): p. 1280-9.

153. Fisher, R.I., S.A. Rosenberg, and G. Fyfe, *Long-term survival update for high-dose recombinant interleukin-2 in patients with renal cell carcinoma.* Cancer J Sci Am, 2000. **6 Suppl 1**: p. S55-7.

154. Fyfe, G., et al., *Results of treatment of 255 patients with metastatic renal cell carcinoma who received high-dose recombinant interleukin-2 therapy.* J Clin Oncol, 1995. **13**(3): p. 688-96.

155. Rini, B.I., et al., *Bevacizumab plus interferon alfa compared with interferon alfa monotherapy in patients with metastatic renal cell carcinoma: CALGB 90206.* J Clin Oncol, 2008. **26**(33): p. 5422-8.

156. Lee, C.H. and R.J. Motzer, *Kidney cancer in 2016: The evolution of anti-angiogenic therapy for kidney cancer.* Nat Rev Nephrol, 2017. **13**(2): p. 69-70.

157. Patel, P.H., et al., *Targeting von Hippel-Lindau pathway in renal cell carcinoma.* Clin Cancer Res, 2006. **12**(24): p. 7215-20.

158. Motzer, R.J., et al., *Kidney Cancer, Version 2.2017, NCCN Clinical Practice Guidelines in Oncology.* J Natl Compr Canc Netw, 2017. **15**(6): p. 804-834.

159. Motzer, R.J., et al., *Overall survival and updated results for sunitinib compared with interferon alfa in patients with metastatic renal cell carcinoma.* J Clin Oncol, 2009. **27**(22): p. 3584-90.

160. Motzer, R.J., et al., *Sunitinib versus interferon alfa in metastatic renal-cell carcinoma.* N Engl J Med, 2007. **356**(2): p. 115-24.

161. Ravaud, A., et al., *Adjuvant Sunitinib in High-Risk Renal-Cell Carcinoma after Nephrectomy.* N Engl J Med, 2016. **375**(23): p. 2246-2254.

162. Motzer, R.J., et al., *Pazopanib versus sunitinib in metastatic renal-cell carcinoma.* N Engl J Med, 2013. **369**(8): p. 722-31.

163. Choueiri, T.K., et al., *Cabozantinib versus sunitinib as initial therapy for metastatic renal cell carcinoma of intermediate or poor risk (Alliance A031203 CABOSUN randomised trial): Progression-free survival by independent review and overall survival update.* Eur J Cancer, 2018. **94**: p. 115-125.

164. Rini, B.I., et al., *Comparative effectiveness of axitinib versus sorafenib in advanced renal cell carcinoma (AXIS): a randomised phase 3 trial.* Lancet, 2011. **378**(9807): p. 1931-9.

165. Bhargava, P. and M.O. Robinson, *Development of second-generation VEGFR tyrosine kinase inhibitors: current status.* Curr Oncol Rep, 2011. **13**(2): p. 103-11.

166. Escudier, B., et al., *Bevacizumab plus interferon alfa-2a for treatment of metastatic renal cell carcinoma: a randomised, double-blind phase III trial.* Lancet, 2007. **370**(9605): p. 2103-11.

167. Yang, J.C., et al., *A randomized trial of bevacizumab, an anti-vascular endothelial growth factor antibody, for metastatic renal cancer.* N Engl J Med, 2003. **349**(5): p. 427-34.

168. Ma, S., et al., *The role of tumor microenvironment in resistance to anti-angiogenic therapy.* 2018. **7**: p. 326.

169. Sternberg, C.N., et al., *Pazopanib in locally advanced or metastatic renal cell carcinoma: results of a randomized phase III trial.* J Clin Oncol, 2010. **28**(6): p. 1061-8.

170. Hutson, T.E., et al., *Axitinib versus sorafenib as first-line therapy in patients with metastatic renal-cell carcinoma: a randomised open-label phase 3 trial.* Lancet Oncol, 2013. **14**(13): p. 1287-94.

171. Lempiainen, H. and T.D. Halazonetis, *Emerging common themes in regulation of PIKKs and PI3Ks.* Embo j, 2009. **28**(20): p. 3067-73.

172. Saxton, R.A. and D.M. Sabatini, *mTOR Signaling in Growth, Metabolism, and Disease.* Cell, 2017. **168**(6): p. 960-976.

173. Hudes, G., et al., *Temsirolimus, interferon alfa, or both for advanced renal-cell carcinoma.* N Engl J Med, 2007. **356**(22): p. 2271-81.

174. Motzer, R.J., et al., *Efficacy of everolimus in advanced renal cell carcinoma: a double-blind, randomised, placebo-controlled phase III trial.* Lancet, 2008. **372**(9637): p. 449-56.

175. Hamid, Y. and D.N. Poller, *Spontaneous regression of renal cell carcinoma: a pitfall in diagnosis of renal lesions.* J Clin Pathol, 1998. **51**(4): p. 334-6.

176. de Riese, W., et al., *Metastatic renal cell carcinoma (RCC): spontaneous regression, long-term survival and late recurrence.* Int Urol Nephrol, 1991. **23**(1): p. 13-25.
177. Yoshihara, K., et al., *Inferring tumour purity and stromal and immune cell admixture from expression data.* Nat Commun, 2013. **4**: p. 2612.
178. Thompson, R.H., et al., *PD-1 is expressed by tumor-infiltrating immune cells and is associated with poor outcome for patients with renal cell carcinoma.* Clin Cancer Res, 2007. **13**(6): p. 1757-61.
179. Senbabaoglu, Y., et al., *Tumor immune microenvironment characterization in clear cell renal cell carcinoma identifies prognostic and immunotherapeutically relevant messenger RNA signatures.* Genome Biol, 2016. **17**(1): p. 231.
180. Leach, D.R., M.F. Krummel, and J.P. Allison, *Enhancement of antitumor immunity by CTLA-4 blockade.* Science, 1996. **271**(5256): p. 1734-6.
181. Hodi, F.S., et al., *Improved survival with ipilimumab in patients with metastatic melanoma.* N Engl J Med, 2010. **363**(8): p. 711-23.
182. Yang, J.C., et al., *Ipilimumab (anti-CTLA4 antibody) causes regression of metastatic renal cell cancer associated with enteritis and hypophysitis.* J Immunother, 2007. **30**(8): p. 825-30.
183. Dong, H., et al., *Tumor-associated B7-H1 promotes T-cell apoptosis: a potential mechanism of immune evasion.* Nat Med, 2002. **8**(8): p. 793-800.
184. Motzer, R.J., et al., *Nivolumab versus Everolimus in Advanced Renal-Cell Carcinoma.* N Engl J Med, 2015. **373**(19): p. 1803-13.
185. Nguyen, L.T. and P.S. Ohashi, *Clinical blockade of PD1 and LAG3--potential mechanisms of action.* Nat Rev Immunol, 2015. **15**(1): p. 45-56.
186. McDermott, D.F., et al., *Atezolizumab, an Anti-Programmed Death-Ligand 1 Antibody, in Metastatic Renal Cell Carcinoma: Long-Term Safety, Clinical Activity, and Immune Correlates From a Phase Ia Study.* J Clin Oncol, 2016. **34**(8): p. 833-42.
187. Brahmer, J.R., et al., *Safety and activity of anti-PD-L1 antibody in patients with advanced cancer.* N Engl J Med, 2012. **366**(26): p. 2455-65.
188. Cottrell, T.R. and J.M. Taube, *PD-L1 and Emerging Biomarkers in Immune Checkpoint Blockade Therapy.* Cancer journal (Sudbury, Mass.), 2018. **24**(1): p. 41-46.
189. Jilaveanu, L.B., et al., *PD-L1 Expression in Clear Cell Renal Cell Carcinoma: An Analysis of Nephrectomy and Sites of Metastases.* J Cancer, 2014. **5**(3): p. 166-72.
190. Patel, S.P. and R. Kurzrock, *PD-L1 Expression as a Predictive Biomarker in Cancer Immunotherapy.* Mol Cancer Ther, 2015. **14**(4): p. 847-56.
191. Choueiri, T.K., et al., *Immunomodulatory activity of nivolumab in previously treated and untreated metastatic renal cell carcinoma (mRCC): Biomarker-based results from a randomized clinical trial.* Journal of Clinical Oncology, 2014. **32**(15_suppl): p. 5012-5012.
192. Choueiri, T.K., et al., *Immunomodulatory activity of nivolumab in metastatic renal cell carcinoma (mRCC): Association of biomarkers with clinical outcomes.* Journal of Clinical Oncology, 2015. **33**(15_suppl): p. 4500-4500.
193. Thompson, R.H., et al., *Costimulatory molecule B7-H1 in primary and metastatic clear cell renal cell carcinoma.* Cancer, 2005. **104**(10): p. 2084-91.
194. Thompson, R.H., et al., *Costimulatory B7-H1 in renal cell carcinoma patients: Indicator of tumor aggressiveness and potential therapeutic target.* Proc Natl Acad Sci U S A, 2004. **101**(49): p. 17174-9.
195. Motzer, R.J., et al., *Nivolumab plus Ipilimumab versus Sunitinib in Advanced Renal-Cell Carcinoma.* New England Journal of Medicine, 2018. **378**(14): p. 1277-1290.
196. Chalmers, Z.R., et al., *Analysis of 100,000 human cancer genomes reveals the landscape of tumor mutational burden.* Genome Med, 2017. **9**(1): p. 34.
197. Miao, D. and C.A. Margolis, *Genomic correlates of response to immune checkpoint therapies in clear cell renal cell carcinoma.* Science, 2018. **359**(6377): p. 801-806.
198. Mahoney, K.M., P.D. Rennert, and G.J. Freeman, *Combination cancer immunotherapy and new immunomodulatory targets.* Nat Rev Drug Discov, 2015. **14**(8): p. 561-84.
199. Fife, B.T., et al., *Interactions between PD-1 and PD-L1 promote tolerance by blocking the TCR-induced stop signal.* Nat Immunol, 2009. **10**(11): p. 1185-92.
200. Rudd, C.E., *The reverse stop-signal model for CTLA4 function.* Nat Rev Immunol, 2008. **8**(2): p. 153-60.
201. Larkin, J., F.S. Hodi, and J.D. Wolchok, *Combined Nivolumab and Ipilimumab or Monotherapy in Untreated Melanoma.* N Engl J Med, 2015. **373**(13): p. 1270-1.
202. Amin, A., et al., *Safety and efficacy of nivolumab in combination with sunitinib or pazopanib in advanced or metastatic 37renal cell carcinoma: the CheckMate 016 study.* J Immunother Cancer, 2018. **6**(1): p. 109.

203. Hammers, H.J., et al., *Expanded cohort results from CheckMate 016: A phase I study of nivolumab in combination with ipilimumab in metastatic renal cell carcinoma (mRCC).* Journal of Clinical Oncology, 2015. **33**(15_suppl): p. 4516-4516.
204. Hammers, H.J., et al., *CheckMate 214: A phase III, randomized, open-label study of nivolumab combined with ipilimumab versus sunitinib monotherapy in patients with previously untreated metastatic renal cell carcinoma.* Journal of Clinical Oncology, 2015. **33**(15_suppl): p. TPS4578-TPS4578.
205. Terme, M., et al., *Modulation of immunity by antiangiogenic molecules in cancer.* Clin Dev Immunol, 2012. **2012**: p. 492920.
206. Desar, I.M., et al., *Sorafenib reduces the percentage of tumour infiltrating regulatory T cells in renal cell carcinoma patients.* Int J Cancer, 2011. **129**(2): p. 507-12.
207. Ko, J.S., et al., *Sunitinib mediates reversal of myeloid-derived suppressor cell accumulation in renal cell carcinoma patients.* Clin Cancer Res, 2009. **15**(6): p. 2148-57.
208. Rini, B.I., et al., *Phase 1 dose-escalation trial of tremelimumab plus sunitinib in patients with metastatic renal cell carcinoma.* Cancer, 2011. **117**(4): p. 758-67.
209. Nadal, R.M., et al., *Results of phase I plus expansion cohorts of cabozantinib (Cabo) plus nivolumab (Nivo) and CaboNivo plus ipilimumab (Ipi) in patients (pts) with with metastatic urothelial carcinoma (mUC) and other genitourinary (GU) malignancies.* Journal of Clinical Oncology, 2018. **36**(6_suppl): p. 515-515.
210. Linehan, W.M., R. Srinivasan, and L.S. Schmidt, *The genetic basis of kidney cancer: a metabolic disease.* Nat Rev Urol, 2010. **7**(5): p. 277-85.
211. Darnell, J.E., Jr., *Transcription factors as targets for cancer therapy.* Nat Rev Cancer, 2002. **2**(10): p. 740-9.
212. Erbel, P.J., et al., *Structural basis for PAS domain heterodimerization in the basic helix--loop--helix-PAS transcription factor hypoxia-inducible factor.* Proc Natl Acad Sci U S A, 2003. **100**(26): p. 15504-9.
213. Greenberger, L.M., et al., *A RNA antagonist of hypoxia-inducible factor-1alpha, EZN-2968, inhibits tumor cell growth.* Mol Cancer Ther, 2008. **7**(11): p. 3598-608.
214. Terzuoli, E., et al., *Aminoflavone, a ligand of the aryl hydrocarbon receptor, inhibits HIF-1alpha expression in an AhR-independent fashion.* Cancer Res, 2010. **70**(17): p. 6837-48.
215. Rapisarda, A., et al., *Identification of small molecule inhibitors of hypoxia-inducible factor 1 transcriptional activation pathway.* Cancer Res, 2002. **62**(15): p. 4316-24.
216. Rapisarda, A., et al., *Topoisomerase I-mediated inhibition of hypoxia-inducible factor 1: mechanism and therapeutic implications.* Cancer Res, 2004. **64**(4): p. 1475-82.
217. Sapra, P., et al., *Novel delivery of SN38 markedly inhibits tumor growth in xenografts, including a camptothecin-11-refractory model.* Clin Cancer Res, 2008. **14**(6): p. 1888-96.
218. Welsh, S., et al., *Antitumor activity and pharmacodynamic properties of PX-478, an inhibitor of hypoxia-inducible factor-1alpha.* Mol Cancer Ther, 2004. **3**(3): p. 233-44.
219. Young, C., et al., *CRLX101 (formerly IT-101)-A Novel Nanopharmaceutical of Camptothecin in Clinical Development.* Curr Bioact Compd, 2011. **7**(1): p. 8-14.
220. Zhang, H., et al., *Digoxin and other cardiac glycosides inhibit HIF-1alpha synthesis and block tumor growth.* Proc Natl Acad Sci U S A, 2008. **105**(50): p. 19579-86.
221. Kong, D., et al., *Echinomycin, a small-molecule inhibitor of hypoxia-inducible factor-1 DNA-binding activity.* Cancer Res, 2005. **65**(19): p. 9047-55.
222. Cook, K.M., et al., *Epidithiodiketopiperazines block the interaction between hypoxia-inducible factor-1alpha (HIF-1alpha) and p300 by a zinc ejection mechanism.* J Biol Chem, 2009. **284**(39): p. 26831-8.
223. Kaluz, S., M. Kaluzova, and E.J. Stanbridge, *Proteasomal inhibition attenuates transcriptional activity of hypoxia-inducible factor 1 (HIF-1) via specific effect on the HIF-1alpha C-terminal activation domain.* Mol Cell Biol, 2006. **26**(15): p. 5895-907.
224. Strese, S., et al., *Effects of hypoxia on human cancer cell line chemosensitivity.* BMC Cancer, 2013. **13**: p. 331.
225. Martinez-Saez, O., et al., *Targeting HIF-2 alpha in clear cell renal cell carcinoma: A promising therapeutic strategy.* Crit Rev Oncol Hematol, 2017. **111**: p. 117-123.
226. Keefe, S.M., et al., *Efficacy of the nanoparticle-drug conjugate CRLX101 in combination with bevacizumab in metastatic renal cell carcinoma: results of an investigator-initiated phase I-IIa clinical trial.* Ann Oncol, 2016. **27**(8): p. 1579-85.
227. Jeong, W., et al., *Pilot trial of EZN-2968, an antisense oligonucleotide inhibitor of hypoxia-inducible factor-1 alpha (HIF-1alpha), in patients with refractory solid tumors.* Cancer Chemother Pharmacol, 2014. **73**(2): p. 343-8.
228. Patnaik, A., et al., *Phase I dose-escalation study of EZN-2208 (PEG-SN38), a novel conjugate of poly(ethylene) glycol and SN38, administered weekly in patients with advanced cancer.* Cancer Chemother Pharmacol, 2013. **71**(6): p. 1499-506.
229. Tibes, R., et al., *Results from a phase I, dose-escalation study of PX-478, an orally available inhibitor of HIF-1α.* Journal of Clinical Oncology, 2010. **28**(15_suppl): p. 3076-3076.

230. Onnis, B., A. Rapisarda, and G. Melillo, *Development of HIF-1 inhibitors for cancer therapy.* J Cell Mol Med, 2009. **13**(9a): p. 2780-6.
231. Gordan, J.D., et al., *HIF-alpha effects on c-Myc distinguish two subtypes of sporadic VHL-deficient clear cell renal carcinoma.* Cancer Cell, 2008. **14**(6): p. 435-46.
232. Key, J., et al., *Principles of ligand binding within a completely buried cavity in HIF2alpha PAS-B.* J Am Chem Soc, 2009. **131**(48): p. 17647-54.
233. Rogers, J.L., et al., *Development of inhibitors of the PAS-B domain of the HIF-2alpha transcription factor.* J Med Chem, 2013. **56**(4): p. 1739-47.
234. Scheuermann, T.H., et al., *Artificial ligand binding within the HIF2alpha PAS-B domain of the HIF2 transcription factor.* Proc Natl Acad Sci U S A, 2009. **106**(2): p. 450-5.
235. Scheuermann, T.H., et al., *Allosteric inhibition of hypoxia inducible factor-2 with small molecules.* Nat Chem Biol, 2013. **9**(4): p. 271-6.
236. Wu, D., et al., *Structural integration in hypoxia-inducible factors.* Nature, 2015. **524**: p. 303.
237. Wallace, E.M., et al., *A Small-Molecule Antagonist of HIF2alpha Is Efficacious in Preclinical Models of Renal Cell Carcinoma.* Cancer Res, 2016. **76**(18): p. 5491-500.
238. Courtney, K.D., et al., *Phase I Dose-Escalation Trial of PT2385, a First-in-Class Hypoxia-Inducible Factor-2α Antagonist in Patients With Previously Treated Advanced Clear Cell Renal Cell Carcinoma.* Journal of Clinical Oncology, 2018. **36**(9): p. 867-874.
239. Chen, W., et al., *Targeting renal cell carcinoma with a HIF-2 antagonist.* Nature, 2016. **539**(7627): p. 112-117.
240. Cho, H., et al., *On-target efficacy of a HIF-2alpha antagonist in preclinical kidney cancer models.* Nature, 2016. **539**(7627): p. 107-111.
241. Ruf, M., H. Moch, and P. Schraml, *PD-L1 expression is regulated by hypoxia inducible factor in clear cell renal cell carcinoma.* Int J Cancer, 2016. **139**(2): p. 396-403.
242. Messai, Y., et al., *Renal Cell Carcinoma Programmed Death-ligand 1, a New Direct Target of Hypoxia-inducible Factor-2 Alpha, is Regulated by von Hippel-Lindau Gene Mutation Status.* Eur Urol, 2016. **70**(4): p. 623-632.
243. Fallah, J. and B.I. Rini, *HIF Inhibitors: Status of Current Clinical Development.* Curr Oncol Rep, 2019. **21**(1): p. 6.
244. Kumar, A., et al., *Renal Cell Carcinoma: Molecular Aspects.* Indian J Clin Biochem, 2018. **33**(3): p. 246-254.
245. Network, C.G.A.R., *Comprehensive molecular characterization of clear cell renal cell carcinoma.* Nature, 2013. **499**(7456): p. 43-9.
246. Lindau, A., *Zur frage der angiomatosis retinæ und ihrer hirnkomplikationen.* Acta Ophthalmologica, 1926. **4**(1-2): p. 193-226.
247. v. Hippel, E., *Über eine sehr seltene Erkrankung der Netzhaut.* Albrecht von Graefes Archiv für Ophthalmologie, 1904. **59**(1): p. 83-106.
248. Chittiboina, P. and R.R. Lonser, *Von Hippel-Lindau disease.* Handb Clin Neurol, 2015. **132**: p. 139-56.
249. Maher, E.R., et al., *Clinical features and natural history of von Hippel-Lindau disease.* Q J Med, 1990. **77**(283): p. 1151-63.
250. Werness, B.A. and J.G. Guccion, *Tumor of the broad ligament in von Hippel-Lindau disease of probable mullerian origin.* Int J Gynecol Pathol, 1997. **16**(3): p. 282-5.
251. Maher, E.R., *Hereditary renal cell carcinoma syndromes: diagnosis, surveillance and management.* World J Urol, 2018. **36**(12): p. 1891-1898.
252. Beroukhim, R., et al., *Patterns of gene expression and copy-number alterations in von-hippel lindau disease-associated and sporadic clear cell carcinoma of the kidney.* Cancer Res, 2009. **69**(11): p. 4674-81.
253. Furge, K.A., et al., *Identification of deregulated oncogenic pathways in renal cell carcinoma: an integrated oncogenomic approach based on gene expression profiling.* Oncogene, 2007. **26**(9): p. 1346-50.
254. Brauch, H., et al., *VHL alterations in human clear cell renal cell carcinoma: association with advanced tumor stage and a novel hot spot mutation.* Cancer Res, 2000. **60**(7): p. 1942-8.
255. Mandriota, S.J., et al., *HIF activation identifies early lesions in VHL kidneys: evidence for site-specific tumor suppressor function in the nephron.* Cancer Cell, 2002. **1**(5): p. 459-68.
256. Turajlic, S., J. Larkin, and C. Swanton, *SnapShot: Renal Cell Carcinoma.* Cell, 2015. **163**(6): p. 1556-1556.e1.
257. Varela, I., et al., *Exome sequencing identifies frequent mutation of the SWI/SNF complex gene PBRM1 in renal carcinoma.* Nature, 2011. **469**(7331): p. 539-42.
258. Macher-Goeppinger, S., et al., *PBRM1 (BAF180) protein is functionally regulated by p53-induced protein degradation in renal cell carcinomas.* J Pathol, 2015. **237**(4): p. 460-71.
259. Brugarolas, J., *Molecular genetics of clear-cell renal cell carcinoma.* J Clin Oncol, 2014. **32**(18): p. 1968-76.

260. Kanu, N., et al., *SETD2 loss-of-function promotes renal cancer branched evolution through replication stress and impaired DNA repair.* Oncogene, 2015. **34**(46): p. 5699-708.
261. Wenger, R.H., et al., *Oxygen-regulated erythropoietin gene expression is dependent on a CpG methylation-free hypoxia-inducible factor-1 DNA-binding site.* Eur J Biochem, 1998. **253**(3): p. 771-7.
262. Simon, J.M., et al., *Variation in chromatin accessibility in human kidney cancer links H3K36 methyltransferase loss with widespread RNA processing defects.* Genome Res, 2014. **24**(2): p. 241-50.
263. Guo, G., et al., *Frequent mutations of genes encoding ubiquitin-mediated proteolysis pathway components in clear cell renal cell carcinoma.* Nat Genet, 2011. **44**(1): p. 17-9.
264. Di Croce, L. and K. Helin, *Transcriptional regulation by Polycomb group proteins.* Nature Structural &Amp; Molecular Biology, 2013. **20**: p. 1147.
265. Hakimi, A.A., et al., *Adverse outcomes in clear cell renal cell carcinoma with mutations of 3p21 epigenetic regulators BAP1 and SETD2: a report by MSKCC and the KIRC TCGA research network.* Clin Cancer Res, 2013. **19**(12): p. 3259-67.
266. van Kessel, A.G., et al., *Renal cell cancer: chromosome 3 translocations as risk factors.* J Natl Cancer Inst, 1999. **91**(13): p. 1159-60.
267. Woodward, E.R., et al., *Population-based survey of cancer risks in chromosome 3 translocation carriers.* Genes Chromosomes Cancer, 2010. **49**(1): p. 52-8.
268. Cohen, A.J., et al., *Hereditary renal-cell carcinoma associated with a chromosomal translocation.* N Engl J Med, 1979. **301**(11): p. 592-5.
269. Bonne, A.C., et al., *Chromosome 3 translocations and familial renal cell cancer.* Curr Mol Med, 2004. **4**(8): p. 849-54.
270. Shen, C., et al., *Genetic and functional studies implicate HIF1alpha as a 14q kidney cancer suppressor gene.* Cancer Discov, 2011. **1**(3): p. 222-35.
271. Zhang, H., et al., *HIF-1 inhibits mitochondrial biogenesis and cellular respiration in VHL-deficient renal cell carcinoma by repression of C-MYC activity.* Cancer Cell, 2007. **11**(5): p. 407-20.
272. Li, L., et al., *SQSTM1 is a pathogenic target of 5q copy number gains in kidney cancer.* Cancer Cell, 2013. **24**(6): p. 738-50.
273. Duran, A., et al., *p62 is a key regulator of nutrient sensing in the mTORC1 pathway.* Mol Cell, 2011. **44**(1): p. 134-46.
274. Dondeti, V.R., et al., *Integrative genomic analyses of sporadic clear cell renal cell carcinoma define disease subtypes and potential new therapeutic targets.* Cancer Res, 2012. **72**(1): p. 112-21.
275. Liu, L., et al., *Enhancer of zeste homolog 2 (EZH2) promotes tumour cell migration and invasion via epigenetic repression of E-cadherin in renal cell carcinoma.* BJU Int, 2016. **117**(2): p. 351-62.
276. Elvidge, G.P., et al., *Concordant regulation of gene expression by hypoxia and 2-oxoglutarate-dependent dioxygenase inhibition: the role of HIF-1alpha, HIF-2alpha, and other pathways.* J Biol Chem, 2006. **281**(22): p. 15215-26.
277. Schonenberger, D., et al., *Formation of Renal Cysts and Tumors in Vhl/Trp53-Deficient Mice Requires HIF1alpha and HIF2alpha.* Cancer Res, 2016. **76**(7): p. 2025-36.
278. Schietke, R.E., et al., *Renal tubular HIF-2alpha expression requires VHL inactivation and causes fibrosis and cysts.* PLoS One, 2012. **7**(1): p. e31034.
279. Kondo, K., et al., *Inhibition of HIF2alpha is sufficient to suppress pVHL-defective tumor growth.* PLoS Biol, 2003. **1**(3): p. E83.
280. Khan, M.N., et al., *Factor inhibiting HIF (FIH-1) promotes renal cancer cell survival by protecting cells from HIF-1alpha-mediated apoptosis.* Br J Cancer, 2011. **104**(7): p. 1151-9.
281. Bracken, C.P., et al., *Cell-specific regulation of hypoxia-inducible factor (HIF)-1alpha and HIF-2alpha stabilization and transactivation in a graded oxygen environment.* J Biol Chem, 2006. **281**(32): p. 22575-85.
282. Schodel, J., et al., *Common genetic variants at the 11q13.3 renal cancer susceptibility locus influence binding of HIF to an enhancer of cyclin D1 expression.* Nat Genet, 2012. **44**(4): p. 420-5, s1-2.
283. Salama, R., et al., *Heterogeneous Effects of Direct Hypoxia Pathway Activation in Kidney Cancer.* PLoS One, 2015. **10**(8): p. e0134645.
284. Gordan, J.D., C.B. Thompson, and M.C. Simon, *HIF and c-Myc: sibling rivals for control of cancer cell metabolism and proliferation.* Cancer Cell, 2007. **12**(2): p. 108-13.
285. Zhang, T., et al., *The contributions of HIF-target genes to tumor growth in RCC.* PLoS One, 2013. **8**(11): p. e80544.
286. Smith, K., et al., *Silencing of epidermal growth factor receptor suppresses hypoxia-inducible factor-2-driven VHL-/- renal cancer.* Cancer Res, 2005. **65**(12): p. 5221-30.
287. Roche, O., et al., *Identification of non-coding genetic variants in samples from hypoxemic respiratory disease patients that affect the transcriptional response to hypoxia.* Nucleic Acids Res, 2016. **44**(19): p. 9315-9330.
288. Wang, Y., et al., *Regulation of endocytosis via the oxygen-sensing pathway.* Nat Med, 2009. **15**(3): p. 319-24.

289. Turner, K.J., et al., *Expression of hypoxia-inducible factors in human renal cancer: relationship to angiogenesis and to the von Hippel-Lindau gene mutation.* Cancer Res, 2002. **62**(10): p. 2957-61.
290. Logsdon, E.A., et al., *A systems biology view of blood vessel growth and remodelling.* J Cell Mol Med, 2014. **18**(8): p. 1491-508.
291. Semenza, G.L., *Regulation of vascularization by hypoxia-inducible factor 1.* Ann N Y Acad Sci, 2009. **1177**: p. 2-8.
292. Kaelin, W.G., Jr., *The VHL Tumor Suppressor Gene: Insights into Oxygen Sensing and Cancer.* Trans Am Clin Climatol Assoc, 2017. **128**: p. 298-307.
293. Kaelin, W.G., Jr., *The von Hippel-Lindau tumor suppressor gene and kidney cancer.* Clin Cancer Res, 2004. **10**(18 Pt 2): p. 6290s-5s.
294. Bos, R., et al., *Hypoxia-inducible factor-1alpha is associated with angiogenesis, and expression of bFGF, PDGF-BB, and EGFR in invasive breast cancer.* Histopathology, 2005. **46**(1): p. 31-6.
295. Abramsson, A., P. Lindblom, and C. Betsholtz, *Endothelial and nonendothelial sources of PDGF-B regulate pericyte recruitment and influence vascular pattern formation in tumors.* J Clin Invest, 2003. **112**(8): p. 1142-51.
296. White, N.M., et al., *Galectin-1 has potential prognostic significance and is implicated in clear cell renal cell carcinoma progression through the HIF/mTOR signaling axis.* Br J Cancer, 2014. **110**(5): p. 1250-9.
297. Schmelzle, T. and M.N. Hall, *TOR, a central controller of cell growth.* Cell, 2000. **103**(2): p. 253-62.
298. Elorza, A., et al., *HIF2alpha acts as an mTORC1 activator through the amino acid carrier SLC7A5.* Mol Cell, 2012. **48**(5): p. 681-91.
299. Hakimi, A.A., C.G. Pham, and J.J. Hsieh, *A clear picture of renal cell carcinoma.* Nat Genet, 2013. **45**(8): p. 849-50.
300. Kim, J.W., et al., *HIF-1-mediated expression of pyruvate dehydrogenase kinase: a metabolic switch required for cellular adaptation to hypoxia.* Cell Metab, 2006. **3**(3): p. 177-85.
301. Papandreou, I., et al., *HIF-1 mediates adaptation to hypoxia by actively downregulating mitochondrial oxygen consumption.* Cell Metab, 2006. **3**(3): p. 187-97.
302. Iyer, N.V., et al., *Cellular and developmental control of O2 homeostasis by hypoxia-inducible factor 1 alpha.* Genes Dev, 1998. **12**(2): p. 149-62.
303. Semenza, G.L., et al., *Hypoxia response elements in the aldolase A, enolase 1, and lactate dehydrogenase A gene promoters contain essential binding sites for hypoxia-inducible factor 1.* J Biol Chem, 1996. **271**(51): p. 32529-37.
304. Ebert, B.L., J.D. Firth, and P.J. Ratcliffe, *Hypoxia and mitochondrial inhibitors regulate expression of glucose transporter-1 via distinct Cis-acting sequences.* J Biol Chem, 1995. **270**(49): p. 29083-9.
305. Ward, P.S. and C.B. Thompson, *Metabolic reprogramming: a cancer hallmark even warburg did not anticipate.* Cancer Cell, 2012. **21**(3): p. 297-308.
306. Hakimi, A.A., et al., *An Integrated Metabolic Atlas of Clear Cell Renal Cell Carcinoma.* Cancer Cell, 2016. **29**(1): p. 104-116.
307. Patra, K.C. and N. Hay, *The pentose phosphate pathway and cancer.* Trends Biochem Sci, 2014. **39**(8): p. 347-54.
308. Fukuda, R., et al., *HIF-1 regulates cytochrome oxidase subunits to optimize efficiency of respiration in hypoxic cells.* Cell, 2007. **129**(1): p. 111-22.
309. Guzy, R.D. and P.T. Schumacker, *Oxygen sensing by mitochondria at complex III: the paradox of increased reactive oxygen species during hypoxia.* Exp Physiol, 2006. **91**(5): p. 807-19.
310. Jeremy M Berg, J.L.T., and Lubert Stryer, *Glucose 6-Phosphate Dehydrogenase Plays a Key Role in Protection Against Reactive Oxygen Species*, in *Biochemistry. 5th edition*, N.Y.W.H. Freeman, Editor. 2002.
311. Gameiro, P.A., et al., *In vivo HIF-mediated reductive carboxylation is regulated by citrate levels and sensitizes VHL-deficient cells to glutamine deprivation.* Cell Metab, 2013. **17**(3): p. 372-85.
312. Mullen, A.R., et al., *Reductive carboxylation supports growth in tumour cells with defective mitochondria.* Nature, 2011. **481**(7381): p. 385-8.
313. Yang, L., S. Venneti, and D. Nagrath, *Glutaminolysis: A Hallmark of Cancer Metabolism.* Annu Rev Biomed Eng, 2017. **19**: p. 163-194.
314. Kang, H.M., et al., *Defective fatty acid oxidation in renal tubular epithelial cells has a key role in kidney fibrosis development.* Nat Med, 2015. **21**(1): p. 37-46.
315. Meierhofer, D., et al., *Decrease of mitochondrial DNA content and energy metabolism in renal cell carcinoma.* Carcinogenesis, 2004. **25**(6): p. 1005-10.
316. Bellot, G., et al., *Hypoxia-induced autophagy is mediated through hypoxia-inducible factor induction of BNIP3 and BNIP3L via their BH3 domains.* Mol Cell Biol, 2009. **29**(10): p. 2570-81.
317. Zhang, H., et al., *Mitochondrial autophagy is an HIF-1-dependent adaptive metabolic response to hypoxia.* J Biol Chem, 2008. **283**(16): p. 10892-903.

318. Qiu, B., et al., *HIF2alpha-Dependent Lipid Storage Promotes Endoplasmic Reticulum Homeostasis in Clear-Cell Renal Cell Carcinoma.* Cancer Discov, 2015. **5**(6): p. 652-67.
319. Walther, T.C. and R.V. Farese, Jr., *Lipid droplets and cellular lipid metabolism.* Annu Rev Biochem, 2012. **81**: p. 687-714.
320. Du, W., et al., *HIF drives lipid deposition and cancer in ccRCC via repression of fatty acid metabolism.* 2017. **8**(1): p. 1769.
321. Sundelin, J.P., et al., *Increased expression of the very low-density lipoprotein receptor mediates lipid accumulation in clear-cell renal cell carcinoma.* PLoS One, 2012. **7**(11): p. e48694.
322. McGarry, J.D. and N.F. Brown, *The mitochondrial carnitine palmitoyltransferase system. From concept to molecular analysis.* Eur J Biochem, 1997. **244**(1): p. 1-14.
323. Ramsay, R.R., R.D. Gandour, and F.R. van der Leij, *Molecular enzymology of carnitine transfer and transport.* Biochim Biophys Acta, 2001. **1546**(1): p. 21-43.
324. Zammit, V.A., *The malonyl-CoA-long-chain acyl-CoA axis in the maintenance of mammalian cell function.* Biochem J, 1999. **343 Pt 3**: p. 505-15.
325. LaGory, E.L., et al., *Suppression of PGC-1alpha Is Critical for Reprogramming Oxidative Metabolism in Renal Cell Carcinoma.* Cell Rep, 2015. **12**(1): p. 116-127.
326. Simonnet, H., et al., *Low mitochondrial respiratory chain content correlates with tumor aggressiveness in renal cell carcinoma.* Carcinogenesis, 2002. **23**(5): p. 759-68.
327. Gnarra, J.R., et al., *Mutations of the VHL tumour suppressor gene in renal carcinoma.* Nature Genetics, 1994. **7**(1): p. 85-90.
328. Maxwell, P.H., et al., *The tumour suppressor protein VHL targets hypoxia-inducible factors for oxygen-dependent proteolysis.* Nature, 1999. **399**: p. 271.
329. Harten, S.K., et al., *Inactivation of the von Hippel-Lindau tumour suppressor gene induces Neuromedin U expression in renal cancer cells.* Mol Cancer, 2011. **10**: p. 89.
330. Cong, L., et al., *Multiplex genome engineering using CRISPR/Cas systems.* Science, 2013. **339**(6121): p. 819-23.
331. Hall, T.A. *BioEdit: a user-friendly biological sequence alignment editor and analysis program for Windows 95/98/NT*. in *Nucleic acids symposium series*. 1999. [London]: Information Retrieval Ltd., c1979-c2000.
332. Leek, R., et al., *Methods: Using Three-Dimensional Culture (Spheroids) as an In Vitro Model of Tumour Hypoxia.* Adv Exp Med Biol, 2016. **899**: p. 167-96.
333. Moore, C.B., et al., *Short hairpin RNA (shRNA): design, delivery, and assessment of gene knockdown.* Methods Mol Biol, 2010. **629**: p. 141-58.
334. Yang, J., et al., *HIF-2α promotes epithelial-mesenchymal transition through regulating Twist2 binding to the promoter of E-cadherin in pancreatic cancer.* Journal of Experimental & Clinical Cancer Research, 2016. **35**(1): p. 26.
335. Gao, T., et al., *The mechanism between epithelial mesenchymal transition in breast cancer and hypoxia microenvironment.* Biomed Pharmacother, 2016. **80**: p. 393-405.
336. Nieto, M.A., et al., *EMT: 2016.* Cell, 2016. **166**(1): p. 21-45.
337. Salman, T., *Spontaneous tumor regression.* Journal of Oncological Science, 2016. **2**(1): p. 1-4.
338. Yu, J., et al., *Antitumor activity of T cells generated from lymph nodes draining the SEA-expressing murine B16 melanoma and secondarily activated with dendritic cells.* Int J Biol Sci, 2009. **5**(2): p. 135-46.
339. Weissman, I.L., L.E. Hood, and W.B. Wood, *Essential concepts in immunology*. 1978: Addison-Wesley.
340. Shiratori, Y., et al., *Effect of splenectomy on hepatic metastasis of colon carcinoma and natural killer activity in the liver.* Dig Dis Sci, 1995. **40**(11): p. 2398-406.
341. Gorelik, E., et al., *Role of NK cells in the control of metastatic spread and growth of tumor cells in mice.* Int J Cancer, 1982. **30**(1): p. 107-12.
342. Osellame, L.D., T.S. Blacker, and M.R. Duchen, *Cellular and molecular mechanisms of mitochondrial function.* Best Pract Res Clin Endocrinol Metab, 2012. **26**(6): p. 711-23.
343. Maranchie, J.K., et al., *The contribution of VHL substrate binding and HIF1-alpha to the phenotype of VHL loss in renal cell carcinoma.* Cancer Cell, 2002. **1**(3): p. 247-55.
344. Zimmer, M., et al., *Inhibition of hypoxia-inducible factor is sufficient for growth suppression of VHL-/- tumors.* Mol Cancer Res, 2004. **2**(2): p. 89-95.
345. Franovic, A., et al., *Human cancers converge at the HIF-2alpha oncogenic axis.* Proc Natl Acad Sci U S A, 2009. **106**(50): p. 21306-11.
346. Westenfelder, C. and R.L. Baranowski, *Erythropoietin stimulates proliferation of human renal carcinoma cells.* Kidney International, 2000. **58**(2): p. 647-657.
347. Warnecke, C., et al., *Differentiating the functional role of hypoxia-inducible factor (HIF)-1alpha and HIF-2alpha (EPAS-1) by the use of RNA interference: erythropoietin is a HIF-2alpha target gene in Hep3B and Kelly cells.* Faseb j, 2004. **18**(12): p. 1462-4.

348. Scortegagna, M., et al., *HIF-2alpha regulates murine hematopoietic development in an erythropoietin-dependent manner.* Blood, 2005. **105**(8): p. 3133-40.
349. Gruber, M., et al., *Acute postnatal ablation of Hif-2alpha results in anemia.* Proc Natl Acad Sci U S A, 2007. **104**(7): p. 2301-6.
350. Wu, P., et al., *The erythropoietin/erythropoietin receptor signaling pathway promotes growth and invasion abilities in human renal carcinoma cells.* PLoS One, 2012. **7**(9): p. e45122.
351. Gunaratnam, L., et al., *Hypoxia inducible factor activates the transforming growth factor-alpha/epidermal growth factor receptor growth stimulatory pathway in VHL(-/-) renal cell carcinoma cells.* J Biol Chem, 2003. **278**(45): p. 44966-74.
352. Wu, D., et al., *Bidirectional modulation of HIF-2 activity through chemical ligands.* Nature Chemical Biology, 2019. **15**(4): p. 367-376.
353. Borowicz, S., et al., *The soft agar colony formation assay.* J Vis Exp, 2014(92): p. e51998.
354. Xu, R., et al., *3-[(1S,2S,3R)-2,3-Difluoro-1-hydroxy-7-methylsulfonylindan-4-yl]oxy-5-fluorobenzo nitrile (PT2977), a Hypoxia-Inducible Factor 2alpha (HIF-2alpha) Inhibitor for the Treatment of Clear Cell Renal Cell Carcinoma.* J Med Chem, 2019. **62**(15): p. 6876-6893.
355. Matak, D., et al., *Colony, hanging drop, and methylcellulose three dimensional hypoxic growth optimization of renal cell carcinoma cell lines.* Cytotechnology, 2017. **69**(4): p. 565-578.
356. Lieubeau-Teillet, B., et al., *von Hippel-Lindau gene-mediated growth suppression and induction of differentiation in renal cell carcinoma cells grown as multicellular tumor spheroids.* Cancer Res, 1998. **58**(21): p. 4957-62.
357. Wang, Y., et al., *HIF-1alpha and HIF-2alpha correlate with migration and invasion in gastric cancer.* Cancer Biol Ther, 2010. **10**(4): p. 376-82.
358. Wang, X. and A. Schneider, *HIF-2alpha-mediated activation of the epidermal growth factor receptor potentiates head and neck cancer cell migration in response to hypoxia.* Carcinogenesis, 2010. **31**(7): p. 1202-10.
359. Li, N.A., et al., *Knockdown of hypoxia inducible factor-2alpha inhibits cell invasion via the downregulation of MMP-2 expression in breast cancer cells.* Oncol Lett, 2016. **11**(6): p. 3743-3748.
360. Yang, J., et al., *HIF-2alpha promotes epithelial-mesenchymal transition through regulating Twist2 binding to the promoter of E-cadherin in pancreatic cancer.* J Exp Clin Cancer Res, 2016. **35**: p. 26.
361. Rankin, E.B., et al., *Direct regulation of GAS6/AXL signaling by HIF promotes renal metastasis through SRC and MET.* Proc Natl Acad Sci U S A, 2014. **111**(37): p. 13373-8.
362. Rodrigues, P., et al., *NF-kappaB-Dependent Lymphoid Enhancer Co-option Promotes Renal Carcinoma Metastasis.* Cancer Discov, 2018. **8**(7): p. 850-865.
363. Emerling, B.M., et al., *Identification of CDCP1 as a hypoxia-inducible factor 2alpha (HIF-2alpha) target gene that is associated with survival in clear cell renal cell carcinoma patients.* Proc Natl Acad Sci U S A, 2013. **110**(9): p. 3483-8.
364. Hanna, S.C., et al., *HIF1alpha and HIF2alpha independently activate SRC to promote melanoma metastases.* J Clin Invest, 2013. **123**(5): p. 2078-93.
365. Gimm, T., et al., *Hypoxia-inducible protein 2 is a novel lipid droplet protein and a specific target gene of hypoxia-inducible factor-1.* Faseb j, 2010. **24**(11): p. 4443-58.
366. Briston, T., et al., *VHL-Mediated Regulation of CHCHD4 and Mitochondrial Function.* Frontiers in Oncology, 2018. **8**(388).
367. Hervouet, E., et al., *HIF and reactive oxygen species regulate oxidative phosphorylation in cancer.* Carcinogenesis, 2008. **29**(8): p. 1528-37.
368. Torres, A., et al., *Extracellular adenosine promotes cell migration/invasion of Glioblastoma Stem-like Cells through A3 Adenosine Receptor activation under hypoxia.* Cancer Lett, 2019. **446**: p. 112-122.
369. Doronkin, S., et al., *Dose-dependent modulation of HIF-1alpha/sima controls the rate of cell migration and invasion in Drosophila ovary border cells.* Oncogene, 2010. **29**(8): p. 1123-34.
370. Zuo, Y., Y. Wu, and C. Chakraborty, *Cdc42 negatively regulates intrinsic migration of highly aggressive breast cancer cells.* J Cell Physiol, 2012. **227**(4): p. 1399-407.
371. Muller, S., et al., *HIF stabilization inhibits renal epithelial cell migration and is associated with cytoskeletal alterations.* Sci Rep, 2018. **8**(1): p. 9497.
372. Yang, H., et al., *Extracellular ATP promotes breast cancer invasion and epithelial-mesenchymal transition via hypoxia-inducible factor 2alpha signaling.* Cancer Sci, 2019. **110**(8): p. 2456-2470.
373. Kim, W.Y., et al., *HIF2alpha cooperates with RAS to promote lung tumorigenesis in mice.* J Clin Invest, 2009. **119**(8): p. 2160-70.
374. Dana, H., et al., *Molecular Mechanisms and Biological Functions of siRNA.* Int J Biomed Sci, 2017. **13**(2): p. 48-57.
375. Hu, H., et al., *Hypoxia-inducible factors enhance glutamate signaling in cancer cells.* Oncotarget, 2014. **5**(19): p. 8853-68.
376. Sumi, C., et al., *Cancerous phenotypes associated with hypoxia-inducible factors are not influenced by the volatile anesthetic isoflurane in renal cell carcinoma.* PLoS One, 2019. **14**(4): p. e0215072.

377. Vanharanta, S., et al., *Epigenetic expansion of VHL-HIF signal output drives multiorgan metastasis in renal cancer.* Nat Med, 2013. **19**(1): p. 50-6.
378. Wierzbicki, P.M., et al., *Prognostic significance of VHL, HIF1A, HIF2A, VEGFA and p53 expression in patients with clearcell renal cell carcinoma treated with sunitinib as firstline treatment.* Int J Oncol, 2019. **55**(2): p. 371-390.
379. Kohno, K., et al., *The pleiotropic functions of the Y-box-binding protein, YB-1.* Bioessays, 2003. **25**(7): p. 691-8.
380. El-Naggar, A.M., et al., *Translational Activation of HIF1alpha by YB-1 Promotes Sarcoma Metastasis.* Cancer Cell, 2015. **27**(5): p. 682-97.
381. Hiraga, T., et al., *Hypoxia and hypoxia-inducible factor-1 expression enhance osteolytic bone metastases of breast cancer.* Cancer Res, 2007. **67**(9): p. 4157-63.
382. Liao, D., et al., *Hypoxia-inducible factor-1alpha is a key regulator of metastasis in a transgenic model of cancer initiation and progression.* Cancer Res, 2007. **67**(2): p. 563-72.
383. Helczynska, K., et al., *Hypoxia-inducible factor-2alpha correlates to distant recurrence and poor outcome in invasive breast cancer.* Cancer Res, 2008. **68**(22): p. 9212-20.
384. Moreno Roig, E., et al., *Prognostic Role of Hypoxia-Inducible Factor-2α Tumor Cell Expression in Cancer Patients: A Meta-Analysis.* Frontiers in Oncology, 2018. **8**(224).
385. Schlesinger-Raab, A., et al., *Metastatic renal cell carcinoma: results of a population-based study with 25 years follow-up.* Eur J Cancer, 2008. **44**(16): p. 2485-95.
386. McKay, R.R., et al., *Impact of bone and liver metastases on patients with renal cell carcinoma treated with targeted therapy.* Eur Urol, 2014. **65**(3): p. 577-84.
387. Gore, M.E., et al., *Final results from the large sunitinib global expanded-access trial in metastatic renal cell carcinoma.* Br J Cancer, 2015. **113**(1): p. 12-9.
388. Nieder, C., et al., *Treatment of brain metastases from renal cell cancer.* Urol Oncol, 2011. **29**(4): p. 405-10.
389. Roser, F., S.K. Rosahl, and M. Samii, *Single cerebral metastasis 3 and 19 years after primary renal cell carcinoma: case report and review of the literature.* J Neurol Neurosurg Psychiatry, 2002. **72**(2): p. 257-8.
390. Kolsi, F., et al., *Delayed brain metastasis from renal cell carcinoma.* Urol Case Rep, 2019. **22**: p. 54-56.
391. Harada, Y., et al., *Clinical study of brain metastasis of renal cell carcinoma.* Eur Urol, 1999. **36**(3): p. 230-5.
392. Everson, T.C., *Spontaneous regression of cancer.* Annals of the New York Academy of Sciences, 1964. **114**(2): p. 721-735.
393. Janiszewska, A.D., S. Poletajew, and A. Wasiutynski, *Spontaneous regression of renal cell carcinoma.* Contemp Oncol (Pozn), 2013. **17**(2): p. 123-7.
394. Jawanda, G.G. and D. Drachenberg, *Spontaneous regression of biopsy proven primary renal cell carcinoma: A case study.* Can Urol Assoc J, 2012. **6**(5): p. E203-5.
395. de Riese, W., et al., *Complete spontaneous regression in metastatic renal cell carcinoma — an update and review.* World Journal of Urology, 1991. **9**(4): p. 184-191.
396. Lim, R., et al., *A unique case of spontaneous regression of metastatic papillary renal cell carcinoma: a case report.* Cases Journal, 2009. **2**(1): p. 7769.
397. Ueda, K., et al., *Spontaneous regression of multiple pulmonary nodules in a patient with unclassified renal cell carcinoma following laparoscopic partial nephrectomy: A case report.* Mol Clin Oncol, 2016. **5**(1): p. 49-52.
398. Yang, T.-Y., W.-R. Lin, and A.W. Chiu, *Spontaneous regression of adrenal metastasis from renal cell carcinoma after sunitinib withdrawal: case report and literature review.* BMC Urology, 2018. **18**(1): p. 105.
399. Lokich, J., *Spontaneous regression of metastatic renal cancer. Case report and literature review.* Am J Clin Oncol, 1997. **20**(4): p. 416-8.
400. Melichar, B., et al., *Spontaneous regression of renal cell carcinoma lung metastases in a patient with psoriasis.* Acta Oncol, 2009. **48**(6): p. 925-7.
401. Peired, A.J., A. Sisti, and P. Romagnani, *Renal Cancer Stem Cells: Characterization and Targeted Therapies.* Stem Cells Int, 2016. **2016**: p. 8342625.
402. Ashkenazi, R., S.N. Gentry, and T.L. Jackson, *Pathways to tumorigenesis--modeling mutation acquisition in stem cells and their progeny.* Neoplasia, 2008. **10**(11): p. 1170-82.
403. Kern, S.E. and D. Shibata, *The fuzzy math of solid tumor stem cells: a perspective.* Cancer Res, 2007. **67**(19): p. 8985-8.
404. Alison, M.R., S.M. Lim, and L.J. Nicholson, *Cancer stem cells: problems for therapy?* J Pathol, 2011. **223**(2): p. 147-61.
405. Pietras, A., et al., *HIF-2α maintains an undifferentiated state in neural crest-like human neuroblastoma tumor-initiating cells.* Proceedings of the National Academy of Sciences, 2009. **106**(39): p. 16805-16810.
406. Li, Z., et al., *Hypoxia-inducible factors regulate tumorigenic capacity of glioma stem cells.* Cancer Cell, 2009. **15**(6): p. 501-13.

407. Rouault-Pierre, K., et al., *HIF-2alpha protects human hematopoietic stem/progenitors and acute myeloid leukemic cells from apoptosis induced by endoplasmic reticulum stress.* Cell Stem Cell, 2013. **13**(5): p. 549-63.
408. Myszczyszyn, A., et al., *The Role of Hypoxia and Cancer Stem Cells in Renal Cell Carcinoma Pathogenesis.* Stem Cell Rev Rep, 2015. **11**(6): p. 919-43.
409. Pavlova, N.N. and C.B. Thompson, *The Emerging Hallmarks of Cancer Metabolism.* Cell Metab, 2016. **23**(1): p. 27-47.
410. Zhang, X.D., et al., *Effect of 2-deoxy-D-glucose on various malignant cell lines in vitro.* Anticancer Res, 2006. **26**(5a): p. 3561-6.
411. Woodward, G.E. and F.B. Cramer, *2-Deoxy-D-glucose as an inhibitor of anaerobic glycolysis in tumor tissues.* J Franklin Inst, 1952. **254**: p. 259-60.
412. Plathow, C. and W.A. Weber, *Tumor cell metabolism imaging.* J Nucl Med, 2008. **49 Suppl 2**: p. 43s-63s.
413. Hu, C.J., et al., *Differential roles of hypoxia-inducible factor 1alpha (HIF-1alpha) and HIF-2alpha in hypoxic gene regulation.* Mol Cell Biol, 2003. **23**(24): p. 9361-74.
414. Uchida, T., et al., *Prolonged hypoxia differentially regulates hypoxia-inducible factor (HIF)-1alpha and HIF-2alpha expression in lung epithelial cells: implication of natural antisense HIF-1alpha.* J Biol Chem, 2004. **279**(15): p. 14871-8.
415. Carracedo, A., L.C. Cantley, and P.P. Pandolfi, *Cancer metabolism: fatty acid oxidation in the limelight.* Nat Rev Cancer, 2013. **13**(4): p. 227-32.
416. Currie, E., et al., *Cellular fatty acid metabolism and cancer.* Cell Metab, 2013. **18**(2): p. 153-61.
417. Mylonis, I., G. Simos, and E. Paraskeva, *Hypoxia-Inducible Factors and the Regulation of Lipid Metabolism.* Cells, 2019. **8**(3).
418. Olzmann, J.A. and P. Carvalho, *Dynamics and functions of lipid droplets.* Nature Reviews Molecular Cell Biology, 2019. **20**(3): p. 137-155.
419. Shyu, P., Jr., et al., *Dropping in on lipid droplets: insights into cellular stress and cancer.* Biosci Rep, 2018. **38**(5).
420. Wilfling, F., et al., *Triacylglycerol synthesis enzymes mediate lipid droplet growth by relocalizing from the ER to lipid droplets.* Dev Cell, 2013. **24**(4): p. 384-99.
421. Lee, S.J., et al., *Mitochondrial dysfunction induces formation of lipid droplets as a generalized response to stress.* Oxid Med Cell Longev, 2013. **2013**: p. 327167.
422. Ploegh, H.L., *A lipid-based model for the creation of an escape hatch from the endoplasmic reticulum.* Nature, 2007. **448**(7152): p. 435-8.
423. Fu, S., et al., *Aberrant lipid metabolism disrupts calcium homeostasis causing liver endoplasmic reticulum stress in obesity.* Nature, 2011. **473**(7348): p. 528-31.
424. Maier, A., et al., *Hypoxia-inducible protein 2 Hig2/Hilpda mediates neutral lipid accumulation in macrophages and contributes to atherosclerosis in apolipoprotein E-deficient mice.* Faseb j, 2017. **31**(11): p. 4971-4984.
425. Greenspan, P. and S.D. Fowler, *Spectrofluorometric studies of the lipid probe, nile red.* J Lipid Res, 1985. **26**(7): p. 781-9.
426. Greenspan, P., E.P. Mayer, and S.D. Fowler, *Nile red: a selective fluorescent stain for intracellular lipid droplets.* J Cell Biol, 1985. **100**(3): p. 965-73.
427. Fam, T.K., A.S. Klymchenko, and M. Collot, *Recent Advances in Fluorescent Probes for Lipid Droplets.* Materials (Basel), 2018. **11**(9).
428. Zhang, H., et al., *HIF-1 Inhibits Mitochondrial Biogenesis and Cellular Respiration in VHL-Deficient Renal Cell Carcinoma by Repression of C-MYC Activity.* Cancer Cell, 2007. **11**(5): p. 407-420.
429. Nilsson, H., et al., *Primary clear cell renal carcinoma cells display minimal mitochondrial respiratory capacity resulting in pronounced sensitivity to glycolytic inhibition by 3-Bromopyruvate.* Cell Death Dis, 2015. **6**: p. e1585.
430. Okamoto, A., et al., *HIF-1-mediated suppression of mitochondria electron transport chain function confers resistance to lidocaine-induced cell death.* Scientific Reports, 2017. **7**(1): p. 3816.
431. Hervouet, E., et al., *A new role for the von Hippel-Lindau tumor suppressor protein: stimulation of mitochondrial oxidative phosphorylation complex biogenesis.* Carcinogenesis, 2005. **26**(3): p. 531-9.
432. Li, F., et al., *Myc stimulates nuclearly encoded mitochondrial genes and mitochondrial biogenesis.* Mol Cell Biol, 2005. **25**(14): p. 6225-34.
433. Leisz, S., et al., *Distinct von Hippel-Lindau gene and hypoxia-regulated alterations in gene and protein expression patterns of renal cell carcinoma and their effects on metabolism.* Oncotarget, 2015. **6**(13): p. 11395-406.
434. Hay, M., et al., *Clinical development success rates for investigational drugs.* Nat Biotechnol, 2014. **32**(1): p. 40-51.
435. Pantziarka, P., et al., *ReDO_DB: the repurposing drugs in oncology database.* Ecancermedicalscience, 2018. **12**: p. 886.
436. Ashburn, T.T. and K.B. Thor, *Drug repositioning: identifying and developing new uses for existing drugs.* Nature Reviews Drug Discovery, 2004. **3**(8): p. 673-683.
437. Koudijs, K.K.M., et al., *Personalised drug repositioning for Clear Cell Renal Cell Carcinoma using gene expression.* Sci Rep, 2018. **8**(1): p. 5250.

438. Koudijs, K.K.M., et al., *The impact of estimated tumour purity on gene expression-based drug repositioning of Clear Cell Renal Cell Carcinoma samples.* Sci Rep, 2019. **9**(1): p. 2495.
439. Rena, G., D.G. Hardie, and E.R. Pearson, *The mechanisms of action of metformin.* Diabetologia, 2017. **60**(9): p. 1577-1585.
440. Tseng, C.H., *Use of metformin and risk of kidney cancer in patients with type 2 diabetes.* Eur J Cancer, 2016. **52**: p. 19-25.
441. Keizman, D., et al., *Metformin Use and Outcome of Sunitinib Treatment in Patients With Diabetes and Metastatic Renal Cell Carcinoma.* Clin Genitourin Cancer, 2016. **14**(5): p. 420-425.
442. Psutka, S.P., et al., *The association between metformin use and oncologic outcomes among surgically treated diabetic patients with localized renal cell carcinoma.* Urol Oncol, 2015. **33**(2): p. 67.e15-23.
443. Shepherd, J., et al., *Prevention of coronary heart disease with pravastatin in men with hypercholesterolemia. 1995.* Atheroscler Suppl, 2004. **5**(3): p. 91-7.
444. Oliver, M.F., *Might treatment of hypercholesterolaemia increase non-cardiac mortality?* Lancet, 1991. **337**(8756): p. 1529-31.
445. Ukomadu, C. and A. Dutta, *p21-dependent inhibition of colon cancer cell growth by mevastatin is independent of inhibition of G1 cyclin-dependent kinases.* J Biol Chem, 2003. **278**(44): p. 43586-94.
446. Seeger, H., D. Wallwiener, and A.O. Mueck, *Statins can inhibit proliferation of human breast cancer cells in vitro.* Exp Clin Endocrinol Diabetes, 2003. **111**(1): p. 47-8.
447. Hoque, A., H. Chen, and X.C. Xu, *Statin induces apoptosis and cell growth arrest in prostate cancer cells.* Cancer Epidemiol Biomarkers Prev, 2008. **17**(1): p. 88-94.
448. Collisson, E.A., et al., *Atorvastatin prevents RhoC isoprenylation, invasion, and metastasis in human melanoma cells.* Mol Cancer Ther, 2003. **2**(10): p. 941-8.
449. Wu, J., et al., *Blocking the Raf/MEK/ERK pathway sensitizes acute myelogenous leukemia cells to lovastatin-induced apoptosis.* Cancer Res, 2004. **64**(18): p. 6461-8.
450. Fang, Z., et al., *Simvastatin inhibits renal cancer cell growth and metastasis via AKT/mTOR, ERK and JAK2/STAT3 pathway.* PLoS One, 2013. **8**(5): p. e62823.
451. Horiguchi, A., et al., *3-hydroxy-3-methylglutaryl-coenzyme a reductase inhibitor, fluvastatin, as a novel agent for prophylaxis of renal cancer metastasis.* Clin Cancer Res, 2004. **10**(24): p. 8648-55.
452. Check, J.H., et al., *Long-term High-quality Survival with Single-agent Mifepristone Treatment Despite Advanced Cancer.* Anticancer Res, 2016. **36**(12): p. 6511-6513.
453. Check, J.H., et al., *Efficacy of the progesterone receptor antagonist mifepristone for palliative therapy of patients with a variety of advanced cancer types.* Anticancer Res, 2010. **30**(2): p. 623-8.
454. Broach, J.R. and J. Thorner, *High-throughput screening for drug discovery.* Nature, 1996. **384**(6604 Suppl): p. 14-6.
455. Chen, D.S. and M.M. Davis, *Molecular and functional analysis using live cell microarrays.* Curr Opin Chem Biol, 2006. **10**(1): p. 28-34.
456. Houck, K.A. and R.J. Kavlock, *Understanding mechanisms of toxicity: insights from drug discovery research.* Toxicol Appl Pharmacol, 2008. **227**(2): p. 163-78.
457. Zhang, Z., et al., *Quality control of cell-based high-throughput drug screening.* Acta Pharmaceutica Sinica B, 2012. **2**(5): p. 429-438.
458. Lundholt, B.K., K.M. Scudder, and L. Pagliaro, *A simple technique for reducing edge effect in cell-based assays.* J Biomol Screen, 2003. **8**(5): p. 566-70.
459. Malo, N., et al., *Statistical practice in high-throughput screening data analysis.* Nat Biotechnol, 2006. **24**(2): p. 167-75.
460. Thompson, J.M., et al., *Targeting the Mevalonate Pathway Suppresses VHL-Deficient CC-RCC through an HIF-Dependent Mechanism.* Mol Cancer Ther, 2018. **17**(8): p. 1781-1792.
461. Vincent, L., et al., *Cerivastatin, an inhibitor of 3-hydroxy-3-methylglutaryl coenzyme a reductase, inhibits endothelial cell proliferation induced by angiogenic factors in vitro and angiogenesis in in vivo models.* Arterioscler Thromb Vasc Biol, 2002. **22**(4): p. 623-9.
462. Nubel, T., et al., *Lovastatin inhibits Rho-regulated expression of E-selectin by TNFalpha and attenuates tumor cell adhesion.* Faseb j, 2004. **18**(1): p. 140-2.
463. Wang, I.K., S.Y. Lin-Shiau, and J.K. Lin, *Suppression of invasion and MMP-9 expression in NIH 3T3 and v-H-Ras 3T3 fibroblasts by lovastatin through inhibition of ras isoprenylation.* Oncology, 2000. **59**(3): p. 245-54.
464. Chong, P.H., J.D. Seeger, and C. Franklin, *Clinically relevant differences between the statins: implications for therapeutic selection.* Am J Med, 2001. **111**(5): p. 390-400.
465. Woodard, J., et al., *Statin-dependent suppression of the Akt/mammalian target of rapamycin signaling cascade and programmed cell death 4 up-regulation in renal cell carcinoma.* Clin Cancer Res, 2008. **14**(14): p. 4640-9.
466. Woodard, J., et al., *AMPK as a therapeutic target in renal cell carcinoma.* Cancer Biol Ther, 2010. **10**(11): p. 1168-77.

467. Farina, H.G., et al., *Lovastatin alters cytoskeleton organization and inhibits experimental metastasis of mammary carcinoma cells.* Clinical & Experimental Metastasis, 2002. **19**(6): p. 551-560.
468. McKay, R.R., et al., *Statins and survival outcomes in patients with metastatic renal cell carcinoma.* European Journal of Cancer, 2016. **52**: p. 155-162.
469. Bjorkhem-Bergman, L., J.D. Lindh, and P. Bergman, *What is a relevant statin concentration in cell experiments claiming pleiotropic effects?* Br J Clin Pharmacol, 2011. **72**(1): p. 164-5.
470. Golomb, B.A. and M.A. Evans, *Statin adverse effects : a review of the literature and evidence for a mitochondrial mechanism.* Am J Cardiovasc Drugs, 2008. **8**(6): p. 373-418.
471. Isaacs, A. and J. Lindenmann, *Virus interference. I. The interferon.* Proc R Soc Lond B Biol Sci, 1957. **147**(927): p. 258-67.
472. Platanias, L.C., *Mechanisms of type-I- and type-II-interferon-mediated signalling.* Nat Rev Immunol, 2005. **5**(5): p. 375-86.
473. Pestka, S., C.D. Krause, and M.R. Walter, *Interferons, interferon-like cytokines, and their receptors.* Immunol Rev, 2004. **202**: p. 8-32.
474. Goubau, D., S. Deddouche, and C. Reis e Sousa, *Cytosolic sensing of viruses.* Immunity, 2013. **38**(5): p. 855-69.
475. Iwasaki, A., *A virological view of innate immune recognition.* Annu Rev Microbiol, 2012. **66**: p. 177-96.
476. Paludan, S.R. and A.G. Bowie, *Immune sensing of DNA.* Immunity, 2013. **38**(5): p. 870-80.
477. Stark, G.R., et al., *How cells respond to interferons.* Annu Rev Biochem, 1998. **67**: p. 227-64.
478. Yoneyama, M., et al., *Shared and unique functions of the DExD/H-box helicases RIG-I, MDA5, and LGP2 in antiviral innate immunity.* J Immunol, 2005. **175**(5): p. 2851-8.
479. Yoneyama, M., et al., *The RNA helicase RIG-I has an essential function in double-stranded RNA-induced innate antiviral responses.* Nat Immunol, 2004. **5**(7): p. 730-7.
480. Kawai, T., et al., *IPS-1, an adaptor triggering RIG-I- and Mda5-mediated type I interferon induction.* Nat Immunol, 2005. **6**(10): p. 981-8.
481. Fitzgerald, K.A., et al., *IKKepsilon and TBK1 are essential components of the IRF3 signaling pathway.* Nat Immunol, 2003. **4**(5): p. 491-6.
482. Sharma, S., et al., *Triggering the interferon antiviral response through an IKK-related pathway.* Science, 2003. **300**(5622): p. 1148-51.
483. Hemmi, H., et al., *The roles of two IkappaB kinase-related kinases in lipopolysaccharide and double stranded RNA signaling and viral infection.* J Exp Med, 2004. **199**(12): p. 1641-50.
484. Lin, R., et al., *Virus-dependent phosphorylation of the IRF-3 transcription factor regulates nuclear translocation, transactivation potential, and proteasome-mediated degradation.* Mol Cell Biol, 1998. **18**(5): p. 2986-96.
485. Sato, M., et al., *Involvement of the IRF family transcription factor IRF-3 in virus-induced activation of the IFN-beta gene.* FEBS Lett, 1998. **425**(1): p. 112-6.
486. Yoneyama, M., et al., *Direct triggering of the type I interferon system by virus infection: activation of a transcription factor complex containing IRF-3 and CBP/p300.* Embo j, 1998. **17**(4): p. 1087-95.
487. Zhang, Z., et al., *The helicase DDX41 senses intracellular DNA mediated by the adaptor STING in dendritic cells.* Nat Immunol, 2011. **12**(10): p. 959-65.
488. Unterholzner, L., et al., *IFI16 is an innate immune sensor for intracellular DNA.* Nature Immunology, 2010. **11**: p. 997.
489. Takaoka, A., et al., *DAI (DLM-1/ZBP1) is a cytosolic DNA sensor and an activator of innate immune response.* Nature, 2007. **448**(7152): p. 501-5.
490. Chen, Q., L. Sun, and Z.J. Chen, *Regulation and function of the cGAS–STING pathway of cytosolic DNA sensing.* Nature Immunology, 2016. **17**: p. 1142.
491. Ishikawa, H., Z. Ma, and G.N. Barber, *STING regulates intracellular DNA-mediated, type I interferon-dependent innate immunity.* Nature, 2009. **461**(7265): p. 788-92.
492. Liu, S., et al., *Phosphorylation of innate immune adaptor proteins MAVS, STING, and TRIF induces IRF3 activation.* Science, 2015. **347**(6227): p. aaa2630.
493. Abe, T. and G.N. Barber, *Cytosolic-DNA-mediated, STING-dependent proinflammatory gene induction necessitates canonical NF-kappaB activation through TBK1.* J Virol, 2014. **88**(10): p. 5328-41.
494. Civril, F., et al., *Structural mechanism of cytosolic DNA sensing by cGAS.* Nature, 2013. **498**(7454): p. 332-7.
495. Sun, L., et al., *Cyclic GMP-AMP synthase is a cytosolic DNA sensor that activates the type I interferon pathway.* Science, 2013. **339**(6121): p. 786-91.
496. Wu, J., et al., *Cyclic GMP-AMP is an endogenous second messenger in innate immune signaling by cytosolic DNA.* Science, 2013. **339**(6121): p. 826-30.
497. Heil, F., et al., *Species-specific recognition of single-stranded RNA via toll-like receptor 7 and 8.* Science, 2004. **303**(5663): p. 1526-9.

498. Krug, A., et al., *Herpes simplex virus type 1 activates murine natural interferon-producing cells through toll-like receptor 9.* Blood, 2004. **103**(4): p. 1433-7.
499. Park, B.S. and J.-O. Lee, *Recognition of lipopolysaccharide pattern by TLR4 complexes.* Experimental &Amp; Molecular Medicine, 2013. **45**: p. e66.
500. Akira, S., S. Uematsu, and O. Takeuchi, *Pathogen recognition and innate immunity.* Cell, 2006. **124**(4): p. 783-801.
501. Honda, K., A. Takaoka, and T. Taniguchi, *Type I interferon [corrected] gene induction by the interferon regulatory factor family of transcription factors.* Immunity, 2006. **25**(3): p. 349-60.
502. Honda, K., et al., *Role of a transductional-transcriptional processor complex involving MyD88 and IRF-7 in Toll-like receptor signaling.* Proc Natl Acad Sci U S A, 2004. **101**(43): p. 15416-21.
503. Kawai, T., et al., *Interferon-alpha induction through Toll-like receptors involves a direct interaction of IRF7 with MyD88 and TRAF6.* Nat Immunol, 2004. **5**(10): p. 1061-8.
504. Yamamoto, M., et al., *TRAM is specifically involved in the Toll-like receptor 4-mediated MyD88-independent signaling pathway.* Nat Immunol, 2003. **4**(11): p. 1144-50.
505. Oganesyan, G., et al., *Critical role of TRAF3 in the Toll-like receptor-dependent and -independent antiviral response.* Nature, 2006. **439**(7073): p. 208-11.
506. Honda, K., et al., *IRF-7 is the master regulator of type-I interferon-dependent immune responses.* Nature, 2005. **434**(7034): p. 772-7.
507. Fuertes, M.B., et al., *Type I interferon response and innate immune sensing of cancer.* Trends Immunol, 2013. **34**(2): p. 67-73.
508. de Weerd, N.A., S.A. Samarajiwa, and P.J. Hertzog, *Type I interferon receptors: biochemistry and biological functions.* J Biol Chem, 2007. **282**(28): p. 20053-7.
509. Cohen, B., et al., *Ligand-induced association of the type I interferon receptor components.* Mol Cell Biol, 1995. **15**(8): p. 4208-14.
510. Stark, G.R. and J.E. Darnell, Jr., *The JAK-STAT pathway at twenty.* Immunity, 2012. **36**(4): p. 503-14.
511. Schneider, W.M., M.D. Chevillotte, and C.M. Rice, *Interferon-stimulated genes: a complex web of host defenses.* Annu Rev Immunol, 2014. **32**: p. 513-45.
512. Blaszczyk, K., et al., *The unique role of STAT2 in constitutive and IFN-induced transcription and antiviral responses.* Cytokine Growth Factor Rev, 2016. **29**: p. 71-81.
513. Schoggins, J.W. and C.M. Rice, *Interferon-stimulated genes and their antiviral effector functions.* Curr Opin Virol, 2011. **1**(6): p. 519-25.
514. Wilmes, S., et al., *Receptor dimerization dynamics as a regulatory valve for plasticity of type I interferon signaling.* J Cell Biol, 2015. **209**(4): p. 579-93.
515. Shi, H.X., et al., *Positive regulation of interferon regulatory factor 3 activation by Herc5 via ISG15 modification.* Mol Cell Biol, 2010. **30**(10): p. 2424-36.
516. Patterson, J.B. and C.E. Samuel, *Expression and regulation by interferon of a double-stranded-RNA-specific adenosine deaminase from human cells: evidence for two forms of the deaminase.* Mol Cell Biol, 1995. **15**(10): p. 5376-88.
517. Miar, A., et al., *Hypoxia induces transcriptional and translational downregulation of the type I interferon (IFN) pathway in multiple cancer cell types.* bioRxiv, 2019: p. 715151.
518. Bidwell, B.N., et al., *Silencing of Irf7 pathways in breast cancer cells promotes bone metastasis through immune escape.* Nat Med, 2012. **18**(8): p. 1224-31.
519. Okabe, Y., et al., *Toll-like receptor-independent gene induction program activated by mammalian DNA escaped from apoptotic DNA degradation.* J Exp Med, 2005. **202**(10): p. 1333-9.
520. Crow, Y.J., et al., *Mutations in the gene encoding the 3’-5’ DNA exonuclease TREX1 cause Aicardi-Goutières syndrome at the AGS1 locus.* Nature Genetics, 2006. **38**(8): p. 917-920.
521. Barbalat, R., et al., *Nucleic acid recognition by the innate immune system.* Annu Rev Immunol, 2011. **29**: p. 185-214.
522. Weiss, G., et al., *MyD88 drives the IFN-beta response to Lactobacillus acidophilus in dendritic cells through a mechanism involving IRF1, IRF3, and IRF7.* J Immunol, 2012. **189**(6): p. 2860-8.
523. Ehrlich, P., *Ueber den jetzigen Stand der Karzinomforschung.* Ned. Tijdschr. voor Geneeskd, 1909. **5**: p. 273-90.
524. Burnet, M., *Cancer: a biological approach. III. Viruses associated with neoplastic conditions. IV. Practical applications.* Br Med J, 1957. **1**(5023): p. 841-7.
525. Thomas, L. and H. Lawrence, *Cellular and humoral aspects of the hypersensitive states.* New York: Hoeber-Harper, 1959: p. 529-532.
526. Stutman, O., *Tumor development after 3-methylcholanthrene in immunologically deficient athymic-nude mice.* Science, 1974. **183**(4124): p. 534-6.

527. Dighe, A.S., et al., *Enhanced in vivo growth and resistance to rejection of tumor cells expressing dominant negative IFN gamma receptors.* Immunity, 1994. **1**(6): p. 447-56.
528. Kaplan, D.H., et al., *Demonstration of an interferon gamma-dependent tumor surveillance system in immunocompetent mice.* Proc Natl Acad Sci U S A, 1998. **95**(13): p. 7556-61.
529. Street, S.E., et al., *Suppression of lymphoma and epithelial malignancies effected by interferon gamma.* J Exp Med, 2002. **196**(1): p. 129-34.
530. Street, S.E., E. Cretney, and M.J. Smyth, *Perforin and interferon-gamma activities independently control tumor initiation, growth, and metastasis.* Blood, 2001. **97**(1): p. 192-7.
531. Trapani, J.A., *Target cell apoptosis induced by cytotoxic T cells and natural killer cells involves synergy between the pore-forming protein, perforin, and the serine protease, granzyme B.* Aust N Z J Med, 1995. **25**(6): p. 793-9.
532. Shankaran, V., et al., *IFNgamma and lymphocytes prevent primary tumour development and shape tumour immunogenicity.* Nature, 2001. **410**(6832): p. 1107-11.
533. Dunn, G.P., et al., *Cancer immunoediting: from immunosurveillance to tumor escape.* Nat Immunol, 2002. **3**(11): p. 991-8.
534. Smyth, M.J., et al., *Differential tumor surveillance by natural killer (NK) and NKT cells.* J Exp Med, 2000. **191**(4): p. 661-8.
535. Gresser, I., et al., *Increased survival in mice inoculated with tumor cells and treated with interferon preparations.* Proc Natl Acad Sci U S A, 1969. **63**(1): p. 51-7.
536. Gresser, I., C. Maury, and D. Brouty-Boye, *Mechanism of the antitumour effect of interferon in mice.* Nature, 1972. **239**(5368): p. 167-8.
537. Gresser, I., et al., *Injection of mice with antibody to interferon enhances the growth of transplantable murine tumors.* J Exp Med, 1983. **158**(6): p. 2095-107.
538. Reid, L.M., et al., *Influence of anti-mouse interferon serum on the growth and metastasis of tumor cells persistently infected with virus and of human prostatic tumors in athymic nude mice.* Proc Natl Acad Sci U S A, 1981. **78**(2): p. 1171-5.
539. Le Bon, A. and D.F. Tough, *Links between innate and adaptive immunity via type I interferon.* Curr Opin Immunol, 2002. **14**(4): p. 432-6.
540. Zhang, X., et al., *Potent and selective stimulation of memory-phenotype CD8+ T cells in vivo by IL-15.* Immunity, 1998. **8**(5): p. 591-9.
541. Kerbel, R. and J. Folkman, *Clinical translation of angiogenesis inhibitors.* Nat Rev Cancer, 2002. **2**(10): p. 727-39.
542. Vicari, A.P. and C. Caux, *Chemokines in cancer.* Cytokine Growth Factor Rev, 2002. **13**(2): p. 143-54.
543. Matzinger, P., *Tolerance, danger, and the extended family.* Annu Rev Immunol, 1994. **12**: p. 991-1045.
544. Gasser, S. and D.H. Raulet, *The DNA damage response arouses the immune system.* Cancer Res, 2006. **66**(8): p. 3959-62.
545. Dunn, G.P., C.M. Koebel, and R.D. Schreiber, *Interferons, immunity and cancer immunoediting.* Nat Rev Immunol, 2006. **6**(11): p. 836-48.
546. Bromberg, J.F., et al., *Transcriptionally active Stat1 is required for the antiproliferative effects of both interferon alpha and interferon gamma.* Proc Natl Acad Sci U S A, 1996. **93**(15): p. 7673-8.
547. Kumar, A., et al., *Defective TNF-alpha-induced apoptosis in STAT1-null cells due to low constitutive levels of caspases.* Science, 1997. **278**(5343): p. 1630-2.
548. Qin, Z. and T. Blankenstein, *CD4+ T cell--mediated tumor rejection involves inhibition of angiogenesis that is dependent on IFN gamma receptor expression by nonhematopoietic cells.* Immunity, 2000. **12**(6): p. 677-86.
549. Loeb, L.A., K.R. Loeb, and J.P. Anderson, *Multiple mutations and cancer.* Proc Natl Acad Sci U S A, 2003. **100**(3): p. 776-81.
550. Budhwani, M., R. Mazzieri, and R. Dolcetti, *Plasticity of Type I Interferon-Mediated Responses in Cancer Therapy: From Anti-tumor Immunity to Resistance.* Front Oncol, 2018. **8**: p. 322.
551. Stone, H.B., L.J. Peters, and L. Milas, *Effect of host immune capability on radiocurability and subsequent transplantability of a murine fibrosarcoma.* J Natl Cancer Inst, 1979. **63**(5): p. 1229-35.
552. Burnette, B.C., et al., *The efficacy of radiotherapy relies upon induction of type i interferon-dependent innate and adaptive immunity.* Cancer Res, 2011. **71**(7): p. 2488-96.
553. Lim, J.Y., et al., *Type I interferons induced by radiation therapy mediate recruitment and effector function of CD8(+) T cells.* Cancer Immunol Immunother, 2014. **63**(3): p. 259-71.
554. Deng, L., et al., *STING-Dependent Cytosolic DNA Sensing Promotes Radiation-Induced Type I Interferon-Dependent Antitumor Immunity in Immunogenic Tumors.* Immunity, 2014. **41**(5): p. 843-52.
555. Casares, N., et al., *Caspase-dependent immunogenicity of doxorubicin-induced tumor cell death.* J Exp Med, 2005. **202**(12): p. 1691-701.

556. Vacchelli, E., et al., *Autocrine signaling of type 1 interferons in successful anticancer chemotherapy.* Oncoimmunology, 2015. **4**(8): p. e988042.
557. Sistigu, A., et al., *Cancer cell-autonomous contribution of type I interferon signaling to the efficacy of chemotherapy.* Nat Med, 2014. **20**(11): p. 1301-9.
558. Pardoll, D.M., *The blockade of immune checkpoints in cancer immunotherapy.* Nat Rev Cancer, 2012. **12**(4): p. 252-64.
559. Sanmamed, M.F. and L. Chen, *Inducible expression of B7-H1 (PD-L1) and its selective role in tumor site immune modulation.* Cancer J, 2014. **20**(4): p. 256-61.
560. Hamid, O., et al., *Safety and tumor responses with lambrolizumab (anti-PD-1) in melanoma.* N Engl J Med, 2013. **369**(2): p. 134-44.
561. Gao, J., et al., *Loss of IFN-gamma Pathway Genes in Tumor Cells as a Mechanism of Resistance to Anti-CTLA-4 Therapy.* Cell, 2016. **167**(2): p. 397-404.e9.
562. Zaretsky, J.M., et al., *Mutations Associated with Acquired Resistance to PD-1 Blockade in Melanoma.* N Engl J Med, 2016. **375**(9): p. 819-29.
563. Shin, D.S., et al., *Primary Resistance to PD-1 Blockade Mediated by JAK1/2 Mutations.* Cancer Discov, 2017. **7**(2): p. 188-201.
564. Gettinger, S., et al., *Impaired HLA Class I Antigen Processing and Presentation as a Mechanism of Acquired Resistance to Immune Checkpoint Inhibitors in Lung Cancer.* Cancer Discov, 2017. **7**(12): p. 1420-1435.
565. Hummel, J.L., E. Safroneeva, and K.L. Mossman, *The role of ICP0-Null HSV-1 and interferon signaling defects in the effective treatment of breast adenocarcinoma.* Mol Ther, 2005. **12**(6): p. 1101-10.
566. Zhang, K.X., et al., *Down-regulation of type I interferon receptor sensitizes bladder cancer cells to vesicular stomatitis virus-induced cell death.* Int J Cancer, 2010. **127**(4): p. 830-8.
567. Li, Q. and M.A. Tainsky, *Epigenetic silencing of IRF7 and/or IRF5 in lung cancer cells leads to increased sensitivity to oncolytic viruses.* PLoS One, 2011. **6**(12): p. e28683.
568. Wilson, E.B., et al., *Blockade of chronic type I interferon signaling to control persistent LCMV infection.* Science, 2013. **340**(6129): p. 202-7.
569. Teijaro, J.R., et al., *Persistent LCMV infection is controlled by blockade of type I interferon signaling.* Science, 2013. **340**(6129): p. 207-11.
570. Kalliolias, G.D. and L.B. Ivashkiv, *Overview of the biology of type I interferons.* Arthritis Res Ther, 2010. **12 Suppl 1**: p. S1.
571. Banchereau, J. and V. Pascual, *Type I interferon in systemic lupus erythematosus and other autoimmune diseases.* Immunity, 2006. **25**(3): p. 383-92.
572. Novick, D., B. Cohen, and M. Rubinstein, *The human interferon alpha/beta receptor: characterization and molecular cloning.* Cell, 1994. **77**(3): p. 391-400.
573. Pioli, P.D., et al., *Sequential proteolytic processing of an interferon-alpha receptor subunit by TNF-alpha converting enzyme and presenilins.* J Interferon Cytokine Res, 2012. **32**(7): p. 312-25.
574. Kumar, K.G., J.J. Krolewski, and S.Y. Fuchs, *Phosphorylation and specific ubiquitin acceptor sites are required for ubiquitination and degradation of the IFNAR1 subunit of type I interferon receptor.* J Biol Chem, 2004. **279**(45): p. 46614-20.
575. Kumar, K.G., et al., *Site-specific ubiquitination exposes a linear motif to promote interferon-alpha receptor endocytosis.* J Cell Biol, 2007. **179**(5): p. 935-50.
576. Kumar, K.G., et al., *Basal ubiquitin-independent internalization of interferon alpha receptor is prevented by Tyk2-mediated masking of a linear endocytic motif.* J Biol Chem, 2008. **283**(27): p. 18566-72.
577. Kalie, E., et al., *The stability of the ternary interferon-receptor complex rather than the affinity to the individual subunits dictates differential biological activities.* J Biol Chem, 2008. **283**(47): p. 32925-36.
578. Chmiest, D., et al., *Spatiotemporal control of interferon-induced JAK/STAT signalling and gene transcription by the retromer complex.* Nat Commun, 2016. **7**: p. 13476.
579. Tomita, S., et al., *Suppression of SOCS3 increases susceptibility of renal cell carcinoma to interferon-alpha.* Cancer Sci, 2011. **102**(1): p. 57-63.
580. Zitzmann, K., et al., *SOCS1 silencing enhances antitumor activity of type I IFNs by regulating apoptosis in neuroendocrine tumor cells.* Cancer Res, 2007. **67**(10): p. 5025-32.
581. Piganis, R.A., et al., *Suppressor of cytokine signaling (SOCS) 1 inhibits type I interferon (IFN) signaling via the interferon alpha receptor (IFNAR1)-associated tyrosine kinase Tyk2.* J Biol Chem, 2011. **286**(39): p. 33811-8.
582. Fenner, J.E., et al., *Suppressor of cytokine signaling 1 regulates the immune response to infection by a unique inhibition of type I interferon activity.* Nat Immunol, 2006. **7**(1): p. 33-9.
583. Dunn, G.P., et al., *IFN unresponsiveness in LNCaP cells due to the lack of JAK1 gene expression.* Cancer Res, 2005. **65**(8): p. 3447-53.

584. Tanaka, T., M.A. Soriano, and M.J. Grusby, *SLIM is a nuclear ubiquitin E3 ligase that negatively regulates STAT signaling.* Immunity, 2005. **22**(6): p. 729-36.
585. Durfee, L.A., et al., *The ISG15 conjugation system broadly targets newly synthesized proteins: implications for the antiviral function of ISG15.* Mol Cell, 2010. **38**(5): p. 722-32.
586. Malakhova, O.A., et al., *Protein ISGylation modulates the JAK-STAT signaling pathway.* Genes Dev, 2003. **17**(4): p. 455-60.
587. Li, Y., et al., *ISG56 is a negative-feedback regulator of virus-triggered signaling and cellular antiviral response.* Proc Natl Acad Sci U S A, 2009. **106**(19): p. 7945-50.
588. Rajsbaum, R., A. Garcia-Sastre, and G.A. Versteeg, *TRIMmunity: the roles of the TRIM E3-ubiquitin ligase family in innate antiviral immunity.* J Mol Biol, 2014. **426**(6): p. 1265-84.
589. Hu, Y., et al., *Guanylate binding protein 4 negatively regulates virus-induced type I IFN and antiviral response by targeting IFN regulatory factor 7.* J Immunol, 2011. **187**(12): p. 6456-62.
590. Noman, M.Z., et al., *Microenvironmental hypoxia orchestrating the cell stroma cross talk, tumor progression and antitumor response.* Crit Rev Immunol, 2011. **31**(5): p. 357-77.
591. Gabrilovich, D.I. and S. Nagaraj, *Myeloid-derived suppressor cells as regulators of the immune system.* Nat Rev Immunol, 2009. **9**(3): p. 162-74.
592. Gabrilovich, D., *Mechanisms and functional significance of tumour-induced dendritic-cell defects.* Nat Rev Immunol, 2004. **4**(12): p. 941-52.
593. Corzo, C.A., et al., *HIF-1alpha regulates function and differentiation of myeloid-derived suppressor cells in the tumor microenvironment.* J Exp Med, 2010. **207**(11): p. 2439-53.
594. Laoui, D., et al., *Tumor hypoxia does not drive differentiation of tumor-associated macrophages but rather fine-tunes the M2-like macrophage population.* Cancer Res, 2014. **74**(1): p. 24-30.
595. Chaturvedi, P., et al., *Hypoxia-inducible factor-dependent signaling between triple-negative breast cancer cells and mesenchymal stem cells promotes macrophage recruitment.* Proc Natl Acad Sci U S A, 2014. **111**(20): p. E2120-9.
596. Doedens, A.L., et al., *Macrophage expression of hypoxia-inducible factor-1 alpha suppresses T-cell function and promotes tumor progression.* Cancer Res, 2010. **70**(19): p. 7465-75.
597. Lin, E.Y., et al., *Macrophages regulate the angiogenic switch in a mouse model of breast cancer.* Cancer Res, 2006. **66**(23): p. 11238-46.
598. Burke, B., et al., *Hypoxia-induced gene expression in human macrophages: implications for ischemic tissues and hypoxia-regulated gene therapy.* Am J Pathol, 2003. **163**(4): p. 1233-43.
599. Fingleton, B., et al., *Matrilysin [MMP-7] expression selects for cells with reduced sensitivity to apoptosis.* Neoplasia, 2001. **3**(6): p. 459-68.
600. Kondelkova, K., et al., *Regulatory T cells (TREG) and their roles in immune system with respect to immunopathological disorders.* Acta Medica (Hradec Kralove), 2010. **53**(2): p. 73-7.
601. Atkuri, K.R., et al., *Importance of culturing primary lymphocytes at physiological oxygen levels.* Proc Natl Acad Sci U S A, 2007. **104**(11): p. 4547-52.
602. Hasmim, M., et al., *Cutting edge: Hypoxia-induced Nanog favors the intratumoral infiltration of regulatory T cells and macrophages via direct regulation of TGF-beta1.* J Immunol, 2013. **191**(12): p. 5802-6.
603. Facciabene, A., et al., *Tumour hypoxia promotes tolerance and angiogenesis via CCL28 and T(reg) cells.* Nature, 2011. **475**(7355): p. 226-30.
604. Thiel, M., et al., *Targeted deletion of HIF-1alpha gene in T cells prevents their inhibition in hypoxic inflamed tissues and improves septic mice survival.* PLoS One, 2007. **2**(9): p. e853.
605. Hatfield, S.M., et al., *Immunological mechanisms of the antitumor effects of supplemental oxygenation.* Sci Transl Med, 2015. **7**(277): p. 277ra30.
606. Jayaprakash, P., et al., *Targeted hypoxia reduction restores T cell infiltration and sensitizes prostate cancer to immunotherapy.* J Clin Invest, 2018. **128**(11): p. 5137-5149.
607. Chouaib, S., et al., *Hypoxic stress: obstacles and opportunities for innovative immunotherapy of cancer.* Oncogene, 2017. **36**(4): p. 439-445.
608. Banchereau, J. and R.M. Steinman, *Dendritic cells and the control of immunity.* Nature, 1998. **392**(6673): p. 245-52.
609. Gabrilovich, D.I., et al., *Production of vascular endothelial growth factor by human tumors inhibits the functional maturation of dendritic cells.* Nat Med, 1996. **2**(10): p. 1096-103.
610. Schito, L. and G.L. Semenza, *Hypoxia-Inducible Factors: Master Regulators of Cancer Progression.* Trends Cancer, 2016. **2**(12): p. 758-770.
611. Noman, M.Z., et al., *PD-L1 is a novel direct target of HIF-1alpha, and its blockade under hypoxia enhanced MDSC-mediated T cell activation.* J Exp Med, 2014. **211**(5): p. 781-90.

612. Curiel, T.J., et al., *Blockade of B7-H1 improves myeloid dendritic cell-mediated antitumor immunity.* Nat Med, 2003. **9**(5): p. 562-7.

613. Baginska, J., et al., *Granzyme B degradation by autophagy decreases tumor cell susceptibility to natural killer-mediated lysis under hypoxia.* Proc Natl Acad Sci U S A, 2013. **110**(43): p. 17450-5.

614. Viry, E., et al., *Autophagic degradation of GZMB/granzyme B: a new mechanism of hypoxic tumor cell escape from natural killer cell-mediated lysis.* Autophagy, 2014. **10**(1): p. 173-5.

615. Gonzalez, S., et al., *NKG2D ligands: key targets of the immune response.* Trends Immunol, 2008. **29**(8): p. 397-403.

616. Groh, V., et al., *Tumour-derived soluble MIC ligands impair expression of NKG2D and T-cell activation.* Nature, 2002. **419**(6908): p. 734-8.

617. Hirschhaeuser, F., U.G. Sattler, and W. Mueller-Klieser, *Lactate: a metabolic key player in cancer.* Cancer Res, 2011. **71**(22): p. 6921-5.

618. Feder-Mengus, C., et al., *Multiple mechanisms underlie defective recognition of melanoma cells cultured in three-dimensional architectures by antigen-specific cytotoxic T lymphocytes.* Br J Cancer, 2007. **96**(7): p. 1072-82.

619. Husain, Z., et al., *Tumor-derived lactate modifies antitumor immune response: effect on myeloid-derived suppressor cells and NK cells.* J Immunol, 2013. **191**(3): p. 1486-95.

620. Dietl, K., et al., *Lactic acid and acidification inhibit TNF secretion and glycolysis of human monocytes.* J Immunol, 2010. **184**(3): p. 1200-9.

621. Gottfried, E., et al., *Tumor-derived lactic acid modulates dendritic cell activation and antigen expression.* Blood, 2006. **107**(5): p. 2013-21.

622. Zhang, W., et al., *Lactate Is a Natural Suppressor of RLR Signaling by Targeting MAVS.* Cell, 2019. **178**(1): p. 176-189.e15.

623. Synnestvedt, K., et al., *Ecto-5'-nucleotidase (CD73) regulation by hypoxia-inducible factor-1 mediates permeability changes in intestinal epithelia.* J Clin Invest, 2002. **110**(7): p. 993-1002.

624. Kobie, J.J., et al., *T regulatory and primed uncommitted CD4 T cells express CD73, which suppresses effector CD4 T cells by converting 5'-adenosine monophosphate to adenosine.* J Immunol, 2006. **177**(10): p. 6780-6.

625. Ohta, A. and M. Sitkovsky, *Extracellular adenosine-mediated modulation of regulatory T cells.* Front Immunol, 2014. **5**: p. 304.

626. Chinnery, P.F. and G. Hudson, *Mitochondrial genetics.* Br Med Bull, 2013. **106**: p. 135-59.

627. Gray, M.W., *The endosymbiont hypothesis revisited.* Int Rev Cytol, 1992. **141**: p. 233-357.

628. Andrews, R.M., et al., *Reanalysis and revision of the Cambridge reference sequence for human mitochondrial DNA.* Nat Genet, 1999. **23**(2): p. 147.

629. Birky, C.W., Jr., *The inheritance of genes in mitochondria and chloroplasts: laws, mechanisms, and models.* Annu Rev Genet, 2001. **35**: p. 125-48.

630. Kasamatsu, H. and J. Vinograd, *Replication of circular DNA in eukaryotic cells.* Annu Rev Biochem, 1974. **43**(0): p. 695-719.

631. Hatefi, Y., *The mitochondrial electron transport and oxidative phosphorylation system.* Annu Rev Biochem, 1985. **54**: p. 1015-69.

632. Taanman, J.W., *The mitochondrial genome: structure, transcription, translation and replication.* Biochim Biophys Acta, 1999. **1410**(2): p. 103-23.

633. Uhler, J.P. and M. Falkenberg, *Primer removal during mammalian mitochondrial DNA replication.* DNA Repair, 2015. **34**: p. 28-38.

634. Schlee, M. and G. Hartmann, *Discriminating self from non-self in nucleic acid sensing.* Nat Rev Immunol, 2016. **16**(9): p. 566-80.

635. Pallen, M.J., *Time to recognise that mitochondria are bacteria?* Trends Microbiol, 2011. **19**(2): p. 58-64.

636. Bours, M.J., et al., *Adenosine 5'-triphosphate and adenosine as endogenous signaling molecules in immunity and inflammation.* Pharmacol Ther, 2006. **112**(2): p. 358-404.

637. Tannahill, G.M., et al., *Succinate is an inflammatory signal that induces IL-1beta through HIF-1alpha.* Nature, 2013. **496**(7444): p. 238-42.

638. Chicco, A.J. and G.C. Sparagna, *Role of cardiolipin alterations in mitochondrial dysfunction and disease.* Am J Physiol Cell Physiol, 2007. **292**(1): p. C33-44.

639. Claypool, S.M. and C.M. Koehler, *The complexity of cardiolipin in health and disease.* Trends Biochem Sci, 2012. **37**(1): p. 32-41.

640. Dieude, M., et al., *Cardiolipin binds to CD1d and stimulates CD1d-restricted gammadelta T cells in the normal murine repertoire.* J Immunol, 2011. **186**(8): p. 4771-81.

641. Iyer, S.S., et al., *Mitochondrial cardiolipin is required for Nlrp3 inflammasome activation.* Immunity, 2013. **39**(2): p. 311-323.

642. Kozak, M., *Comparison of initiation of protein synthesis in procaryotes, eucaryotes, and organelles.* Microbiol Rev, 1983. **47**(1): p. 1-45.

643. Carp, H., *Mitochondrial N-formylmethionyl proteins as chemoattractants for neutrophils.* J Exp Med, 1982. **155**(1): p. 264-75.

644. Campbell, C.T., J.E. Kolesar, and B.A. Kaufman, *Mitochondrial transcription factor A regulates mitochondrial transcription initiation, DNA packaging, and genome copy number.* Biochim Biophys Acta, 2012. **1819**(9-10): p. 921-9.

645. Chaung, W.W., et al., *Mitochondrial transcription factor A is a proinflammatory mediator in hemorrhagic shock.* Int J Mol Med, 2012. **30**(1): p. 199-203.

646. Crouser, E.D., et al., *Monocyte activation by necrotic cells is promoted by mitochondrial proteins and formyl peptide receptors.* Crit Care Med, 2009. **37**(6): p. 2000-9.

647. Julian, M.W., et al., *Mitochondrial transcription factor A, an endogenous danger signal, promotes TNFalpha release via RAGE- and TLR9-responsive plasmacytoid dendritic cells.* PLoS One, 2013. **8**(8): p. e72354.

648. Pullerits, R., et al., *Extracellular cytochrome c, a mitochondrial apoptosis-related protein, induces arthritis.* Rheumatology (Oxford), 2005. **44**(1): p. 32-9.

649. Hemmi, H., et al., *A Toll-like receptor recognizes bacterial DNA.* Nature, 2000. **408**(6813): p. 740-5.

650. Lund, J., et al., *Toll-like receptor 9-mediated recognition of Herpes simplex virus-2 by plasmacytoid dendritic cells.* J Exp Med, 2003. **198**(3): p. 513-20.

651. Zhang, Q., et al., *Circulating mitochondrial DAMPs cause inflammatory responses to injury.* Nature, 2010. **464**(7285): p. 104-7.

652. Zhou, R., et al., *A role for mitochondria in NLRP3 inflammasome activation.* Nature, 2011. **475**: p. 122.

653. Rongvaux, A., et al., *Apoptotic caspases prevent the induction of type I interferons by mitochondrial DNA.* Cell, 2014. **159**(7): p. 1563-77.

654. Collins, L.V., et al., *Endogenously oxidized mitochondrial DNA induces in vivo and in vitro inflammatory responses.* Journal of Leukocyte Biology, 2004. **75**(6): p. 995-1000.

655. Shimada, K., et al., *Oxidized Mitochondrial DNA Activates the NLRP3 Inflammasome during Apoptosis.* Immunity, 2012. **36**(3): p. 401-414.

656. Krüger, A., et al., *Human TLR8 senses UR/URR motifs in bacterial and mitochondrial RNA.* EMBO reports, 2015. **16**(12): p. 1656-1663.

657. Dhir, A., et al., *Mitochondrial double-stranded RNA triggers antiviral signalling in humans.* Nature, 2018. **560**(7717): p. 238-242.

658. Yla-Anttila, P., et al., *3D tomography reveals connections between the phagophore and endoplasmic reticulum.* Autophagy, 2009. **5**(8): p. 1180-5.

659. Yen, W.L., et al., *The conserved oligomeric Golgi complex is involved in double-membrane vesicle formation during autophagy.* J Cell Biol, 2010. **188**(1): p. 101-14.

660. Hailey, D.W., et al., *Mitochondria supply membranes for autophagosome biogenesis during starvation.* Cell, 2010. **141**(4): p. 656-67.

661. Ravikumar, B., et al., *Plasma membrane contributes to the formation of pre-autophagosomal structures.* Nat Cell Biol, 2010. **12**(8): p. 747-57.

662. Mizushima, N., *Autophagy: process and function.* Genes Dev, 2007. **21**(22): p. 2861-73.

663. Egan, D.F., et al., *Phosphorylation of ULK1 (hATG1) by AMP-activated protein kinase connects energy sensing to mitophagy.* Science, 2011. **331**(6016): p. 456-61.

664. Jewell, J.L., R.C. Russell, and K.L. Guan, *Amino acid signalling upstream of mTOR.* Nat Rev Mol Cell Biol, 2013. **14**(3): p. 133-9.

665. Bellot, G., et al., *Hypoxia-Induced Autophagy Is Mediated through Hypoxia-Inducible Factor Induction of BNIP3 and BNIP3L via Their BH3 Domains.* Molecular and Cellular Biology, 2009. **29**(10): p. 2570-2581.

666. Wu, H. and Q. Chen, *Hypoxia activation of mitophagy and its role in disease pathogenesis.* Antioxid Redox Signal, 2015. **22**(12): p. 1032-46.

667. Kubli, D.A. and A.B. Gustafsson, *Mitochondria and mitophagy: the yin and yang of cell death control.* Circ Res, 2012. **111**(9): p. 1208-21.

668. Hanna, R.A., et al., *Microtubule-associated protein 1 light chain 3 (LC3) interacts with Bnip3 protein to selectively remove endoplasmic reticulum and mitochondria via autophagy.* J Biol Chem, 2012. **287**(23): p. 19094-104.

669. Quinsay, M.N., et al., *Bnip3-mediated mitochondrial autophagy is independent of the mitochondrial permeability transition pore.* Autophagy, 2010. **6**(7): p. 855-62.

670. Novak, I., et al., *Nix is a selective autophagy receptor for mitochondrial clearance.* EMBO Rep, 2010. **11**(1): p. 45-51.

671. Schwarten, M., et al., *Nix directly binds to GABARAP: a possible crosstalk between apoptosis and autophagy.* Autophagy, 2009. **5**(5): p. 690-8.
672. Sandoval, H., et al., *Essential role for Nix in autophagic maturation of erythroid cells.* Nature, 2008. **454**(7201): p. 232-5.
673. Schweers, R.L., et al., *NIX is required for programmed mitochondrial clearance during reticulocyte maturation.* Proc Natl Acad Sci U S A, 2007. **104**(49): p. 19500-5.
674. Dorn, G.W., 2nd, *Mitochondrial pruning by Nix and BNip3: an essential function for cardiac-expressed death factors.* J Cardiovasc Transl Res, 2010. **3**(4): p. 374-83.
675. Chandel, N.S., et al., *Mitochondrial reactive oxygen species trigger hypoxia-induced transcription.* Proc Natl Acad Sci U S A, 1998. **95**(20): p. 11715-20.
676. Cooper, C.E. and C. Giulivi, *Nitric oxide regulation of mitochondrial oxygen consumption II: Molecular mechanism and tissue physiology.* Am J Physiol Cell Physiol, 2007. **292**(6): p. C1993-2003.
677. Cooper, C.E., *Nitric oxide and cytochrome oxidase: substrate, inhibitor or effector?* Trends Biochem Sci, 2002. **27**(1): p. 33-9.
678. Buckler, K.J. and R.D. Vaughan-Jones, *Effects of hypoxia on membrane potential and intracellular calcium in rat neonatal carotid body type I cells.* J Physiol, 1994. **476**(3): p. 423-8.
679. Premkumar, D.R., et al., *Intracellular pathways linking hypoxia to activation of c-fos and AP-1.* Adv Exp Med Biol, 2000. **475**: p. 101-9.
680. Chiche, J., et al., *Hypoxic enlarged mitochondria protect cancer cells from apoptotic stimuli.* J Cell Physiol, 2010. **222**(3): p. 648-57.
681. Frezza, C., et al., *Metabolic profiling of hypoxic cells revealed a catabolic signature required for cell survival.* PLoS One, 2011. **6**(9): p. e24411.
682. Jung, J., et al., *Mitochondrial NIX Promotes Tumor Survival in the Hypoxic Niche of Glioblastoma.* Cancer Res, 2019. **79**(20): p. 5218-5232.
683. Tang, W., et al., *PTEN-mediated mitophagy and APE1 overexpression protects against cardiac hypoxia/reoxygenation injury.* In Vitro Cell Dev Biol Anim, 2019.
684. Zhang, J. and P.A. Ney, *Role of BNIP3 and NIX in cell death, autophagy, and mitophagy.* Cell Death Differ, 2009. **16**(7): p. 939-46.
685. Ferber, E.C., et al., *FOXO3a regulates reactive oxygen metabolism by inhibiting mitochondrial gene expression.* Cell Death Differ, 2012. **19**(6): p. 968-79.
686. Jensen, K.S., et al., *FoxO3A promotes metabolic adaptation to hypoxia by antagonizing Myc function.* Embo j, 2011. **30**(22): p. 4554-70.
687. Gutsaeva, D.R., et al., *Transient hypoxia stimulates mitochondrial biogenesis in brain subcortex by a neuronal nitric oxide synthase-dependent mechanism.* J Neurosci, 2008. **28**(9): p. 2015-24.
688. Zhu, L., et al., *Hypoxia induces PGC-1alpha expression and mitochondrial biogenesis in the myocardium of TOF patients.* Cell Res, 2010. **20**(6): p. 676-87.
689. Arner, E.S. and S. Eriksson, *Mammalian deoxyribonucleoside kinases.* Pharmacol Ther, 1995. **67**(2): p. 155-86.
690. Fasullo, M. and L. Endres, *Nucleotide salvage deficiencies, DNA damage and neurodegeneration.* International journal of molecular sciences, 2015. **16**(5): p. 9431-9449.
691. Eriksson, S. and L. Wang, *Substrate Specificities, Expression and Primary Sequences of Deoxynucleoside Kinases; Implications for Chemotherapy.* Nucleosides and Nucleotides, 1997. **16**(5-6): p. 653-659.
692. King, M.P. and G. Attardi, *Human cells lacking mtDNA: repopulation with exogenous mitochondria by complementation.* Science, 1989. **246**(4929): p. 500-3.
693. Gregoire, M., et al., *On auxotrophy for pyrimidines of respiration-deficient chick embryo cells.* Eur J Biochem, 1984. **142**(1): p. 49-55.
694. King, M.P. and G. Attardi, *Isolation of human cell lines lacking mitochondrial DNA.* Methods Enzymol, 1996. **264**: p. 304-13.
695. Gaude, E., et al., *NADH Shuttling Couples Cytosolic Reductive Carboxylation of Glutamine with Glycolysis in Cells with Mitochondrial Dysfunction.* Mol Cell, 2018. **69**(4): p. 581-593.e7.
696. Hertzog, J., et al., *Infection with a Brazilian isolate of Zika virus generates RIG-I stimulatory RNA and the viral NS5 protein blocks type I IFN induction and signaling.* Eur J Immunol, 2018. **48**(7): p. 1120-1136.
697. Sung, P.S., et al., *Roles of unphosphorylated ISGF3 in HCV infection and interferon responsiveness.* Proc Natl Acad Sci U S A, 2015. **112**(33): p. 10443-8.
698. Kato, H., et al., *Length-dependent recognition of double-stranded ribonucleic acids by retinoic acid-inducible gene-I and melanoma differentiation-associated gene 5.* J Exp Med, 2008. **205**(7): p. 1601-10.

699. Weber, F., et al., *Double-stranded RNA is produced by positive-strand RNA viruses and DNA viruses but not in detectable amounts by negative-strand RNA viruses.* J Virol, 2006. **80**(10): p. 5059-64.

700. Mattern, I.E., *Mutagenicity of ethidium bromide after metabolic activation in vitro.* Mutation Research/Environmental Mutagenesis and Related Subjects, 1976. **38**(2): p. 120-121.

701. Starnes, M.C. and Y.C. Cheng, *Cellular metabolism of 2',3'-dideoxycytidine, a compound active against human immunodeficiency virus in vitro.* J Biol Chem, 1987. **262**(3): p. 988-91.

702. Nelson, I., et al., *Depletion of mitochondrial DNA by ddC in untransformed human cell lines.* Somat Cell Mol Genet, 1997. **23**(4): p. 287-90.

703. Oran, A.R., et al., *Multi-focal control of mitochondrial gene expression by oncogenic MYC provides potential therapeutic targets in cancer.* Oncotarget, 2016. **7**(45): p. 72395-72414.

704. Bousquet, P.A., et al., *Hypoxia Strongly Affects Mitochondrial Ribosomal Proteins and Translocases, as Shown by Quantitative Proteomics of HeLa Cells.* Int J Proteomics, 2015. **2015**: p. 678527.

705. Liu, X. and G. Hajnoczky, *Altered fusion dynamics underlie unique morphological changes in mitochondria during hypoxia-reoxygenation stress.* Cell Death Differ, 2011. **18**(10): p. 1561-72.

706. Thomas, L.W., et al., *CHCHD4 Regulates Intracellular Oxygenation and Perinuclear Distribution of Mitochondria.* Front Oncol, 2017. **7**: p. 71.

707. Al-Mehdi, A.B., et al., *Perinuclear mitochondrial clustering creates an oxidant-rich nuclear domain required for hypoxia-induced transcription.* Sci Signal, 2012. **5**(231): p. ra47.

708. Swiger, B., et al., *Hypoxia causes perinuclear mitochondrial clustering and nuclear oxidant stress in pulmonary artery endothelial cells (PAECS) via a dynein-dependent molecular motor.* The FASEB Journal, 2008. **22**(1_supplement): p. 1174.16-1174.16.

709. Baccelli, I., et al., *Mubritinib Targets the Electron Transport Chain Complex I and Reveals the Landscape of OXPHOS Dependency in Acute Myeloid Leukemia.* Cancer Cell, 2019. **36**(1): p. 84-99.e8.

710. Nagasawa, J., et al., *Novel HER2 selective tyrosine kinase inhibitor, TAK-165, inhibits bladder, kidney and androgen-independent prostate cancer in vitro and in vivo.* Int J Urol, 2006. **13**(5): p. 587-92.

711. Gorini, S., et al., *Chemotherapeutic Drugs and Mitochondrial Dysfunction: Focus on Doxorubicin, Trastuzumab, and Sunitinib.* Oxid Med Cell Longev, 2018. **2018**: p. 7582730.

712. Stagg, J., et al., *Anti–ErbB-2 mAb therapy requires type I and II interferons and synergizes with anti–PD-1 or anti-CD137 mAb therapy.* Proceedings of the National Academy of Sciences, 2011. **108**(17): p. 7142-7147.

713. Kang, B.H., et al., *Combinatorial drug design targeting multiple cancer signaling networks controlled by mitochondrial Hsp90.* J Clin Invest, 2009. **119**(3): p. 454-64.

714. Fiesel, F.C., et al., *Mitochondrial targeted HSP90 inhibitor Gamitrinib-TPP (G-TPP) induces PINK1/Parkin-dependent mitophagy.* Oncotarget, 2017. **8**(63): p. 106233-106248.

715. McKeown, S.R., *Defining normoxia, physoxia and hypoxia in tumours-implications for treatment response.* Br J Radiol, 2014. **87**(1035): p. 20130676.

716. Gingras, A.C., B. Raught, and N. Sonenberg, *Regulation of translation initiation by FRAP/mTOR.* Genes Dev, 2001. **15**(7): p. 807-26.

717. Koumenis, C., et al., *Regulation of protein synthesis by hypoxia via activation of the endoplasmic reticulum kinase PERK and phosphorylation of the translation initiation factor eIF2alpha.* Mol Cell Biol, 2002. **22**(21): p. 7405-16.

718. van den Beucken, T., M. Koritzinsky, and B.G. Wouters, *Translational control of gene expression during hypoxia.* Cancer Biol Ther, 2006. **5**(7): p. 749-55.

719. Liu, L., et al., *Hypoxia-induced energy stress regulates mRNA translation and cell growth.* Mol Cell, 2006. **21**(4): p. 521-31.

720. Thomas, J.D. and G.J. Johannes, *Identification of mRNAs that continue to associate with polysomes during hypoxia.* Rna, 2007. **13**(7): p. 1116-31.

721. Thomas, J.D., L.M. Dias, and G.J. Johannes, *Translational repression during chronic hypoxia is dependent on glucose levels.* Rna, 2008. **14**(4): p. 771-81.

722. Fahling, M., *Surviving hypoxia by modulation of mRNA translation rate.* J Cell Mol Med, 2009. **13**(9a): p. 2770-9.

723. Minter, M.R., et al., *Type-1 interferons contribute to oxygen glucose deprivation induced neuro-inflammation in BE(2)M17 human neuroblastoma cells.* J Neuroinflammation, 2014. **11**: p. 43.

724. Wang, H., et al., *ADAR1 Suppresses the Activation of Cytosolic RNA-Sensing Signaling Pathways to Protect the Liver from Ischemia/Reperfusion Injury.* Sci Rep, 2016. **6**: p. 20248.

725. Weiss, G.J., et al., *Phase 1 study of the safety, tolerability, and pharmacokinetics of TH-302, a hypoxia-activated prodrug, in patients with advanced solid malignancies.* Clin Cancer Res, 2011. **17**(9): p. 2997-3004.

726. Engel, C., et al., *RIG-I Resists Hypoxia-Induced Immunosuppression and Dedifferentiation.* Cancer Immunol Res, 2017. **5**(6): p. 455-467.

727. De Luna, N., et al., *Hypoxia triggers IFN-I production in muscle: Implications in dermatomyositis.* Sci Rep, 2017. **7**(1): p. 8595.

728. Cui, X.G., et al., *HIF1/2alpha mediates hypoxia-induced LDHA expression in human pancreatic cancer cells.* Oncotarget, 2017. **8**(15): p. 24840-24852.

729. Johnson, A.B., N. Denko, and M.C. Barton, *Hypoxia induces a novel signature of chromatin modifications and global repression of transcription.* Mutat Res, 2008. **640**(1-2): p. 174-9.

730. Batie, M., et al., *Hypoxia induces rapid changes to histone methylation and reprograms chromatin.* Science, 2019. **363**(6432): p. 1222-1226.

731. Aloni, Y. and G. Attardi, *Symmetrical in vivo transcription of mitochondrial DNA in HeLa cells.* Proc Natl Acad Sci U S A, 1971. **68**(8): p. 1757-61.

732. Young, P.G. and G. Attardi, *Characterization of double-stranded RNA from HeLa cell mitochondria.* Biochem Biophys Res Commun, 1975. **65**(4): p. 1201-7.

733. Parker, R. and U. Sheth, *P bodies and the control of mRNA translation and degradation.* Mol Cell, 2007. **25**(5): p. 635-46.

734. Borowski, L.S., et al., *Human mitochondrial RNA decay mediated by PNPase-hSuv3 complex takes place in distinct foci.* Nucleic Acids Res, 2013. **41**(2): p. 1223-40.

735. Li, Y., et al., *Ribonuclease L mediates the cell-lethal phenotype of double-stranded RNA editing enzyme ADAR1 deficiency in a human cell line.* eLife, 2017. **6**.

736. Leonova, K.I., et al., *p53 cooperates with DNA methylation and a suicidal interferon response to maintain epigenetic silencing of repeats and noncoding RNAs.* Proc Natl Acad Sci U S A, 2013. **110**(1): p. E89-98.

737. Wiatrek, D.M., et al., *Activation of innate immunity by mitochondrial dsRNA in mouse cells lacking p53 protein.* Rna, 2019. **25**(6): p. 713-726.

738. Ralston, A., *Simultaneous gene transcription and translation in bacteria.* Nature Education, 2008. **1**(4).

739. Chevrollier, A., et al., *ANT2 expression under hypoxic conditions produces opposite cell-cycle behavior in 143B and HepG2 cancer cells.* Mol Carcinog, 2005. **42**(1): p. 1-8.

740. Liu, H., et al., *Hypoxia increases tumor cell sensitivity to glycolytic inhibitors: a strategy for solid tumor therapy (Model C).* Biochem Pharmacol, 2002. **64**(12): p. 1745-51.

741. Matsubara, T., et al., *Additive Influence of Extracellular pH, Oxygen Tension, and Pressure on Invasiveness and Survival of Human Osteosarcoma Cells.* Front Oncol, 2013. **3**: p. 199.

742. Matsuda, N., et al., *PINK1 stabilized by mitochondrial depolarization recruits Parkin to damaged mitochondria and activates latent Parkin for mitophagy.* J Cell Biol, 2010. **189**(2): p. 211-21.

743. Narendra, D., et al., *Parkin is recruited selectively to impaired mitochondria and promotes their autophagy.* J Cell Biol, 2008. **183**(5): p. 795-803.

744. Sliter, D.A., et al., *Parkin and PINK1 mitigate STING-induced inflammation.* Nature, 2018. **561**(7722): p. 258-262.

745. Zhang, L., et al., *Altered brain energetics induces mitochondrial fission arrest in Alzheimer's Disease.* Sci Rep, 2016. **6**: p. 18725.

746. Wu, W., et al., *FUNDC1 is a novel mitochondrial-associated-membrane (MAM) protein required for hypoxia-induced mitochondrial fission and mitophagy.* Autophagy, 2016. **12**(9): p. 1675-1676.

747. Ong, S.B., et al., *Inhibiting mitochondrial fission protects the heart against ischemia/reperfusion injury.* Circulation, 2010. **121**(18): p. 2012-22.

748. Valko, M., et al., *Role of oxygen radicals in DNA damage and cancer incidence.* Mol Cell Biochem, 2004. **266**(1-2): p. 37-56.

749. Manoochehri Khoshinani, H., S. Afshar, and R. Najafi, *Hypoxia: A Double-Edged Sword in Cancer Therapy.* Cancer Invest, 2016. **34**(10): p. 536-545.

750. Moeller, B.J. and M.W. Dewhirst, *HIF-1 and tumour radiosensitivity.* Br J Cancer, 2006. **95**(1): p. 1-5.

751. Reznik, E., et al., *Mitochondrial DNA copy number variation across human cancers.* eLife, 2016. **5**.

752. Schofield, C.J. and P.J. Ratcliffe, *Oxygen sensing by HIF hydroxylases.* Nat Rev Mol Cell Biol, 2004. **5**(5): p. 343-54.

9. Appendix

Publications during the PhD

1. Miar A, **Arnaiz E**, Bridges E, Beedie S, Cribbs AP, Downes DJ, Beagrie R, Rehwinkel J, Harris AL. *Hypoxia induces transcriptional and translational downregulation of the type I interferon (IFN) pathway in multiple cancer cell types*. Submitted to Cancer Research.
2. **Arnaiz E**, Miar A, Dias AG, Prasad N, Schulze U, Waithe D, Rehwinkel J, Harris AL. *Hypoxia regulates endogenous double-stranded RNA production via reduced mitochondrial DNA transcription.* Under preparation.
3. **Arnaiz E**, Miar A, Bridges E, Prasad N, Lawrie CH, Harris AL. *HIF2α involvement in renal cancer metastasis.* Under preparation.